



**THURBER** ENGINEERING LTD.

# **PILE DESIGN RECOMMENDATIONS BASED ON ANALYSIS OF PILE LOAD TESTS IN ONTARIO**

## **MTO FOUNDATIONS**

**Report**

to

**Ministry of Transportation Ontario (MTO)**

**Prepared by**

Mohamed Hosney, Ph.D., P.Eng.  
Associate, Senior Geotechnical Engineer

Keli Shi, M.Eng., P.Eng.  
Principal, Senior Geotechnical Engineer

P.K. Chatterji, Ph.D., P.Eng.  
Designated Principal Contact

Date: August 31, 2023  
File: 31000



## TABLE OF CONTENTS

1.	INTRODUCTION .....	1
1.1	Objectives .....	2
2.	BACKGROUND .....	3
2.1	Summary of the Pile Load Test Database .....	3
2.2	Static Pile Load Test Analysis .....	5
2.3	Measured vs. Predicted Geotechnical Resistance of Piles .....	9
3.	PROPOSED FRAMEWORK FOR EVALUATING THE ULTIMATE AXIAL GEOTECHNICAL RESISTANCE OF PILES .....	10
3.1	Ultimate Shaft Resistance in Cohesionless Soils .....	11
3.2	Ultimate Shaft Resistance in Cohesive Soils .....	20
3.3	Ultimate End Bearing Resistance in Cohesionless Soils .....	29
3.4	Ultimate End Bearing in Cohesive Soils .....	33
3.5	Ultimate Geotechnical Resistance for Piles Driven into Till .....	34
3.5.1	Geotechnical Capacity of Driven Piles into Till based on MSPT Correlations .....	35
3.6	Geotechnical Resistance of Steel Piles Founded on Bedrock .....	36
3.6.1	Piles Driven to Refusal on Sound Bedrock .....	36
3.6.2	Piles Driven to Refusal within Fractured Bedrock .....	39
3.6.3	Piles Driven into Completely Weathered Bedrock (Residual Soil) .....	43
3.7	Geotechnical Resistance of Rock Sockets .....	43
4.	STRENGTH GAIN .....	47
4.1	Effect of Re-consolidation .....	49
4.2	Effect of Long-term Aging .....	51
4.3	Comparison with Measured Change in Pile Capacity .....	51
5.	RELAXATION .....	55
6.	IMPACT OF CONSTRUCTION MEANS AND METHODS ON PILE CAPACITY .....	56
7.	SOIL STRUCTURE INTERACTION .....	57
8.	SUMMARY AND CONCLUSIONS .....	63
9.	RECOMMENDATIONS FOR FUTURE WORK .....	69
	ACKNOWLEDGEMENT .....	69
	REFERENCES .....	70

## LIST OF TABLES

Table 2-1. Summary of Soil Conditions and Pile Properties .....	4
Table 3-1. Recommended values for $k$ , $\delta$ , and $\beta$ (extracted from CHBDC, 2019) .....	12
Table 3-2. Unplugged versus Plugged Section of Steel Piles .....	16
Table 3-3. Recommended Values for Decay Parameter in Various Cohesionless Soils .....	19
Table 3-4. Measured Versus Predicted Shaft Resistance for Piles Driven Through Cohesionless Soil Layers .....	19
Table 3-5. Examined Total Stress ( $\alpha$ ) methods and Factors Considered in Each Method ..	22
Table 3-6. Examined Effective Stress Approach ( $\beta$ Method) and Factors Considered in Each Method .....	25
Table 3-7. Measured Versus Predicted Shaft Resistance for Piles Driven Through Cohesive Soil Layers .....	28
Table 3-8. Recommended values for $N_q$ and $N_t$ (extracted from CHBDC, 2019 and CFEM, 2006) .....	30
Table 3-9. Measured Versus Predicted End Bearing Resistance of Steel H-Piles (310 x110) Rest on Cohesionless Soil .....	33
Table 3-10. Recommended Value of the Parameter $N_{cr}$ for Computing the Ultimate End Bearing Resistance of Driven Steel Piles Rest on Bedrock .....	37
Table 3-11. Recommended Value of Friction Angle of Rock Mass (excerpt from Tomlinson 2004) .....	38
Table 3-12. Pile Load Test of Piles Driven to Bedrock at MTO Sites .....	39
Table 3-13. Characterization of Rock Masses on the Basis of Interlocking and Join Alteration (Hoek and Brown, 1998) .....	41
Table 3-14. Values of $m_i$ for intact rock group (Hoek, 2007) .....	42
Table 3-15. Pile Load Test of Rock Sockets at MTO Sites .....	46
Table 4-1. Strength Gain Observation for All Relevant MTO Sites .....	53

## LIST OF FIGURES

Figure 1-1. Location of the 41 Pile Load Test Sites in Ontario, Canada (Extracted from MTO report, 1993) .....	2
Figure 1-2. Location of the Studies Recent 9 Sites in Ontario, Canada.....	2
Figure 2-1. Load-Displacement Curve and Predicted Ultimate Pile Resistance For Pile Load Test Conducted at Highway 401-Fletcher's Creek Site.....	8
Figure 2-2. Settlement Vs. Settlement/Load Based on Pile Load Test Conducted at Highway 401-Fletcher's Creek Site (Modified Chin Method) .....	8
Figure 2-3. Fitted Load-Displacement Curve Based on Pile Load Test Conducted at Highway 401-Fletcher's Creek Site (Brinch Hansen's Method) .....	9
Figure 2-4. Measured Versus Predicted Ultimate Geotechnical Resistance of Piles for the Subject 50 MTO Sites.....	10
Figure 3-1. Idealized and Field Profiles of Shaft Friction with Depth (after Randolph et al., 1994).....	13
Figure 3-2. Local shear stresses during installation of an instrumented pile (after Lehane 1992).....	14
Figure 3-3. Variation of $N_q$ with $\phi$ (after Berezantzev et al., 1961) .....	16
Figure 3-4. Measured Unit Shaft Resistance Vs. Predicted Values With and Without Considering Friction Fatigue for 36 m Long Test Pile – Hwy 400/89 Interchange .....	17
Figure 3-5. Measured Unit Shaft Resistance Vs. Predicted Values With and Without Considering Friction Fatigue For 51 m Long production Piles – Hwy 400/89 Interchange ..	18
Figure 3-6. Measured Versus Predicted Ultimate Geotechnical Resistance of Piles for Group-3 Sites.....	20
Figure 3-7. Variation of $\alpha$ with $S_u$ (excerpt from CHBDC, 2019) .....	21
Figure 3-8. NGI-05 Pile Design Method (after Karlsrud et al. 2005) .....	23
Figure 3-9. Proposed $\alpha$ value as per Karlsrud et al. 2012.....	23
Figure 3-10. Proposed $\beta$ value as per Burland (1993) .....	24
Figure 3-11. Proposed $\beta$ value as per Karlsrud (2012) .....	25
Figure 3-12. Measured Unit Shaft Resistance Vs. Predicted Values for 44 m Long Test Pile – Blanche River Site using (a) $\alpha$ -Method and (b) $\beta$ -Method.....	27
Figure 3-13. Measured Versus Predicted Ultimate Geotechnical Resistance of Piles for Group-4 Sites.....	28
Figure 3-14. Ultimate Unit End Bearing Resistance ( $q_b$ ) for Cohesionless Soils (excerpt from Fleming et al., 2009).....	31





Figure 3-15. Correction Factor for Ultimate Unit End Bearing Resistance for Open-Ended (Small Displacement) Driven Piles Rest on Cohesionless Soil .....	32
Figure 3-16. Relationship Between Friction Angle and GSI (after Hoek et. al., 1998).....	41
Figure 3-17. End bearing and shaft resistance of rock socket as function of socket displacement.....	45
Figure 3-18. Relationship between peak and post peak shear stress as function of the normal stress of the rock-concrete interface (excerpt from Vizini and Futai, 2019) .....	46
Figure 4-1. Soil Movement During Driving of Pile (adopted from Baligh, 1985).....	47
Figure 4-2. Change in Pile Resistance with Time for 310x110 Steel H-pile Driven through Stiff Clay Soil at the Highway 569-Blanche River Site.....	48
Figure 4-3. Build-up of the Shaft Friction During the Re-consolidation Phase (excerpt from NGI-2013) .....	49
Figure 4-4. Time Factor Values at Different Degrees of Consolidation (excerpt from Karlsrud, 2012).....	50
Figure 4-5. Typical Range of Normalized $G_{50}/S_u$ (excerpt from Karlsrud, 2012).....	51
Figure 4-6. Measured vs. Predicted Change in Pile Resistance with Time for 310x110 Steel H-pile Driven through Stiff Clay Soil at the Highway 569-Blanche River Site. ....	52

## **APPENDICES**

Appendix A: Background Information and Pile Load Test Assessment For the 50 MTO Site

Appendix B: Results of PLTs Carried out at 9 MOT Sites Across Ontario Between 2016 - 2019

Appendix C: Summary of the Suggested Design Methods

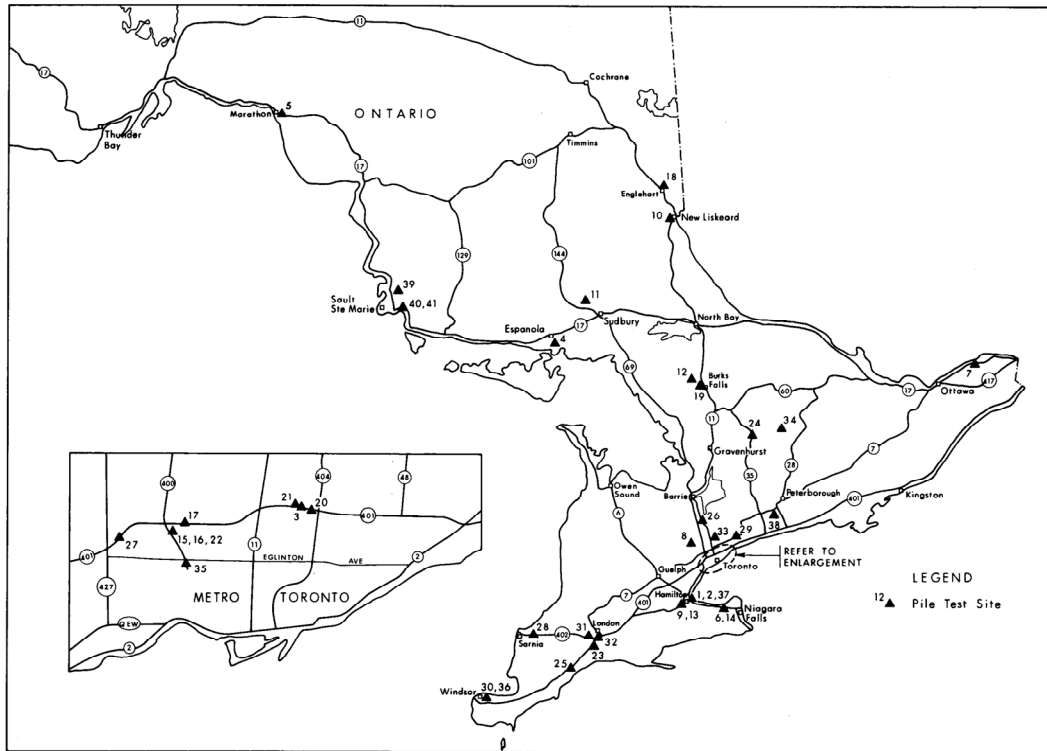


## 1. INTRODUCTION

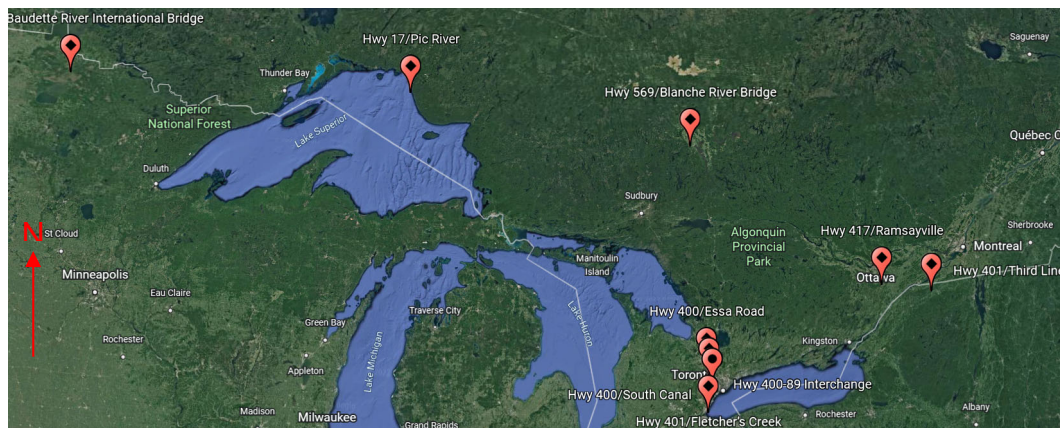
Deep foundations are typically being used at bridge sites where the near surface soils cannot provide adequate support for the structural loads. Originally, driven timber piles had been used as foundations for structures where deep foundations were required. As technology advanced, higher strength materials such as concrete or steel are being used more commonly in order to be able to sustain large structural loads. Although there is widespread use of piles, the commonly used methods for estimating the static axial geotechnical resistance of piles (e.g., methods recommended in Canadian Foundation Engineering Manual (CFEM), 2006; Canadian Highway Bridge Design Code (CHBDC), 2019; Federal Highway Administration (FHWA), 2016; etc.) remain mainly empirical or semi-empirical. These methods were calibrated to the equipment and methods used at the time of assessment (e.g., several decades ago) and might not be suitable for use with modern test equipment and current methods. As a result, the estimation of the axial capacity of piles still involves considerable level of uncertainty (Randolph et al., 1994; White and Bolton, 2002). Therefore, the widely used design methods can result in overconservative or unconservative design.

In order to improve and better assess the geotechnical design of piles in Ontario, the Ministry of Transportation of Ontario (MTO) developed the Pile Load and Extraction Tests report (MTO, 1993), which aimed at compiling the results of more than 100 pile load tests (PLTs) carried out at 41 sites across Ontario between 1952 and 1992 (Figure 1-1). In addition, results of the PLT carried out at nine (9) sites across Ontario between 2016 and 2019 have also been collected (Figure 1-2). The results of the PLTs carried out between 2016 and 2019 are presented in Appendix B.

The result of the 1952-1992 pile load tests and the available pile driving records were used by Rauf and Rothenburg (2011) to develop a guideline for estimating the axial capacity of driven piles in Ontario using dynamic formulae. Moreover, Liu and Jesswein (2022) used the same pile load test results to evaluate the reliability of the existing standard penetration test (SPT) based design methods and to develop a new SPT-based design method for driven piles in Ontario.



**Figure 1-1. Location of the 41 Pile Load Test Sites in Ontario, Canada (Extracted from MTO report, 1993)**



**Figure 1-2. Location of the Studies Recent 9 Sites in Ontario, Canada**

## 1.1 Objectives

An initial assessment of the pile load test data indicated significant difference between predicted geotechnical capacity of piles and actual capacity measured during pile load



test. The objective of this study is to assess the reasons for this observed discrepancy and to develop a framework/guideline for evaluating realistic geotechnical resistance of piles driven or augered through different Ontario geological overburden to dense soils or bedrock. To achieve this objective, the ultimate geotechnical capacity of the piles tested in the 41 historic sites (MTO, 1993) and the 9 recent sites have been assessed based on the analysis of all available static pile load tests and the driving records (i.e., Pile Driving Analyzer (PDA) and Case Pile Wave Analysis Program (CAPWAP) analysis). Subsequently, the commonly used design methods proposed by the CFEM and the CHBDC have been used to predict the geotechnical capacity of the test piles at the aforementioned 50 sites. The comparison between the measured geotechnical resistance of piles versus the predicted values provided an opportunity to better understand the performance of driven or augered piles in Ontario. Design guideline has been developed, as presented herein, to allow the designer to predict the geotechnical capacity of piles with a reasonable level of accuracy.

Furthermore, the effect of the time on the ultimate shaft resistance of piles driven through cohesive layers has been evaluated based on the analysis of the PLT and PDA carried out at a subject site at different points of time. Based on this evaluation, a simplified semi-empirical design procedure to account for the increase in pile resistance with time is presented.

## **2. BACKGROUND**

### **2.1 Summary of the Pile Load Test Database**

A total number of 133 static pile load tests have been carried out by MTO at the 41 historic sites and the 9 recent sites. The majority of the test piles are steel (i.e., 45 steel H-piles and 38 steel tubes). The rest of the piles are timber (38 piles), cast-in-place concrete (7 piles), and pre-cast concrete (5 piles).

The 50 MTO test pile sites can be classified into eight (8) different site groups based on the subsurface conditions along the pile length, the founding stratum at the tip of the pile, and the method of installation (see Table 2-1).

**Table 2-1. Summary of Soil Conditions and Pile Properties**

Site Group	Installation	Soil Along Pile Length	Design Founding Stratum	Pile Material	Length of piles (m)	No. of PLT
Group 1	Driven	Stratified deposits [cohesive and non-cohesive layers]	Cohesionless layer	Steel HP 310 x 110	14.8 to 51.0	9
				Steel Tubes (324 mm to 559 mm O.D)	8.0 to 32.7	12
				Pre-cast Concrete (305 mm x 305 mm)	14.6 to 34.9	2
				Timber piles (tip dia. 216 mm to 350 mm)	3.3 to 17.1	9
Group 2	Driven	Cohesive deposits	Cohesionless layer	Steel HP	9.6 to 30.5	8
Group 3	Driven	Cohesionless deposits	Cohesionless layer	Steel HP	14.5 to 38.9	11
				Steel Tubes (305 mm to 324 mm O.D)	5.8 to 22.8	8
				Timber piles (tip dia. 216 mm to 273 mm)	5.2 to 14.3	11
Group 4	Driven / Caisson	Cohesive deposits	Cohesive layer	Steel HP	3.1 to 40.0	9
				Steel Tubes (324 mm O.D)	3.0 to 42.7	12
				Pre-cast concrete (305 mm x 305 mm)	5.8 to 11.0	3
				Cast-in-place concrete (508 mm dia.)	9.5	1
				Timber piles (tip dia. 191 mm to 305 mm)	3.1 to 22.0	11
Group 5	Driven	Stratified deposits [cohesive and non-cohesive layers]	Shale or Limestone Bedrock	Steel HP	12.6 to 50.0	6
				Steel Tubes (324 mm O.D)	21.3 to 40.0	2
Group 6	Caisson	Cohesionless deposits	Cohesionless layer	Cast-in-place (2.44 m dia.)	26.0	1
Group 7	Driven / Caisson	Stratified deposits [cohesive and non-cohesive layers]	Cohesive layer	Steel HP	21.5 to 22.3	2
				Steel Tubes (324 mm O.D)	15.3 to 36.0	4
				Cast-in-place concrete (559 to 763 mm dia.)	7.3 to 18.6	2
				Timber piles (tip dia. 203 mm to 254 mm)	9.0 to 14.5	7
Group 8	Caisson	Rock Socket	Shale Bedrock	Cast-in-place concrete (590 to 640 mm dia.)	0.91 to 1.4 rock socket length	3
<b>TOTAL NUMBER OF PILE LOAD TESTS (PLT)</b>						<b>133</b>



The piles at Group 1 sites are driven piles through stratified deposits (i.e., cohesive and non-cohesive soil/till layers) with the pile tip into cohesionless deposit. Group 2 sites include steel H-piles driven through cohesive soil layers and the founding stratum is cohesionless layer.

The piles at Group 3 sites are driven piles through cohesionless soil layers and the soil at the tip elevation is cohesionless as well. The soil layers along the pile length and at the pile tip are both cohesive at the Group 4 sites. Group 4 includes both driven piles and cast-in-place reinforced concrete bored piles (caissons). Sites where driven steel H-piles or steel tube piles are supported on bedrock (shale or limestone) are classified as Group 5 sites. Group 6 site includes a case of large diameter caisson augered through cohesionless soil layers and founded on cohesionless soil layer. Group 7 sites include both driven piles and caissons where cohesive and cohesionless soil layers are encountered along the length of the piles/caisson, whereas the soil at the tip elevation of the piles/caissons is cohesive. The caisson under Group 8 site is socketed into the sound shale bedrock. Reference is made to the Pile Load and Extraction Tests report (MTO, 1993) for the Record of Borehole Logs at the pile load test locations for the 41 historic sites. The load-displacement curves for all tested piles are also included in the MTO report. The subsurface conditions and the results of the piles load tests at the recent 9 sites have been provided directly by MTO.

In addition to the static pile load tests, PDA tests and CAPWAP analysis were carried out at eight (8) sites during the driving of 28 pre-production test piles and 49 production piles. The PDA and CAPWAP were carried out at the End of Initial Drive and Beginning of Restrike of the subject piles. The PDA and CAPWAP results have been used to determine the shaft resistance and the end bearing resistance of the examined piles.

## **2.2 Static Pile Load Test Analysis**

Multiple analytical methods are available and commonly used to assess the ultimate geotechnical resistance of a pile based on the static pile load test results. Among those, several methods have been proposed over the last decades to identify the yield point or the failure load based on the characteristics of the load-displacement curve obtained from the pile load test. The methods of analysis can be divided into two main categories: gradual failure methods and plunging failure methods. The gradual failure methods define the ultimate pile capacity as the point near the greatest curvature on the load-



displacement curve; whereas, the plunging methods locate the ultimate pile capacity near the plunging failure where the rate of pile settlement increases without corresponding increase in the test load.

One of the commonly used gradual failure methods is the Davisson Offset Limit Load Method (1973). The Brinch Hansen's 90% Method (1963) and the Modified Chin Method (1970) are commonly used plunging failure methods for analyzing the pile load tests. These three methods, which are recommended by the CFEM and the CHBDC, have been used in this study to analyze the pile load test results from all sites.

Davisson Offset Limit Load may be considered the most popular method used to predict the ultimate geotechnical resistance of piles by considering the elastic shortening of the pile when having various loads placed on it during pile load tests. According to this method, the ultimate resistance of pile corresponds to a specified pile head displacement (s) given by the following equation:

$$S = \frac{Q \cdot L}{E \cdot A} + (4 + 8d) \quad (1)$$

Where:      S = movement of the pile head (mm),  
              Q = the applied load,  
              L = length of the pile,  
              E = Young's modulus of the pile material,  
              A = the cross-section area of the pile, and  
              d = the pile diameter or pile width.

The point of intersection between the offset theoretical elastic compression line of the pile and the measured load-displacement curve is defined as the ultimate pile capacity as per the Davisson Offset Limit Load method (see Figure 2-1). However, it should be noted that the Davisson Offset Limit Load method was developed for end bearing driven piles assuming that little to no resistance is contributed by skin friction, the pile head is free, and the pile tip is fixed. These assumptions are not always representative; therefore, use of such method may be very conservative.

The Brinch Hansen's 90% Method (1963) and the Modified Chin Method (1970) assume that the load-displacement curve is hyperbolic. However, when the settlement (S) is





plotted versus the settlement over load ( $S/Q$ ), the relationship becomes straight line as shown in Figure 2-2. The ultimate pile resistance can be computed based on the Modified Chin Method (1970) using the following equation:

$$Q_{ult} = \frac{1}{1.2 \cdot b} \quad (2)$$

Where:  $Q_{ult}$  = the ultimate geotechnical resistance, and  
 $b$  = the slope of the line obtained from Figure 2-2.

For the Brinch Hansen's 90% Method (1963), the hyperbolic load-displacement curve is plotted using the following equation:

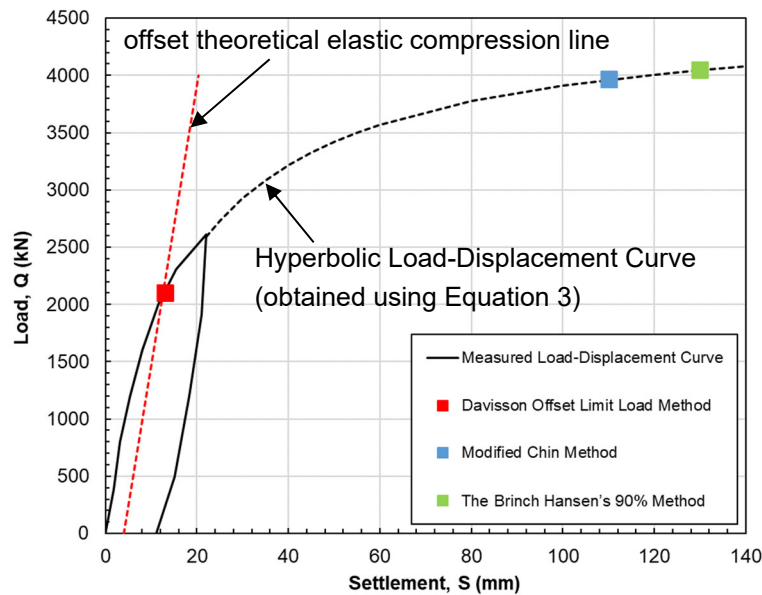
$$Q = \frac{S}{(a+b \cdot S)} \quad (3)$$

Where:  $Q$  = the applied load,  
 $S$  = settlement, and  
 $a$  and  $b$  = values obtained from Figure 2-2.

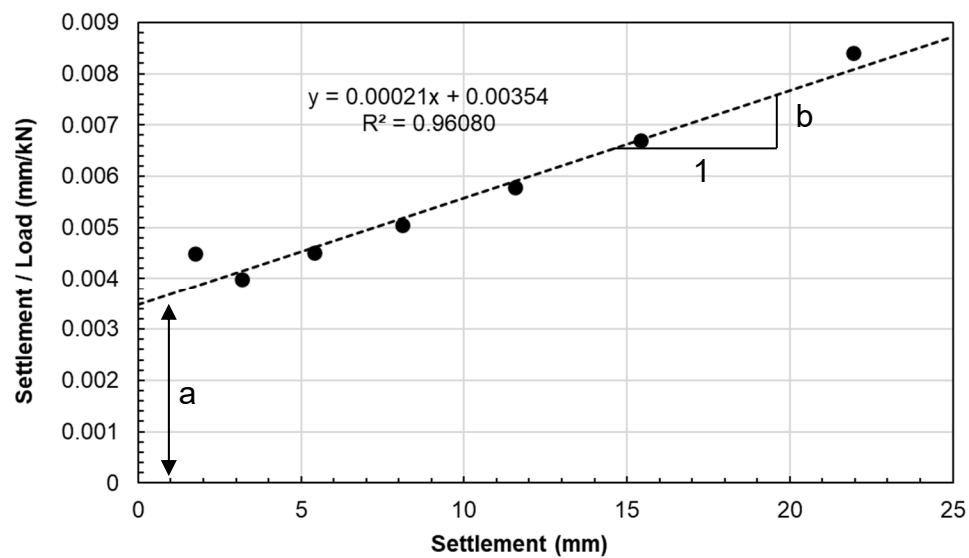
The ultimate geotechnical resistance ( $Q_{ult}$ ) is defined as per Brinch Hansen's 90% Method as the load where the settlement ( $2\Delta$ ) corresponding to this load is equal to double the settlement ( $\Delta$ ) corresponding to 90% of  $Q_{ult}$  (see Figure 2-3)

As shown in Figure 2-1, the estimated ultimate geotechnical resistances from the Brinch Hansen's 90% Method and the Modified Chin Method are typically higher than the value obtained based on the Davisson Offset Limit Load Method. However, if plunging failure has not been reached during the pile load test (e.g., the pile load test at Highway 401-Fletcher's Creek site), then the standard practice is to assume that the maximum applied load is the load which causes failure. Therefore, for all pile load tests carried out at the 50 MTO sites, the ultimate resistance is taken to be the maximum value obtained from the three methods of analysis as long as the value is less than the maximum load applied during the pile load test. Otherwise, the maximum load applied during the pile load test was considered as the ultimate geotechnical resistance of the pile. The interpreted ultimate geotechnical resistance for the 133 pile load tests obtained from the above three interpretive methods are presented in Table A-1 of Appendix A.

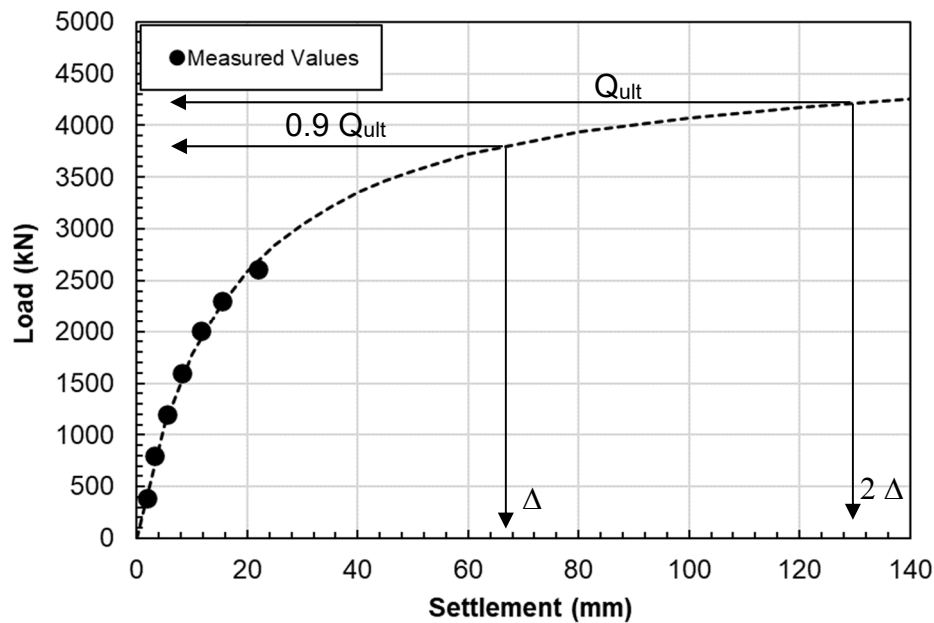




**Figure 2-1. Load-Displacement Curve and Predicted Ultimate Pile Resistance For Pile Load Test Conducted at Highway 401-Fletcher's Creek Site**



**Figure 2-2. Settlement Vs. Settlement/Load Based on Pile Load Test Conducted at Highway 401-Fletcher's Creek Site (Modified Chin Method)**

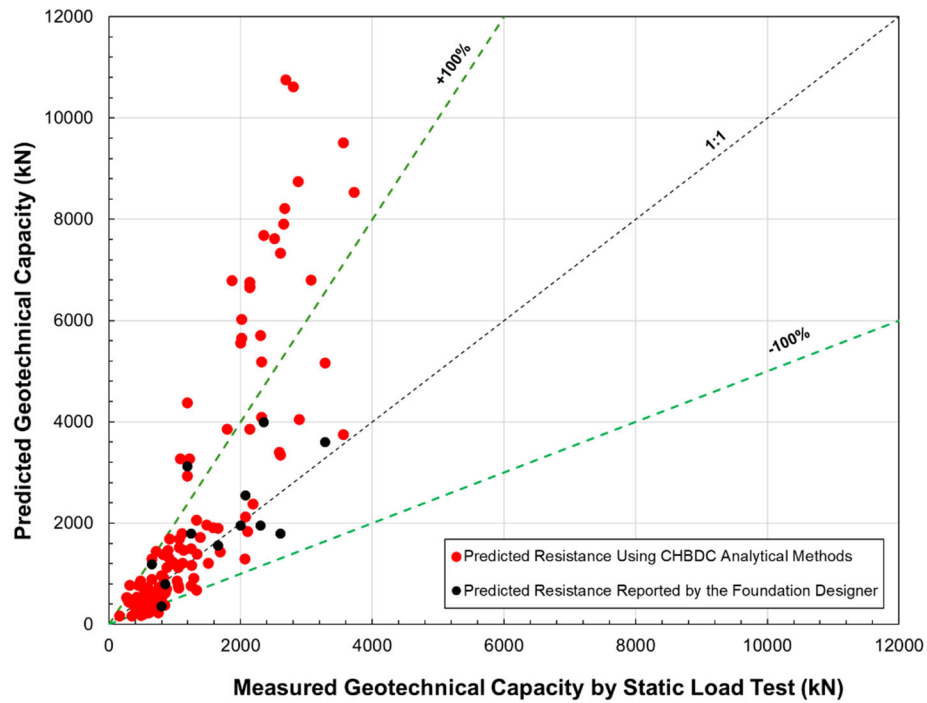


**Figure 2-3. Fitted Load-Displacement Curve Based on Pile Load Test Conducted at Highway 401-Fletcher's Creek Site (Brinch Hansen's Method)**

### 2.3 Measured vs. Predicted Geotechnical Resistance of Piles

As indicated earlier, one of the main reasons for the assessment presented herein is the MTO observation of the significant difference between the predicted geotechnical resistance of piles versus the actual values measured by the static pile load tests and the driving records. Figure 2-4 shows a comparison between the measured geotechnical capacity by the static pile load tests conducted in the subject 50 sites versus the predicted geotechnical capacity obtained by using the analytical methods presented in the CHBDC. The available predicted geotechnical capacities assessed by the foundation consultant are also shown in Figure 2-4. It could be seen that the ratio between the predicted geotechnical resistance to the measured geotechnical resistance of the examined piles can range from 0.3 to 4.0. This significant difference between the measured and predicted resistances can result in either conservative foundation design if the predicted capacity is conservative or construction complications/claims if the measured capacity is significantly lower than the value predicted by the foundation designer. The next sections of the report present the possible explanation for such significant difference between the

measured and predicted capacity of piles along with a proposed framework of design to more accurately determine the geotechnical resistance of piles in Ontario.



**Figure 2-4. Measured Versus Predicted Ultimate Geotechnical Resistance of Piles for the Subject 50 MTO Sites**

### 3. PROPOSED FRAMEWORK FOR EVALUATING THE ULTIMATE AXIAL GEOTECHNICAL RESISTANCE OF PILES

The ultimate axial geotechnical resistance of a single pile can be estimated by adding the ultimate shaft resistance along the embedment length of the pile to the ultimate end bearing resistance at the pile toe elevation, as expressed by the following equation:

$$Q_{ult} = P_s + P_b = \Sigma q_s \cdot C \cdot \Delta L + q_b \cdot A_b \quad (4)$$

Where:

- $P_s$  = the ultimate shaft resistance,
- $P_b$  = the ultimate end bearing resistance,
- $q_s$  = the ultimate unit shaft resistance along the portion of the pile ( $\Delta L$ ) embedded within each soil layer,

$C$  = the pile perimeter along the shaft,

$q_b$  = the ultimate unit end bearing resistance at the toe of the pile, and

$A_b$  = the area of the pile at the tip elevation.

There are several empirical methods available to assess the values of unit shaft resistance and unit end bearing resistance, some of which are discussed in the CHBDC (2019) and the CFEM (2006). The following sections present an evaluation of the methods presented in the CHBDC and CFEM for the calculation of the ultimate geotechnical resistance of a pile in cohesionless and cohesive soils. Recommendations for additional considerations to be included during design are also presented.

### 3.1 Ultimate Shaft Resistance in Cohesionless Soils

The value of the ultimate shaft resistance of piles in cohesionless soils can be calculated as follows:

$$P_s = k \cdot \tan(\delta) \cdot \sigma_v \cdot A_s = \beta \cdot \sigma_v \cdot A_s \quad (5)$$

Where:  $k$  = the coefficient of lateral earth pressure,  
 $\delta$  = the angle of interface friction between the pile and the surrounding soil,  
 $\sigma_v$  = the average vertical effective stress along the pile shaft, and  
 $A_s$  is the surface area of the pile shaft.

Recommended values for the  $k$ ,  $\delta$ , and  $\beta$  are presented in the CFEM and CHBDC as shown in Table 3-1.

Based on Equation 5, the shaft resistance of a pile embedded in a homogeneous cohesionless soil layer increase linearly with the depth, as shown schematically in Figure 3-1 (red dotted line). However, it has been observed based on back analysis of field and lab tests on instrumented piles (e.g., Vésic, 1969; Hanna and Tan, 1973; Heerema, 1978; Toolan et al., 1990; Lehane 1992; Chow, 1997; De Nicola, 1996; Bruno, 1999; Lehane et al., 1993, 2005; and many other researchers) that even in homogenous cohesionless deposit, the unit shaft resistance along driven piles does not increase linearly with depth, as shown schematically in Figure 3-1 (blue solid line). The difference between the theoretical and the actual field performance represents the over-estimation in assessment of the shaft resistance. Several attempts have been made to obtain unit shaft resistance

distribution which could match the average shaft resistance measured from a pile load test.

**Table 3-1. Recommended values for  $k$ ,  $\delta$ , and  $\beta$  (extracted from CHBDC, 2019)**

**Lateral earth pressure co-efficient,  $K$   
(after NAVFAC DM 7.02)**

Pile type	$K$ (piles under compression)	$K$ (piles under tension — uplift piles)
Driven H-piles	0.5–1.0	0.3–0.5
Driven displacement piles (round and square)	1.0–1.5	0.6–1.0
Driven displacement tapered piles	1.5–2.0	1.0–1.3
Driven jetted piles	0.4–0.9	0.3–0.6
Bored piles (less than 600 mm diameter)	0.7	0.4

**Values of pile shaft friction angles,  $\delta$   
(after NAVFAC, 1986)**

Pile type	$\delta$
Steel piles	20°
Timber piles	$3/4 \phi$
Concrete piles	$3/4 \phi$

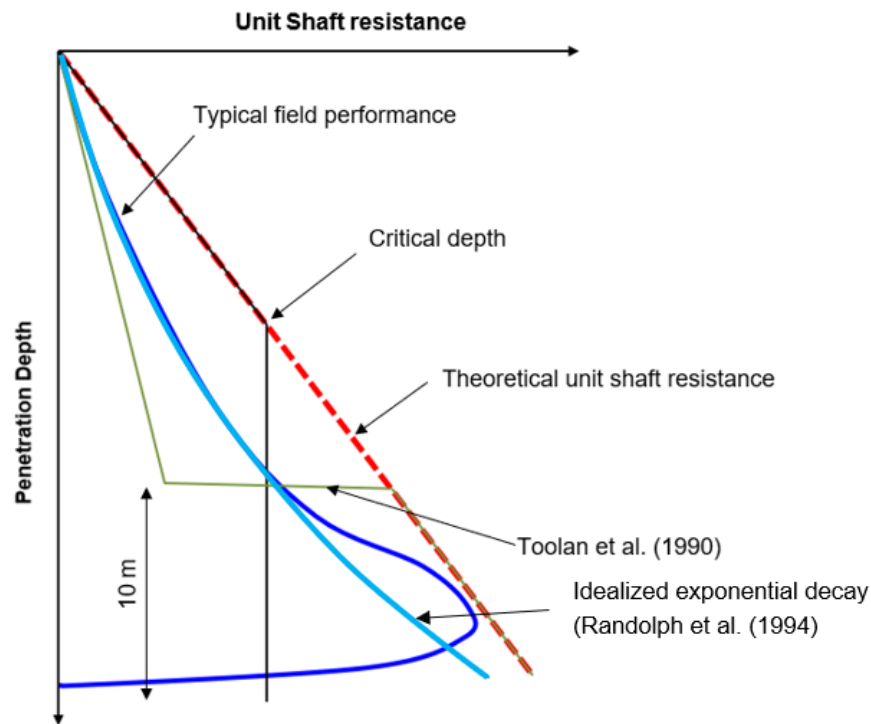
**Variation of  $\beta$  values with  $\phi'$  for (a) driven piles and for (b) drilled shafts**

(a) Driven piles

$\phi'$	$\beta$
28°	0.44
35°	0.75
37°	1.20

(b) Drilled shafts

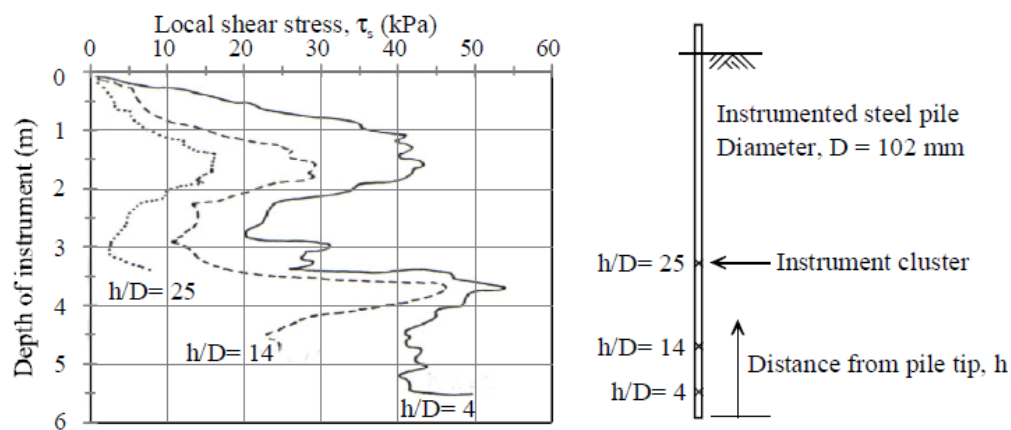
$\phi'$	$\beta$
33°	0.1
35°	0.2
37°	0.35



**Figure 3-1. Idealized and Field Profiles of Shaft Friction with Depth (after Randolph et al., 1994)**

For example, the CHBDC (2019) recommends the “critical depth” concept where the unit shaft resistance is assumed to increase linearly with depth until a specific depth (i.e., the critical depth) below which the unit shaft resistance is constant. In contrast to the critical depth concept, Toolan et. al. (1990) proposes a low lateral earth pressure coefficient ( $k$ ) for the upper portion of the pile and a higher  $k$  value for the lower portion of the pile (see Figure 3-1). These two methods, and several others, are relatively simple but don’t capture either the actual phenomenon of the change in the local shaft friction with depth or the unit shaft resistance distribution as measured from the instrumented pile load tests. Therefore, the shaft resistance obtained using these methods can result in over or under estimation of the geotechnical resistance of piles depending on the pile length and the subsurface conditions. This is believed to be one of the main reasons for the significant difference between the measured and predicted pile resistance noted at the various pile load test sites for piles driven through cohesionless deposits.

The decrease in the horizontal effective stress, and hence the local shaft friction, acting on driven pile shaft at a specific depth as the pile tip penetrates deeper is known as the “friction fatigue”. Several field and laboratory experiments have been carried out to better understand this phenomenon. For example, Lehane (1992), carried out a series of field experiments on instrumented displacement piles driven through different types of soils including medium dense sand. It has been observed that within the same soil layer, the shaft resistance at a specific depth decreases as the distance between the point of interest and the pile tip elevation increase (see Figure 3-2).



**Figure 3-2. Local shear stresses during installation of an instrumented pile (after Lehane 1992)**

White and Bolton (2002) explained, based on a laboratory calibration chamber testing, that the friction fatigue occurs due to the gradual densification of soil adjacent to the pile shaft under the cyclic shearing action of installation. This process is enhanced by the diffusion of the fine broken particles away from the pile-soil interface into the more open matrix of uncrushed soil in the far field. These two actions result in volume reduction in the boundary layer at the pile-soil interface combined with horizontal unloading of the far field. Given that the soil zones closer to the ground surface experience higher level of shearing during installation and higher potential of breakage, the friction fatigue is more pronounced at higher elevations.

Randolph et al. (1994) introduced a design framework to capture the effect of the friction fatigue on the shaft friction by predicting the horizontal earth pressure coefficient ( $k$ ) to

decay exponentially with distance from the pile tip (see Figure 3-1) as expressed by Equation 6:

$$k = k_{min} + (k_{max} - k_{min}) e^{-\left(\frac{\mu h}{d}\right)} \quad (6)$$

Where:  $k_{min}$  = the active earth pressure coefficient,  
 $\mu$  = the decay rate parameter (which can be taken as  $\sim 0.05$  as per Randolph et al. 1994),  
 $h$  = the distance from the pile tip,  
 $d$  = the pile diameter or width, and  
 $k_{max}$  can be computed using the following equation:

$$k_{max} = S_t \cdot N_q \quad (7)$$

Where:  $S_t$  = the ratio of the radial effective stress acting in the vicinity of the pile tip at shaft failure to the end bearing capacity, and  
 $N_q$  = the bearing capacity coefficient.

Fleming et al. (1992) suggested a value of 0.02 for the factor  $S_t$ . The value of the factor  $S_t$  can also be computed using the following equation as a function of the soil friction angle ( $\phi$ ):

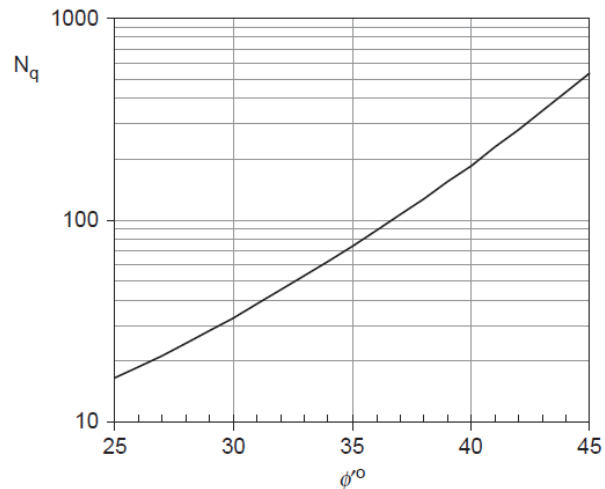
$$S_t = 0.1 e^{(-3 \cdot \tan \phi)} \quad (8)$$

The value of  $N_q$  quoted in the literature vary considerably but those derived by Berezantzev et al. (1961) are used most widely for the design of deep foundations (Figure 3-3).

The shaft resistance along all driven piles penetrated through cohesionless soil/till layers at the subject MTO sites has been obtained using Equation 5 in conjunction with the  $k$  values estimated following Randolph et al. (1994) framework (i.e., Equation 6). The  $\delta$  value has been obtained to be equal to  $0.54 \phi$  for steel piles,  $0.76 \phi$  for wood and concrete piles penetrated through sand layers, and  $0.5 \phi$  for wood and concrete piles penetrated through silt layers. For steel H-piles, the shaft area was taken as the perimeter of a plugged section (Table 3-2) times the pile length, as long as the conditions presented in the commentary of the CHBDC (2019) is satisfied (e.g., the ratio of the pile embedment

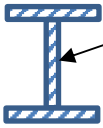
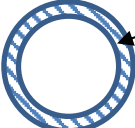
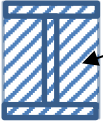
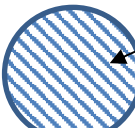


length to pile diameter or width is greater than 20 to 35 in medium dense to dense soils, etc.).



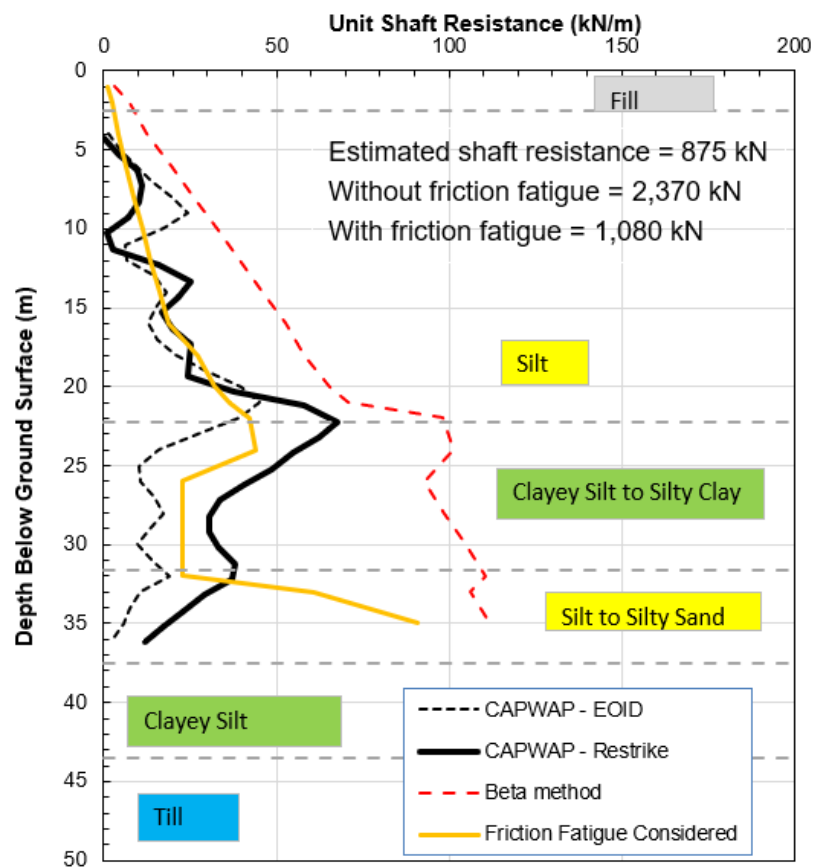
**Figure 3-3. Variation of  $N_q$  with  $\phi$  (after Berezantzev et al., 1961)**

**Table 3-2. Unplugged versus Plugged Section of Steel Piles**

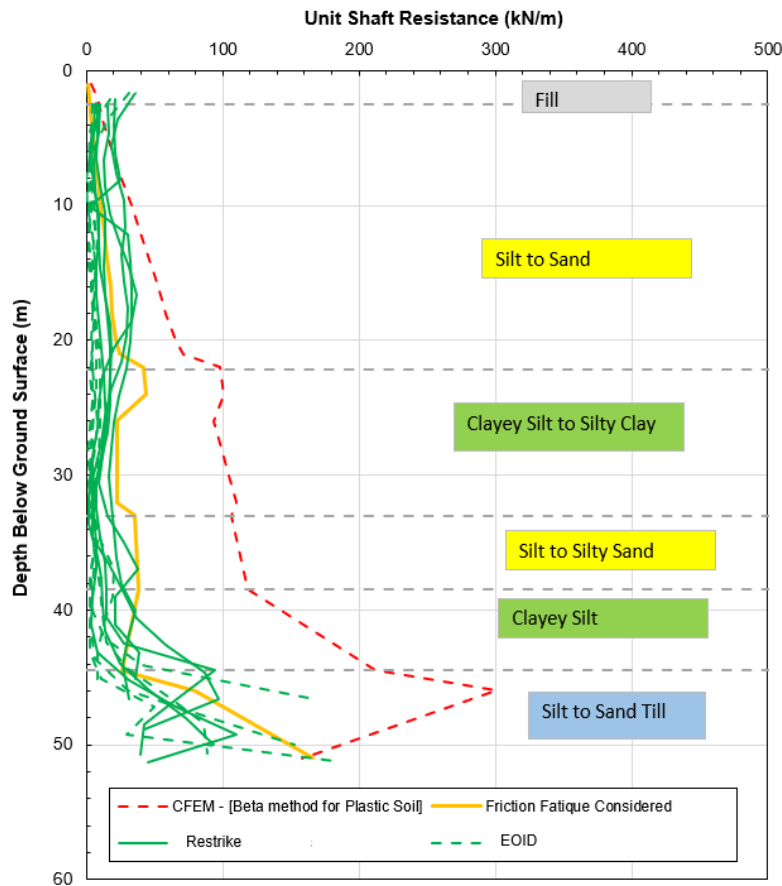
Steel Section	H-Pile	Pipe
Unplugged Section [Steel Section Only]		
Plugged Section [Steel Section and Soil Plug]		

As an example, Figure 3-4 presents the measured unit shaft resistance with depth at the end of initial driving (EOID) and during the restrrike for an HP 310x110 test pile penetrated through stratified deposits at Highway 400/89 interchange site. Without considering the effect of the friction fatigue, the estimated unit shaft friction was much larger than the measured values. On the other hand, the unit shaft resistance profile obtained

considering the friction fatigue as described above and with  $\mu$  value of 0.05 was very close to the field measured values. Ignoring the friction fatigue results in overestimation of the pile capacity by a factor of 2.5 (see Table A-1; Appendix A) and resulted in the need to increase the embedment depth of the pile from 36 m to 51 m to achieve required pile capacity. The unit shaft resistances measured for six (6) production piles are shown in Figure 3-5. The estimated unit shaft resistance considering the friction fatigue matches well with the measured shaft resistance.



**Figure 3-4. Measured Unit Shaft Resistance Vs. Predicted Values With and Without Considering Friction Fatigue for 36 m Long Test Pile – Hwy 400/89 Interchange**



**Figure 3-5. Measured Unit Shaft Resistance Vs. Predicted Values With and Without Considering Friction Fatigue For 51 m Long production Piles – Hwy 400/89 Interchange**

Based on the analysis of all pile load tests carried out at all relevant MTO sites, the recommended values for the decay parameter ( $\mu$ ) based on the soil condition and the method of pile installation are shown in Table 3-3.

Using the above recommended method for obtaining the shaft friction along piles in cohesionless soils, the results of the predicted ultimate pile resistance matches well with the measured resistance as shown in Figure 3-6 for the Group-3 sites. In addition, the measured shaft resistance of piles penetrated through cohesionless soils and tested in the MTO recent sites (where PDA and CAPWAP analysis carried out) were compared to the predicted shaft resistance assessed based on the aforementioned recommended

method (Table 3-4). A good match can be observed between the measured and predicted shaft resistances.

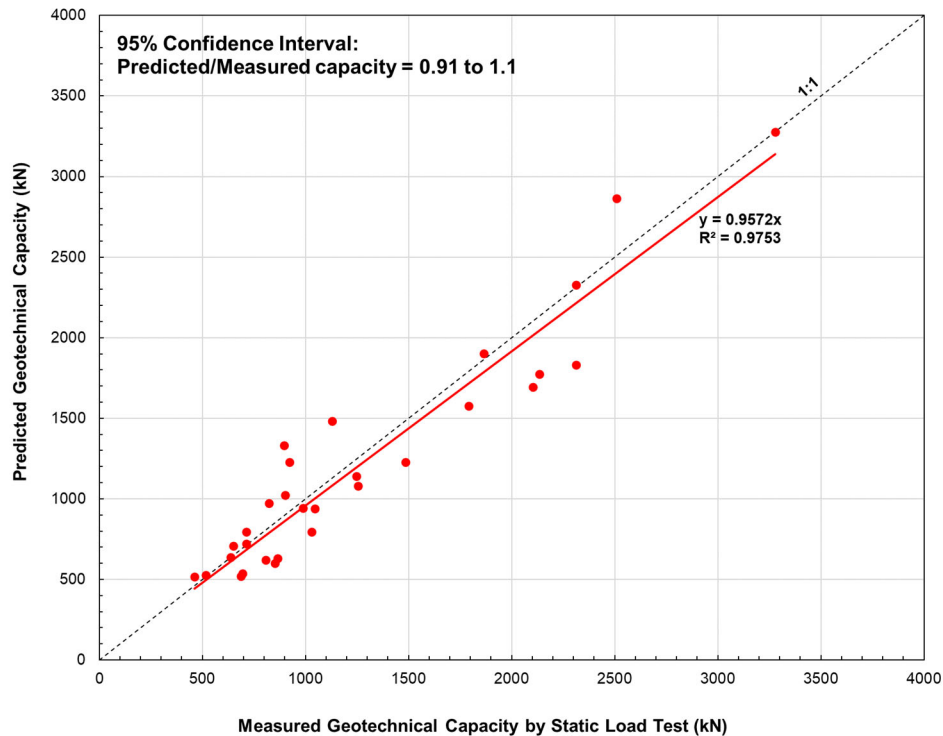
**Table 3-3. Recommended Values for Decay Parameter in Various Cohesionless Soils**

Soil Type	Installation Method	Recommended Decay parameter ( $\mu$ )
Silty Sand to Sandy Silt [Compact to Very Dense]	Driven	0.03 to 0.05
<ul style="list-style-type: none"> <li>- Very Loose to Loose Cohesionless soils</li> <li>- Gravel [any level of compaction]</li> <li>- Silt [any level of compaction]</li> </ul>	Driven	0 to 0.03
All Cohesionless Soils	Augered	0

As illustrated above, the soil friction angle is the main shear strength parameter required to determine the shaft resistance within the cohesionless soils. The friction angle can be determined through laboratory testing (i.e., Drained Direct Shear Test or Consolidated Drained Triaxial Test) or estimated based on empirical correlations with the SPT “N” values and/or results of Cone Penetration Test (CPT). It's important to note that the accurate determination of the soil friction angle is obtained through laboratory testing. However, empirical correlations can provide reasonable estimates when laboratory testing is not feasible or when preliminary information is required.

**Table 3-4. Measured Versus Predicted Shaft Resistance for Piles Driven Through Cohesionless Soil Layers**

Site Group	Site Name	Soil Along Pile Length	Pile Length (m)	Measured Ultimate Shaft Resistance (kN)	Predicted Ultimate Shaft Resistance (kN)
Group 1	HWY 400 - 89	Steel H-Pile [310x110] penetrated through stratified deposits	36.0	875	1080
Group 1	HWY 400 - 89	Steel H-Pile [310x110] penetrated through stratified deposits	51.0	1827	1920
Group 3	HWY 400 - Essa Rd.	Steel H-Pile [310x110] penetrated through Silt to sand	31.6	2330	2320



**Figure 3-6. Measured Versus Predicted Ultimate Geotechnical Resistance of Piles for Group-3 Sites**

### **3.2 Ultimate Shaft Resistance in Cohesive Soils**

Piles in cohesive soils develop a high portion of their ultimate axial geotechnical resistance along the shaft. Therefore, a considerable effort has been made over the last century for developing a reliable method for estimating the value of the shaft friction of piles in clay by back analyzing the results of pile load tests. The methods which have been developed can be grouped into two main approaches: the total stress approach ( $\alpha$  method) or the effective stress approach ( $\beta$  method).

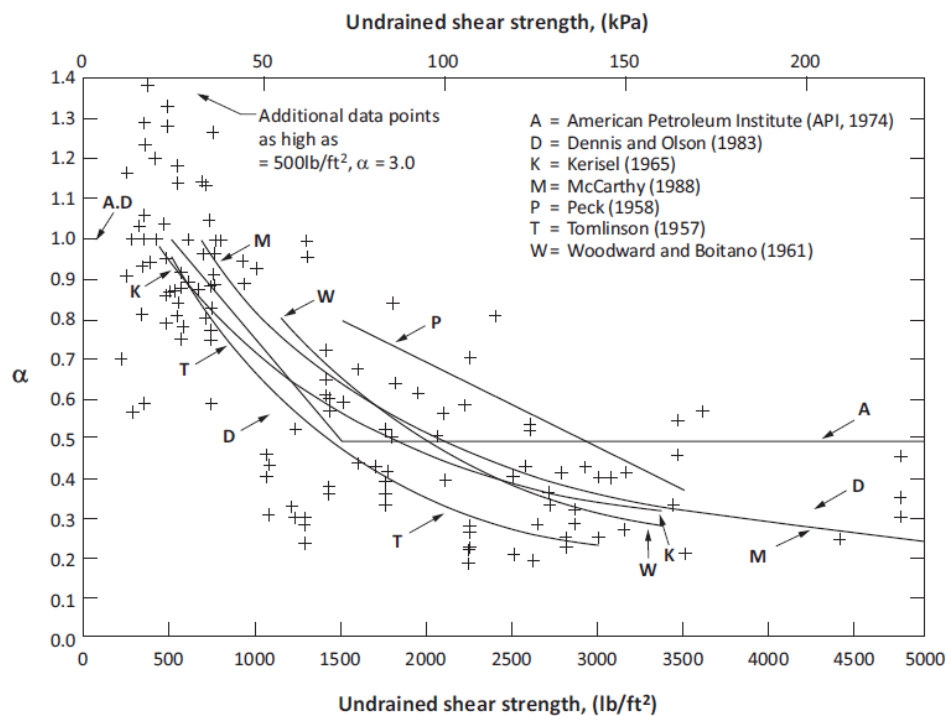
The total stress approach ( $\alpha$  method) links the average shaft resistance ( $P_s$ ) to the average undrained shear strength ( $S_u$ ) of the clay along the pile shaft through an adhesion factor ( $\alpha$ ) via the following general formula:

$$P_s = \alpha \cdot S_u \cdot A_s \quad (9)$$

Where:  $\alpha$  = adhesion factor, and

$A_s$  = the shaft surface area of the pile (i.e.,  $A_s$  = pile perimeter x pile length).

Several attempts have been made between 1950s and 1980s (e.g., Tomlinson 1957) on developing a correlation between the  $\alpha$  value and the  $S_u$  of the clay (Figure 3-7). Many of these initial correlations were developed from static load tests on un-instrumented piles driven through multiple soil strata with variable undrained strengths which resulted in considerable uncertainty in the estimated  $\alpha$  coefficient for a given site as could be seen in Figure 3-7 (Chow 1997).



**Figure 3-7. Variation of  $\alpha$  with  $S_u$  (excerpt from CHBDC, 2019)**

The CHBDC and the CFEM recommend obtaining the  $\alpha$  value based on Tomlinson (1957) method. However, it has been shown in literature that the shaft friction will depend not only on the  $S_u$  value but also on other factors such as pile stiffness, stress history of clay deposits, and clay plasticity (e.g., Kolk and van der Velde, 1996; Karlsrud et al., 2005; Karlsrud, 2012). In this research, the measured shaft resistance from the piles from

subject 50 MTO sites was compared to the predicted shaft friction obtained from four total stress ( $\alpha$ ) method as shown in Table 3-5. The  $\alpha$  value can be obtained as follows:

1- Tomlinson (1957): as per Figure 3-7.

2- Kolk and Van Der Velde (1996):

$$\alpha = 0.9 F_L \left( \frac{s_u}{\sigma_v} \right)^{-0.3} \quad (10)$$

Where  $F_L$  is the depth factor obtained from the following relationship:

$$F_L = \left( \frac{L-Z}{D} \right)^{-0.2} \quad (11)$$

Where  $L$  = depth from the surface to the pile tip,  $Z$  = depth from the surface to the point considered,  $D$  = outside diameter of pile.

3- NGI-05 (Karlsrud et al. 2005): as per Figure 3-8.

4- Karlsrud (2012): as per Figure 3-9.

**Table 3-5. Examined Total Stress ( $\alpha$ ) methods and Factors Considered in Each Method**

Method/Reference	Pile Length Effect	Stress History	Plasticity Index ( $I_p$ )	Shear Strength ( $s_u$ )	Effective Vertical Stress ( $\sigma_v$ )
Tomlinson (1957)	x	x	x	✓	x
Kolk and Van Der Velde (1996)	✓	✓	x	✓	✓
NGI-05 (Karlsrud et al. 2005)	x	✓	✓	✓	✓
Karlsrud (2012)	x	✓	✓	✓	✓

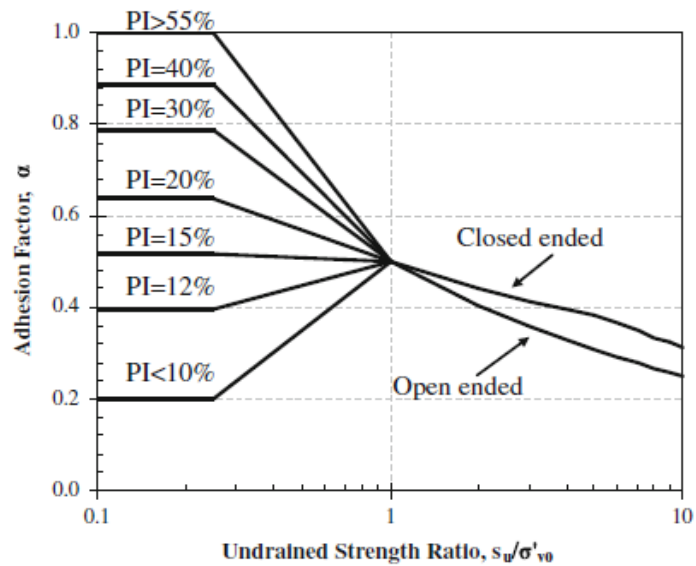


Figure 3-8. NGI-05 Pile Design Method (after Karlsrud et al. 2005)

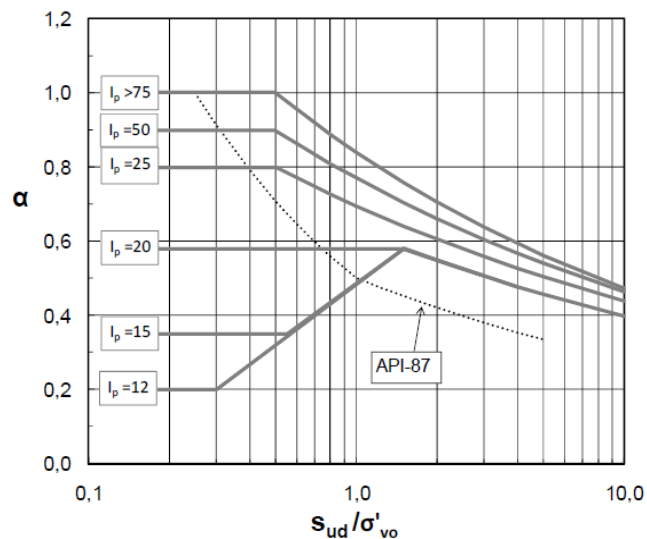


Figure 3-9. Proposed  $\alpha$  value as per Karlsrud et al. 2012

The effective stress approach ( $\beta$  method) assumes that the drained conditions prevail at the pile-soil interface resulting in the shaft friction being a function of the horizontal effective stress and the interface friction angle. Under this condition, the ultimate shaft resistance ( $P_s$ ) is computed via the following general formula:



$$P_s = k_s \cdot \tan(\delta) \cdot \sigma_v \cdot A_s = \beta \cdot \sigma_v \cdot A_s \quad (12)$$

Where:  $\beta$  = the shaft friction coefficient, and

$A_s$  = the shaft area of the pile (i.e.,  $A_s$  = pile perimeter x pile length).

The CFEM recommends a  $\beta$  value in the range of 0.25 to 0.32. The CHBDC recommends the following equation to compute the  $\beta$  value for driven piles (as per Meyerhof, 1976):

$$\beta = (1 - \sin \varphi) \tan(\delta) \cdot OCR^{0.5} \quad (13)$$

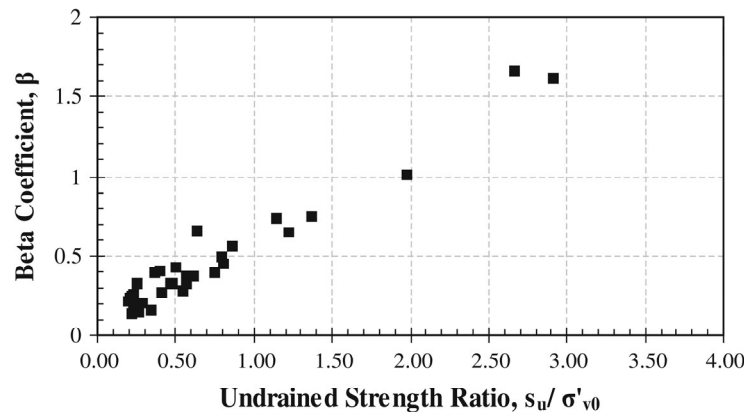
Where: OCR = the overconsolidation ratio

With more collected pile load test data, several attempts have been made after Meyerhof (1976) to better assess the  $\beta$  value. In this research, the measured shaft resistance of the piles from relevant MTO sites was compared to the predicted shaft friction obtained from four effective stress approach ( $\beta$  method; Table 3-6) as listed below:

- 1- Meyerhof (1976):  $\beta$  value to be computed as per equation 13.
- 2- Flaate and Selnes (1977): the following equation proposed to obtain the  $\beta$  value:

$$\beta = (0.3 \text{ to } 0.5) \cdot OCR^{0.5} \cdot \left( \frac{L+20}{2L+20} \right) \quad (14)$$

- 3- Burland (1993): as per Figure 3-10.



**Figure 3-10. Proposed  $\beta$  value as per Burland (1993)**

- 4- Karlsrud (2012): as per Figure 3-11.

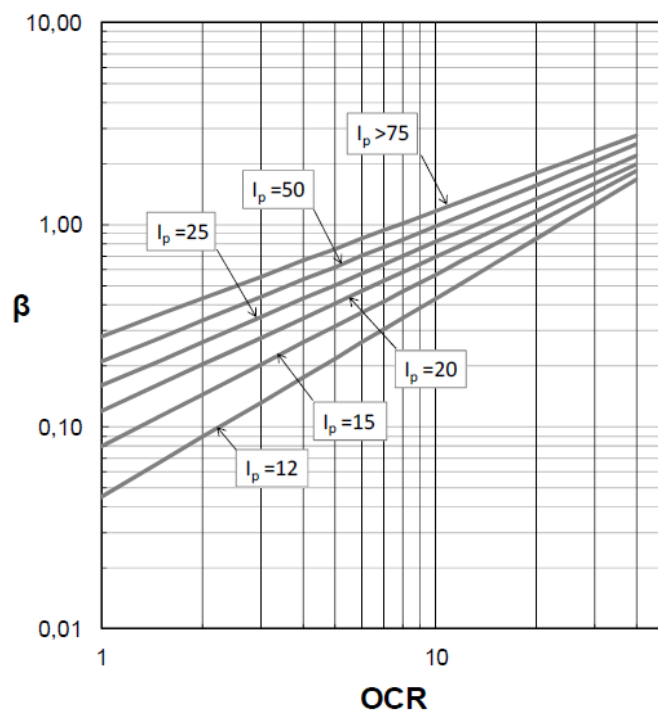


Figure 3-11. Proposed  $\beta$  value as per Karlsrud (2012)

Table 3-6. Examined Effective Stress Approach ( $\beta$  Method) and Factors Considered in Each Method

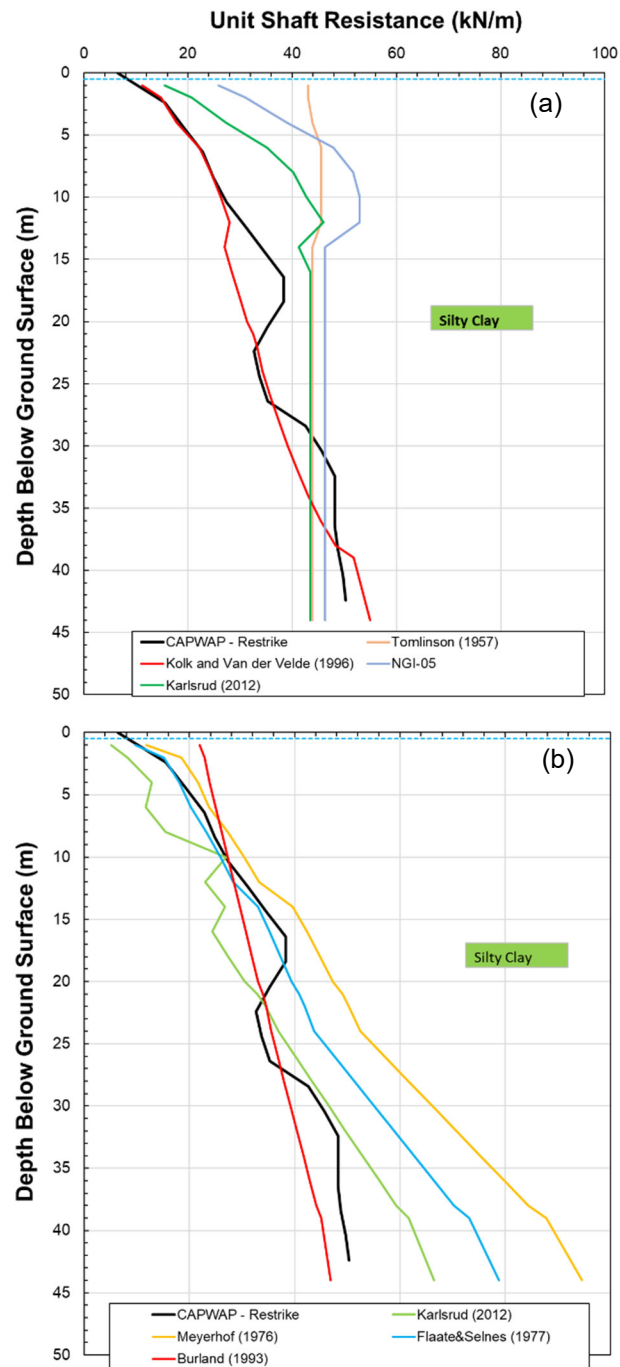
Method/Reference	Adhesion Factor ( $\delta$ )	Friction Angle ( $\phi$ )	Overconsolidation Ratio (OCR)	Effective Vertical Stress ( $\sigma_v$ )	Pile Length (L)	Shear Strength ( $S_u$ )	Plasticity Index ( $I_p$ )
Meyerhof (1976)	✓	✓	✓	✓	✗	✗	✗
Flaate and Selnes (1977)	✗	✗	✓	✓	✓	✗	✗
Burland (1993)	✗	✗	✓	✓	✗	✓	✗
Karlsrud (2012)	✗	✗	✓	✓	✗	✗	✓

The shaft resistance along all driven piles penetrated through cohesive soil layers at the subject MTO sites has been obtained using the  $\alpha$ -method (Equation 9) and  $\beta$ -method (Equation 12) using the methods listed in tables 3-4 and 3-5 for obtaining the  $\alpha$  and  $\beta$  values, respectively. For open ended piles (e.g., Steel H-piles), the shaft surface area was taken as the perimeter of the plugged section times the pile length, as long as ratio of the pile penetration depth to pile diameter is greater than 10, as per CHBDC (2019).

The following observations have been made based on the assessment of all Group-4 sites (36 pile load tests, Table 2-1):

- 1- There is no one method/approach that always gives the best match between the measured and predicted shaft resistance of piles driven through cohesive layers,
- 2- Out of the examined  $\alpha$ -methods, Kolk and Van Der Velde (1996) and Karlsrud (2012) provide the best match with the measured shaft resistance (Figure 3-12,a). The Tomlinson (1957) and NGI-05 typically overestimate the shaft capacity.
- 3- Out of the examined  $\beta$ -methods, Burland (1993) and Karlsrud (2012) provide the best match with the measured shaft resistance (Figure 3-12,b). Meyerhof (1976) and Flaate and Selnes (1977) typically overestimate the shaft capacity.
- 4- Based on the above, it is recommended that the ultimate shaft resistance of piles in contact with cohesive layers be estimated based on Kolk and Van Der Velde (1996), Burland (1993), and Karlsrud (2012;  $\alpha$  and  $\beta$  methods). The design value should be the minimum predicted resistance obtained from the aforementioned methods.

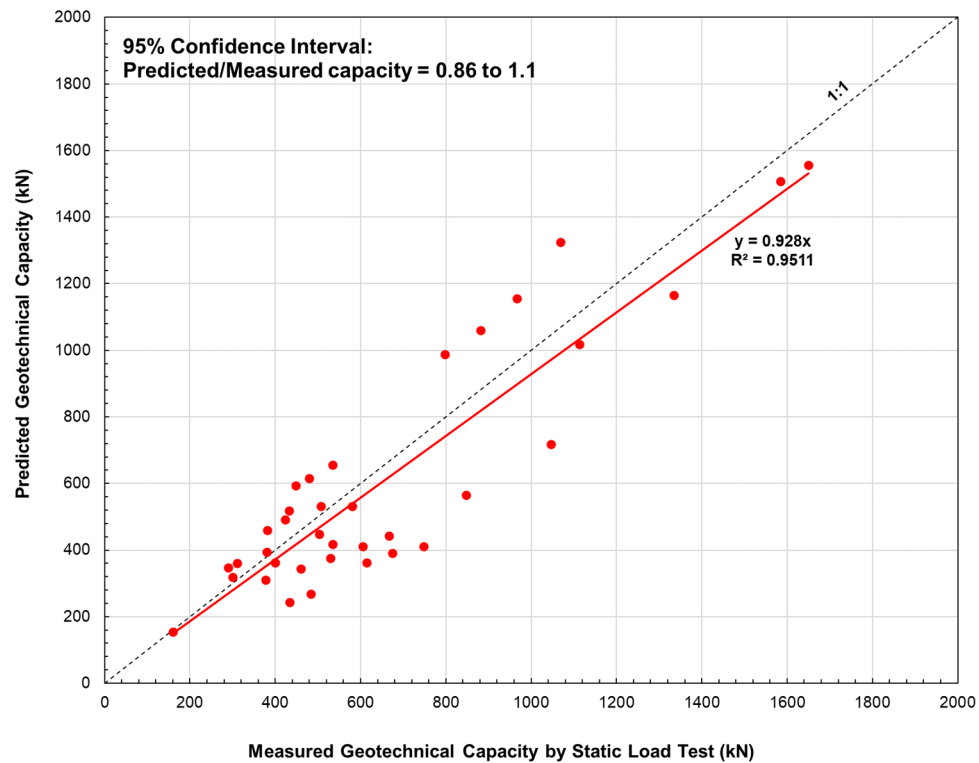
Using the above recommended approach for obtaining the shaft friction along piles in cohesive soils, the results of the predicted ultimate pile resistance matches well with the measured resistance as shown in Figure 3-13 for the Group-4 sites. In addition, the measured shaft resistance of piles penetrated through cohesive soils and tested in the MTO recent sites (where PDA and CAPWAP analysis carried out) were compared to the predicted shaft resistance assessed based on the aforementioned recommended approach (Table 3-7). A good match can be observed between the measured and predicted shaft resistances.



**Figure 3-12. Measured Unit Shaft Resistance Vs. Predicted Values for 44 m Long Test Pile – Blanche River Site using (a)  $\alpha$ -Method and (b)  $\beta$ -Method**

**Table 3-7. Measured Versus Predicted Shaft Resistance for Piles Driven Through Cohesive Soil Layers**

Site Group	Site Name	Soil Along Pile Length	Pile Length (m)	Measured Shaft Resistance (kN)	Predicted Shaft Resistance (kN)
Group 2	Hwy 400 - South Canal	Steel H-Pile [310x110] Penetrated through Clayey Silt soil	16.5	1568	1222
Group 2	HWY 401 - Fletcher's Creek	Steel H-Pile [310x110] Penetrated through Clayey Silt till	9.6	775	784
Group 4	Hwy 569- Blance River Bridge	Steel H-Pile [310x110] penetrated through firm Varved Clay	40.0	1607	1552



**Figure 3-13. Measured Versus Predicted Ultimate Geotechnical Resistance of Piles for Group-4 Sites**

To obtain the shaft resistance within the cohesive soils, the soil undrained shear strength ( $S_u$ ), Atterberg Limits, and OCR values shall be determined. The undrained shear strength can be determined through laboratory testing (e.g., Unconfined Compression Test or Unconsolidated Undrained Triaxial Test), or estimated based on empirical correlations with other soil parameters, such as the plasticity index or based on correlations with field tests such as CPT. The plasticity index values can be obtained via Atterberg Limits test. The OCR can be determined through laboratory testing (such as One-Dimensional Consolidation Test, etc.) or estimated based on correlations with field test results (e.g., CPT).

It's important to note that field and laboratory testing provide an accurate determination of soil properties, especially for critical engineering projects. However, empirical correlations can be used for preliminary assessments or when laboratory testing is not feasible.

### **3.3 Ultimate End Bearing Resistance in Cohesionless Soils**

The ultimate end bearing resistance of piles founded in cohesionless soil is typically expressed as:

$$P_b = q_b \cdot A_b = N_q \text{ (or } N_t) \cdot \sigma_v \cdot A_b \quad (15)$$

Where:

- $q_b$  = the ultimate unit end bearing resistance,
- $N_q$  and  $N_t$  = as defined by the CHBDC (2019) and the CFEM (2006), are the tip bearing capacity factor (see Table 3-8),
- $\sigma_v$  = the effective vertical stress at the level of the pile base, and
- $A_b$  = the resisting area.

As per Equation 15, it is expected that the ultimate end bearing resistance of piles in a uniform cohesionless deposit would increase linearly with the vertical effective stress (i.e., with depth). However, previous research (e.g., Kulhawy, 1984; Neely, 1988) showed that the end bearing resistance may continue to increase with depth but at a decreasing rate. This phenomenon is mainly due to the reduction in the peak friction angle of cohesionless soils with increasing confining pressure (Bolton, 1986). Thus, the value of the  $N_q$  or  $N_t$  is expected to decrease with depth. The effect of the reduction in the peak friction angle with depth on the ultimate end bearing resistance of piles in cohesionless soils has been

quantified by Fleming et. al (2009) and resulted in the design charts shown in Figure 3-14. In this method, the ultimate unit end bearing resistance is a function of the effective vertical stress ( $\sigma_v$ ), the effective critical state friction angle ( $\phi_{cv}$ ), and the uncorrected relative density of soil ( $I_D$ ) at the tip elevation of the pile.

**Table 3-8. Recommended values for  $N_q$  and  $N_t$  (extracted from CHBDC, 2019 and CFEM, 2006)**

**The values of for various  $\phi'$  values and pile types  
(after NAVFAC DM 7.2)**

$\phi$	26	28	30	31	32	33	34	35	36	37	38	39	40
$N_q$ (for driven piles)	10	15	21	24	29	35	42	50	62	77	86	120	145
$N_q$ (for bored piles)	5	8	10	12	14	17	21	25	30	38	43	60	72

*Range of  $N_t$  Factors*

Soil Type	Cast-in-Place Piles	Driven Piles
Silt	10 – 30	20 – 40
Loose sand	20 – 30	30 – 80
Medium sand	30 – 60	50 – 120
Dense sand	50 – 100	100 – 120
Gravel	80 - 150	150 - 300

For example, if the  $\sigma_v$  at the tip elevation of a pile is 200 kPa and the relative density at this level is 75%, then the  $q_b$  is anticipated to be 7 MPa if the  $\phi_{cv} = 27^\circ$  or 10 MPa if the  $\phi_{cv} = 30^\circ$  (see Figure 3-14). The value of the  $\phi_{cv}$  can be computed using the following equation:

$$\phi_{cv} = \phi' - 3 \cdot I_R \quad (16)$$

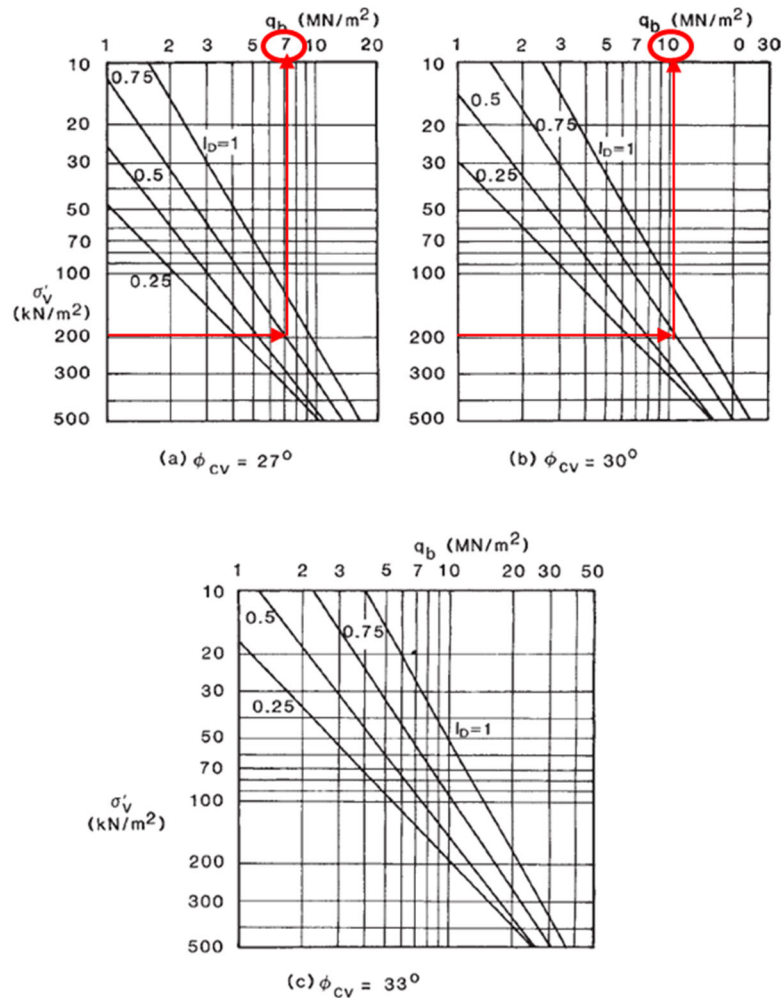
$$I_R = I_D \left[ 5.4 - \ln \left( \frac{p'}{p_a} \right) \right] - 1 \quad (17)$$

Where:  $\phi'$  = the effective friction angle,

$I_R$  = the corrected relative density,

$p'$  = mean effective stress level at the pile tip elevation ( $\sim \sqrt{\sigma_v \cdot N_q}$ ), and

$p_a$  = the atmospheric pressure.



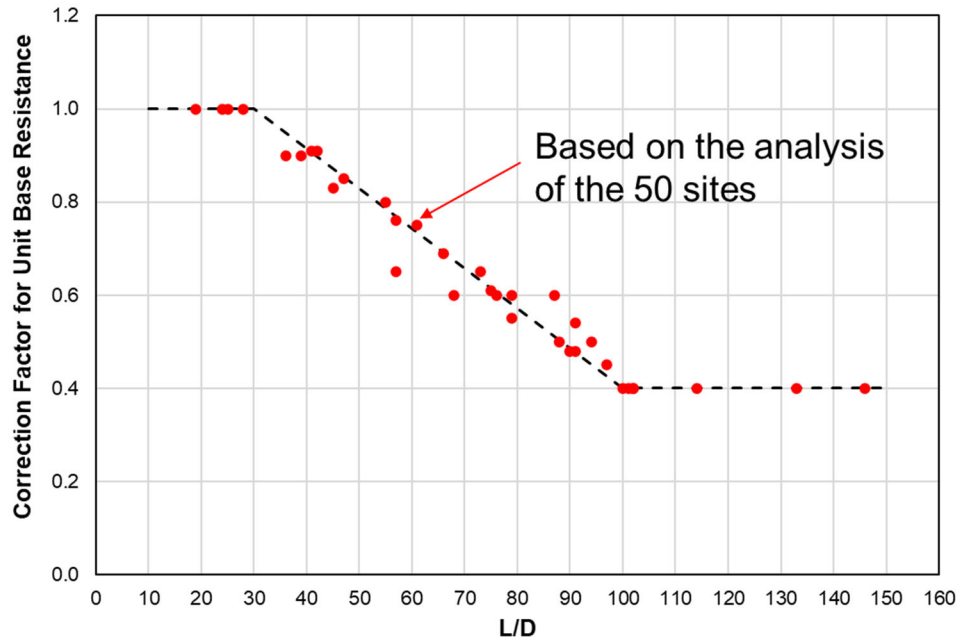
**Figure 3-14. Ultimate Unit End Bearing Resistance ( $q_b$ ) for Cohesionless Soils (excerpt from Fleming et al., 2009)**

The unit end bearing pressure values presented in Figure 3-14 are considered reasonable for displacement driven piles (e.g., closed pipe piles). For small displacement piles (e.g., H-piles), Fleming et al. (2009) suggested to multiply the  $q_b$  value obtain from Figure 3-14 by a correction factor of 0.8. However, based on the analyses of all subject MTO sites, a correction factor based on the Length over Diameter ( $L/D$ ) ratio is proposed in Figure 3-15.

For bored (non-displacement) piles, Fleming et al. (2009) suggested to multiply the  $q_b$  value obtain from Figure 3-14 by a correction factor of 0.5 to 0.7. This range seems to be



reasonable based on the assessment of the pile load test carried out on one large diameter caisson at one of the subject MTO sites (Site Group-6).



**Figure 3-15. Correction Factor for Ultimate Unit End Bearing Resistance for Open-Ended (Small Displacement) Driven Piles Rest on Cohesionless Soil**

Based on the above, it is recommended that the ultimate end bearing resistance of piles in cohesionless soil be taken as the minimum of the value obtained from Equation 15 (with using  $N_q$  as per CHBDC, 2019) and the value obtained for the Fleming et al. (2009) charts (Figure 3-14). The soil friction angle can be obtained as discussed in Section 3.1.

The measured end bearing resistance of piles with tip elevation within cohesionless soils and tested in the MTO recent sites (where PDA and CAPWAP analysis carried out) were compared to the predicted end bearing resistance assessed based on the aforementioned recommended approach (Table 3-9). A good match can be observed between the measured and predicted end bearing resistances.

**Table 3-9. Measured Versus Predicted End Bearing Resistance of Steel H-Piles (310 x110)  
Rest on Cohesionless Soil**

Site Type	Site Name	Soil Along Pile Length	Pile Length (m)	Measured Ultimate End Bearing Resistance (kN)	Predicted Ultimate End Bearing Resistance (kN)
Group 1	HWY 400 - 89	Very Dense Silt to Sandy Silt (lower deposit) followed by very stiff clayey silt layer	36.0	275	360
Group 1	HWY 400 - 89	"100-blow" clayey silt to silt and sand till	51.0	525	650
Group 2	Hwy 400 - South Canal	Very Dense Sand to Silt soil	16.5	500	690
Group 2	HWY 401 - Fletcher's Creek	Very Dense Sand to Silt till	9.6	1825	1480
Group 3	HWY 400 - Essa Rd.	Very Dense Silty Sand	31.6	950	955

### 3.4 Ultimate End Bearing in Cohesive Soils

As recommended by the CFEM (2006) and CHBDC (2019), the ultimate end bearing resistance of a pile founded in cohesive soil can be estimated based on the following equation:

$$P_b = q_b \cdot A_b = (S_u \cdot N_c + \sigma_v \cdot N_q + \frac{\gamma \cdot d}{2} N_\gamma) \cdot A_b \quad (18)$$

Where:

- $q_b$  = the ultimate unit end bearing resistance,
- $A_b$  = the resisting area,
- $d$  = the pile diameter or width,
- $S_u$  = the cohesion of soil within a distance of  $2d$  below the base,
- $\sigma_v$  = the effective vertical stress at the level of the pile base,
- $\gamma$  = the unit weight of soil, and
- $N_c$ ,  $N_q$ , and  $N_\gamma$  = the bearing capacity factors.



The drained end bearing resistance of piles in clay will be significantly larger than the undrained end bearing resistance. However, the drained end bearing resistance can only be achieved with large pile settlement which typically exceeds the design tolerance for foundation settlement. Therefore, the ultimate end bearing resistance of piles in clay is commonly computed for the undrained condition (i.e.,  $\phi = 0$ ) to limit the pile settlement. Under this condition, the ultimate end bearing capacity can be computed using the following equation:

$$P_b = S_u \cdot N_c \cdot A_b \quad (19)$$

The value of bearing capacity factor  $N_c$  is typically taken as 9 (Skempton, 1951). A lower  $N_c$  may be used where the pile tip is embedded a shallow distance in a strong clay layer underlying a weak layer. A linear interpolation between  $N_c$  of 6 for pile tip resting on the strong layer and  $N_c$  of 9 for pile tip embedded a minimum of 3 to 5 times pile diameter or width in the strong bearing stratum.

Based on the assessment of all pile load tests where piles were founded on cohesive layers (i.e., Groups 4 and 7 sites), we recommend using Equation 19 to obtain the ultimate end bearing capacity of piles rest on cohesive soils. The soil cohesion can be obtained as discussed in Section 3.2.

### **3.5 Ultimate Geotechnical Resistance for Piles Driven into Till**

The main factor impacting the estimation of the geotechnical capacity of piles is either the penetrated and founding deposits behave as cohesive or non-cohesive material. Therefore, the recommended design methods presented under Sections 3.1 to 3.4 of this report were found to be applicable for glacial till deposits.

The glacial till deposits are typically heavily overconsolidated. Therefore, obtaining the geotechnical design parameters (such as cohesion, friction angle, etc.) based on empirical correlations developed for “non-till” deposits may result in conservative design. Therefore, for relatively large projects, it is crucial to acquire the geotechnical design parameters through a comprehensive field and laboratory investigation program. This program should include activities like pressuremeter field testing, triaxial testing, and consolidation testing on undisturbed samples. By conducting these investigations, accurate and site-specific design parameters can be determined.

During the preliminary design stage or for projects with limited number of piles, it is possible to obtain design parameters using empirical correlations specifically developed for glacial till deposits (e.g., Cao et al., 2015, Long 2016). Additionally, information from field and laboratory testing conducted on glacial till and reported in relevant literature (e.g., Manzari et al., 2014) can also be utilized to inform the design process. This combination of empirical correlations and data from glacial till investigations will aid in developing reliable design parameters.

### **3.5.1 Geotechnical Capacity of Driven Piles into Till based on MSPT Correlations**

Previous researches have been carried out to obtain correlations between the unit shaft friction and unit end bearing of piles driven into intermediate geotechnical materials (IGM; such as very dense/hard glacial tills) with SPT values (e.g., Long 2016).

The proposed correlations presented in Long (2016) are based on modified SPT (MSPT) values. MSPT values are recorded during conventional standard penetration testing. However, instead of counting blows for every 6", MSPT records spoon penetration in inches for every 10 blows until a total count of 100 blows. MSPT value is taken as the slope of the linear portion of spoon penetration vs. blow counts curve and has the same unit of "blow per foot (bpf)" as the conventional SPT-N value. MSPT value is usually higher than the conventional SPT-N value because the spoon penetration per inch tends to decrease as blow count increases. However, conversion between the two is straightforward and most time the two can be equal. The report proposes  $MSPT = 1.27 \times SPT-N$ .

Given MSPT field procedure is not practiced in Ontario, conversion between MSPT and conventional SPT-N could be done as follows:

- If spoon penetration is less than 6", e.g., 100 blows for 4", then  $MSPT = SPT-N = 100/(4/12) = 300$  bpf
- If spoon penetration is between 6" and 12", e.g., 45-55/3" (100 blows for 9" penetration), then  $MSPT = 55/(3/12) = 220$  bpf (neglecting first 6")
- If spoon penetration is between 12" and 18", e.g., 20-30-50/3" (100 blows for 15"), then  $MSPT = 80/(9/12) = 106$  bpf (neglecting first 6")
- If spoon penetration is 18" or more, e.g., 25-35-40-50/4" (150 blows for 22"), then  $MSPT = SPT-N = 35+40 = 75$  bpf (neglecting first 6" and last 4")

Long (2016) obtained the capacity of piles driven into IGMs (or “100-blow” materials) based on analyzing the results of seven static load test and PDA/CAPWAP test results. Then, design recommendations for unit shaft friction and end bearing for piles driven into IGMs were developed as correlation with the MSPT. The correlations can typically be applied to IGMs with SPT-N over 50 bpf or UCS between 0.5 to 5 MPa (i.e.,  $S_u = 0.25$  to 2.5 MPa). The following correlations are proposed by Long (2016):

- Shaft Friction:  $f_s = 1.05 \cdot \text{MSPT}$  ( $\leq 100$  kPa) for cohesive material  
 $f_s = 45 \cdot (\text{MSPT})^{0.25}$  ( $\leq 150$  kPa) for cohesionless material
- End Bearing:  $q_t = 0.04675 \cdot \text{MSPT}$  ( $\leq 10$  MPa) for cohesive material  
 $q_t = 3.25 \cdot \text{MSPT}^{0.3}$  ( $\leq 15$  MPa) for cohesionless material

Similar correlations can be established for till materials in Ontario utilizing the PDA/CAPWAP and static load test results.

### **3.6 Geotechnical Resistance of Steel Piles Founded on Bedrock**

Piles driven to refusal on sound bedrock are typically designed as end bearing piles ignoring any shaft resistance that may be developed along the pile length. The prediction of the rock behaviour under axial loading condition is complex because the rock is typically brittle and its failure in shear is a function of both the intact rock properties (such as unconfined strength) and the nature of discontinuities in the rock mass. Due to this complexity, the design codes (such as CFEM, 2006, and CHBDC, 2019) either suggest using very conservative approaches for computing the pile capacity or suggest using engineering judgment and/or local experience.

#### **3.6.1 Piles Driven to Refusal on Sound Bedrock**

The surface of the sound bedrock at each site shall be defined by a professional geotechnical engineer via assessment of the field investigation results (e.g., drilled rock cores, televiwer, etc.). In general, the sound bedrock can be defined as the moderately weathered to fresh bedrock, with Rock Quality Designation (RQD) of greater than 75%, and Fracture Index (FI) less than 5 fractures/0.3 m (CFEM, 2006).

In general, the ultimate end bearing resistance of piles founded on sound bedrock can be computed as follows:

$$Q_{ult} = N_{cr} \cdot q_u \cdot A_b \quad (20)$$

Where:  $q_u$  = the unconfined compressive strength of rock,  
 $A_b$  = the resisting area of the pile section, and  
 $N_{cr}$  = parameter typically obtained based on fitting field and lab test results.

Suggested value for the  $N_{cr}$  has been provided in several previous research as shown in Table 3-10. The resisting area for the piles rest on shale bedrock can be assumed to be the plugged area of the pile section; whereas, the resisting area for piles rest on hard rock (e.g., granite) could be the steel area of the pile.

**Table 3-10. Recommended Value of the Parameter  $N_{cr}$  for Computing the Ultimate End Bearing Resistance of Driven Steel Piles Rest on Bedrock**

Reference	$N_{cr}$
Rehman and Broms (1971)	4 to 6
Pells and Turner (1978)	3.0
Goodman (1980)	$N\Phi + 1 = \tan^2(45+\Phi/2) + 1$ <p>Where <math>\Phi</math> is the friction angle of rock mass. Recommended values as shown in Table 3-11.</p>
Tomlinson (2004)	$2 N\Phi = 2 \cdot \tan^2(45+\Phi/2)$
Morton (2012)	7.5

**Table 3-11. Recommended Value of Friction Angle of Rock Mass (excerpt from Tomlinson 2004)**

Classification	Type	Friction angle (degrees)
Low friction	Schists (high mica content)	20 to 27
	Shale	
	Marl	
Medium friction	Sandstone	27 to 34
	Siltstone	
	Chalk	
	Gneiss	
	Slate	
High friction	Basalt	34 to 40
	Granite	

The ultimate capacity of the eight piles driven to bedrock at the MTO sites listed in Table 3-12 have been assessed based on the results of the static pile load test. Issues have been reported for 7 out of the 8 pie load tests as shown in Table 3-12 (e.g., failure in reaction pile system) which result in unrealistic assessment for the pile capacity. The only site where pile load test done with no known issues is the one at Hwy 417-Ramsayville site.

Based on the analysis of the pile load test at HWY 417-Ramsayville site, the ultimate geotechnical resistance of rock is interpreted to be 6410 kN (as per Modified Chin Method). However, the test has been terminated at 4350 kN as the pile material was almost at yield. Therefore, the ultimate resistance of the pile was mainly governed by the structural capacity of the pile material. The ultimate geotechnical capacity of the steel H-pile at HWY 417-Ramsayville site obtained using Equation 20 and  $N_{cr}$  value of 7.5 is estimated to be 6970 kN, which matches well with the interpreted geotechnical resistance from the pile load test. Therefore, the ultimate geotechnical resistance of piles driven to sound bedrock is recommended to be estimated using Equation 20 and  $N_{cr}$  value of 7.5.

The unconfined compressive strength of rock can be obtained by conducting laboratory unconfined compressive strength tests.

**Table 3-12. Pile Load Test of Piles Driven to Bedrock at MTO Sites**

Site Name	Pile Type	Rock Type	Pile Length (m)	Maximum Applied Load During the PLT (kN)	Maximum Measured Settlement (mm)	Interpreted Geotechnical Resistance based on the Modified Chin Method (kN)	Predicted Geotechnical Resistance using Morton (2012) Method (kN)	Notes
HWY 417 - Ramsayville	Steel HP 310x110	Shale	50.0	4350	70 mm	6410	6970	-
HWY 401 - Third Line (Bainsville)	Steel HP 310x79	Limestone	12.6	1960	25 mm	2778	5610	failure in reaction pile system
Site 9: HWY 403 at King and Main Street Interchange (1961)	Steel Tube 324 mm OD x 6.3 mm [Filled with concrete]	Shale	21.3	1778	10 mm	2222	6180	failure not reached
Site 9: HWY 403 at King and Main Street Interchange (1961)	14BP73	Shale	21.3	1778	10 mm	2199	6970	failure not reached
Site 17: HWY 401 Basket Weave Bridges Between Keele & Jane St. (1963)	Steel HP 310x110	Shale	26.5	2669	80 mm	2904	6970	Most likely tip of the pile is at the till above the sound bedrock
Site 30: E.C. Row Expressway And C. & O. Railway (1974)	steel tube 324 OD x 6.3 mm thick (concreted filled)	Limestone	40.0	3559	55 mm	5241	3540	failure not reached
Site 37: Q.E.W. and Burlington Skyway (1982)	HP 310 x 79	Shale	39.3	2313	30 mm	NA	5700	failure not reached
Site 37: Q.E.W. and Burlington Skyway (1982)	HP 310 x 79	Shale	38.7	2313	30 mm	NA	5700	failure not reached

### 3.6.2 Piles Driven to Refusal within Fractured Bedrock

Designing driven piles that rest on weathered fractured rock (i.e., highly weathered rock with RQD less than 75% and FI greater 5 fractures/0.3 m) presents significant complexity. The highly weathered and fractured rock formations may exhibit variations in strength, degree of weathering, joint orientations, clay infill thickness, etc.; making it difficult to accurately assess the pile's performance and ultimate capacity. Therefore, achieving a





successful design in these circumstances necessitates a comprehensive understanding of the rock mass behavior alongside with the observation of the pile penetration during the pile installation to achieve the target set condition/refusal criteria.

The preliminary capacity of driven piles penetrated through and founded on the weathered bedrock can be assessed using Equation 20 with  $N_{cr}$  value obtained based on Goodman (1980) (i.e.,  $N_{cr} = \tan^2(45+\Phi/2) + 1$ ). The value of the rock mass friction angle can be obtained from Figure 3-16 based on the rock mass condition (represented by the Geological Strength Index, GSI, and the rock mass strength factor,  $m_i$ ).

The GSI and  $m_i$  values can be obtained from Table 3-13 and Table 3-14, respectively.


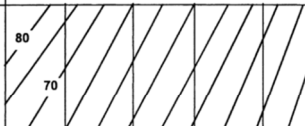




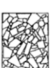
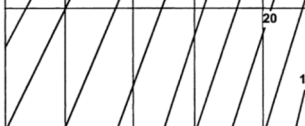
The effect of pile penetration into the fractured rock has been assessed by Ladanyi and Roy (1971) where they proposed a depth factor =  $1+0.5 \times (\text{penetration depth into the fractured rock/pile width}) \times \cos(\Phi)$ . Therefore, the geotechnical capacity can be expected to increase with increasing the penetration depth into the fractured rock.

For example, the ultimate geotechnical capacity of steel H-pile 310X110 driven to fractured shale with GSI of 35% and UCS of 10 MPa can be obtained as following:

- The rock mass strength factor ( $m_i$ ) = 6 [Table 3-14]
- Rock mass friction angle =  $22^\circ$  [Figure 3-16]
- $N_{cr} = \tan^2(45+\Phi/2) + 1 = 3.2$
- $Q_{ult} = N_{cr} \times q_u \times A_b = 3.2 \times 10,000 \times 0.09548 = 3,050 \text{ kN}$ .
- Factored geotechnical resistance =  $0.4 \times 3,050 = 1,220 \text{ kN}$ .

In the example above, the factored geotechnical resistance is estimated to be 2,000 kN if the tip of the pile is advanced into the fractured rock by about 450 mm.

**Table 3-13. Characterization of Rock Masses on the Basis of Interlocking and Joint Alteration (Hoek and Brown, 1998)**

Geological Strength Index		Surface conditions	
<p>From the description of structure and surface conditions of the rock mass, pick an appropriate box in this chart. Estimate the average value to the Geological Strength Index (GSI) from the contours. Do not attempt to be too precise. Quoting a range of GSI from 36 to 42 is more realistic than stating that <math>GSI = 38</math>. It is also important to recognize that the Hoek-Brown criterion should only be applied to rock masses where the size of individual blocks is small compared with the size of the excavation under consideration.</p>		<p>Very good Very rough and fresh unweathered surfaces</p> <p>Good Rough, maybe slightly weathered or iron stained surfaces</p> <p>Fair Smooth and/or moderately weathered and altered surfaces</p> <p>Poor Sticksided or highly weathered surfaces or compact coatings with fillings of angular fragments</p> <p>Very poor Sticksided and highly weathered surfaces with soft clay coatings or fillings</p>	
Structure		Decreasing surface quality →	
 <p>Blocky – very well interlocked undisturbed rock mass consisting of cubical blocks formed by three orthogonal discontinuity sets</p>			
 <p>Very Blocky – interlocked, partially disturbed rock mass with multifaceted angular blocks formed by four or more discontinuity sets</p>			
 <p>Blocky/disturbed – folded and/or faulted with angular blocks formed by many intersecting discontinuity sets</p>			
 <p>Disintegrated – poorly interlocked, heavily broken rock mass with a mixture of angular and rounded rock pieces</p>			
	Decreasing interlocking of rock pieces ↓		

**Table 3-14. Values of  $m_i$  for intact rock group (Hoek, 2007)**

Texture			
Coarse	Medium	Fine	Very fine
Sedimentary rock types			
Conglomerates (21 ± 3)	Sandstone (17 ± 4)	Siltstone (7 ± 2)	Claystone (4 ± 2)
Breccia (19 ± 5)		Greywacke (18 ± 3)	Shales (6 ± 2)
Crystalline limestone (12 ± 3)	Sparitic limestone (10 ± 2)	Micritic limestone (9 ± 2)	Dolomites (9 ± 3)
			Chalk (7 ± 2)
Metamorphic			
Marble (9 ± 3)	Hornfels (19 ± 4)	Quartzite (20 ± 3)	
	Metasandstone (19 ± 3)		
Migmatite (29 ± 3)	Amphibolite (26 ± 6)		
Gneiss (28 ± 5)	Schist (12 ± 3)	Phyllite (7 ± 3)	Slate (7 ± 4)
Igneous			
Granite (32 ± 3)	Diorite (25 ± 5)		
Granodiorite (29 ± 3)			
Gabbro (29 ± 3)	Dolerite (16 ± 5)		
Norite (20 ± 5)			
Porphyrite (20 ± 5)		Diabase (15 ± 5)	Peridotite (25 ± 5)
	Rhyolite (25 ± 5)	Dacite (25 ± 3)	Obsidian (19 ± 3)
	Andesite (25 ± 5)	Basalt (25 ± 5)	
Agglomerate (19 ± 3)	Breccia (19 ± 5)	Tuff (13 ± 5)	

### **3.6.3 Piles Driven into Completely Weathered Bedrock (Residual Soil)**

As observed by the pile load tests carried out at HWY 401 basket weave bridges site (Site No. 17), the geotechnical capacity of the driven piles founded within the completely weathered bedrock (i.e., residual soil) can be much smaller than that for piles fully driven to rest on the sound bedrock. Therefore, the PDA results shall be properly assessed to verify whether the pile is resting on the sound bedrock.

The geotechnical capacity of piles driven to refusal within the completely weathered bedrock can be obtained using the design methodologies for piles driven into till, as presented in Sections 3.5 of this report. The pile geotechnical capacity shall be estimated considering that the entire thickness of completely weathered bedrock will act like soil with both cohesive and cohesionless behaviour.

### **3.7 Geotechnical Resistance of Rock Sockets**

Three piles load tests were carried out at one of the MTO sites (i.e., Site 27, HWY 401 and Airport Road). The tests were carried out on 0.59 m to 0.64 m diameter cast-in-place concrete caissons socketed into sound shale bedrock. The socket length for the three tested piles varies between 0.9 m and 1.4 m. The ultimate capacity of the rock sockets results from a combination of the rock socket shaft resistance and the end bearing resistance. The values of the shaft resistance and end bearing resistance are sensitive to the construction means and methods and the level of base cleaning to minimize presence of sediment between the load bearing rock and the concrete at the base of the caissons. The ultimate unfactored end bearing resistance can be assessed using the following equation (CFEM, 2006):

$$P_b = q_b \cdot A_b = (q_u \cdot 3 \cdot K_{sp} \cdot D_F) \cdot A_b \quad (21)$$

Where:

- $q_b$  = the ultimate unit end bearing resistance,
- $A_b$  = the resisting base area,
- $q_u$  = the unconfined compressive strength of the intact rock core,
- $K_{sp}$  = empirical factor that depends on the spacing between discontinuities within the rock mass, and
- $D_F$  = the depth factor ( $=1+0.4 L_s/D_s \leq 3$ ; where  $L_s$  is the rock socket length and  $D_s$  is the rock socket diameter).

The ultimate peak shaft resistance can be assessed using the following equation (CFEM, 2006):

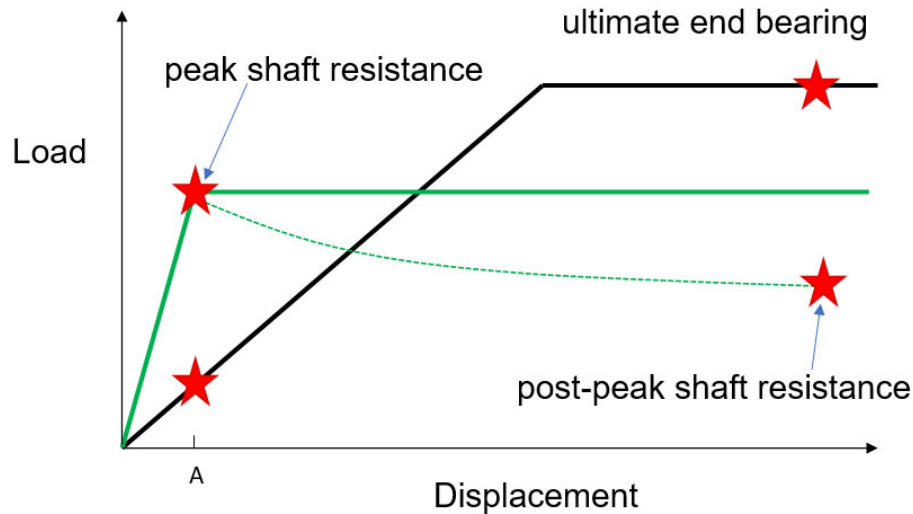
$$P_s = q_s \cdot A_s = a (q_u)^b \cdot \pi \cdot D_s \cdot L_s \quad (22)$$

Where:

- $q_s$  = the ultimate average peak unit shaft resistance,
- $A_s$  = the resisting area,
- $q_u$  = the unconfined compressive strength of the intact rock core (MPa),
- $L_s$  = the rock socket length,
- $D_s$  = the rock socket diameter, and
- $a$  and  $b$  = curve fitting parameters with value of 0.2 and 0.5, respectively (Horvath and Kenney, 1979), for the preliminary design. A statistical analysis using  $a$  and  $b$  values from other publications is recommended to be carried out.

It is known that the rock-concrete ultimate shaft friction resistance can be mobilized at relatively small displacement compared to the ultimate end bearing resistance (Figure 3-16). After reaching the peak shaft resistance, the rock-concrete shaft interface friction undergoes a reduction in the post-peak stage. Therefore, when both shaft and end bearing resistances are to be considered for estimating the socket capacity, adding the ultimate end bearing and peak shaft resistance (as per Equation 21 and 22) will result in an overestimation of the rock socket capacity as the ultimate end bearing and the peak shaft resistance do not occur at the same level of deformation. Therefore, the rock socket capacity should be the greater of the following two values:

- i- peak shaft resistance plus the portion of the end bearing mobilized at the corresponding level of deformation (e.g., deformation at point A; Figure 3-17),
- ii- Ultimate end bearing resistance + post-peak shaft resistance.



**Figure 3-17. End bearing and shaft resistance of rock socket as function of socket displacement**

Determination of the portion of end bearing resistance corresponding to the peak shaft resistance can be computed as described in Section 18.6.5 of the CFEM (2006). For the initial stage of design, the ratio of the peak to the post-peak rock-concrete shaft resistance may be obtained using the relationship shown in Figure 3-18. It should be noted that the behaviour of the shaft resistance of the rock-concrete interface depends on the rock and concrete properties. Therefore, it is highly recommended to obtain the value of the peak and post-peak shaft resistance based on laboratory direct shear tests carried out on rock-concrete specimens prepared using rock core samples and concrete samples with similar properties (e.g. compressive strength) to the concrete that will be used for the construction of the production caissons.

The measured ultimate geotechnical resistance of rock sockets obtained from the pile load tests at the subject MTO sites and the ultimate geotechnical resistance predicted by the aforementioned recommendations are shown in Table 3-15. A reasonably good match could be seen between the measured and predicted values.

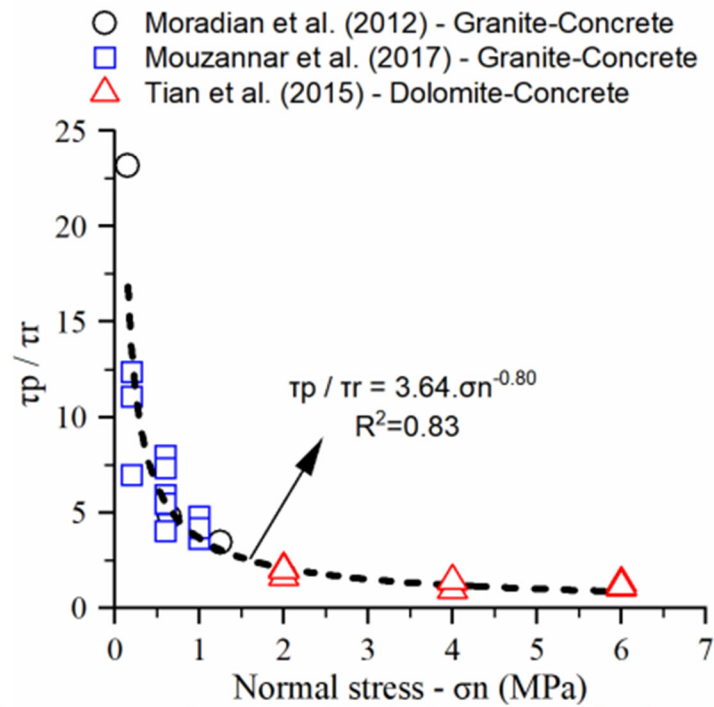


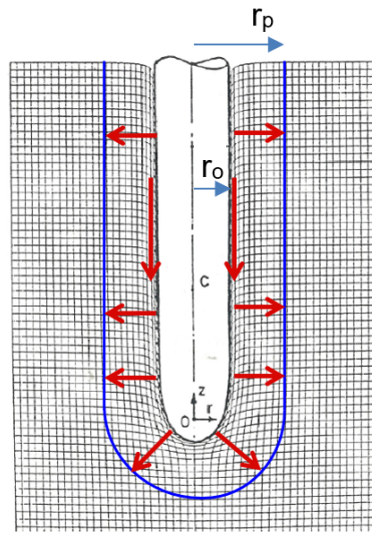
Figure 3-18. Relationship between peak and post peak shear stress as function of the normal stress of the rock-concrete interface (excerpt from Vizini and Futai, 2019)

Table 3-15. Pile Load Test of Rock Sockets at MTO Sites

Site Name	Soil Along Pile Length	Pile Type	Design Founding Stratum	Rock socket length (m)	Measured Unfactored Ultimate Geotechnical Resistance (kN)	Predicted Unfactored Ultimate Geotechnical Resistance (kN)
Site 27: HWY 401 and Airport Road	rock socket	0.64 m dia. cast in place concrete	Shale bedrock	0.9	4450	4892
		0.59 m dia. cast in place concrete		1.4	4450	5382
		0.64 m dia. cast in place concrete		1.0	4450	5222

#### 4. STRENGTH GAIN

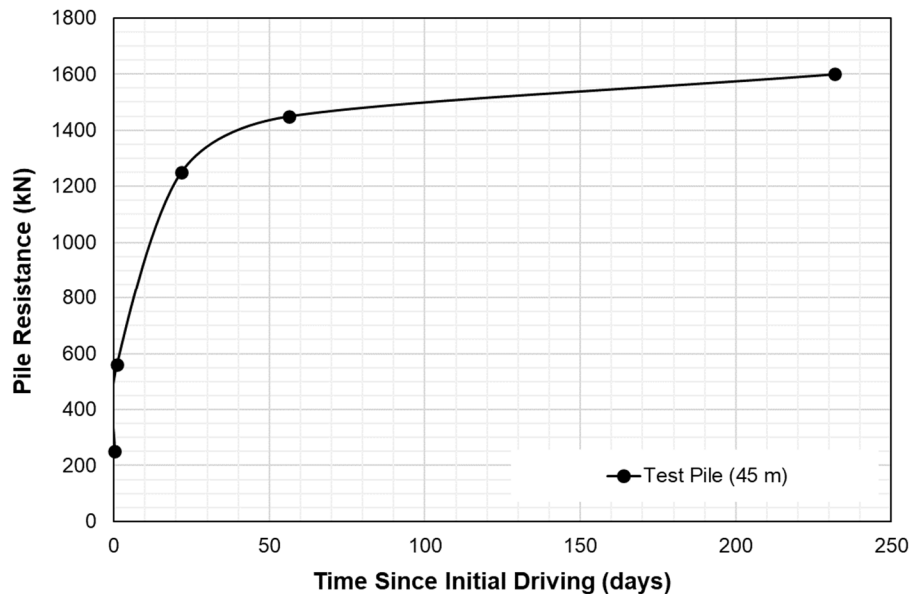
Piles driven through cohesive soil layers induce relatively high excess pore water pressure in the zone around the pile shaft and below the tip of the pile due to the consolidation and/or the shearing of the soil at the pile/soil interface (Figure 4-1). This results in increase in the geotechnical resistance of pile with time as driving induced excess pore pressure around the pile dissipates, which can take several months based on the soil characteristics and the pile type and dimensions.



**Figure 4-1. Soil Movement During Driving of Pile (adopted from Baligh, 1985)**

One of the clear examples of the strength gain is the increase in the geotechnical capacity of the driven steel H-pile 310X110 through the firm to stiff clay at the Highway 569-Blanche River Bridge site (Figure 4-2). The measured pile resistance at the end of initial driving was 250 kN. After two months, the pile capacity increased to 1450 kN; as measured by static pile load test. After 7 months, the pile capacity was measured by a static pile load test to be 1600 kN.





**Figure 4-2. Change in Pile Resistance with Time for 310x110 Steel H-pile Driven through Stiff Clay Soil at the Highway 569-Blanche River Site.**

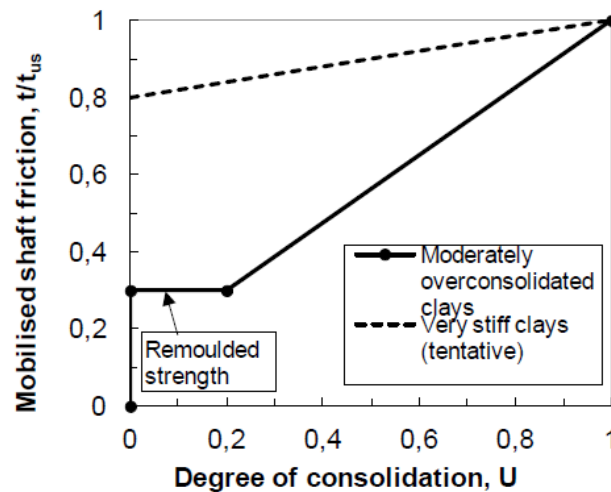
There are several factors contributing to the increase in the geotechnical resistance of driven piles through clay soils. The main two factors are:

- 1- The classical effect of the re-consolidation, which is mainly the increase in the radial effective stress in the clay surrounding the pile shaft due to the dissipation of the excess pore water pressure generated during the driving of the pile, and
- 2- The long-term aging effect, which starts near the end of re-consolidation phase due to the potential enhancement of the chemical bonding between the clay particles and/or further increase in the mean effective stress due to creep effects.

Analytical approaches (such as the Capacity Expansion Method and the Strain Path Method) have been developed over the last decades to predict the change in the stress and strain conditions caused by driving of piles and therefore predict the change in the geotechnical resistance with time. However, such analytical methods require going through complicated mathematical computations with several assumptions and simplifications that impact the accuracy of the assessment of the change in resistance with time.

#### 4.1 Effect of Re-consolidation

NGI (2013) proposed a simplified semi-empirical approach to predict the change in the pile capacity with time during the re-consolidation phase. The approach was developed based on testing the axial capacity of 406 mm to 508 mm diameter, 10 m to 23.6 m long, piles driven through low to medium plastic, normally consolidated to over-consolidated clay soil/till at six different sites. The piles were tested 1, 2, 6, 12, and 24 months after installation. Based on that, the change in the shaft resistance with the degree of consolidation was developed as shown in Figure 4-3. The plot presents the change in the shaft resistance ratio (i.e., the ratio of the mobilized shaft resistance at a specific point in time to the ultimate shaft resistance computed as per Section 3.2) as a function of the degree of consolidation (U).



**Figure 4-3. Build-up of the Shaft Friction During the Re-consolidation Phase (excerpt from NGI-2013)**

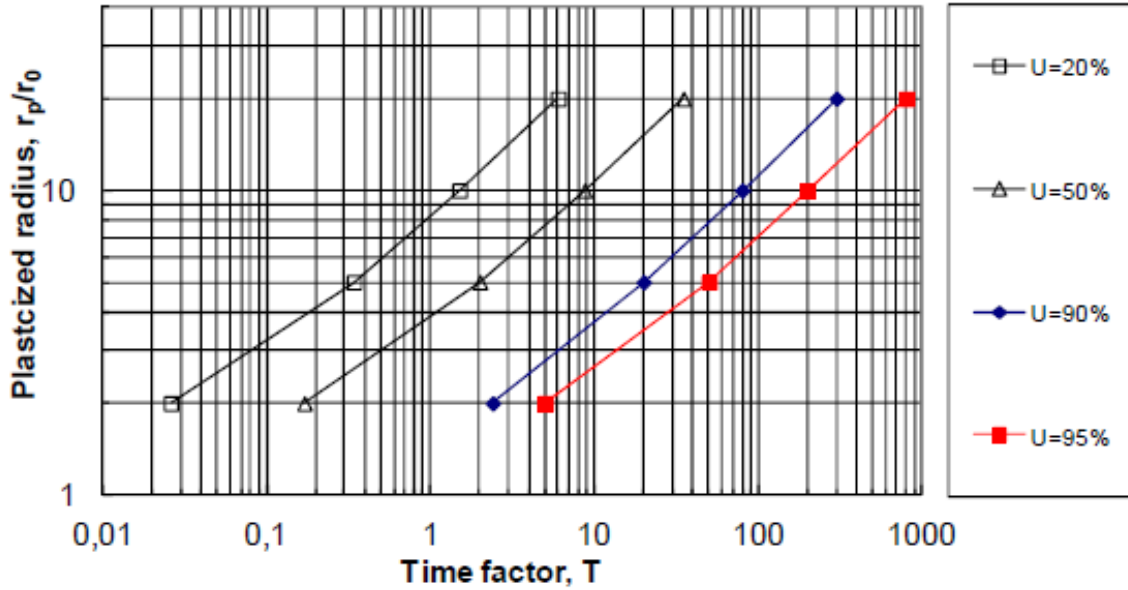
The time required to reach a specific degree of consolidation Time (U%) can be computed as following:

$$Time (U\%) = T(U\%) \cdot \frac{(r_o)^2}{c_h} \quad (23)$$

Where:  $T(U\%)$  = time factor as a function of degree of consolidation, (see Figure 4-4)

$r_o$  = pile radius or half the pile width

$c_h$  = horizontal coefficient of consolidation



**Figure 4-4. Time Factor Values at Different Degrees of Consolidation (excerpt from Karlsrud, 2012)**

The normalized plasticized radius shown in Figure 4-4 ( $r_p/r_o$ ; see Figure 4-1) can be computed as following:

$$\frac{r_p}{r_o} = \left( \frac{G_{50}}{s_u} \right)^{0.5} \cdot \left[ \frac{r_o^2 - r_{ie}^2}{r_o^2} \right]^{0.5} \quad (24)$$

Where:  $G_{50}$  = secant shear modulus at 50% mobilization of the undrained shear strength.  
Typical range of the normalized  $G_{50}/s_u$  is shown in Figure 4-5.

$r_{ie}$  = equivalent internal pile radius (e.g., for unplugged piles =  $r_o - t$ ; where  $t$  is the wall thickness of the pile)

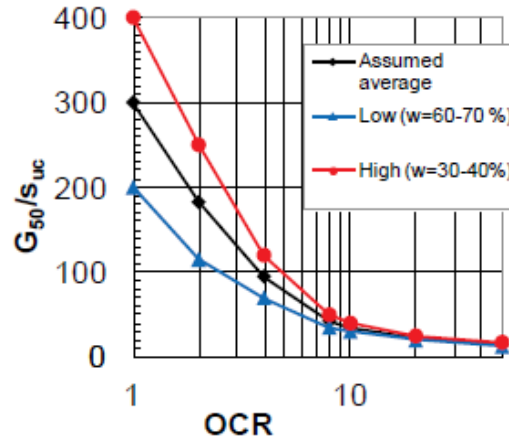


Figure 4-5. Typical Range of Normalized  $G_{50}/S_u$  (excerpt from Karlsrud, 2012)

#### 4.2 Effect of Long-term Aging

NGI (2000) proposed the following equation to consider the increase in the pile capacity after the end of the re-consolidation phase:

$$Q(t) = Q(100) \cdot [1 + \Delta 10 \cdot \log_{10}(\frac{t}{100})] \quad (25)$$

Where:

$$\Delta 10 = 0.1 + 0.4 \left(1 - \frac{Ip}{50}\right) \cdot OCR^{-0.8}$$

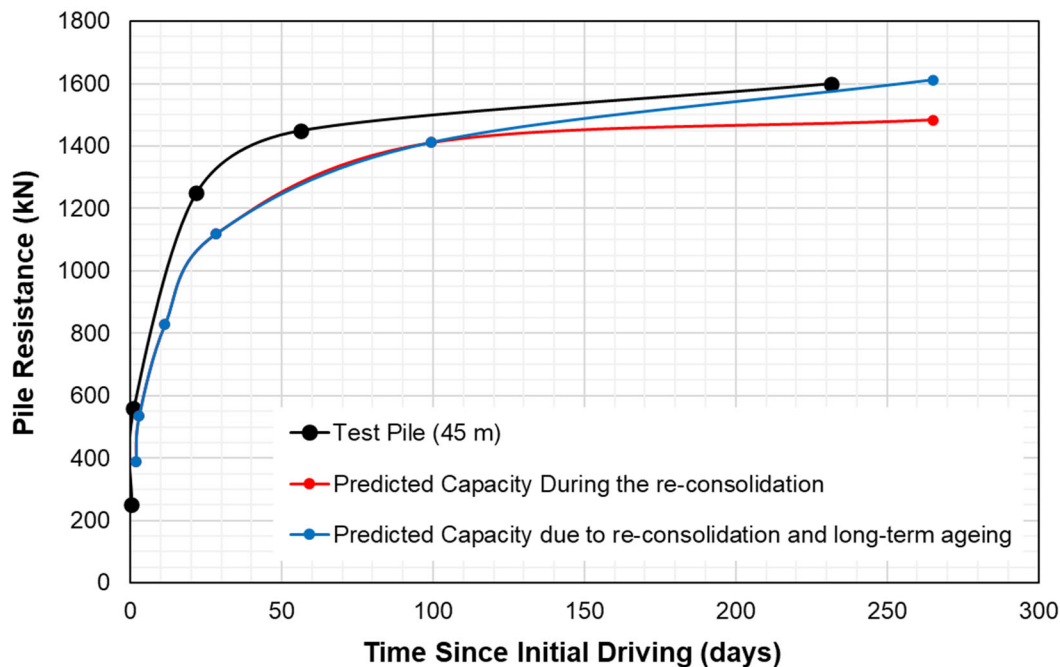
t = time in days after the pile installation

Q(100) = capacity of the pile after 100 days or the end of the re-consolidation phase,

Q(t) = capacity at a later time

#### 4.3 Comparison with Measured Change in Pile Capacity

The change in the pile capacity with time during the re-consolidation phase and the long-term ageing described above has been assessed for the pile load test carried out at the Highway 569- Blanche River Site. The predicted change in the geotechnical axial capacity with time using the NGI method with the measured axial capacity at different points of time are plotted in Figure 4-6. Good match could be seen between the measured and predicted change in the axial pile capacity with time.



**Figure 4-6. Measured vs. Predicted Change in Pile Resistance with Time for 310x110 Steel H-pile Driven through Stiff Clay Soil at the Highway 569-Blanche River Site.**

The change in the axial pile capacity with time in 20 MTO sites are summarized in Table 4-1. The following observations can be made on the measured axial capacity with time:

- i. The significant portion of the change in the pile capacity with time take place during the first two month after pile installation,
- ii. The strength gain is anticipated to be negligible for short piles (< 10 m long),
- iii. Field observations have shown that the axial capacity of piles driven through stratified soil layers (i.e., alternating cohesive and non-cohesive layers) can increase with time by up to 35% (note: same observation reported by Chow et al., 1998). Fleming et. al (2009) explained that this increase may be due to corrosion at the pile-soil interface or relaxation of the arching of highly stressed sand surrounding the pile. However, it is recommended not to consider this increase in the design of piles penetrated through stratified layers as the increase in the shaft capacity may be brittle (i.e., reduces rapidly with the pile movement).

- iv. The strength gain can be also observed for pile penetrated through fine sand and silt deposits. The strength gain under such subsurface condition shall be assessed based on conducting PDA tests at different point of time as discussed in Section 5.

**Table 4-1. Strength Gain Observation for All Relevant MTO Sites**

Site Group	Site Name	Soil Along Pile Length	Pile Type	Design Founding Stratum	Pile Length (m)	Strength Gain Observation
Group 1	HWY 400 - 89	Steel H-Pile penetrated through stratified deposits [stiff to hard clayey silt, hard clayey silt till]	Steel HP 310x110	Very Dense Silt to Sandy Silt (lower deposit) followed by very stiff clayey silt layer	36 to 51 m	Based on PDA only: 0% to 35% increase after 7 days of initial driving. Based on PDA and SLT: 40% to 60% increase after 33 days of driving
Group 2	Hwy 400 - South Canal	Steel H-Pile [310x110] Penetrated through soft to very stiff Clayey Silt	Steel HP 310x110	Very Dense Sand to Silt soil	16.5	Based on PDA only: 0% to 14% increase after 6 days of initial driving. Based on PDA and SLT: 80% increase after 9 months of driving
Group 2	HWY 401 - Fletcher's Creek	Steel H-Pile [310x110] Penetrated through very soft to firm clayey silt and firm to hard Clayey Silt till	Steel HP 310x110	Very Dense Sand to Silt till	9.6	Based on PDA and SLT: 18% increase after 5 months of driving
Group 7	Site 19: HWY 50 and North Creek	Timber pile penetrated through stratified deposits [cfirm to stiff clayey silt]	Timber Size 36 (treated Timber) [Butt f = 356 mm , tip f = 203 mm]	Firm to stff silty clay to clayey silt	13.7	Based on SLT: increase by 8% in the first day followed by no increase
Group 4	Hwy 569- Blance River Bridge	Steel H-Pile [310x110] penetrated through firm Varved Clay	Steel HP 310x110	Firm Varved Clay	40.0	Based on PDA and SLT: Rapid increase during the first 2 month (capacity increase by 600% ) followed by a slower rate of increase for up to 1.6 years (capacity increased by 700%).
Group 4	Site 10: HWY 11 and O.N.R.	Drivem Timber Pile penetrated through firm to stiff silty clay soil	Timber Size 32 (untreated Timber) [Butt f = 324 mm , tip f = 197 mm]	Firm to Stiff Silty Clay	15.1	Based on SLT: 40 to 50% % increase in the capacity after 2 months followed by no increase.
Group 4	Site 18: HWY 624 and Blanche River	Timber pile penetrated through very stiff to firm silty clay	Timber Size 30 (treated Timber) [Butt f = 305 mm , tip f = 203 mm]	Firm varved clay	12.5	Based on SLT: rapid increase by 30 to 300% in the first 2 month followed by no increase.
Group 4	Site 23: HWY 401 and Country Road 14	Timber pile penetrated through very stiff to hard silty clay	Timber Size 36 (treated Timber) [Butt f = 356 mm , tip f = 254 mm]	very stiff to hard silty clay	3.1	No increase

Site Group	Site Name	Soil Along Pile Length	Pile Type	Design Founding Stratum	Pile Length (m)	Strength Gain Observation
Group 4	Site 23: HWY 401 and Country Road 14	Steel tube penetrated through very stiff to hard silty clay	steel tube 324 OD x 6.3 mm thick (concreted filled)	very stiff to hard silty clay	3.0	No increase
Group 4	Site 23: HWY 401 and Country Road 14	Timber pile penetrated through very stiff to hard silty clay	HP 310 x 110	very stiff to hard silty clay	3.1	No increase
Group 4	Site 25: HWY 401 and Elgin County Road 5	steel tube penetrated through stiff to very stiff silty clay	steel tube 324 OD x 6.3 mm thick (concreted filled)	Stif to very stiff silty clay	5.6	Based on SLT: increase by 30% after 13 months
Group 4	Site 25: HWY 401 and Elgin County Road 5	HP penetrated through stiff to very stiff silty clay	HP 310 x 79	Stif to very stiff silty clay	18.4	Based on SLT: increase by 10% after 13 months
Group 4	Site 25: HWY 401 and Elgin County Road 5	steel tube penetrated through stiff to very stiff silty clay	steel tube 324 OD x 6.3 mm thick (concreted filled)	Stif to very stiff silty clay	18.4	Based on SLT: increase by 30% after 13 months
Group 4	Site 25: HWY 401 and Elgin County Road 5	steel tube penetrated through stiff to very stiff silty clay	steel tube 324 OD x 6.3 mm thick (concreted filled)	Stif to very stiff silty clay	9.3	Based on SLT: increase by 20% after 13 months
Group 4	Site 25: HWY 401 and Elgin County Road 5	HP penetrated through stiff to very stiff silty clay	HP 310 x 79	Stif to very stiff silty clay	9.4	No increase
Group 4	Site 26: HWY 11 and Schomberg River	steel tube penetrated through peat and organic cohesive soil	steel tube 324 OD x 6.3 mm thick (concreted filled)	soft to firm organic silt and clay	12.2	Based on SLT: increase by 50% after 17 months
Group 4	Site 26: HWY 11 and Schomberg River	steel tube penetrated through peat, organic cohesive soil, and stiff to hard clayey silt	steel tube 324 OD x 6.3 mm thick (concreted filled)	stiff clayey silt	30.5	No increase
Group 4	Site 26: HWY 11 and Schomberg River	steel tube penetrated through peat, organic cohesive soil, and stiff to hard clayey silt	steel tube 324 OD x 6.3 mm thick (concreted filled)	stiff clayey silt	42.7	Based on SLT: increase by 30% after 17 months
Group 4	Site 26: HWY 11 and Schomberg River	timber pile penetrated through peat, organic cohesive soil, and stiff to hard clayey silt	Timber Size 36 [Butt f = 429 mm, tip f = 203 mm]	stiff to hard clayey silt	22.0	No increase
Group 4	Site 26: HWY 11 and Schomberg River	timber pile penetrated through peat and organic cohesive soil	Timber Size 36 [Butt f = 490 mm, tip f = 241 mm]	soft to firm organic silt and clay	12.2	No increase



## 5. RELAXATION

The previous section discussed the increase in the geotechnical capacity of driven pile with time due to strength gain. On the other hand, piles driven into dense to very dense saturated fine sands and silts, heavily over-consolidated clays, or weak laminated bedrocks (e.g., shale, mudstone, claystone, and siltstone) may experience decrease in the geotechnical capacity with time; a phenomenon known as “relaxation”.

Several researchers have explained the relaxation phenomenon (e.g., Thompson and Thompson, 1985; York et al., 1994; Herrera, 2015; etc.). In essence, shearing dense cohesionless soil/ heavily over-consolidated clays during pile installation can result in soil dilation. The soil dilation will result in negative pore pressure to be temporarily generated during pile driving, which in turn will result in a temporary increase in the effective stresses. Therefore, analysis of pile driving tests at the end of pile installation will show an “apparent” high geotechnical capacity due to this temporary increase in the effective stresses. As the negative pore pressure is being dissipated, the effective stresses will be decreased, and the pile capacity will decrease as well.

The relaxation of driven piles founded on weak laminated rocks may be attributed to the shale softening caused by migration of water to the toe of the pile in the peripheral opening created by the driving of pile. As clarified in the FHWA-NHI-16-009, the utilization of the slake durability test (ASTM D4644-16) proves valuable in evaluating the potential weathering and deterioration of rocks. By assessing the slake durability index, lower values can indicate deposits where driven piles are more susceptible to relaxation. Another potential relaxation mechanism is the release of the locked-in horizontal stresses following the pile driving (Thompson and Thompson, 1985).

As reported by Thompson and Thompson (1985), it is uncommon for driven piles to experience relaxation when bearing in the glacial till deposits commonly found in southern Canada.

Because of the relaxation, several guidelines (e.g., FHWA-NHI-16-009) propose that static load testing or dynamic test restrikes should be conducted once the soil has regained equilibrium conditions. In cases where piezometers are not available to provide site-specific pore pressure data, it is advisable to postpone static load testing or restriking





of piles in dense silts and fine sands or highly over-consolidated clays for a few days to a week after driving, or even longer if feasible. Similarly, in shale formations prone to relaxation, it is recommended to delay static load testing or restrike testing for a minimum of ten days to two weeks following the driving process.

There is no relaxation observed from the pile load test results for the MTO historic sites and the 9 recent sites. There is also limited published cases on the magnitude of relaxation for different soil and rock types. Thompson and Thompson (1985) and Hussein et al. (1993) suggest relaxation factors (i.e., ultimate geotechnical resistance after negative pore pressure dissipation divided by the ultimate geotechnical resistance at the end of initial driving) for piles founded in shales prone of relaxation can range from 0.5 to 0.9. For driven piles founded in dense sands, relaxation factors of 0.5 and 0.8 have also been observed.

When piles are driven into materials that are prone to relaxation, it is advisable to drive the piles to a capacity higher than the required ultimate capacity to accommodate some subsequent relaxation.

## **6. IMPACT OF CONSTRUCTION MEANS AND METHODS ON PILE CAPACITY**

There is currently no available data gathered from past or recent MTO sites that allows for a quantitative assessment of the effect of construction means and methods on the capacity of piles. Nevertheless, it is important to note that the means and methods employed during construction can exert a significant influence on the capacity of the piles.

For instance, when driving piles through challenging conditions such as glacial tills containing boulders, cobbles, or harder/denser zones in order to achieve the required tip elevations and soil resistance, it is generally recommended to reinforce the pile tips with driving shoes or pile points, such as the Titus Steel Standard Points for H-Piles or any other approved equivalent. The driving shoes, which are steel plates attached to the outer perimeter of the H-pile and are not flush with the pile flange, can adversely affect the capacity of the piles, particularly for friction piles.

Another example involves the utilization of bentonite slurry when installing caissons. This practice can potentially result in a reduction of the shaft friction resistance with uncertainty filter cake removal, thus impacting the overall capacity of the pile.

In summary, it is evident that the means and methods employed during construction exert a direct impact on the capacity of piles. Therefore, careful consideration should be given to ensure that the chosen techniques and processes are suitable for achieving the desired load-bearing capacity and long-term performance of the piles. It is crucial to take into account the potential effects of various construction methods, such as the use of driving shoes and bentonite slurry, to ensure the optimal design and construction of pile foundations.

## **7. SOIL STRUCTURE INTERACTION**

The ultimate geotechnical resistance of a pile is mobilized at a pile head settlement typically equivalent to 10 to 15% of pile diameter or width depending on multiple factors, including pile slenderness ratio ( $L/d$ ), pile-soil stiffness ratio ( $E_p/E_s$ ), pile section area ratio (plugged or unplugged for open section), etc. These factors will affect the distribution and magnitude of the elastic shortening of the pile shaft under axial load and impact the load transfer mechanism along the pile shaft and consequently relative contribution of the shaft friction and end bearing in resisting the ultimate failure load.

In uniform soil conditions, short piles (e.g.,  $L/d \leq 30$ ) will generally experience less elastic shortening than long piles (e.g.,  $L/d \geq 70$ ) before fully mobilizing the ultimate end bearing. For short piles, small elastic compression of the pile shaft allows the ultimate shaft friction along the entire pile length to develop almost simultaneously largely due to near constant relative pile-soil movement at all depths. For long piles, the relative pile-soil movement is much greater along the upper portion of the pile shaft than along the lower portion prior to mobilization of significant end bearing. The shaft friction along the upper portion of a long pile can reach post peak shear strength while the shaft friction along the lower portion remains below the linear elastic limit. In some cases, pile to soil slippage may occur along the upper shaft and result in large pile head movement without appreciable increase in pile capacity. A possible scenario for long piles would be upon mobilization of ultimate end bearing a significantly large portion of the pile shaft may have developed post peak or residual friction resistance. Further increase in pile length yields no corresponding increase in the pile stiffness (or load settlement ratio). This limiting pile behaviour makes designing a long pile to reach unyielding load bearing stratum less attractive due to excessive pile shortening associated with higher design load and inefficient use of shaft friction resistance.

Typical methods to estimate pile settlement in the context of soil pile interaction include closed-form solutions, load transfer method, elastic theory-based analysis and finite element analysis. The elastic theory-based analysis utilizes Mindlin's equations for the displacements within a soil mass caused by loading within the mass and discretization of pile elements and surrounding soil mass to permit superposition of stresses and displacements. Implementation of both elastic theory-based analysis and finite element analysis require intensive matrix computation assisted by a computer and therefore are not further discussed herein. The following sections provide brief descriptions of closed-form solutions and load transfer method.

#### ○ *Closed-Form Solutions*

Approximate closed-form solutions including elastic solution and hyperbolic method are discussed in the sections below. These methods generally integrate rigorous theoretical derivations with empirical experience.

#### • Elastic Solution

Elastic solutions to predict pile settlement under vertical working load were developed by various researchers such as Frank (1974), Cooke (1974), Randolph and Wroth (1978), Mylonakis and Gazetas (1998), etc., for both rigid and compressible piles. These solutions assume uniform shear stress distribution on the circumference of concentric cylinders of soil surrounding the pile. A maximum radius ( $r_m$ ) representing the limit of zone of influence of the pile-soil interface shear stress was introduced to compute the shear stress on each cylindrical surface. The maximum radius is a function of the pile slenderness ratio ( $L/d$ ) and variation of soil modulus along the pile shaft and below the pile toe. The load settlement ratio of the pile head can be estimated by the equation below:

$$\frac{P_t}{w_t d G_L} = \frac{\frac{2\eta}{(1-\nu)\xi} + \frac{2\pi\rho \tanh(\mu L) L}{\xi \mu L} \frac{L}{d}}{1 + \frac{8\eta}{\pi\lambda(1-\nu)\xi} \frac{\tanh(\mu L) L}{\mu L} \frac{L}{d}}$$

In which,  $P_t$  and  $w_t$  are the axial load and settlement at the pile head;  $G_L$  is the soil modulus at the pile base;  $\nu$  is the Poisson's ratio of soil;  $\eta$  is the ratio of pile shaft diameter  $d$  to base diameter  $d_b$  (e.g., 1 for typical pipe pile and H-pile);  $\xi$  is the ratio of soil modulus at the pile base  $G_L$  to soil modulus below the base  $G_b$ ;  $\rho$  is the ratio of average soil modulus  $\bar{G}$  along pile length to soil modulus at the pile base  $G_L$ ;  $\lambda$  is the pile-soil stiffness ratio

$E_p/G_L$ , where  $E_p$  is the equivalent pile modulus  $(EA)_p/(\pi d^2/4)$ ,  $(EA)_p$  is the cross-sectional rigidity of the pile material and  $\pi d^2/4$  is the equivalent circular area of pile section (plugged or unplugged);  $\zeta$  is a measure of radius of influence of pile  $\ln(2r_m/d)$ , where  $r_m$  is the maximum radius of influence  $\{0.25 + \xi[2.5\rho(1-\nu)-0.25]\}L$ ;  $\mu L$  is a measure of pile compressibility  $2\sqrt{2/\zeta\lambda}(L/d)$ .

The load at the pile base and the base stiffness can be estimated by the equation below as a percentage of the total load:

$$\frac{P_b}{P_t} = \frac{\frac{\eta}{(1-\nu)\xi} \frac{1}{\cosh(\mu L)}}{\frac{\eta}{(1-\nu)\xi} + \frac{\pi\rho \tanh(\mu L) L}{\zeta \mu L d}}$$

$$\frac{P_b}{w_b} = \frac{2d_b G_b}{(1-\nu)}$$

In which,  $P_b$  and  $w_b$  are the load at the pile base and pile base settlement, respectively.

For a typical steel HP 310x110 driven into uniform stiff to very stiff cohesive soil with full plug development, pile-soil stiffness ratio  $\lambda$  will be in the order of 1,500 to 3,000. The pile may be treated as rigid (incompressible) if the slenderness ratio  $L/d$  is less than 10 to 15. If the slenderness ratio  $L/d$  exceeds 60 to 90, the load settlement ratio or pile stiffness at the pile head ( $P_t/w_t$ ) will become independent of the pile length.  $d$  should be taken as the equivalent circular diameter of the plugged section.

This closed-form solution provides a simple and quick approach for estimating pile settlement and relative magnitudes of shaft friction and end bearing under the design working load. However, if a pile load vs. settlement curve is to be constructed, it may be arbitrary and time-consuming to vary the strain-dependent soil moduli ( $\bar{G}$ ,  $G_L$  and  $G_b$ ) at each load increment to capture the non-linear soil behaviour in shaft friction and end bearing.

- Hyperbolic Method

Fleming (1992) proposed a pile settlement prediction method based on the hyperbolic method used in Chin (1970) for interpretation of pile load test results. The hyperbolic

method has been widely used to define ultimate loads in static pile load tests. The Chin method defines the ultimate load ( $U$ ) to be the inverse of the slope ( $m$ ) of settlement/load ( $\Delta/P$ ) plotted against the settlement ( $\Delta$ ) of the pile head. Chin (1970, 1972) suggests that the hyperbolic function applies for piles deriving load carrying capacity mostly from shaft friction or end bearing. A bilinear relationship exists between pile head settlement and settlement/load with the first linear part representing shaft friction and the second linear part representing base bearing.

For a perfectly rigid pile (e.g., incompressible pile), the shaft and base displacements will be exactly the same under pile head load and are given by the following equations:

- Shaft Displacement:  $\Delta_S = \frac{M_S D_S P_S}{U_S - P_S}$
- Base Displacement:  $\Delta_B = \frac{0.6 U_B P_B}{D_B E_B (U_B - P_B)}$

Where  $D_S$  and  $D_B$  are the pile shaft diameter and base diameter, respectively;  $U_S$  and  $U_B$  are ultimate shaft friction capacity and ultimate base bearing capacity, respectively, and are typically estimated using conventional static analysis and field/lab test data;  $P_S$  and  $P_B$  are mobilized shaft friction load and base bearing load, respectively, corresponding to the shaft and base displacements;  $M_S$  is a shaft flexibility factor relating shaft movement to shaft diameter and typically varies from 0.0005 in very stiff soils or soft rocks to 0.001-0.002 in stiff over-consolidated clays to 0.004 in soft to firm or loose soils;  $E_B$  is secant soil modulus beneath the pile base corresponding to a base load equal to 25% of ultimate base bearing capacity.

Elastic compression ( $\Delta_e$ ) of a compressible pile is estimated assuming a friction-free or low friction zone ( $L_0$ ) in the upper portion of the pile and a friction transfer zone ( $L_F = L_P - L_0$ ). The friction-free or low friction zone ( $L_0$ ) accounts for any weak, soft soils or unconsolidated alluvial deposits near the surface or gap formed around a pile at a shallow depth caused by pile “whip” during driving.

- $\Delta_e = \frac{P(L_0 + K_e L_F)}{A_P E_P}$  if applied total load  $P$  (i.e.,  $P_S + P_B$ ) is less than ultimate shaft friction  $U_S$ .
- $\Delta_e = \frac{P L_P - L_F U_S (1 - K_e)}{A_P E_P}$  if applied total load  $P$  is greater than ultimate shaft friction  $U_S$ .

Where  $L_P$ ,  $A_P$  and  $E_P$  are the total pile length, section area and elastic modulus of the pile material;  $K_e$  is effective column length of the friction transfer portion ( $L_F$ ) of the pile and

typically ranges between 0.45 and 0.55.

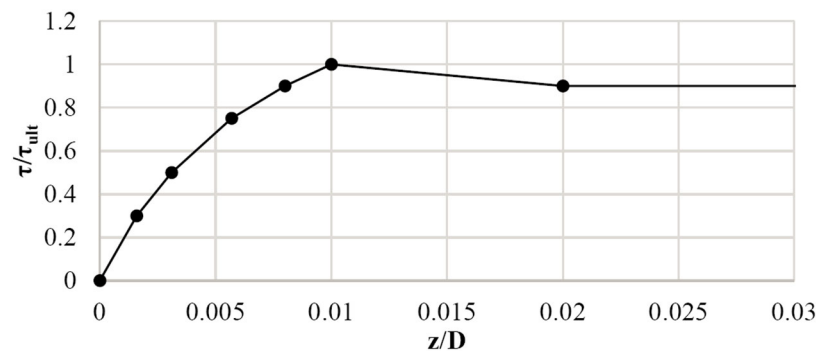
A load displacement curve can be established by incrementally increasing pile settlement to calculate corresponding shaft friction load and base bearing load for an incompressible pile. The total load ( $P$ ) combining shaft friction ( $P_S$ ) and base bearing ( $P_B$ ) will then be used to estimate elastic compression to be added to the shaft settlement. The shaft friction load will be re-calculated based on the updated shaft settlement through iterations until convergence is achieved. The iterative procedure will be terminated when or before the ultimate pile capacity  $U$  (i.e.,  $U_S + U_B$ ) is reached.

The accuracy of the predicted ultimate shaft friction and end bearing capacities governs the quality of the interpreted load displacement curve and will be heavily reliant on the method of static analysis used and availability of high-quality test data such as past results of PDA or static load tests carried out in the same deposit.

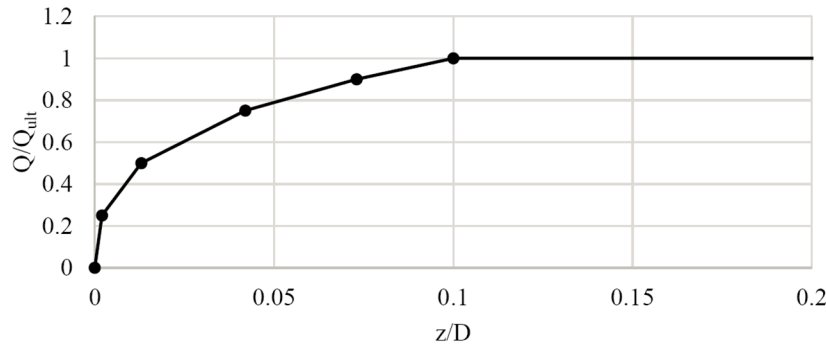
#### ○ *Load Transfer Method*

Coyle and Reese (1966) proposed Load Transfer Method based on soil test data measured from instrumented piles in the field and laboratory. Empirical load transfer curves for shaft friction and end bearing were also developed by Seed and Reese (1957), Mosher (1984), Reese and O'Neill (1988), API (2002), etc., for both sands and clays. The shaft friction and end bearing load transfer curves for API-Clay are illustrated below as an example. Both load transfer curves are normalized by the ultimate unit resistance on the load axis and pile diameter on the displacement axis.

#### • API-Clay Shaft Friction (t-z) Load Transfer Curve



- API-Clay End Bearing (Q-z) Load Transfer Curve



Poulos and Davis (1980) provides a step-by-step iterative procedure that can be readily implemented in an Excel spreadsheet for pile settlement computation based on load transfer method. Commercial geotechnical software RSPile (by Rocscience Inc.) has been developed based on the load transfer method in conjunction with basic 1-D finite element discretization of pile segments. The implementation of finite element formulation was only intended for pile discretization rather than continuum modelling, i.e., the soil surrounding each pile segment is modelled as an individual shear spring that has no direct interaction with the adjacent springs.

The iterative procedure starts by assuming a small movement at the pile toe ( $\rho_t$ ) followed by:

1. The pile toe reaction ( $q_t$ ) corresponding to the assumed toe movement is estimated based on the end bearing Load Transfer Curve (Q-z) or elastic solution such as Boussinesq theory.
2. The same pile shaft movement is assumed for the entire bottom pile segment to estimate the shaft friction ( $\tau_s$ ) using shaft friction Load Transfer Curve (t-z). The shaft friction is assumed to be uniform along the pile segment.
3. With the estimated shaft friction ( $\tau_s$ ) and base bearing ( $q_t$ ), the load at the top of bottom pile segment (Q) and elastic compression ( $\delta$ ) at the mid-point of the segment can be calculated.
4. The new shaft movement ( $\rho_t + \delta$ ) at the mid-point of the bottom pile segment is used to estimate the new shaft friction ( $\tau_s'$ ) based on the t-z curve.
5. If the difference between the new shaft friction ( $\tau_s'$ ) and the original shaft friction ( $\tau_s$ ) does not meet the specified tolerance (e.g., 1%), Step 3 to 4 is repeated to calculate the new elastic compression ( $\delta'$ ) and mid-point movement until the

tolerance is achieved.

6. Upon meeting the tolerance, the next pile segment up is considered based on the calculated load and movement at the top of the bottom pile segment and the segment-by-segment iteration moves up along the pile shaft until the load and displacement at the top of the uppermost pile segment are obtained.

The above procedure is repeated with incremental increase in pile toe movement to produce a load-settlement curve of the pile head.

The quality of the load transfer curves in representing the actual soil-pile interaction along the pile length, especially in stratified soil conditions, will govern the accuracy of the pile settlement prediction. The accuracy in prediction is also limited to some degree by the assumption of discrete soil springs represented by the load transfer curves or lack of interaction between adjacent springs.

## 8. SUMMARY AND CONCLUSIONS

The Ministry of Transportation of Ontario (MTO) has conducted 123 static pile load tests on both driven piles and caissons throughout Ontario between 1952 to 1992. The results of these pile load tests are compiled in the MTO publication titled “Pile Load and Extraction Tests, 1954-1992”, dated 1993. An addition of 10 recent pile load tests have been carried out at various other sites in Ontario. These piles has been installed through a variety of overburden soils including cohesionless, cohesive and stratified deposits and they were terminated on a variety of deposits. Piles have been driven to bedrock and caissons socketed into bedrock have been load tested as well. In many cases the predicted ultimate resistance of the foundation unit were either lower or higher than the actual capacity measured by the load tests. This study has attempted to explain the reasons for such differences between measured and predicted geotechnical resistances. Based on the results of this study. The summary of the recommended design methods are presented in Appendix C and presented below in more details.

### 1. Ultimate Pile Resistance in Cohesionless deposits

The predicted geotechnical resistance of piles driven in cohesionless deposits using the empirical methods recommend by the CFEM (2006) and the CHBDC (2019) is generally higher than the measured resistance from pile load tests. There are several reasons for the difference between the predicted and measured pile capacity as follows:



- a- Ignoring the reduction in the shaft resistance due to the effect of the friction fatigue, as discussed in Section 3.1.
- b- Assuming that the end bearing of the piles increase linearly with depth; whereas, the end bearing may continue to increase with depth but at a decreasing rate, as discussed in Section 3.3.

Based on the analysis of the 71 pile load tests carried out on driven piles and caissons in cohesionless soil, it is recommended the unit shaft resistance be estimated using the following equation:

$$P_s = k \cdot \tan(\delta) \cdot \sigma_v \cdot A_s$$

Where k is obtained based on the framework proposed by Randolph et al. (1994) using the following equation:

$$k = k_{min} + (k_{max} - k_{min}) e^{-\left(\frac{\mu h}{d}\right)}$$

Where:  $k_{min}$  = the active earth pressure coefficient

$$k_{max} = S_t \cdot N_q$$

$$S_t = 0.1 \exp(-3 \cdot \tan \phi)$$

$\mu$  = decay rate parameter

= 0.03 to 0.05 → for compact to very dense silty sand to sandy silt,

= 0 to 0.03 → for very loose to loose soil, very loose to very dense gravel or silt,

= 0 → for caissons

For the end bearing resistance, it is recommended that the ultimate end bearing resistance of piles in cohesionless deposits to be estimated as the minimum of: (i) the value obtained from Equation 15 (with using  $N_q$  as per CHBDC, 2019), and (ii) the value obtained for the Fleming et al. (2009) charts (Figure 3-14) with using the proper corrections factored as discussed in Section 3.3.

## 2. Ultimate Pile Resistance in Cohesive deposits

Several attempts have been made in the past for developing correlations between the shaft resistance in cohesive deposits and the properties of the soil (e.g., shear strength,

Plasticity Index, OCR, etc.). However, most of these correlations were developed from static load tests on un-instrumented piles driven through multiple soil strata with variable undrained strengths, which resulted in considerable uncertainty in the estimated shaft resistance.

The methods which have been developed can be grouped into two main categories: the total stress approach ( $\alpha$  method) or the effective stress approach ( $\beta$  method). The following have been concluded based on the assessment of all 51 pile load tests where the piles were driven through cohesive layers:

- a- There is no one method/approach that always give the best match between the measured and predicted shaft resistance of piles driven through cohesive layers,
- b- Out of the examined  $\alpha$ -methods, Kolk and Van Der Velde (1996) and Karlsrud (2012) provide the best match with the measured shaft resistance.
- c- Out of the examined  $\beta$ -methods, Burland (1993) and Karlsrud (2012) provide the best match with the measured shaft resistance.
- d- It is recommended that the ultimate shaft resistance of piles in contact with cohesive layers to be estimated based on Kolk and Van Der Velde (1996), Burland (1993), and Karlsrud (2012;  $\alpha$  and  $\beta$  methods). The design value should be the minimum predicted resistance obtained from the aforementioned methods.

For the end bearing resistance, it is recommended to use the following equation as per CFEM (2006):

$$P_b = S_u \cdot N_c \cdot A_b$$

Where:

- $S_u$  = the cohesion of soil within a distance of 2d below the base,
- $N_c$  = the bearing capacity factor =
  - = 6 for pile tip resting on the strong layer, or
  - = 9 for pile tip embedded a minimum of 3 to 5 times pile diameter or width in the strong bearing stratum.
- $A_b$  = the resisting area

### 3. Ultimate Resistance of Piles Driven to Bedrock

The results of load tests on 8 piles rest on bedrock have been provided by MTO. However, the pile load test has only been successfully loaded to failure for one pile.

For piles driven to refusal on the surface of sound bedrock, it is recommended that the following equation to be used to assess the ultimate geotechnical resistance of piles driven to bedrock (Morton, 2012):

$$Q_{ult} = N_{cr} \cdot q_u \cdot A_b$$

Where:  $q_u$  = the unconfined compressive strength of intact rock core,

$A_b$  = the plugged area of the pile section for soft rock and steel area for hard rock,

$$N_{cr} = 7.5$$

For pile driven to refusal within relatively weak and fractured bedrock, it is recommended to compute the  $N_{cr}$  to be  $= \tan^2(45+\Phi/2) + 1$ .

The geotechnical capacity of piles driven to found within the completely weathered bedrock (residual soil) can be obtained using the design methodologies for piles driven to found on soil. The pile geotechnical capacity shall be estimated assuming that the entire thickness of completely weathered bedrock will act like soil with both plastic and non-plastic behaviour.

### 4. Ultimate Resistance of Rock Sockets

The ultimate end bearing and peak shaft resistances of caissons socketed in bedrock can be assessed using the equations proposed by the CFEM, 2006 (i.e., Equations 21 and 22; Section 3.6). However, the rock-concrete ultimate peak shaft resistance can be mobilized at relatively small displacement compared to the ultimate end bearing resistance. Therefore, the rock socket capacity should be the maximum of the following values:

- i- peak shaft resistance + the portion of the end bearing mobilized at the corresponding level of deformation (e.g., deformation at point A; Figure 3-16),



- ii- Ultimate end bearing resistance + post-peak shaft resistance.

Determination of the portion of end bearing corresponding to the peak shaft resistance can be computed as described in Section 18.6.5 of the CFEM (2006). For the initial stage of design, the ratio of the peak to the post-peak rock-concrete shaft resistance may be obtained using the relationship shown in Figure 3-17

### 5. Strength Gain

Piles driven through cohesive soil layers generate excess pore water pressure in the zone around the pile shaft and below the tip of the pile due to the driving and/or the shearing of the soil at the pile/soil interface. The geotechnical resistance of these piles increases with time as the excess pore water pressure dissipates and due to other geochemical effects. The simplified semi-empirical method proposed by NGI (2013) provides a good estimate for the increase in the capacity of the driven piles in cohesive soil with time (see Section 6.1). It should be noted that an adequate level of field and laboratory investigation (i.e. CPT testing with pore pressure dissipation, oedometer testing on undisturbed samples, etc.) must be carried out for a reasonable prediction of the change in the ultimate geotechnical capacity with time. It is also important to carry out PDA and CAPWAP analysis on the driven piles at the end of driving and 1 to 2 weeks subsequent to installation to be able to verify and adjust the estimated increase in the pile resistance as assessed using the NGI (2013).

### 6. Relaxation

Piles driven into dense to very dense saturated fine sands and silts, heavily over-consolidated clays, or weak laminated bedrocks (e.g., shale) may experience a decrease in the geotechnical capacity with time (i.e., relaxation). There is no relaxation observed from the pile load test results carried out on the subject MTO sites. There is also limited published cases on the magnitude of relaxation for different soil and rock types. Based on literature, the ultimate geotechnical resistance of piles founded in dense sands or shales prone to relaxation can range from being decreased by 20% to 50%.

To be able to justify the reduction in capacity due to relaxation, if any, several guidelines (e.g., FHWA-NHI-16-009) propose that static load testing or dynamic test restrikes should be conducted once the soil has regained equilibrium conditions which may be about one



week after driving. Similarly, in shale formations prone to relaxation, it is recommended to delay static load testing or restrike testing for a minimum of ten days to two weeks following the driving process.

#### 7. Impact of Construction Means and Methods on Pile Capacity

There is no data collected from the historic or the recent MTO sites which allow quantitatively assess the effect of construction means and methods on the pile capacity. However, it should be noted that the means and methods of construction can have a significant impact on the capacity of piles. For example, in order to prevent pile damage while driving through boulders, cobbles and harder/denser zones to achieve the required tip elevations and soil resistance, it is typically recommended that the pile tips be reinforced with driving shoes such as the Titus Steel Standard Points for H-Piles or approved equivalent. The use of pile driving shoes which is welded to the outside perimeter of H-pile and not flushed with the pile flange will adversely impact the capacity of the piles driven into soil.

Another example is the use of bentonite slurry for augering rock sockets which can result in reduction in the shaft resistance of rock.

Overall, the means and methods of construction have a direct impact on pile capacity, and careful consideration should be given to ensure that the chosen techniques and processes are suitable for achieving the desired load-bearing capacity and long-term performance of the piles.

#### 8. Soil Structure Interaction

Three analytical methods are presented to illustrate settlement prediction of a single pile, including approximate elastic method, hyperbolic method and load transfer method taking into account pile stiffness, soil modulus, load transfer mechanism of shaft friction and end bearing, and interpretation of static pile load test results. Accuracy of the settlement prediction will largely hinge on the quality of soil test data and actual pile installation methods. These methods can be useful in estimating geotechnical resistance at serviceability limit state in comparison to simply applying an overall factor of safety to the ultimate geotechnical resistance value.



It is recommended as part of future study that calibration of the predictive methods against available static pile load test results with high quality soil test data be conducted to help improve accuracy of pile settlement prediction in similar geological deposits in the future.

## **9. RECOMMENDATIONS FOR FUTURE WORK**

As more pile load tests are conducted at MTO bridge sites, the results of future tests should be analyzed based on the proposed methods and conclusions in this report. This will further confirm and augment the conclusions in this report.

## **ACKNOWLEDGEMENT**

The Authors are grateful to MTO and in particular to Tony Sangiuliano, Brady Lin, and Breanne Stramenga for their support during the course of this study.

## REFERENCES

- ASTM D4644-16. Standard Test Method for Slake Durability of Shales and Other Similar Weak Rocks.
- Baligh, M.M. 1984. The Simple-pile Approach to Pile Installation in Clays. Analysis and Design of Pile Foundations. *Proceedings of the Symposium On Codes and Standards*, ASCE National Conv., San Francisco, 310-330.
- Berezantzev, V.G., Khristoforov, V.S., and Golubkov, V. N. 1961. Load bearing capacity and deformation of piled foundations. *Proceedings of the 5th International Conference on Soil Mechanics and Foundation Engineering*, 2, 11-15.
- Bruno, D. 1999. *Dynamic and static load testing of driven piles in sand*. PhD thesis, University of Western Australia.
- Burland, J.P. 1993. Closing address. Proceedings of Recent Large-Scale Fully Instrumented Pile Tests in Clay. Institute of Civil Engineers, London, 590–595.
- Bolton, M.D. 1986. The strength and dilatancy of sands. *Géotechnique*, 36(1): 65–78.
- Cao, L., Peaker, S., and Ahmad, S. 2015. Engineering characteristics of glacial tills in GTA. *Proceedings of GeoQuebec*.
- Chow, F.C. 1997. *Investigations into the behaviour of displacement piles for offshore foundations*. PhD thesis, University of London (Imperial College).
- De Nicola, A. 1996. *The performance of pipe piles in sand*. PhD thesis, University of Western Australia.
- Federal Highway Administration (FHWA), 2016. *Design and Construction of Driven Pile Foundations*, Volume I, Report No. FHWA-NHI-16-009, Washington DC.
- Flaate, K., and Selnes, P. 1977. Side friction of piles in clay. Proceedings of the 9<sup>th</sup> International Conference on Soil Mechanics and Foundation Engineering, Tokyo, 517–522.
- Fleming, W. G. K. 1992. A new method for single pile settlement prediction and analysis. *Geotechnique*, 42, No. 3, 411-425
- Goodman, R.E. 2004. *Introduction to rock mechanics*. 2<sup>nd</sup> Edition, John Wiley & Sons.
- Hoek, E. 2007. *Practical Rock Engineering*, <https://www.rocscience.com/assets/resources>.
- Hoek, E., and Brown, E.T. 1998. Practical estimates of rock mass strength. *International Journal of Rock Mechanics and Mining Sciences*, 34:1165-1186

- Hoek, E., Marinos, P., and Benissi, M. 1998. Applicability of the Geological Strength Index (GSI) Classification for very weak and sheared rock masses. The case of the Athens Schist Formation. *Bulletin of Engineering Geology and the Environment*, 57: 151-160.
- Hanna, T. H., and Tan, R. H. S. 1973. The Behavior of Long Piles Under Compressive Loads in Sand. *Canadian Geotechnical Journal*, 10(3): 311-340.
- Horvath, R.G., and Kenney, T.C. 1979. Shaft resistance in rock socketed drilled piers. *Proceedings of the symposium on deep foundations*, ASCE, Reston, 182-214.
- Heerema, E. P. 1978. Predicting pile driveability: Heather as an illustration of the friction fatigue theory. In *Proceedings of the SPE European Petroleum Conference*, London.
- Herrera, R. 2015. Relaxation of Driven Pile Resistance in Granular Soils, *Geotechnical and Materials Engineers Committee Conference*, Cocoa Beach, Florida.
- Hussein, M.H., Likins, G.E., and Hannigan, P.J. 1993. Pile Evaluation by Dynamic Testing During Restrike. *11<sup>th</sup> Southeast Asian Geotechnical Conference*, Singapore, 535-539.
- Karlsrud, K., Clausen, C.J.F., and Aas, P.M. 2005. Bearing capacity of driven piles in clay, the NGI approach." *Proceedings of the International Symposium on Frontiers in Offshore Geotechnics*, 775-782.
- Karlsrud, K. 2012. *Prediction of load-displacement behavior and capacity of axially-loaded piles in clay based on analyses and interpretation of pile load test results*. PhD Dissertation, Norwegian University of Science and Technology.
- Kolk, H.J, and Van der Velde, E. 1996. A reliable method to determine the friction capacity of piles driven into clays. *Proceedings of 28<sup>th</sup> Annual Offshore Technology Conference*, Houston, TX, 337–346.
- Kulhawy, F.H. 1984. Limiting tip and side resistance: Fact or fallacy. *Proceedings of Symposium On Analysis and Design of Pile Foundations*, San Francisco, 80–98.
- Lehane, B. 1992. *Experimental investigations of pile behaviour using instrumented field piles*. Ph.D. thesis, University of London (Imperial College).
- Lehane, B.M., Jardine, R.J., Bond, A.J., and Frank, R. 1993. Mechanisms of shaft friction in sand from instrumented pile tests. *Journal of Geotechnical Engineering*, 119(1): 19-35.
- Lehane, B.M., Schneider J.A., and Xu, X. 2005. *A review of design methods for offshore driven piles in siliceous sand*. Research Report Geo:05358, Geomechanics Group, The University of Western Australia.



- Liu, J., and Jesswein, M. 2022. *Improving Pile Design in Ontario Soils*. MTO, Highway Standards Branch Report.
- Long, J. H. 2016. Static Pile Load Tests on Driven Piles into Intermediate Geo Materials. Report No. WHRP 0092-12-08
- Meyerhof, G.G. 1976. Bearing capacity and settlement of pile foundations. *Journal of Geotechnical Engineering Division*, 102:195–228
- Tomlinson, M. and Woodward, J. 2008. *Pile Design and Construction Practice*. Fifth edition. MTO Report EM-48. 1993. *Pile Load and Extraction Tests 1954-1992*. Ministry of Transportation, Ontario. Toronto, Ontario, Canada.
- Neely, W.J. 1990. Bearing capacity of expanded-base piles in sand. *Journal of Geotechnical Engineering*. 116(1): 73–87.
- Norwegian Geotechnical Institute (NGI). 2000. Bearing Capacity of Driven Piles, Piles in Clay. Report 525211-1.
- Norwegian Geotechnical Institute (NGI). 2013. Time Effects on Pile Capacity. Report 20061251-00-279-R.
- Pells, P.J.N., and Turner, R.M. 1978. *Theoretical and model studies relating to footings and piles on rock*. Report No. R314, University of Sydney.
- Poulos, H. G. and Davis, E. H. 1980. *Pile Foundation Analysis and Design*. The University of Sydney
- Rehman, S.E. and Broms, B.B. 1971. Bearing capacity of piles driven into rock. *Canadian Geotechnical Journal*, 8(2): 151-162.
- Randolph, M.F., Dolwin, J., and Beck, R. 1994. Design of driven piles in sand. *Géotechnique*, 44(3): 427-448.
- Rauf, A., and Rothenburg, L. 2011. *Development of guidelines for estimation of pile capacity and construction control of pile driving*. MTO Highway Infrastructure innovation Funding Program.
- Manzari, M., Drevininkas, A., Olshansky, D., and Galaa, A. 2014. Behaviour modelling of Toronto Glacial Soils and implementation in numerical modelling. *Proceedings of GeoRegina*.
- Morton, T. 2012. *Assessment of Driven Pile Capacity on Rock Using Empirical Approaches*. MSc thesis, Dalhousie University, Halifax, Canada.

- Thompson, C.D., and Thompson, D.E. 1985. Real and Apparent Relaxation of Driven Piles. American Society of Civil Engineers, *Journal of Geotechnical Engineering*: (111) 2: 225-237.
- Tomlinson, M.J. 1957. The adhesion of piles driven in clay soils. *Proceedings of the 4<sup>th</sup> International Conference on Soil Mechanics and Foundation Engineering*, London, Volume. 2: 66-71.
- Tomlinson, M.J. 2004. *Pile Design and Construction Practice*. 4<sup>th</sup> Edition, E & FN SPON.
- Toolan, F.E., Lings, M.L., and Mirza, U.A. 1990. An appraisal of API RP2A recommendations for determining skin friction of piles in sand. *Proc. 22<sup>nd</sup> Offshore Technology Conference*, Houston, OTC 6422, 33-42.
- Vesic, A.S. 1969. Experiments with instrumented pile groups in sand. ASTM STP 444, 177–222.
- Vizini, V.O.S. and Futai, M.M. 2019. Shear Strength of Rock-Concrete Interface via Direct Shear Test-a data compile. *Proceedings of the 14<sup>th</sup> International Congress on Rock Mechanics and Rock Engineering, Brazil*.
- White, D.J. and Bolton, M.D., 2002. Observing friction fatigue on a jacked pile. Springman, S. (ed.), In *Proceedings of the Workshop on Constitutive and Centrifuge Modelling: Two Extremes*. CRC Press / Balkema, 347-354.
- York, D.L., Brusey, W.G., Clémente, F.M., and Law, S.K. 1994. Setup and Relaxation in Glacial Sand. *American Society of Civil Engineers, Journal of Geotechnical Engineering*, 120(9): 1498-1513.



## **Appendix A**

### **Background Information and Pile Load Test Assessment For the 50 MTO Sites**

**Table A-1. Site Condition, Pile Load Test Assessment, and Predicted Ultimate Geotechnical Resistance by the Foundation Designer**

Site	Soil Along Pile Length	Pile Type	Design Founding Stratum	Pile Length (m)	Ultimate Geotechnical Resistance (kN) Predicted by Foundation Designer	Ultimate Pile Capacity - Static Pile Load Test (kN)				Ultimate Pile Capacity - PDA and CAPWP analysis		
						Max. Applied Load during the Test (kN)	Modified Chin Method (1970)	Brinch Hansen's 90% Method (1963)	Davisson Offset Limit Load Method	Ultimate Pile Capacity (kN)	Shaft Capacity (kN)	Toe Capacity (kN)
HWY 400 - 89	Steel H-Pile [310x110] penetrated through stratified deposits [cohesive and non-cohesive layers]	Steel HP 310x110	Very Dense Silt to Sandy Silt (lower deposit) followed by very stiff clayey silt layer	36.0	3125	1194	1190	1260	860	1150	875	275
HWY 400 - 89	Steel H-Pile [310x110] penetrated through stratified deposits [cohesive and non-cohesive layers]	Steel HP 310x110	"100-blow" clayey silt to silt and sand till	51.0	4000	2352	2990	2700	1650	1500	975	525
Hwy 400 - South Canal	Steel H-Pile [310x110] Penetrated through Clayey Silt soil	Steel HP 310x110	Very Dense Sand to Silt soil	16.5	2550	2196	2068	1858	1400	1106	606	500
HWY 401 - Fletcher's Creek	Steel H-Pile [310x110] Penetrated through Clayey Silt till	Steel HP 310x110	Very Dense Sand to Silt till	9.6	1800	2600	3968	4046	2100	2200	375	1825
HWY 400 - Essa Rd.	Steel H-Pile [310x110] penetrated through Silt to sand	Steel HP 310x110	Very Dense Silty Sand	31.6	3600	3280	5869	5236	3150	1550	600	950
Hwy 569-Blanche River Bridge	Steel H-Pile [310x110] penetrated through firm Varved Clay	Steel HP 310x110	Firm Varved Clay	40.0	1563	1650	1667	1391	1600	1600	1557	43

Site	Soil Along Pile Length	Pile Type	Design Founding Stratum	Pile Length (m)	Ultimate Geotechnical Resistance (kN) Predicted by Foundation Designer	Ultimate Pile Capacity - Static Pile Load Test (kN)				Ultimate Pile Capacity - PDA and CAPWP analysis		
						Max. Applied Load during the Test (kN)	Modified Chin Method (1970)	Brinch Hansen's 90% Method (1963)	Davisson Offset Limit Load Method	Ultimate Pile Capacity (kN)	Shaft Capacity (kN)	Toe Capacity (kN)
HWY 17 - Pic River	Steel H-Pile [310x79] Silty clay (installed in 1959)	Steel H-Pile [310x79]	Varved Clay over Artesian Silt (with electro-osmotic treatment)	16.5	358	700	798	717	700	N/A	N/A	N/A
HWY 417 - Ramsayville	Steel H-Pile [310x110] penetrated through Firm to stiff silty clay to clay	Steel HP 310x110	Shale Bedrock	50.0	3750	4350	6410	5740	4100	2124	924	1200
HWY 401 - Third Line (Bainsville)	Steel H-Pile [310x79] penetrated through stratified deposits [Cohesive and non-cohesive layers]	Steel HP 310x79	Limestone Bedrock	12.6	1500	1960	2778	2514	1850	N/A	N/A	N/A
Rainy River - Baudette River International Bridge	2.44 m diameter drilled shaft - soil along shaft is generally sand to silt and sand Till	2.44 m Diameter Caisson	"100-blow" Sand to Silty Sand Till	26.0	30000	50000	N/A	N/A	N/A	N/A	N/A	N/A
Site 1: Q.E.W. at Burlington Bay Skyway (Hamilton)	Driven Timber Pile penetrated through Compact Sand	Timber Size 35 (Red Pine) [Butt $\phi$ = 324 mm , tip f = 216 mm	Compact to Dense Sand	7.2	N/A	694	749	670	600	N/A	N/A	N/A
Site 2: Q.E.W. at Windermere Cut-Off Burlington Beach	Steel tube with concrete plug penetrated through very loose to loose sand to gravelly sand	Steel Tube (305 mm O.D x 3.6 mm wall) - Concrete Filled - driven with concrete plug	very dense gravel	7.5	1792	1246	1729	1558	1450	N/A	N/A	N/A

Site	Soil Along Pile Length	Pile Type	Design Founding Stratum	Pile Length (m)	Ultimate Geotechnical Resistance (kN) Predicted by Foundation Designer	Ultimate Pile Capacity - Static Pile Load Test (kN)				Ultimate Pile Capacity - PDA and CAPWP analysis		
						Max. Applied Load during the Test (kN)	Modified Chin Method (1970)	Brinch Hansen's 90% Method (1963)	Davisson Offset Limit Load Method	Ultimate Pile Capacity (kN)	Shaft Capacity (kN)	Toe Capacity (kN)
Site 2: Q.E.W. at Windermere Cut-Off Burlington Beach	Steel tube penetrated through very loose to loose sand	Steel Tube (305 mm O.D x 4.4 mm wall) - Concrete filled - Driver open ended	very dense gravel	5.8	796	979	852	763	675	N/A	N/A	N/A
Site 3: HWY 401 and Little Don River	Steel tube with concrete plug penetration through stratified deposits [cohesive and non-cohesive layers]	Steel Tube [559 mm O.D) - driven with concrete plug - filled with concrete	Compact to Dense Sand	8.0	1960	1779	1998	1793	N/A	N/A	N/A	N/A
Site 3: HWY 401 and Little Don River	Steel tube with concrete plug penetration through stratified deposits [cohesive and non-cohesive layers]	Steel Tube [559 mm O.D) - driven with concrete plug - filled with concrete	Compact to Dense Sand	12.3	1960	1779	2296	2078	N/A	N/A	N/A	N/A
Site 4: HWY 68 and Spanish River	Steel tube penetrated through stratified deposits (cohesive and non-cohesive layers)	Steel Tube (324 mm O.D x 4.8 mm wall) - filled with concrete - driven with closed end with steel plate	Very stiff Clayey Silt	36.0	1195	712	650	588	500	N/A	N/A	N/A
Site 6: QEW Over Welland Canal	Steel H-Pile Penetrated through Silty Clay to Clayey Silt soil	HP 280x 112 [11" x 11"]	Very Dense Sand and Gravel [Till]	27.6	N/A	2134	2723	2466	N/A	N/A	N/A	N/A
Site 6: QEW Over Welland Canal	Steel H-Pile Penetrated through Silty Clay to Clayey Silt soil	HP 370 x 108 [14"x14"]	Very Dense Sand and	27.6	N/A	1779	5787	5220	N/A	N/A	N/A	N/A

Site	Soil Along Pile Length	Pile Type	Design Founding Stratum	Pile Length (m)	Ultimate Geotechnical Resistance (kN) Predicted by Foundation Designer	Ultimate Pile Capacity - Static Pile Load Test (kN)				Ultimate Pile Capacity - PDA and CAPWP analysis		
						Max. Applied Load during the Test (kN)	Modified Chin Method (1970)	Brinch Hansen's 90% Method (1963)	Davisson Offset Limit Load Method	Ultimate Pile Capacity (kN)	Shaft Capacity (kN)	Toe Capacity (kN)
			Gravel [Till]									
Site 6: QEW Over Welland Canal	Steel H-Pile Penetrated through Silty Clay to Clayey Silt soil	HP 370 x 108 [14"x14"]	Very Dense Sand and Gravel [Till]	23.0	N/A	1779	2680	2932	N/A	N/A	N/A	N/A
Site 6: QEW Over Welland Canal	Steel H-Pile Penetrated through Silty Clay to Clayey Silt soil	HP 280x 112 [11" x 11"]	Very Dense Sand and Gravel [Till]	30.5	N/A	2134	3064	2761	N/A	N/A	N/A	N/A
Site 6: QEW Over Welland Canal	Steel H-Pile Penetrated through Silty Clay to Clayey Silt soil	HP 280x 112 [11" x 11"]	Very Dense Sand and Gravel [Till]	29.6	N/A	2134	4045	3666	N/A	N/A	N/A	N/A
Site 6: QEW Over Welland Canal	Steel H-Pile Penetrated through Silty Clay to Clayey Silt soil	HP 280x 112 [11" x 11"]	Very Dense Sand and Gravel [Till]	27.3	N/A	2134	3218	2895	N/A	N/A	N/A	N/A
Site 7: Azatika Creek (Alfred Twp.)	Steel H-Pile [310x79] penetrated through stratified deposits [cohesive and non-cohesive layers]	HP 310 x 79	Stiff to very stiff silty clay	22.3	N/A	845	832	754	800	N/A	N/A	N/A
Site 8: HWY 50 and Humber River	Driven Timber Pile penetrated through loose to dense sandy silt to silt	Timber Size 36 (Untreated Timber) [Butt $\phi$ = 356 mm , tip f = 254 mm]	compact silt	9.9	N/A	578	516	463	400	N/A	N/A	N/A
Site 8: HWY 50 and Humber River	Driven Timber Pile penetrated through loose to	Timber Size 36 (Untreated Timber)	compact silt	10.1	N/A	667	636	576	390	N/A	N/A	N/A

Site	Soil Along Pile Length	Pile Type	Design Founding Stratum	Pile Length (m)	Ultimate Geotechnical Resistance (kN) Predicted by Foundation Designer	Ultimate Pile Capacity - Static Pile Load Test (kN)				Ultimate Pile Capacity - PDA and CAPWP analysis		
						Max. Applied Load during the Test (kN)	Modified Chin Method (1970)	Brinch Hansen's 90% Method (1963)	Davisson Offset Limit Load Method	Ultimate Pile Capacity (kN)	Shaft Capacity (kN)	Toe Capacity (kN)
	dense sandy silt to silt	[Butt $\phi$ = 394 mm , tip f = 273 mm]										
Site 9: HWY 403 at King and Main Street Interchange	Driven Steel Tube 324 mm OD x 6.3 mm [Filled with concrete] penetrate through stiff to hard silty clay	Steel Tube 324 mm OD x 6.3 mm [Filled with concrete]	Shale Bedrock	21.3	N/A	1778	2222	1999	2300	N/A	N/A	N/A
Site 9: HWY 403 at King and Main Street Interchange	Driven Steel HP 370 x 108 penetrate through stiff to hard silty clay	Steel HP 370x108	Shale Bedrock	21.3	1500	1778	2199	1978	2000	N/A	N/A	N/A
Site 10: HWY 11 and O.N.R.	Driven Timber Pile penetrated through silty clay soil	Timber Size 32 (untreated Timber) [Butt f = 324 mm , tip f = 197 mm]	Firm to Stiff Silty Clay	15.1	N/A	356	298	270	300	N/A	N/A	N/A
Site 10: HWY 11 and O.N.R.	Driven Timber Pile penetrated through silty clay soil	Timber Size 36 (untreated Timber) [Butt f = 356 mm , tip f = 191 mm]	Firm to Stiff Silty Clay	15.5	N/A	310	269	242	290	N/A	N/A	N/A
Site 11: County Road and Vermilion River	Steel HP driven through loose to compact sand to silt	HP 310 x 79	Compact Silt	26.8	N/A	712	741	667	650	N/A	N/A	N/A
Site 12: Magnetawan River and Dev. Road 605	Timber pile penetrated through stratified deposits [cohesive and non-cohesive layers]	Timber Size 30 (treated Timber) [Butt f = 305 mm ,	Soft clayey silt to silty clay	13.4	N/A	489	713	639	660	N/A	N/A	N/A



Site	Soil Along Pile Length	Pile Type	Design Founding Stratum	Pile Length (m)	Ultimate Geotechnical Resistance (kN) Predicted by Foundation Designer	Ultimate Pile Capacity - Static Pile Load Test (kN)				Ultimate Pile Capacity - PDA and CAPWP analysis		
						Max. Applied Load during the Test (kN)	Modified Chin Method (1970)	Brinch Hansen's 90% Method (1963)	Davisson Offset Limit Load Method	Ultimate Pile Capacity (kN)	Shaft Capacity (kN)	Toe Capacity (kN)
		tip f = 203 mm]										
Site 13: HWY 50 and Humber River	Driven Timber Pile penetrated through dense to very dense silty sand	Timber Size 30 (Untreated Timber) [Butt $\phi$ = 305 mm , tip f = 203 mm]	dense to very dense silty sand	4.6	N/A	445	651	582	250	N/A	N/A	N/A
Site 13: HWY 50 and Humber River	Driven Timber Pile penetrated through loose to compact silty sand	Timber Size 30 (Untreated Timber) [Butt $\phi$ = 305 mm , tip f = 203 mm]	dense to very dense silty sand	6.7	N/A	445	712	638	300	N/A	N/A	N/A
Site 13: HWY 50 and Humber River	Driven Timber Pile penetrated through loose to compact silty sand	Timber Size 30 (Untreated Timber) [Butt $\phi$ = 298 mm , tip f = 203 mm]	very loose to very dense silty sand	6.4	N/A	445	1046	938	250	N/A	N/A	N/A
Site 13: HWY 50 and Humber River	Driven Timber Pile penetrated through compact to very dense sand to sandy silt	Timber Size 30 (Untreated Timber) [Butt $\phi$ = 305 mm , tip f = 203 mm]	very dense sandy silt	5.2	N/A	445	1938	1729	350	N/A	N/A	N/A
Site 13: HWY 50 and Humber River	Steel tube penetrated through compact to very dense sand to sandy silt	Steel Tube 324 mm OD x 6.3 mm [Filled	very dense sandy silt	19.8	N/A	1468	2104	1881	1850	N/A	N/A	N/A

Site	Soil Along Pile Length	Pile Type	Design Founding Stratum	Pile Length (m)	Ultimate Geotechnical Resistance (kN) Predicted by Foundation Designer	Ultimate Pile Capacity - Static Pile Load Test (kN)				Ultimate Pile Capacity - PDA and CAPWP analysis		
						Max. Applied Load during the Test (kN)	Modified Chin Method (1970)	Brinch Hansen's 90% Method (1963)	Davisson Offset Limit Load Method	Ultimate Pile Capacity (kN)	Shaft Capacity (kN)	Toe Capacity (kN)
		with concrete]										
Site 13: HWY 50 and Humber River	Steel tube penetrated through loose to very dense silty sand	Steel Tube 324 mm OD x 6.3 mm [Filled with concrete]	very dense sandy silt	12.5	N/A	712	902	812	850	N/A	N/A	N/A
Site 14: Q.E.W. and Niagara Street	Firm to very stiff Silty Clay	Steel Tube 324 mm OD x 5 mm [Filled with concrete]	Stiff Silty Clay	18.3	N/A	311	263	236	220	N/A	N/A	N/A
Site 14: Q.E.W. and Niagara Street	Firm to very stiff Silty Clay	Steel Tube 324 mm OD x 6.3 mm [Filled with concrete]	Hard Clayey Silt	29.0	N/A	1334	1694	1525	1520	N/A	N/A	N/A
Site 14: Q.E.W. and Niagara Street	Firm to very stiff Silty Clay	HP 310 x 110	hard Clayey Silt	29.0	N/A	1068	2548	2292	2100	N/A	N/A	N/A
Site 15: HWY 401 and Jane Street	Steel tube penetrated through stratified deposits [cohesive and non-cohesive layers]	Franki caisson 0.559 m dia.	Firm to stiff clayey silt to silty clay	7.3	N/A	1334	1201	1073	550	N/A	N/A	N/A
Site 15: HWY 401 and Jane Street	Timber pile penetrated through stratified deposits [cohesive and non-cohesive layers]	Timber Size 36 (untreated Timber) [Butt f = 368 mm , tip f = 229 mm]	Firm to stiff clayey silt to silty clay	9.0	N/A	934	926	830	710	N/A	N/A	N/A

Site	Soil Along Pile Length	Pile Type	Design Founding Stratum	Pile Length (m)	Ultimate Geotechnical Resistance (kN) Predicted by Foundation Designer	Ultimate Pile Capacity - Static Pile Load Test (kN)				Ultimate Pile Capacity - PDA and CAPWP analysis		
						Max. Applied Load during the Test (kN)	Modified Chin Method (1970)	Brinch Hansen's 90% Method (1963)	Davisson Offset Limit Load Method	Ultimate Pile Capacity (kN)	Shaft Capacity (kN)	Toe Capacity (kN)
Site 16: HWY 401 and Black Creek	Timber pile penetrated through stratified deposits [cohesive and non-cohesive layers]	Timber Size 36 (untreated Timber) [Butt f = 368 mm , tip f = 216 mm]	Compact Silt	12.2	N/A	1290	1294	1175	1100	N/A	N/A	N/A
Site 17: HWY 401 Basket Weave Bridges Between Keele & Jane St.	Steel HP pile penetrated through stratified deposits [cohesive and non-cohesive layers]	HP 310 x 110	Very dense Till	25.7	N/A	2669	3360	3041	2400	N/A	N/A	N/A
Site 17: HWY 401 Basket Weave Bridges Between Keele & Jane St.	Steel HP pile penetrated through stratified deposits [firm to stiff clayey silt, dense to very dense silty sand, and very dense till]	HP 310 x 110	Shale Bedrock	26.5	N/A	2669	2904	2589	2400	N/A	N/A	N/A
Site 18: HWY 624 and Blanche River	Timber pile penetrated through very stiff to firm clay	Timber Size 30 (treated Timber) [Butt f = 305 mm , tip f = 203 mm]	Firm varved clay	12.5	N/A	445	377	346	410	N/A	N/A	N/A
Site 18: HWY 624 and Blanche River	Timber pile penetrated through very stiff to firm clay	Timber Size 36 (treated Timber) [Butt f = 381 mm , tip f = 229 mm]	Firm varved clay	12.3	N/A	578	529	477	550	N/A	N/A	N/A
Site 18: HWY 624 and Blanche River	Timber pile penetrated through very stiff to firm clay	Timber Size 32 (treated Timber)	Firm varved clay	12.4	N/A	489	460	411	450	N/A	N/A	N/A

Site	Soil Along Pile Length	Pile Type	Design Founding Stratum	Pile Length (m)	Ultimate Geotechnical Resistance (kN) Predicted by Foundation Designer	Ultimate Pile Capacity - Static Pile Load Test (kN)				Ultimate Pile Capacity - PDA and CAPWP analysis		
						Max. Applied Load during the Test (kN)	Modified Chin Method (1970)	Brinch Hansen's 90% Method (1963)	Davisson Offset Limit Load Method	Ultimate Pile Capacity (kN)	Shaft Capacity (kN)	Toe Capacity (kN)
		[Butt f = 318 mm , tip f = 197 mm]										
Site 18: HWY 624 and Blanche River	Timber pile penetrated through very stiff to firm clay	Cast-in-place Concrete pile 0.508 m dia.	Firm varved clay	9.5	N/A	489	432	394	400	N/A	N/A	N/A
Site 19: HWY 50 and North Creek	Timber pile penetrated through stratified deposits [cohesive and non-cohesive layers]	Timber Size 36 (treated Timber) [Butt f = 356 mm , tip f = 203 mm]	Firm to stiff silty clay to clayey silt	13.7	N/A	712	772	696	580	N/A	N/A	N/A
Site 19: HWY 50 and North Creek	Timber pile penetrated through very loose silty sand to silt	Timber Size 36 (treated Timber) [Butt f = 356 mm , tip f = 254 mm]	Firm to stiff silty clay to clayey silt	8.8	N/A	378	343	311	250	N/A	N/A	N/A
Site 20: Hwy 401 and Don Mills Road	Steel encased displacement pile penetrated through stratified deposits [cohesive and non-cohesive layers]	steel encased pile 406 mm dia.	very dense sand	16.5	N/A	2135	5787	5233	N/A	N/A	N/A	N/A
Site 21: HWY 401 and Leslie Street	Cast-in-place caisson penetrated through stratified deposits [cohesive and non-cohesive layers]	cast in place 0.762 m caisson	Hard Till	18.6	N/A	3559	3840	3425	2000	N/A	N/A	N/A

Site	Soil Along Pile Length	Pile Type	Design Founding Stratum	Pile Length (m)	Ultimate Geotechnical Resistance (kN) Predicted by Foundation Designer	Ultimate Pile Capacity - Static Pile Load Test (kN)				Ultimate Pile Capacity - PDA and CAPWP analysis		
						Max. Applied Load during the Test (kN)	Modified Chin Method (1970)	Brinch Hansen's 90% Method (1963)	Davisson Offset Limit Load Method	Ultimate Pile Capacity (kN)	Shaft Capacity (kN)	Toe Capacity (kN)
Site 21: HWY 401 and Leslie Street	HP 370 x 108 penetrated through stratified deposits [cohesive and non-cohesive layers]	HP 370 x 108 [14"x14"]	Hard Till	21.5	N/A	2224	2187	1969	1900	N/A	N/A	N/A
Site 22: Hwy 400 and Jane Street	Steel tube penetrated through stratified deposits [cohesive and non-cohesive layers]	steel tube 324 OD x 5.2 mm thick (concreted filled)	Firm to very stiff clayey silt	15.3	N/A	278	264	239	200	N/A	N/A	N/A
Site 22: Hwy 400 and Jane Street	Steel tube penetrated through stratified deposits [cohesive and non-cohesive layers]	steel tube 324 OD x 6.3 mm thick (concreted filled)	very stiff to hard clayey silt	30.2	N/A	1223	1108	1003	950	N/A	N/A	N/A
Site 22: Hwy 400 and Jane Street	Steel tube penetrated through stratified deposits [cohesive and non-cohesive layers]	steel tube 324 OD x 5.2 mm thick (concreted filled)	Firm to very stiff clayey silt	15.3	N/A	334	274	247	220	N/A	N/A	N/A
Site 22: Hwy 400 and Jane Street	timber pile penetrated through stratified deposits [cohesive and non-cohesive layers]	Timber Size 36 (treated Timber) [Butt f = 375 mm , tip f = 203 mm]	very stiff to hard clayey silt	14.5	N/A	818	1033	927	800	N/A	N/A	N/A
Site 23: HWY 401 and Country Road 14	Timber pile penetrated through very stiff to hard silty clay	Timber Size 36 (treated Timber) [Butt f = 356 mm , tip f = 254 mm]	very stiff to hard silty clay	3.1	N/A	445	382	346	320	N/A	N/A	N/A

Site	Soil Along Pile Length	Pile Type	Design Founding Stratum	Pile Length (m)	Ultimate Geotechnical Resistance (kN) Predicted by Foundation Designer	Ultimate Pile Capacity - Static Pile Load Test (kN)				Ultimate Pile Capacity - PDA and CAPWP analysis		
						Max. Applied Load during the Test (kN)	Modified Chin Method (1970)	Brinch Hansen's 90% Method (1963)	Davisson Offset Limit Load Method	Ultimate Pile Capacity (kN)	Shaft Capacity (kN)	Toe Capacity (kN)
Site 23: HWY 401 and Country Road 14	Steel tube penetrated through very stiff to hard silty clay	steel tube 324 OD x 6.3 mm thick (concreted filled)	very stiff to hard silty clay	3.0	N/A	589	503	453	390	N/A	N/A	N/A
Site 23: HWY 401 and Country Road 14	Timber pile penetrated through very stiff to hard silty clay	HP 310 x 110	very stiff to hard silty clay	3.1	N/A	445	380	340	300	N/A	N/A	N/A
Site 24: HWY 35 and Beech River	Timber pile penetrated through compact to dense sand to silt	Timber Size 36 (treated Timber) [Butt f = 381 mm , tip f = 251 mm]	compact to dense silt	14.3	N/A	1157	1029	921	712	N/A	N/A	N/A
Site 24: HWY 35 and Beech River	steel tube penetrated through compact to dense sand to silt	steel tube 324 OD x 5.2 mm thick (concreted filled)	compact to dense silt	15.4	N/A	1112	987	892	596	N/A	N/A	N/A
Site 24: HWY 35 and Beech River	steel tube penetrated through loose to dense sand to silt	steel tube 324 OD x 5.2 mm thick (concreted filled)	compact sand	22.4	N/A	1068	922	828	756	N/A	N/A	N/A
Site 24: HWY 35 and Beech River	Steel HP loose to dense sand to silt	HP 310 x 79	compact sand	22.4	N/A	1539	1485	1349	1200	N/A	N/A	N/A
Site 24: HWY 35 and Beech River	Steel HP penetrated through compact to dense sand to silt	HP 310 x 79	compact to dense silt	15.4	N/A	979	823	741	660	N/A	N/A	N/A
Site 25: HWY 401 and Elgin County Road 5	steel tube penetrated through stiff to very stiff silty clay	steel tube 324 OD x 6.3 mm thick	Stiff to very stiff silty clay	5.6	N/A	489	423	376	400	N/A	N/A	N/A

Site	Soil Along Pile Length	Pile Type	Design Founding Stratum	Pile Length (m)	Ultimate Geotechnical Resistance (kN) Predicted by Foundation Designer	Ultimate Pile Capacity - Static Pile Load Test (kN)				Ultimate Pile Capacity - PDA and CAPWP analysis		
						Max. Applied Load during the Test (kN)	Modified Chin Method (1970)	Brinch Hansen's 90% Method (1963)	Davisson Offset Limit Load Method	Ultimate Pile Capacity (kN)	Shaft Capacity (kN)	Toe Capacity (kN)
		(concreted filled)										
Site 25: HWY 401 and Elgin County Road 5	HP penetrated through stiff to very stiff silty clay	HP 310 x 79	Stif to very stiff silty clay	18.4	N/A	1094	967	873	950	N/A	N/A	N/A
Site 25: HWY 401 and Elgin County Road 5	steel tube penetrated through stiff to very stiff silty clay	steel tube 324 OD x 6.3 mm thick (concreted filled)	Stif to very stiff silty clay	18.4	N/A	916	881	796	800	N/A	N/A	N/A
Site 25: HWY 401 and Elgin County Road 5	steel tube penetrated through stiff to very stiff silty clay	steel tube 324 OD x 6.3 mm thick (concreted filled)	Stif to very stiff silty clay	9.3	N/A	623	534	484	480	N/A	N/A	N/A
Site 25: HWY 401 and Elgin County Road 5	HP penetrated through stiff to very stiff silty clay	HP 310 x 79	Stif to very stiff silty clay	9.4	N/A	534	448	403	440	N/A	N/A	N/A
Site 26: HWY 11 and Schomberg River	steel tube penetrated through peat and organic cohesive soil	steel tube 324 OD x 6.3 mm thick (concreted filled)	soft to firm organic silt and clay	12.2	N/A	178	160	145	130	N/A	N/A	N/A
Site 26: HWY 11 and Schomberg River	steel tube penetrated through peat, organic cohesive soil, and stiff to hard clayey silt	steel tube 324 OD x 6.3 mm thick (concreted filled)	stiff clayey silt	30.5	N/A	1246	1113	999	950	N/A	N/A	N/A
Site 26: HWY 11 and Schomberg River	steel tube penetrated through peat, organic cohesive soil, and stiff to hard clayey silt	steel tube 324 OD x 6.3 mm thick (concreted filled)	stiff clayey silt	42.7	N/A	1779	1584	1422	1584	N/A	N/A	N/A

Site	Soil Along Pile Length	Pile Type	Design Founding Stratum	Pile Length (m)	Ultimate Geotechnical Resistance (kN) Predicted by Foundation Designer	Ultimate Pile Capacity - Static Pile Load Test (kN)				Ultimate Pile Capacity - PDA and CAPWP analysis		
						Max. Applied Load during the Test (kN)	Modified Chin Method (1970)	Brinch Hansen's 90% Method (1963)	Davisson Offset Limit Load Method	Ultimate Pile Capacity (kN)	Shaft Capacity (kN)	Toe Capacity (kN)
Site 26: HWY 11 and Schomberg River	timber pile penetrated through peat, organic cohesive soil, and stiff to hard clayey silt	Timber Size 36 [Butt f = 429 mm , tip f = 203 mm]	stiff to hard clayey silt	22.0	N/A	1068	1047	950	890	N/A	N/A	N/A
Site 26: HWY 11 and Schomberg River	timber pile penetrated through peat and organic cohesive soil	Timber Size 36 [Butt f = 490 mm , tip f = 241 mm]	soft to firm organic silt and clay	12.2	N/A	534	484	432	445	N/A	N/A	N/A
Site 27: HWY 401 and Airport Road	rock socket	0.64 m dia. cast in place concrete socketed into shale bedrock	Shale bedrock	0.91 (rock socket length)	N/A		N/A	N/A	N/A	N/A	N/A	N/A
Site 27: HWY 401 and Airport Road	rock socket	0.59 m dia. cast in place concrete socketed into shale bedrock	Shale bedrock	1.4 (rock socket length)	N/A		N/A	N/A	N/A	N/A	N/A	N/A
Site 27: HWY 401 and Airport Road	rock socket	0.64 m dia. cast in place concrete socketed into shale bedrock	Shale bedrock	1.04 (rock socket length)	N/A		N/A	N/A	N/A	N/A	N/A	N/A
Site 28: HWY 402 and Blackwell Road	Steel HP penetrated through firm to very stiff clayey silt soil	HP 310 x 79	firm to vey stiff clayey silt	6.1	N/A	507	434	392	400	N/A	N/A	N/A
Site 28: HWY 402 and Blackwell Road	Steel HP penetrated through firm to very stiff clayey silt soil	HP 310 x 79	firm to vey stiff clayey silt	18.3	N/A	534	480	480	480	N/A	N/A	N/A



Site	Soil Along Pile Length	Pile Type	Design Founding Stratum	Pile Length (m)	Ultimate Geotechnical Resistance (kN) Predicted by Foundation Designer	Ultimate Pile Capacity - Static Pile Load Test (kN)				Ultimate Pile Capacity - PDA and CAPWP analysis		
						Max. Applied Load during the Test (kN)	Modified Chin Method (1970)	Brinch Hansen's 90% Method (1963)	Davisson Offset Limit Load Method	Ultimate Pile Capacity (kN)	Shaft Capacity (kN)	Toe Capacity (kN)
Site 28: HWY 402 and Blackwell Road	Steel HP penetrated through firm to very stiff clayey silt soil	HP 310 x 79	firm to vey stiff clayey silt	12.2	N/A	596	534	534	534	N/A	N/A	N/A
Site 28: HWY 402 and Blackwell Road	Precast reinforced concrete penetrated through firm to very stiff clayey silt soil	Herkules Type # 800 pre-cast concrete (avg. diameter 0.33 m)	firm to vey stiff clayey silt	11.9	N/A	507	400	400	400	N/A	N/A	N/A
Site 28: HWY 402 and Blackwell Road	Precast reinforced concrete penetrated through firm to very stiff clayey silt soil	Herkules Type # 800 pre-cast concrete (avg. diameter 0.33 m)	firm to vey stiff clayey silt	18.0	N/A	747	580	580	580	N/A	N/A	N/A
Site 28: HWY 402 and Blackwell Road	Precast reinforced concrete penetrated through firm to very stiff clayey silt soil	Herkules Type # 800 pre-cast concrete (avg. diameter 0.33 m)	firm to vey stiff clayey silt	5.8	N/A	774	748	748	748	N/A	N/A	N/A
Site 28: HWY 402 and Blackwell Road	steel tube penetrated through firm to very stiff clayey silt soil	steel tube 324 OD x 6.3 mm thick (concreted filled)	firm to vey stiff clayey silt	6.1	N/A	712	605	605	605	N/A	N/A	N/A
Site 28: HWY 402 and Blackwell Road	steel tube penetrated through firm to very stiff clayey silt soil	steel tube 324 OD x 6.3 mm thick (concreted filled)	firm to vey stiff clayey silt	18.3	N/A	774	507	507	507	N/A	N/A	N/A
Site 28: HWY 402 and Blackwell Road	steel tube penetrated through firm to very stiff clayey silt soil	steel tube 324 OD x 6.3 mm thick (concreted filled)	firm to vey stiff clayey silt	12.0	N/A	658	614	614	614	N/A	N/A	N/A

Site	Soil Along Pile Length	Pile Type	Design Founding Stratum	Pile Length (m)	Ultimate Geotechnical Resistance (kN) Predicted by Foundation Designer	Ultimate Pile Capacity - Static Pile Load Test (kN)				Ultimate Pile Capacity - PDA and CAPWP analysis		
						Max. Applied Load during the Test (kN)	Modified Chin Method (1970)	Brinch Hansen's 90% Method (1963)	Davisson Offset Limit Load Method	Ultimate Pile Capacity (kN)	Shaft Capacity (kN)	Toe Capacity (kN)
Site 29: HWY 7 and Duffin Creek	Timber pile penetrated through stratified deposits [cohesive and non-cohesive layers]	Timber Size 33 [Butt f = 338 mm , tip f = 229 mm]	Compact Sandy Silt	13.7	N/A	756	832	746	650	N/A	N/A	N/A
Site 30: E.C. Row Expressway And C. & O. Railway	Steel tube rest on top of limestone bedrock	steel tube 324 OD x 6.3 mm thick (concreted filled)	Limestone Bedrock	40.0	N/A	3559	5241	4693	4000	N/A	N/A	N/A
Site 31: HWY 4 and HWY 402	timber pile penetrated through stiff to hard clayey silt	Timber Size 36 [Butt f = 302 mm , tip f = 254 mm]	stiff to hard clayey silt	6.6	N/A	934	847	769	847	N/A	N/A	N/A
Site 31: HWY 4 and HWY 402	timber pile penetrated through stiff to hard clayey silt	Timber Size 30 [Butt f = 305 mm , tip f = 229 mm]	stiff to hard clayey silt	4.7	N/A	756	667	605	550	N/A	N/A	N/A
Site 31: HWY 4 and HWY 402	timber pile penetrated through stiff to hard clayey silt	Timber Size 36 [Butt f = 356 mm , tip f = 305 mm]	stiff to hard clayey silt	3.5	N/A	756	675	605	550	N/A	N/A	N/A
Site 32: HWY 402 and Broken Front Road	Timber pile penetrated through stratified deposits [cohesive and non-cohesive layers]	Timber Size 36 [Butt f = 375 mm , tip f = 216 mm]	very loose silt	13.5	N/A	934	867	775	800	N/A	N/A	N/A
Site 32: HWY 402 and Broken Front Road	Timber pile penetrated through stratified deposits [cohesive and	Timber Size 33 [Butt f = 337 mm , tip f = 248 mm]	very stiff to hard clayey silt	9.1	N/A	1201	1060	955	1000	N/A	N/A	N/A

Site	Soil Along Pile Length	Pile Type	Design Founding Stratum	Pile Length (m)	Ultimate Geotechnical Resistance (kN) Predicted by Foundation Designer	Ultimate Pile Capacity - Static Pile Load Test (kN)				Ultimate Pile Capacity - PDA and CAPWP analysis		
						Max. Applied Load during the Test (kN)	Modified Chin Method (1970)	Brinch Hansen's 90% Method (1963)	Davisson Offset Limit Load Method	Ultimate Pile Capacity (kN)	Shaft Capacity (kN)	Toe Capacity (kN)
	non-cohesive layers]											
Site 32: HWY 402 and Broken Front Road	Timber pile penetrated through stratified deposits [cohesive and non-cohesive layers]	Timber Size 30 [Butt f = 292 mm , tip f = 216 mm]	very stiff to hard clayey silt	7.6	N/A	756	613	554	550	N/A	N/A	N/A
Site 33: HWY 404 and 16th Ave.	Steel HP penetrated through stratified deposits [cohesive and non-cohesive layers]	HP 310 x 110	dense to very dense silty sand to sandy silt	34.9	N/A	3559	4873	4380	3400	N/A	N/A	N/A
Site 33: HWY 404 and 16th Ave.	Steel tube penetrated through stratified deposits [cohesive and non-cohesive layers]	steel tube 324 OD x 6.3 mm thick (concreted filled)	dense to very dense silty sand to sandy silt	32.7	N/A	2669	2654	2374	2600	N/A	N/A	N/A
Site 33: HWY 404 and 16th Ave.	Reinforced concrete pile penetrated through stratified deposits [cohesive and non-cohesive layers]	RC 0.305 x 0.305	dense to very dense silty sand to sandy silt	34.9	N/A	2891	2874	2586	2600	N/A	N/A	N/A
Site 33: HWY 404 and 16th Ave.	timber pile penetrated through stratified deposits [cohesive and non-cohesive layers]	Timber Size 36 [Butt f = 406 mm , tip f = 305 mm]	dense silty sand to sandy silt	8.7	N/A	1334	1327	1203	890	N/A	N/A	N/A
Site 34: HWY 648 at Pursey and Grace Lake	steel tube penetrated through sandy silt	steel tube 324 OD x 6.3 mm thick	compact sandy silt	18.6	N/A	507	462	415	520	N/A	N/A	N/A

Site	Soil Along Pile Length	Pile Type	Design Founding Stratum	Pile Length (m)	Ultimate Geotechnical Resistance (kN) Predicted by Foundation Designer	Ultimate Pile Capacity - Static Pile Load Test (kN)				Ultimate Pile Capacity - PDA and CAPWP analysis		
						Max. Applied Load during the Test (kN)	Modified Chin Method (1970)	Brinch Hansen's 90% Method (1963)	Davisson Offset Limit Load Method	Ultimate Pile Capacity (kN)	Shaft Capacity (kN)	Toe Capacity (kN)
		(concreted filled)										
Site 35: NWMA at C.N.R. and C.P.R.	Steel HP penetrated through stratified deposits [cohesive and non-cohesive layers]	HP 310 x 110	compact to dense silty sand	14.8	N/A	1868	1684	1508	1400	N/A	N/A	N/A
Site 35: NWMA at C.N.R. and C.P.R.	Steel tube penetrated through stratified deposits [cohesive and non-cohesive layers]	steel tube 324 OD x 6.3 mm thick (concreted filled)	compact to dense silty sand	14.7	N/A	1690	1504	1354	1400	N/A	N/A	N/A
Site 35: NWMA at C.N.R. and C.P.R.	Steel HP penetrated through stratified deposits [cohesive and non-cohesive layers]	HP 310 x 110	compact to dense silty sand	27.6	N/A	2891	2987	2704	2700	N/A	N/A	N/A
Site 35: NWMA at C.N.R. and C.P.R.	Steel tube penetrated through stratified deposits [cohesive and non-cohesive layers]	steel tube 324 OD x 6.3 mm thick (concreted filled)	compact to dense silty sand	27.4	N/A	2669	2588	2330	2500	N/A	N/A	N/A
Site 35: NWMA at C.N.R. and C.P.R.	timber pile penetrated through stratified deposits [cohesive and non-cohesive layers]	Timber Size 36 [Butt f = 356 mm , tip f = 229 mm]	compact to dense silty sand	12.7	N/A	890	814	726	650	N/A	N/A	N/A
Site 35: NWMA at C.N.R. and C.P.R.	pre-cast concrete penetrated through stratified deposits [cohesive and	305 mm x 305 mm concrete	compact to dense silty sand	14.6	N/A	2313	2063	1854	1800	N/A	N/A	N/A

Site	Soil Along Pile Length	Pile Type	Design Founding Stratum	Pile Length (m)	Ultimate Geotechnical Resistance (kN) Predicted by Foundation Designer	Ultimate Pile Capacity - Static Pile Load Test (kN)				Ultimate Pile Capacity - PDA and CAPWP analysis		
						Max. Applied Load during the Test (kN)	Modified Chin Method (1970)	Brinch Hansen's 90% Method (1963)	Davisson Offset Limit Load Method	Ultimate Pile Capacity (kN)	Shaft Capacity (kN)	Toe Capacity (kN)
	non-cohesive layers]											
Site 36: E.C. Row Expressway and C.P.R.	Steel tube penetrated through stratified deposits [cohesive and non-cohesive layers]	steel tube 324 OD x 6.3 mm thick (concreted filled)	very dense sandy silt to silt	29.6	N/A	2011	2153	1954	1800	N/A	N/A	N/A
Site 36: E.C. Row Expressway and C.P.R.	Steel tube penetrated through stratified deposits [cohesive and non-cohesive layers]	steel tube 324 OD x 6.3 mm thick (concreted filled)	very dense sandy silt to silt	31.4	N/A	2011	4045	3228	3000	N/A	N/A	N/A
Site 37: Q.E.W. and Burlington Skyway	Steel HP rest on shale bedrock	HP 310 x 79	shale bedrock	39.3	N/A	2313	N/A	N/A	N/A	N/A	N/A	N/A
Site 37: Q.E.W. and Burlington Skyway	Steel HP rest on shale bedrock	HP 310 x 79	shale bedrock	38.7	N/A	2313	N/A	N/A	N/A	N/A	N/A	N/A
Site 37: Q.E.W. and Burlington Skyway	steel HP penetrated through compact to very dense silty sand to sandy silt	HP 310 x 79	compact to very dense silty sand to sandy silt	14.5	N/A	1197	1128	1027	1100	N/A	N/A	N/A
Site 37: Q.E.W. and Burlington Skyway	steel HP penetrated through compact to very dense silty sand to sandy silt	HP 310 x 79	compact to very dense silty sand to sandy silt	38.9	N/A	2313	4085	3690	3000	N/A	N/A	N/A
Site 37: Q.E.W. and Burlington Skyway	steel HP penetrated through compact to very dense silty sand to sandy silt	HP 310 x 79	compact to very dense silty sand to sandy silt	31.2	N/A	1933	1792	1614	1700	N/A	N/A	N/A

Site	Soil Along Pile Length	Pile Type	Design Founding Stratum	Pile Length (m)	Ultimate Geotechnical Resistance (kN) Predicted by Foundation Designer	Ultimate Pile Capacity - Static Pile Load Test (kN)				Ultimate Pile Capacity - PDA and CAPWP analysis		
						Max. Applied Load during the Test (kN)	Modified Chin Method (1970)	Brinch Hansen's 90% Method (1963)	Davisson Offset Limit Load Method	Ultimate Pile Capacity (kN)	Shaft Capacity (kN)	Toe Capacity (kN)
Site 37: Q.E.W. and Burlington Skyway	steel HP penetrated through compact to very dense silty sand to sandy silt	HP 310 x 79	compact to very dense silty sand to sandy silt	14.5	N/A	1069	897	801	750	N/A	N/A	N/A
Site 37: Q.E.W. and Burlington Skyway	steel HP penetrated through compact to very dense silty sand to sandy silt	HP 310 x 79	compact to very dense silty sand to sandy silt	45.3	N/A	2313	2854	2563	2600	N/A	N/A	N/A
Site 37: Q.E.W. and Burlington Skyway	steel HP penetrated through compact to very dense silty sand to sandy silt	HP 310 x 79	compact to very dense silty sand to sandy silt	30.9	N/A	2135	2945	2628	2400	N/A	N/A	N/A
Site 37: Q.E.W. and Burlington Skyway	timber pile penetrated through loose to dense sand to silty sand	Timber Size 36 [Butt f = 356 mm , tip f = 229 mm]	dense sand	9.6	N/A	761	686	612	600	N/A	N/A	N/A
Site 37: Q.E.W. and Burlington Skyway	timber pile penetrated through loose to dense sand to silty sand	Timber Size 36 [Butt f = 356 mm , tip f = 229 mm]	dense sand	10.4	N/A	956	808	727	700	N/A	N/A	N/A
Site 38: HWY 115 and Country Road 10	Steel HP penetrated through stratified deposits [cohesive and non-cohesive layers]	HP 310 x 110	very dense sandy silt to silty sand	16.2	N/A	2669	3720	3328	2400	N/A	N/A	N/A
Site 38: HWY 115 and Country Road 10	timber pile penetrated through silty clay to clayey silt	Timber Size 36 [Butt f = 400 mm , tip f = 350 mm]	compact to dense sand	3.3	N/A	554	517	466	450	N/A	N/A	N/A
Site 38: HWY 115 and Country Road 10	timber pile penetrated through stratified deposits	Timber Size 34 [Butt f = 340 mm ,	compact to dense sand	5.0	N/A	547	483	488	400	N/A	N/A	N/A

Site	Soil Along Pile Length	Pile Type	Design Founding Stratum	Pile Length (m)	Ultimate Geotechnical Resistance (kN) Predicted by Foundation Designer	Ultimate Pile Capacity - Static Pile Load Test (kN)				Ultimate Pile Capacity - PDA and CAPWP analysis		
						Max. Applied Load during the Test (kN)	Modified Chin Method (1970)	Brinch Hansen's 90% Method (1963)	Davisson Offset Limit Load Method	Ultimate Pile Capacity (kN)	Shaft Capacity (kN)	Toe Capacity (kN)
	[cohesive and non-cohesive layers]	tip f = 220 mm]										
Site 38: HWY 115 and Country Road 10	steel tube penetrated through stratified deposits [cohesive and non-cohesive layers]	steel tube 324 OD x 9.5 mm thick (concreted filled)	very dense sandy silt to silty sand	11.9	N/A	1112	1063	950	700	N/A	N/A	N/A
Site 38: HWY 115 and Country Road 10	steel tube penetrated through stratified deposits [cohesive and non-cohesive layers]	steel tube 324 OD x 9.5 mm thick (concreted filled)	very dense sandy silt to silty sand	16.1	N/A	2615	2604	2329	1800	N/A	N/A	N/A
Site 39: HWY 552 and Goulais River	timber pile penetrated through stratified deposits [cohesive and non-cohesive layers]	Timber Size 36 [Butt f = 400 mm , tip f = 245 mm]	compact silt	17.1	N/A	1245	1368	1228	1200	N/A	N/A	N/A
Site 39: HWY 552 and Goulais River	Steel HP penetrated through stratified deposits [cohesive and non-cohesive layers]	HP 310 x 110	compact silt	25.5	N/A	1468	1329	1201	1300	N/A	N/A	N/A
Site 39: HWY 552 and Goulais River	steel tube penetrated through stratified deposits [cohesive and non-cohesive layers]	steel tube 324 OD x 9.5 mm thick (concreted filled)	compact silt	25.4	N/A	1512	1382	1250	1300	N/A	N/A	N/A
Site 40: HWY 17 and Garden River	timber pile penetrated through stratified deposits [cohesive and	Timber Size 36 [Butt f = 360 mm ,	dense to very dense sand	14.7	N/A	1219	1247	1247	1200	N/A	N/A	N/A

Site	Soil Along Pile Length	Pile Type	Design Founding Stratum	Pile Length (m)	Ultimate Geotechnical Resistance (kN) Predicted by Foundation Designer	Ultimate Pile Capacity - Static Pile Load Test (kN)				Ultimate Pile Capacity - PDA and CAPWP analysis		
						Max. Applied Load during the Test (kN)	Modified Chin Method (1970)	Brinch Hansen's 90% Method (1963)	Davisson Offset Limit Load Method	Ultimate Pile Capacity (kN)	Shaft Capacity (kN)	Toe Capacity (kN)
	non-cohesive layers]	tip f = 240 mm]										
Site 40: HWY 17 and Garden River	Steel HP penetrated through stratified deposits [cohesive and non-cohesive layers]	HP 310 x 110	dense to very dense sand	24.5	N/A	1254	1190	1070	1100	N/A	N/A	N/A
Site 40: HWY 17 and Garden River	steel tube penetrated through stratified deposits [cohesive and non-cohesive layers]	steel tube 324 OD x 9.5 mm thick (concreted filled)	dense to very dense sand	17.2	N/A	1192	1079	982	1100	N/A	N/A	N/A
Site 41: HWY 17 and Root River	timber pile penetrated through very loose to compact sand	Timber Size 36 [Butt f = 400 mm , tip f = 245 mm]	compact sand	8.0	N/A	934	866	775	800	N/A	N/A	N/A
Site 41: HWY 17 and Root River	Steel HP penetrated through very loose to compact sand	HP 310 x 110	very dense sand	19.5	N/A	1779	2510	2268	2300	N/A	N/A	N/A
Site 41: HWY 17 and Root River	steel tube penetrated through very loose to compact sand	steel tube 324 OD x 9.5 mm thick (concreted filled)	very dense sand	16.0	N/A	1779	1864	1691	1800	N/A	N/A	N/A





## **Appendix B**

**Results of PLTs Carried out at 9 MOT Sites Across Ontario Between 2016 - 2019**

## **Appendix B**

**Results of PLTs Carried out at 9 MOT Sites Across Ontario Between 2016 - 2019**

## Recent SPLT Reports - 9 MTO Sites

a. Hwy 401 - Fletcher's Creek

b. Hwy 400 - South Canal

c. Hwy 401 - Third Line (Bainsville)

d. Hwy 569 - Blanche River Bridge)

e. Hwy 400 - 89 Interchange)

f. Hwy 417 - Ramsayville)

g. Hwy 400 - Essa Rd

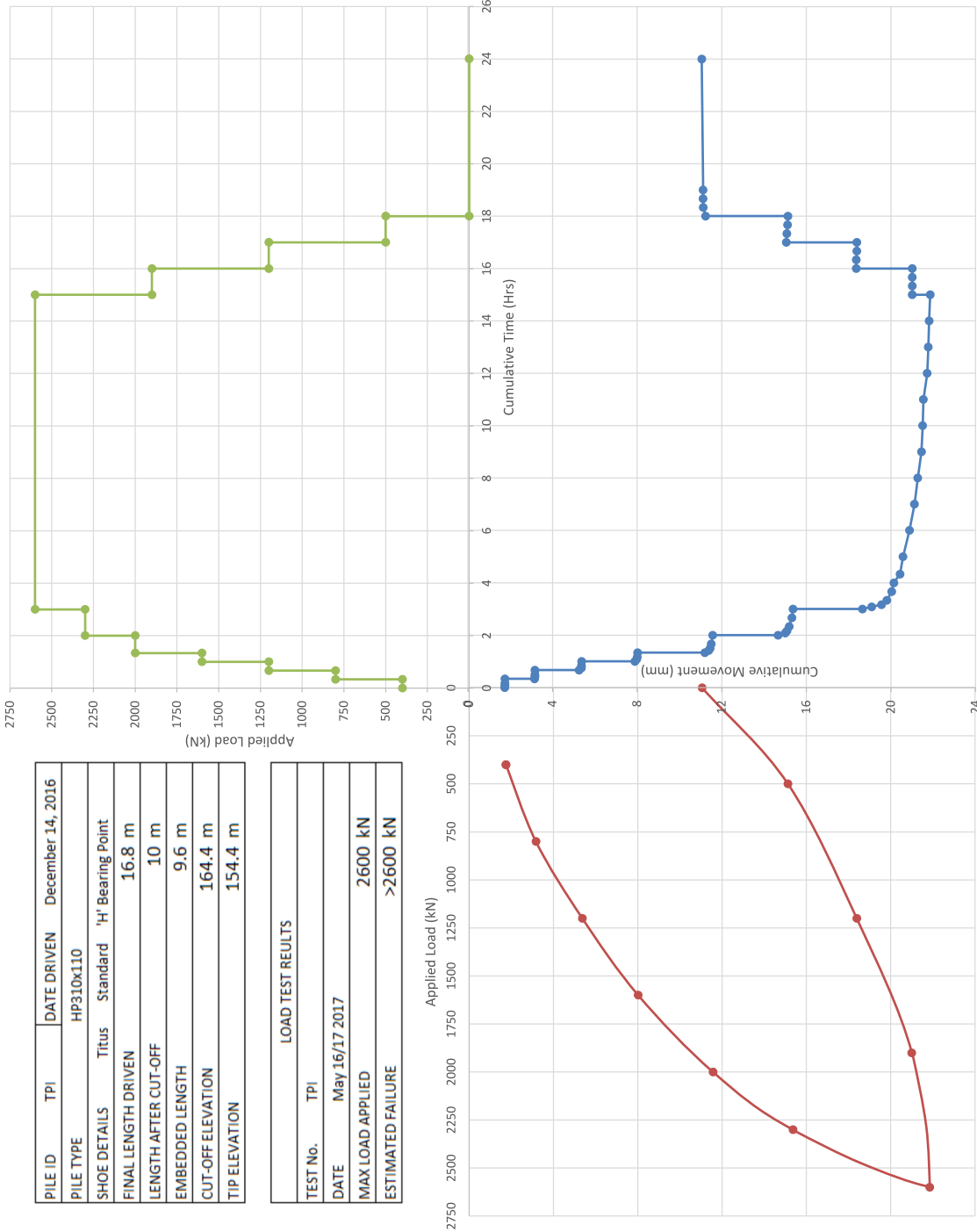
h. Rainy River - Baudette River International Bridge

i. Hwy 17 - Pic River

**a. Hwy 401 - Fletcher's Creek**

PILE ID	TPI	DATE DRIVEN	December 14, 2016
HP310x110			
SHOE DETAILS	Titus	Standard	'H' Bearing Point
FINAL LENGTH DRIVEN	16.8 m		
LENGTH AFTER CUT-OFF	10 m		
EMBEDDED LENGTH	9.6 m		
CUT-OFF ELEVATION	164.4 m		
TIP ELEVATION	154.4 m		

LOAD TEST RESULTS			
TEST No.	TPI		
DATE	May 16/17 2017		
MAX LOAD APPLIED	2600 kN		
ESTIMATED FAILURE	>2600 kN		



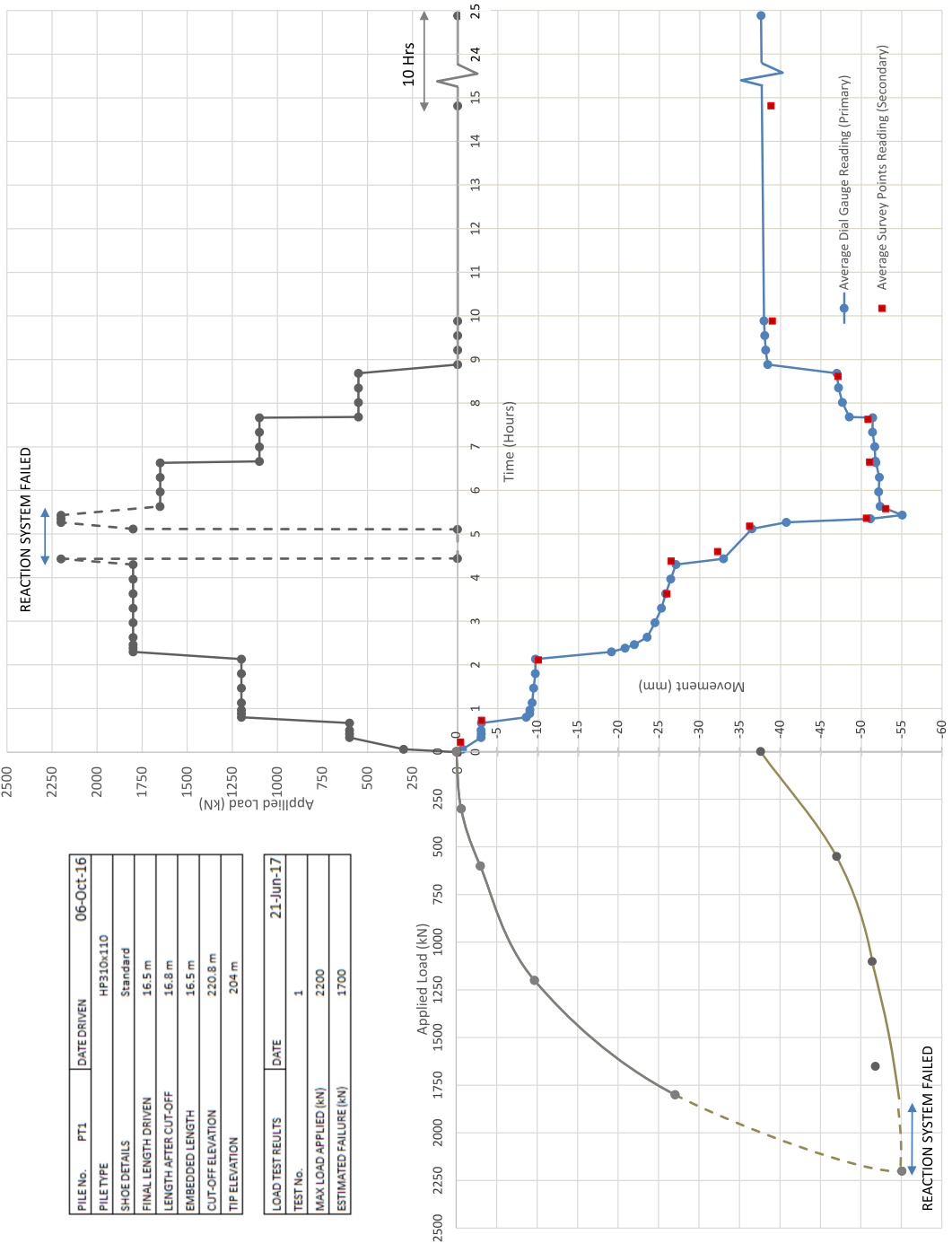
PROJECT  
HIGHWAY 401- FLETCHER'S CREEK BRIDGE  
MISSISSAUGA, ONTARIO

TITLE  
STATIC PILE LOAD TEST RESULTS

CLIENT	AECOM / MTO	CONSULTANT	YYY-AAA-DD	2017-10-06
PREPARED	DH	DESIGN	DH	
REVIEW	KJB	APPROVED	MSDJMAC	



**b. Hwy 400 - South Canal**

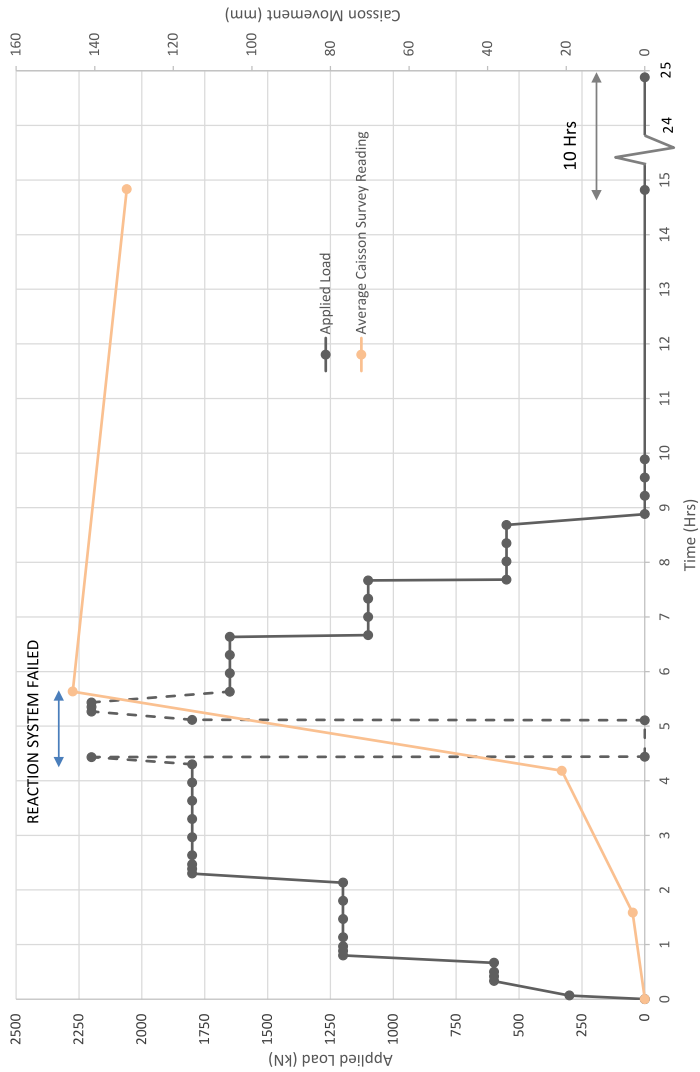


PILE No.	PT1	DATE DRIVEN	06-Oct-16
PILE TYPE	HP310x110		
SHOE DETAILS	Standard		
FINAL LENGTH DRIVEN	16.5 m		
LENGTH AFTER CUT-OFF	16.8 m		
EMBEDDED LENGTH	16.5 m		
CUT-OFF ELEVATION	220.8 m		
TIP ELEVATION	204 m		

LOAD TEST RESULTS	DATE	21-Jun-17
TEST No.	1	
MAX LOAD APPLIED (kN)	2200	
ESTIMATED FAILURE (kN)	1700	

PILE No.	PT1	DATE DRIVEN	06-Oct-16
PILE TYPE			
SHOE DETAILS			
Standard			
FINAL LENGTH DRIVEN			
16.5 m			
LENGTH AFTER CUT-OFF			
16.8 m			
EMBEDDED LENGTH			
16.5 m			
CUT-OFF ELEVATION			
220.8 m			
TIP ELEVATION			
204 m			

LOAD TEST RESULTS	DATE	21-Jun-17
TEST No.		
1		
MAX LOAD APPLIED (kN)		
2200		
ESTIMATED FAILURE (kN)		
1700		



CLIENT  
AECOM / MTO

PROJECT  
HIGHWAY 400 – SOUTH CANAL BRIDGE  
NEWMARKET, ONTARIO

CONSULTANT  
Golder Associates

PREPARED  
DH

DESIGN  
DH

REVIEW  
###

APPROVED  
###

TITLE  
RESPONSE OF REACTION SYSTEM  
(CAISSONS) DURING PILE LOAD TEST

PROJECT No.  
09-1111-0018



**c. Hwy 401 - Third Line (Brainsville)**



**Ottawa (Head Office)**  
589 Rideau St., Unit 212  
Ottawa, ON - K1N 6A1  
Tel: 613.789.6333 Fax: 613.789.5333

Toll Free: 1.877.789.6333  
Email: [info@aattechscientific.com](mailto:info@aattechscientific.com)  
Web: [www.aattechscientific.com](http://www.aattechscientific.com)

**Calgary**  
100, 111 - 5 Avenue SW  
Suite 312  
Calgary, AB - T2P 3Y6  
Tel: 403.261.0023 Fax: 403.261.0024

**New York**  
26000 U.S RT 11, Suite 194  
Evans Mills, NY 13637  
Tel: 315.703.9677 Fax: 315.703.9668

# 3<sup>rd</sup> Line Bridge – Hwy 401, MTO – 2017-4048 Bainsville, ON

## Report 2 Static Compression Loading Test

Project No. 94671802

Prepared for

Dufresne Piling Company Ltd  
Tomlinson Group  
100 Citigate Drive,  
Ottawa, ON K2J 6K7

August 30, 2018



**Ottawa (Head Office)**  
589 Rideau St., Unit 212  
Ottawa, ON - K1N 6A1  
Tel: 613.789.6333 Fax: 613.789.5333

Toll Free: 1.877.789.6333  
Email: [info@aattechscientific.com](mailto:info@aattechscientific.com)  
Web: [www.aattechscientific.com](http://www.aattechscientific.com)

**Calgary**  
100, 111 - 5 Avenue SW  
Suite 312  
Calgary, AB - T2P 3Y6  
Tel: 403.261.0023 Fax: 403.261.0024

**New York**  
26000 U.S RT 11, Suite 194  
Evans Mills, NY 13637  
Tel: 315.703.9677 Fax: 315.703.9668

# 3<sup>rd</sup> Line Bridge – Hwy 401, MTO – 2017-4048 Bainsville, ON

## Report 2 Static Compression Loading Test

Project No. 94671802

Prepared for

Dufresne Piling Company Ltd  
Tomlinson Group  
100 Citigate Drive,  
Ottawa, ON K2J 6K7

August 30, 2018

Prepared by:

Mudasser Noor, B.A.Sc., P. Eng.



30/08/2018

H. (Sam) Salem, M.A.Sc., P. Eng.

## Table of contents

<b><u>Section</u></b>	<b><u>Page</u></b>
INTRODUCTION .....	1
SITE CHARACTERISTICS.....	1
PILE LAYOUT AND TEST SETUP .....	1
TEST RESULTS .....	3
CONCLUSIONS AND RECOMMENDATIONS.....	6

### **Appendices:**

**Appendix 1:** Design drawings by ASI

**Appendix 2:** Static loading test data

## INTRODUCTION

AA Tech Scientific Inc. (ASI) was retained by Dufresne Piling Company (1967) Ltd. (Dufresne), a part of Tomlinson Group, to perform a static and dynamic loading tests on existing piles at the demolished Pier 1 of the 3<sup>rd</sup> Line Bridge over HWY 401 in Bainsville, ON. This report presents the factual results of a compression test performed on Pile TP 2 at this site. The test was performed over two visits on 8<sup>th</sup> and 20<sup>th</sup> of August 2018.

The objective of this test was to verify capacity of the pile which was installed in 1961, based on available documents. The maximum test load, as provided by MTO specifications, is 2,000 kN.

The testing and the interpretation provided in this report are in accordance with ASTM Standard D1143-07(14), Maintained test.

## SITE CHARACTERISTICS

As per the geotechnical report by Thurber Engineering Ltd. dated September 2017, the site below Pier 1 consists of about 6 m to 8 m of soft to stiff silty clay followed by about 4 to 5 m of compact to dense sandy till down to limestone bedrock where the piles are seated.

## PILE LAYOUT AND TEST SETUP

The test pile was identified as an HP310x79 steel section and is located at the center of the north pile bend. The total length of the pile was about 12.6 m, as verified by ASI during pile extraction, with about 12.4 m below the underside of the cap (excavated grade) at the time of testing. The test pile was loaded against a reaction system, initially connected to two existing piles at the east and west extremities of the pier. A first test on August 8, 2018 was terminated prematurely as the welded brackets were shearing off the top of the web of the reaction piles. At the same time, the early results of the partial loading test suggested that the reaction piles would not have enough pullout resistance to complete the test. Therefore, additional reaction was proposed using dowels epoxied into the concrete cap near the reaction piles for the second test. The dowels were connected to the reaction frame with sufficient slack to allow for them to be loaded only after the reaction piles are fully engaged. Details on the reaction setup can be found in ASI's design drawings dated August 13, 2018, enclosed in Appendix 1. A photo of the actual test setup is shown in Figure 1.

One 200-tonne ASI hydraulic jack was used to apply the load. One Geokon (model 3000) resistive load cell and Novotechnik TRS electronic displacement transducers were used to control and monitor the test while sampled simultaneously by a specialized datalogger. Two displacement transducers were installed at opposite sides of the pile to monitor pile head movement against a reference beam and one transducer was placed on each reaction pile to monitor their performance. The pile and test layout are illustrated in Figure 2.

Data was collected simultaneously at 10-second intervals throughout most of the test. A lower collection rate was used through periods of long-duration sustained loading. A copy of the complete data is enclosed in Appendix 2.



Figure 1. Pile, instrumentation, and reaction system

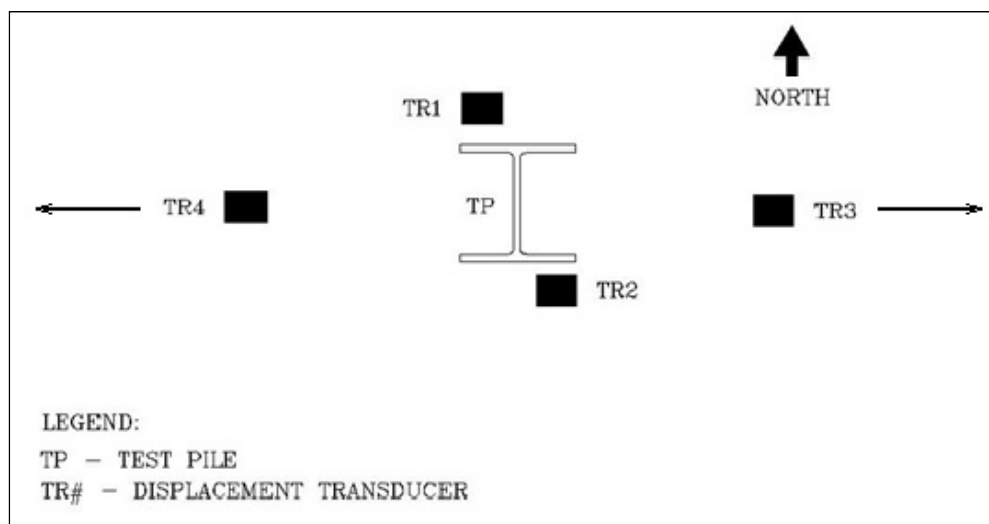


Figure 2. Pile and test layout (not to scale)

## TEST RESULTS

The load was applied in increments of 250 kN, per ASTM, Procedure B (maintained test). Each increment was sustained between 20 minutes and 120 minutes, depending on the rate of pile head movement, and the maximum load was sustained for the balance of 12 hours of test duration where the movement rate threshold of 0.25 mm/h was not exceeded. The pile was unloaded in four equal decrements sustained for 60 minutes each.

Graphical results of both the initial partial test and the final test (first and second tests) are shown as load vs. average displacement in Figure 3 and Figure 4 shows the measurements from all displacement transducers including those at the reaction piles. Despite the backup connection to the pier block, the eastern reaction pile started pulling out excessively near the end of the loading cycle (see Figure 4), and became unsustainable just before reaching the 2,000 kN load. As can be seen in Figure 3, the applied load had to be dropped to about 1,900 kN to maintain it. It was apparent from later inspection that the concrete cap had cracked and was breaking free from the edge piles while lifting up with the reaction pile. The test was successfully sustained around 1,850 kN to 1,900 kN for the remainder of the test duration.

Load vs. Displacement - Pile TP2

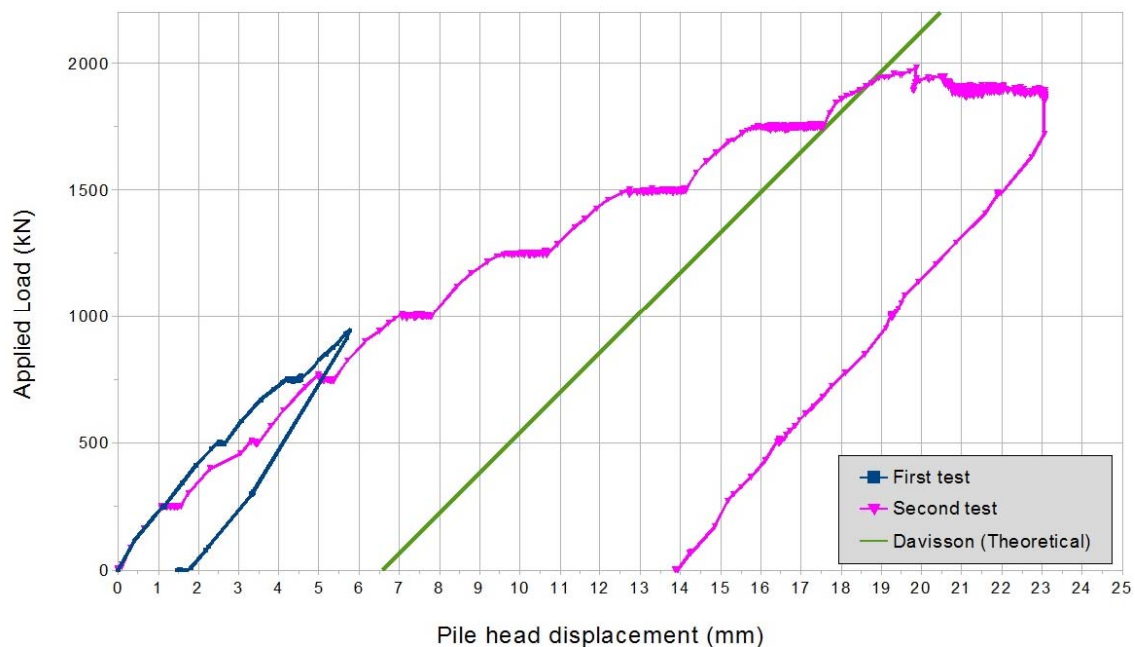
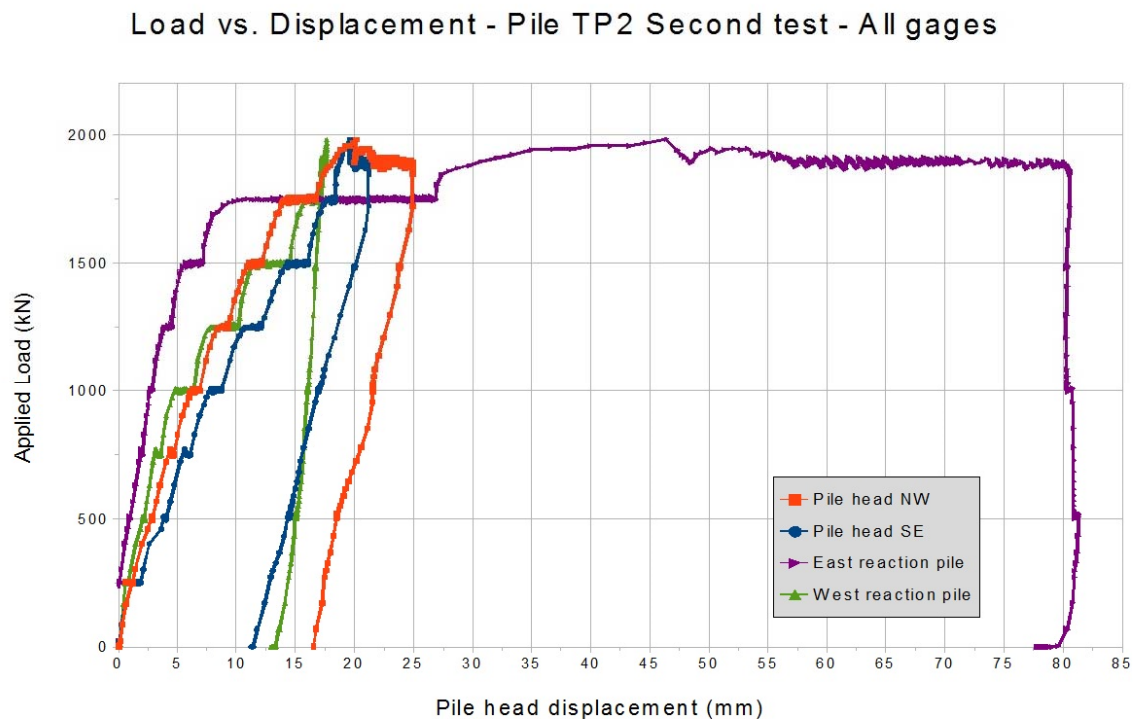


Figure 3: Load vs. averaged pile head movement (first and second tests)



**Figure 4: Load vs. pile head movement (final test, both transducers), plus reaction pile movement**

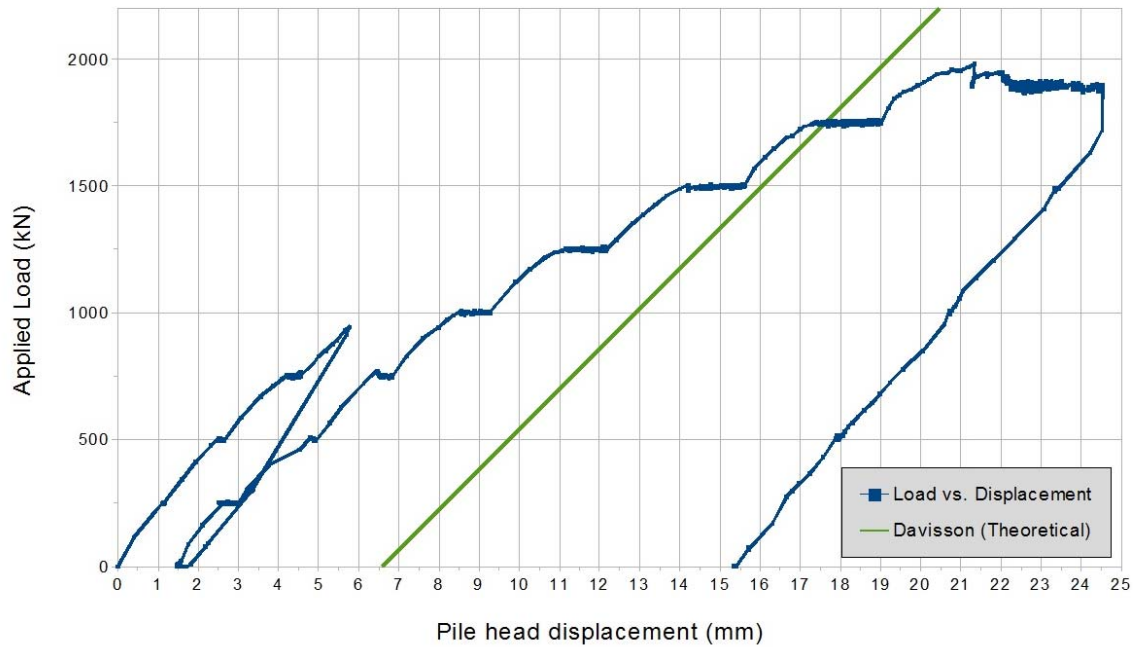
While the pile may offer further resistance, it can be seen in Figure 3 that the Davisson offset failure criterion was exceeded (practical serviceability criterion). This can be further accentuated when the two tests are plotted sequentially as shown in Figure 5, which is a more accurate way to represent the test results.

The data for pile head movement with time at the maximum applied load through to the unloading at the end of the test is shown in Figure 6. The data shows that the pile was stable under the applied load towards the end of the loading cycle.

A maximum pile head movement of 24.54 mm was reached at the end of the sequential loading cycle before final unloading. A residual displacement of 15.35 mm was measured at the end of the sequential testing with negligible time-dependent rebound after complete unloading.

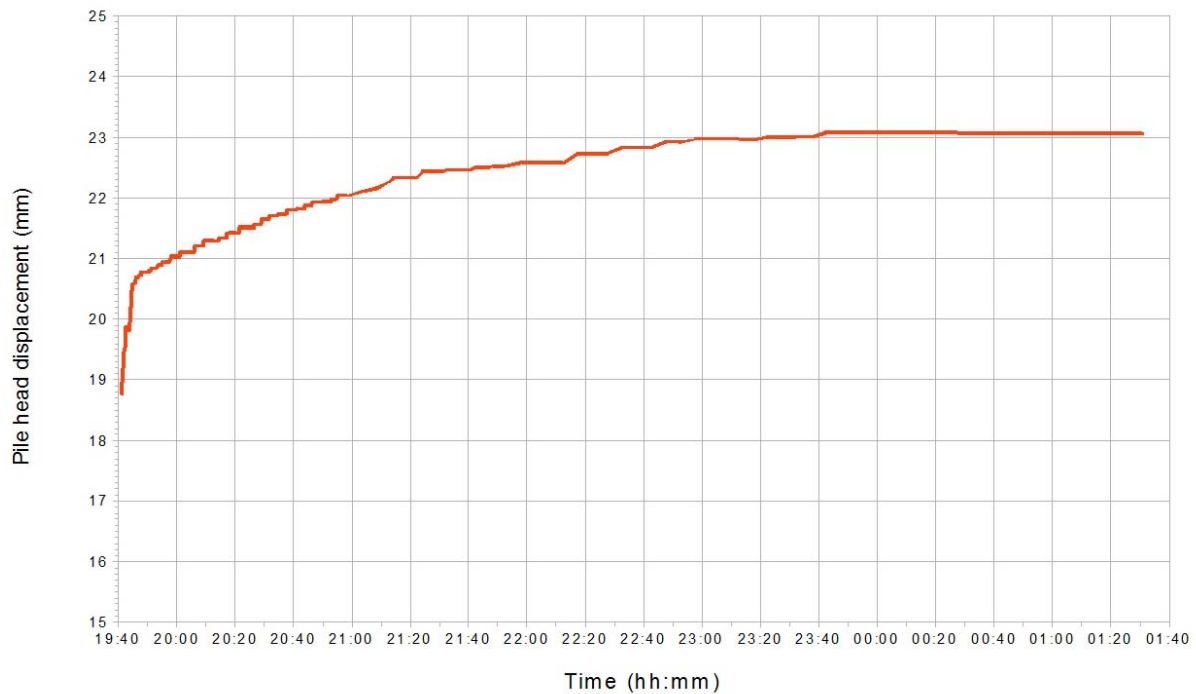


### Load vs. Displacement - Pile TP2 - Sequential test data



**Figure 5: Load vs. pile head movement, first and second tests plotted in sequence.**

### Displacement vs. time at max. load - Pile TP2



**Figure 6: Pile head movement with time while the maximum load was sustained.**

## CONCLUSIONS AND RECOMMENDATIONS

The test pile was loaded to about 2,000 kN; however, a load of about 1,900 kN was sustained due to excessive movement in the west side reaction support. A prior partial test that was terminated prematurely is also reported herein and the two tests are presented in a sequential fashion to account for the entire loading history.

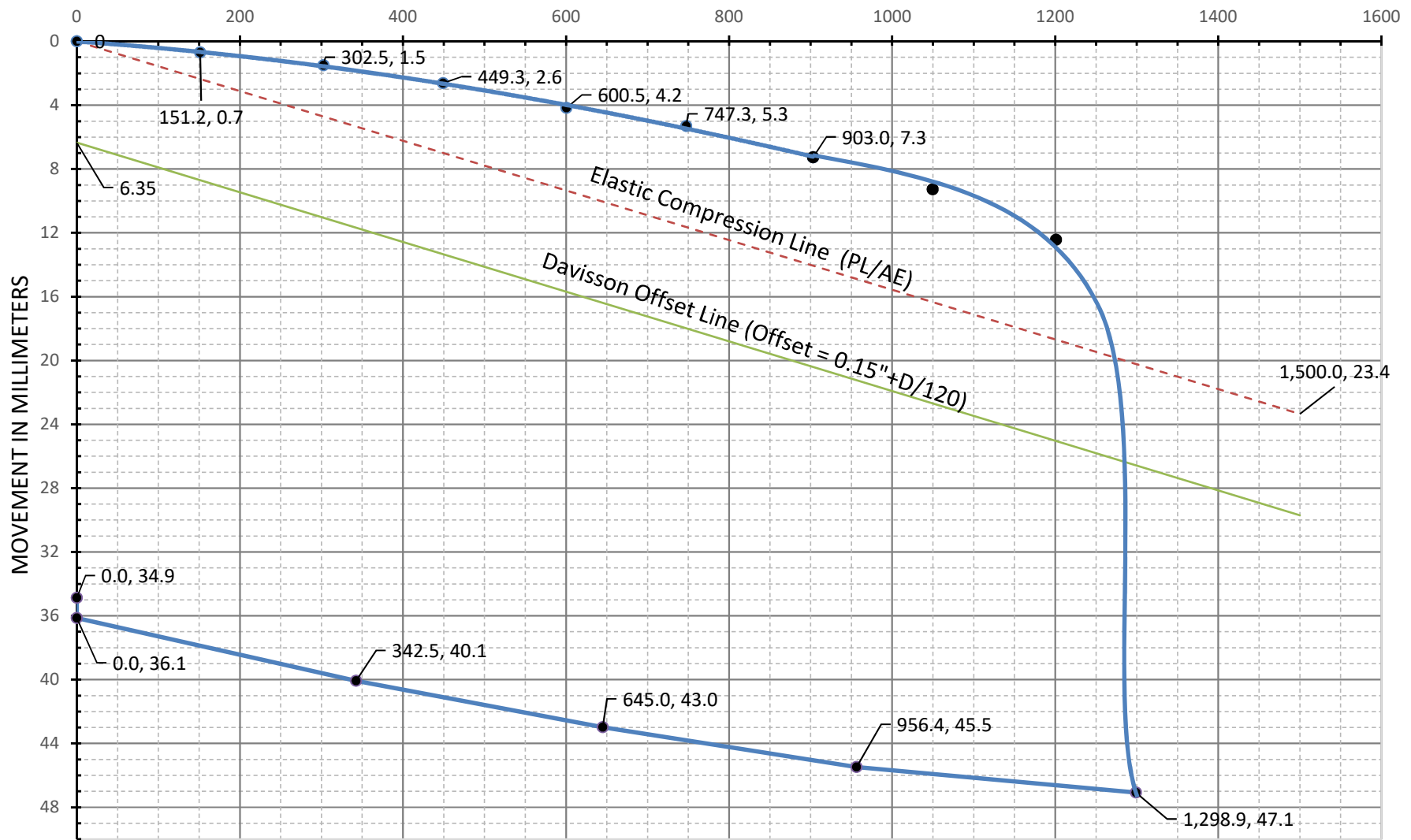
The data for pile head movement with time at the maximum applied load shows that the pile was stable under the applied load towards the end of the loading cycle. While the pile may be capable of sustaining higher loads, Davisson offset criterion (practical serviceability criterion) was exceeded before the final load increment.

A maximum pile head movement of 24.54 mm was reached at the end of the sequential loading cycle before final unloading. A residual displacement of 15.35 mm was measured at the end of the sequential testing with negligible time-dependent rebound after complete unloading.

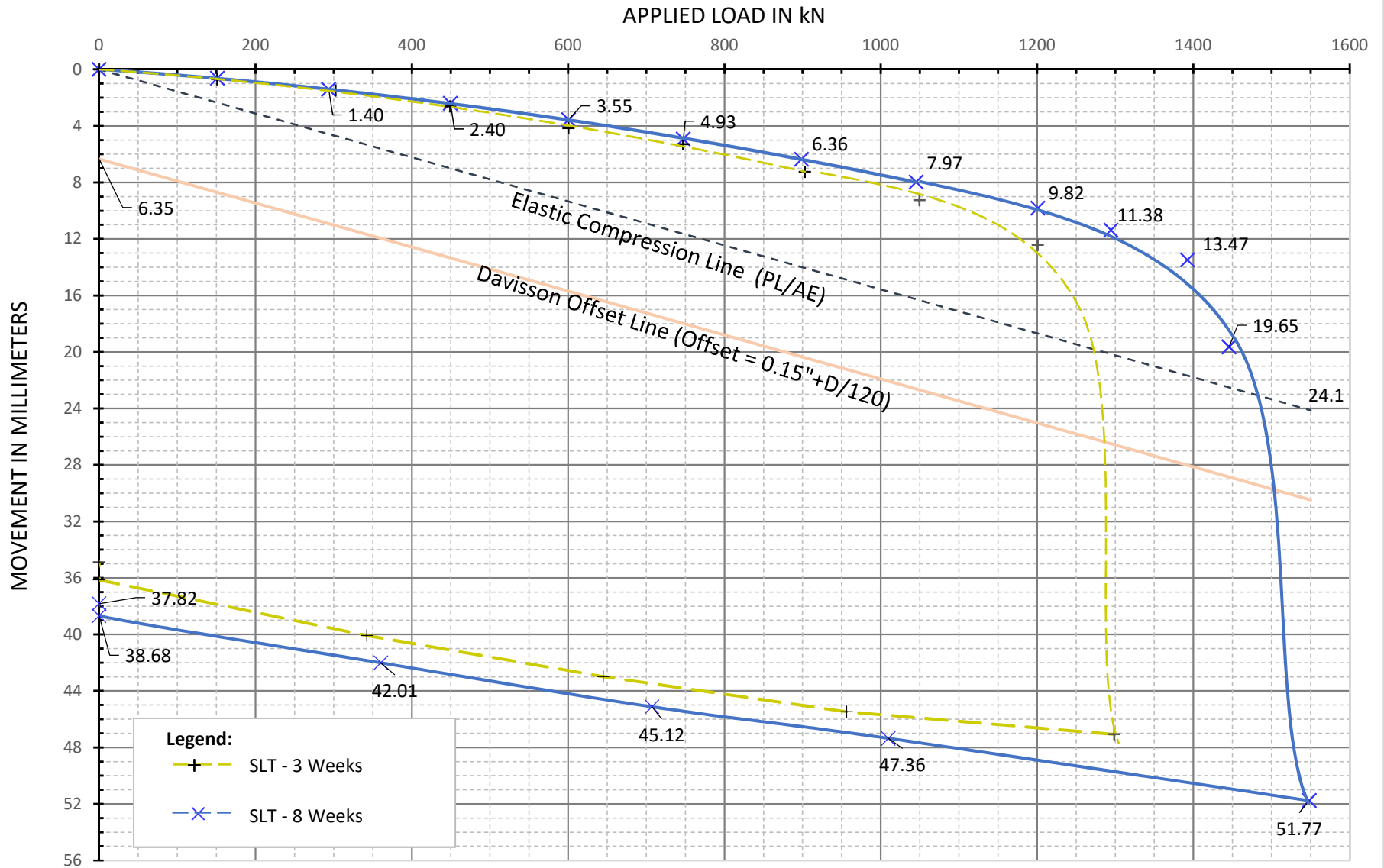
These results apply only to the tested pile. Extending these test results to other piles at the site is dependent on site conditions and other factors, and is beyond the scope of this report.

**d. Hwy 569 - Blanche River Bridge**

DRAWING 1  
 STATIC LOAD TEST ON PILE TP1 (3 WEEKS AFTER DRIVING)  
 LOAD MOVEMENT PLOT  
 APPLIED LOAD IN kN

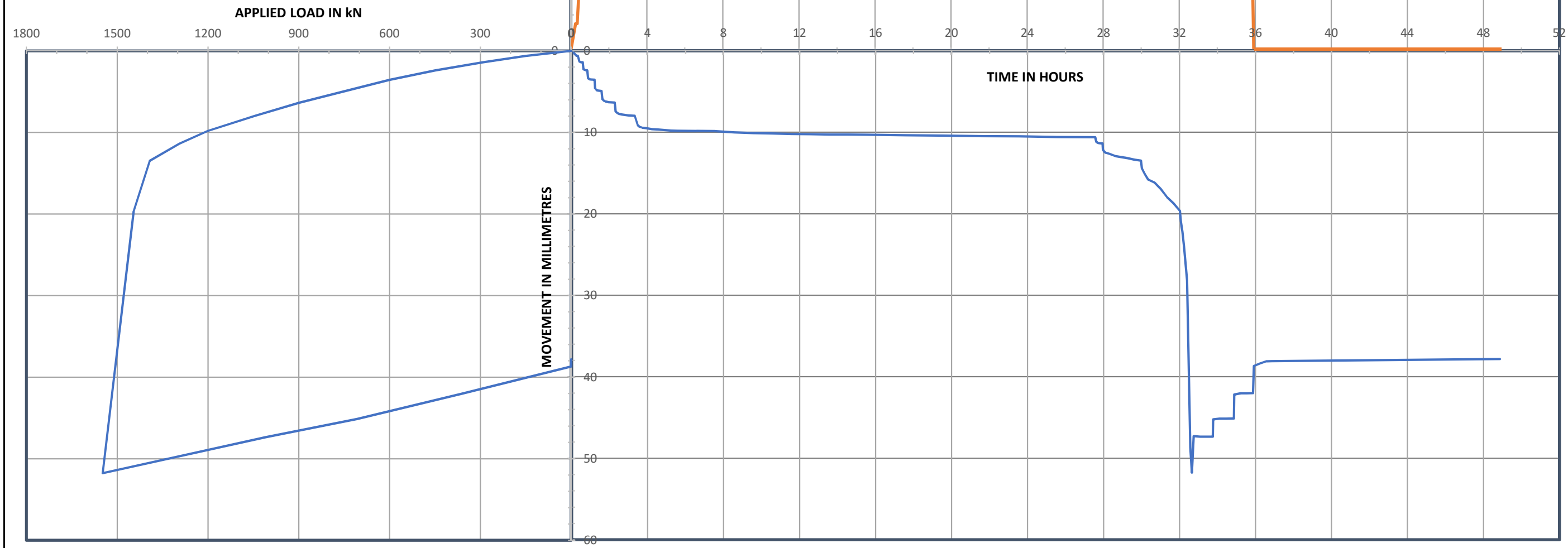
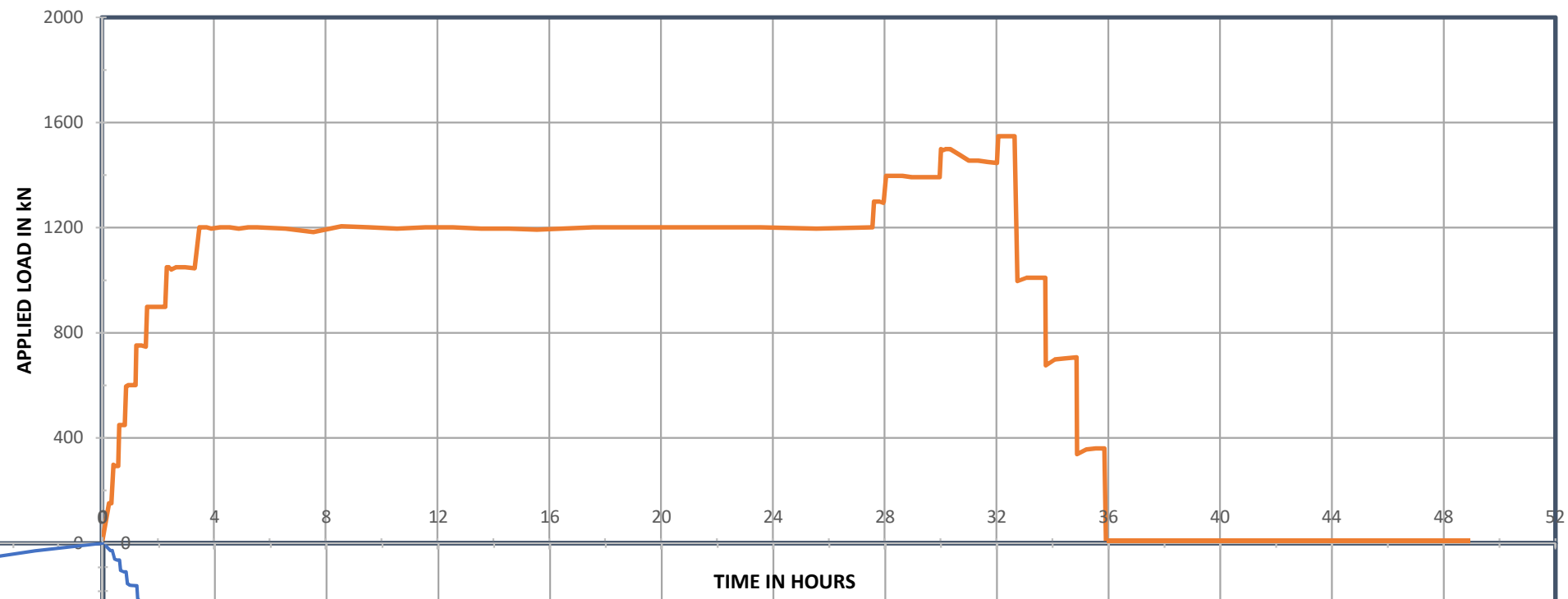


# DRAWING 1 - STATIC LOAD TEST ON PILE TP1 - 8 WEEKS AFTER DRIVING LOAD MOVEMENT PLOT

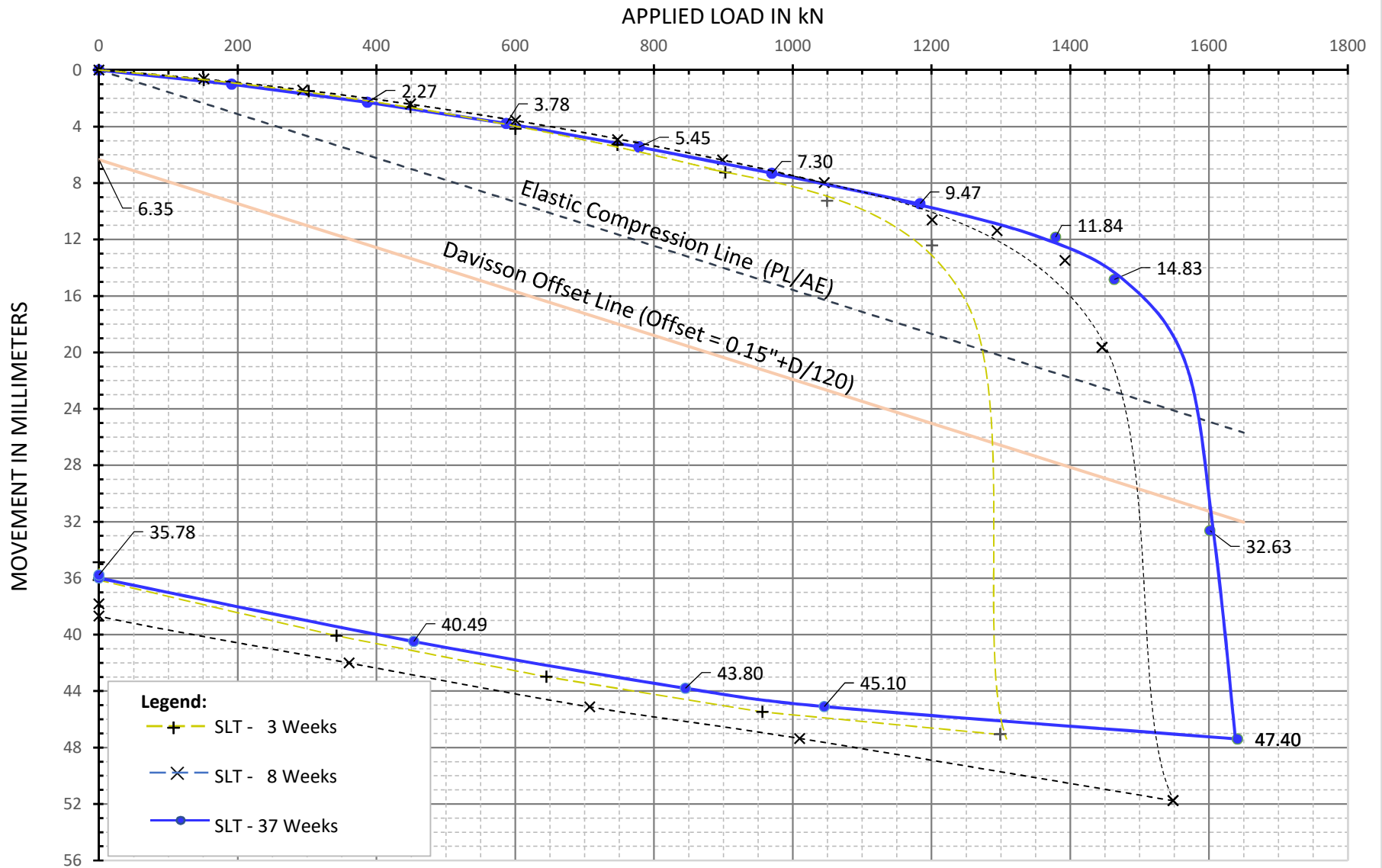


LOCATION : Blanche River Bridge  
Hwy 569 & Blanche River  
10 km North of Temiskaming Shores  
(New Liskeard)  
MTO CONT WP No. : 5163-13-00  
MTO Site No. : 47-38  
GEOCRES No. : 31M-120

PILE NO. : TP1  
DATE DRIVEN : 2018 SEPTEMBER 5  
DATE OF TEST : 2018 NOVEMBER 6 to 8  
PILE TYPE : STEEL 'H' HP 310 x 110  
SHOE DETAILS : NONE  
TOTAL PILE LENGTH : 45.0 m  
EMBEDDED PILE LENGTH : 44.0 m



# STATIC LOAD TEST ON PILE TP1 - 37 WEEKS AFTER DRIVING LOAD MOVEMENT PLOT



**e. Hwy 400 - 89 Interchange**





**Load Increment 250 kN**

PILE NO: Test Pile

Urkkada Job No. 1905CS1373

Project: MTO 2018-2024

**Date:** Oct 7, 2019

Location: HWY 400 & 89

**Start Time:** 12:42 PM

Owner: MTO

**Pile Size:** 310x110

**Contractor:** Fermar Paving Limited

**Pile Type:** H-Pile

Inspector: S. Ferguson/M. El Kotob

Embedment (m): 36.34

[illegible]



**Load Increment 450 kN**

PILE NO: Test Pile

Urkkada Job No. 1905CS1373

Project: MTO 2018-2024

**Date:** Oct 7, 2019

Location: HWY 400 & 89

**Start Time:** 01:08 PM

Owner: MTO

**Pile Size:** 310x110

**Contractor:** Fermar Paving Limited

**Pile Type:** H-Pile

Inspector: S. Ferguson/M. El Kotob

Embedment (m): 36.34

[illegible]



**Load Increment 600 kN**

PILE NO: Test Pile

Urkkada Job No. 1905CS1373

Project: MTO 2018-2024

**Date:** Oct 7, 2019

**Location:** HWY 400 & 89

**Start Time:** 01:35 PM

Owner: MTO

**Pile Size:** 310x110

**Contractor:** Fermar Paving Limited

**Pile Type:** H-Pile

Inspector: S. Ferguson/M. El Kotob

Embedment (m): 36.34

[illegible]



Load Increment 750 kN

PILE NO: \_\_\_\_\_ Test Pile

Urkkada Job No. 1905CS1373

Project: \_\_\_\_\_ MTO 2018-2024

Date: \_\_\_\_\_ Oct 7, 2019

Location: \_\_\_\_\_ HWY 400 &amp; 89

Start Time: \_\_\_\_\_ 02:21 PM

Owner: \_\_\_\_\_ MTO

Pile Size: \_\_\_\_\_ 310x110

Contractor: \_\_\_\_\_ Fermar Paving Limited

Pile Type: \_\_\_\_\_ H-Pile

Inspector: \_\_\_\_\_ S. Ferguson/M. El Kotob

Embedment (m): \_\_\_\_\_ 36.34

Date	Time		Applied Load (kN)	Gauge Reading (psi)	Test Pile								Wire Line Reading (cm)	Movement from Wire Line (cm)	Reaction Pile 1 (cm)	Reaction Pile 2 (cm)	Reaction Pile 3 (cm)	Reaction Pile 4 (cm)
					Vertical Gauge #1 (in)	Vertical Gauge #2 (in)	Gauge #1 Δ (mm)	Gauge #2 Δ (mm)	Average Δ Gauge (mm)	Lateral #1 (in)	Lateral #2 (in)							
	ZERO		0	0	3.480	1.085		-	-	0.200	0.876	29.00			55.9	60.5	67.2	65.9
2019-10-07	0 min	02:21 PM	719	850	3.101	0.665	9.63	10.67	10.15	0.178	0.930	28.20	0.80					
	2 min	02:23 PM	701	825	3.097	0.664	9.73	10.69	10.21	0.178	0.929	28.20	0.80					
	5 min	02:26 PM	681	800	3.095	0.661	9.78	10.77	10.27	0.177	0.928	28.20	0.80					
	10 min	02:31 PM	680	800	3.094	0.659	9.80	10.82	10.31	0.178	0.928	28.20	0.80	55.9	60.3	67.2	65.9	
	20 min	02:41 PM	670	800	3.092	0.658	9.86	10.85	10.35	0.177	0.929	28.10	0.90					
	40 min	03:01 PM	664	800	3.088	0.655	9.96	10.92	10.44	0.177	0.929	28.10	0.90					
	60 min	03:21 PM	659	800	3.088	0.655	9.96	10.92	10.44	0.178	0.929	28.10	0.90					
	80 min	0.65	654	800	3.088	0.654	9.96	10.95	10.45	0.178	0.929	28.10	0.90					



Load Increment 900 kN

PILE NO: \_\_\_\_\_ Test Pile  
 Project: \_\_\_\_\_ MTO 2018-2024  
 Location: \_\_\_\_\_ HWY 400 & 89  
 Owner: \_\_\_\_\_ MTO  
 Contractor: \_\_\_\_\_ Fermar Paving Limited  
 Inspector: \_\_\_\_\_ S. Ferguson/M. El Kotob

Urkkada Job No. \_\_\_\_\_ 1905CS1373  
 Date: \_\_\_\_\_ Oct 7, 2019  
 Start Time: \_\_\_\_\_ 03:49 PM  
 Pile Size: \_\_\_\_\_ 310x110  
 Pile Type: \_\_\_\_\_ H-Pile  
 Embedment (m): \_\_\_\_\_ 36.34

Goulder requested pump up back to target load at 40 & 60 min intervals

Date	Time		Applied Load (kN)	Gauge Reading (psi)	Test Pile									Reaction			
					Vertical Gauge #1 (in)	Vertical Gauge #2 (in)	Gauge #1 Δ (mm)	Gauge #2 Δ (mm)	Average Δ Gauge (mm)	Lateral #1 (in)	Lateral #2 (in)	Wire Line Reading (cm)	Movement from Wire Line (cm)	Reaction Pile 1 (cm)	Reaction Pile 2 (cm)	Reaction Pile 3 (cm)	Reaction Pile 4 (cm)
	ZERO		0	0	3.480	1.085		-	-	0.200	0.876	29.00		55.9	60.5	67.2	65.9
2019-10-07	0 min	03:49 PM	855	950	2.901	0.475	14.71	15.49	15.10	0.174	0.933	27.50	1.50				
	2 min	03:51 PM	797	925	2.907	0.472	14.55	15.57	15.06	0.174	0.933	27.60	1.40				
	5 min	03:54 PM	791	925	2.904	0.470	14.63	15.62	15.13	0.173	0.931	27.80	1.20				
	10 min	03:59 PM	780	925	2.901	0.467	14.71	15.70	15.20	0.173	0.931	27.70	1.30				
	20 min	04:09 PM	769	900	2.899	0.464	14.76	15.77	15.27	0.173	0.930	27.70	1.30				
	40 min	04:29 PM	760	900	2.895	0.460	14.86	15.88	15.37	0.172	0.930	27.70	1.30				
	41 min	04:30 PM	841	950	2.855	0.422	15.88	16.84	16.36	0.174	0.930	27.50	1.50	56.0	60.8	67.3	66.0
	60 min	04:49 PM	788	900	2.847	0.412	16.08	17.09	16.59	0.175	0.932	27.50	1.50				
	61 min	04:50 PM	855	975	2.819	0.384	16.79	17.81	17.30	0.178	0.935	27.40	1.60				
	80 min	05:09 PM	809	925	2.812	0.377	16.97	17.98	17.48	0.178	0.933	27.40	1.60				
	100 min	05:29 PM	802	925	2.809	0.374	17.04	18.06	17.55	0.177	0.932	27.40	1.60				
	120 min	05:49 PM	802	925	2.805	0.371	17.15	18.14	17.64	0.177	0.932	27.40	1.60				



**Load Increment 1050 kN**

Vertical Gauge #2 was adjusted at 10 min interval to allow more travel

Pre-Adjustment was 0.084" equal to Post-adjustment 1.709"

PILE NO: Test Pile

Urkkada Job No. 1905CS1373

**Project:** MTO 2018-2024

**Date:** Oct 7, 2019

**Location:** HWY 400 & 89

**Start Time:** 05:56 PM

Owner: MTO

**Pile Size:** 310x110

**Contractor:** Fermar Paving Limited

**Pile Type:** H-Pile

Inspector: S. Ferguson/M. El Kotob

Embedment (m): 36.34

[illegible]

**Unloading Cycle - 25% Decrements**

Vertical Gauge #2 was adjusted during 1050 kN loading. Subtract 1.625"  
from all readings to obtain true relative reading

PILE NO: \_\_\_\_\_ Test Pile  
Project: \_\_\_\_\_ MTO 2018-2024  
Location: \_\_\_\_\_ HWY 400&89  
Owner: \_\_\_\_\_ MTO  
Contractor: \_\_\_\_\_ Fermar Paving Limited  
Inspector: \_\_\_\_\_ S. Ferguson

Urkkada Job No. 1905CS1373  
Date: Oct 7 & 8, 2019  
Start Time: 06:50 PM  
Pile Size: 310x110  
Pile Type: H-Pile  
Embedment (m): 36.34

Date	Time		Applied Load (kN)	Gauge Reading (psi)	Test Pile								Wire Line Reading (cm)	Movement from Wire Line (cm)	Reaction Pile 1 (cm)	Reaction Pile 2 (cm)	Reaction Pile 3 (cm)	Reaction Pile 4 (cm)
					Vertical Gauge #1 (in)	Vertical Gauge #2 (in)	Gauge #1 Δ (mm)	Gauge #2 Δ (mm)	Average Δ Gauge (mm)	Lateral #1 (in)	Lateral #2 (in)							
	ZERO		0	0	3.480	1.085		-	-	0.200	0.876	29.00			55.9	60.5	67.2	65.9
2019-10-07		750 kN																
	0 min	06:50 PM	878	900	2.357	1.545	28.52	29.59	29.06	0.178	0.935	26.20	2.80					
	20 min	07:10 PM	878	900	2.356	1.544	28.55	29.62	29.08	0.178	0.936	26.30	2.70	57.0	61.8	68.0	66.5	
	40 min	07:30 PM	876	900	2.355	1.543	28.58	29.64	29.11	0.179	0.936	26.30	2.70					
	60 min	07:50 PM	876	900	2.354	1.543	28.60	29.64	29.12	0.179	0.937	26.40	2.60					
		500 kN																
	0 min	07:58 PM	521	550	2.438	1.634	26.47	27.33	26.90	0.191	0.926	26.50	2.50					
	20 min	08:18 PM	533	550	2.438	1.635	26.47	27.31	26.89	0.191	0.925	26.50	2.50					
	40 min	08:38 PM	533	550	2.438	1.635	26.47	27.31	26.89	0.191	0.925	26.50	2.50					
	60 min	08:58 PM	533	550	2.438	1.635	26.47	27.31	26.89	0.191	0.925	26.50	2.50					

2019-10-07		<b>250 kN</b>															
	0 min	09:01 PM	227	300	2.446	1.757	26.26	24.21	25.23	0.204	0.913	26.80	2.20				
	20 min	09:21 PM	237	300	2.447	1.759	26.24	24.16	25.20	0.203	0.913	26.80	2.20				
	40 min	09:41 PM	239	300	2.448	1.759	26.21	24.16	25.18	0.203	0.912	26.80	2.20				
	60 min	10:01 PM	239	300	2.448	1.759	26.21	24.16	25.18	0.203	0.912	26.80	2.20				
		<b>0 kN</b>															
	0 min	10:14 PM	44	0	2.682	1.913	20.27	20.24	20.26	0.210	0.886	27.30	1.70				
	5 min	10:19 PM	0	0	2.698	1.924	19.86	19.96	19.91	0.210	0.886	27.40	1.60	57.3	62.0	68.2	66.8
10-08	12 hr	10:12 AM	0	0	2.705	1.931	19.69	19.79	19.74	0.210	0.886	27.30	1.70	57.3	62.1	68.2	66.8





**Load Increment 500kN**

PILE NO: \_\_\_\_\_ Test Pile

Urkkada Job No. 1905CS1373

**Project:** MTO 2018-2024

**Date:** Oct 9, 2019

**Location:** HWY 400&89

**Start Time:** 10:09 AM

**Owner:** MTO

<b>Pile Size:</b>	310x110
-------------------	---------

<b>Contractor:</b>	Fermar Paving
--------------------	---------------

<b>Pile Type:</b>	H-Pile
-------------------	--------

**Inspector:** S. Ferguson/M. Ferguson

Embedment (m):	36.34
----------------	-------

[illegible]



Load Increment 700kN

PILE NO: Test Pile

Urkkada Job No. 1905CS1373

**Project:** MTO 2018-2024

**Date:** Oct 9, 2019

Location: HWY 400&89

**Start Time:** 11:30 AM

Owner: MTO

**Pile Size:** 310x110

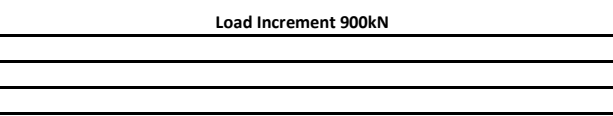
**Contractor:** Fermar Paving

**Pile Type:** H-Pile

Inspector: S. Ferguson/M. Ferguson

Embedment (m): 36.34

[illegible]



**Urkkada Job No.** 1905CS1373

Date:	Oct 9, 2019
Start Time:	12:07 PM
Pile Size:	310x110
Pile Type:	H-Pile
Embedment (m):	36.34



# Load Increment 1100kN

Load increased to target value at 10, 40 & 80 minute intervals

Vertical Dial #1 Reset for additional trave at 100 minute interval

Pre-adjustment: 0.851" = Post-adjustment: 2.002"

PILE NO: \_\_\_\_\_ Test Pile \_\_\_\_\_

Urkkada Job No. 1905CS1373

Project: MTO 2018-2024

Date: Oct 9, 2019

Location: HWY 400&89

Start Time: 02:23 PM

Owner: MTO

Pile Size: 310x110

Contractor: Fermar Paving

Pile Type: H-Pile

Inspector: S. Ferguson/M. Ferguson

Embedment (m): 36.34

Date	Time		Applied Load (kN)	Gauge Reading (psi)	Test Pile												
					Vertical Gauge #1 (in)	Vertical Gauge #2 (in)	Gauge #1 Δ (mm)	Gauge #2 Δ (mm)	Average Δ Gauge (mm)	Lateral #1 (in)	Lateral #2 (in)	Wire Line Reading (cm)	Movement from Wire Line (cm)	Reaction Pile 1 (cm)	Reaction Pile 2 (cm)	Reaction Pile 3 (cm)	Reaction Pile 4 (cm)
	ZERO		0	0	1.991	3.819		-	-	0.400	0.736	27.20		42.6	47.2	54.2	52.8
2019-10-09	0 min	02:23 PM	1070	1100 (+)	1.049	2.819	23.93	25.40	24.66	0.378	0.821	24.80	2.40				
	2 min	02:25 PM	1011	1100	1.042	2.816	24.10	25.48	24.79	0.378	0.820	24.60	2.60				
	5 min	02:28 PM	996	1100 (-)	1.040	2.813	24.16	25.55	24.85	0.379	0.819	24.60	2.60				
	10 min	02:33 PM	985	1100 (-)	1.037	2.810	24.23	25.63	24.93	0.379	0.818	24.60	2.60				
	11 min	02:34 PM	1055	1100	0.994	2.765	25.32	26.77	26.05	0.384	0.819	24.40	2.80				
	20 min	02:43 PM	995	1100 (-)	0.986	2.760	25.53	26.90	26.21	0.386	0.819	24.40	2.80				
	40 min	03:03 PM	977	1050 (+)	0.981	2.757	25.65	26.97	26.31	0.386	0.816	24.40	2.80				
	41 min	03:23 PM	1085	1100 (+)	0.918	2.691	27.25	28.65	27.95	0.387	0.817	24.20	3.00	42.0	46.6	53.6	52.2
	60 min	03:43 PM	1002	1100 (-)	0.907	2.682	27.53	28.88	28.21	0.387	0.816	24.20	3.00				
	80 min	04:03 PM	994	1100 (-)	0.902	2.678	27.66	28.98	28.32	0.386	0.815	24.20	3.00				
	81 min	04:04 PM	1073	1100 (+)	0.863	2.635	28.65	30.07	29.36	0.388	0.819	24.20	3.00				
	100 min	04:23 PM	1019	1100 (-)	2.002	2.626	28.96	30.30	29.63	0.388	0.816	24.10	3.10				
	120 min	04:43 PM	1010	1100 (-)	2.002	2.622	28.96	30.40	29.68	0.388	0.815	24.10	3.10				



# Load Increment 1300kN

Load increased to target value at 10, 20, 40 & 60 minute intervals

Pile displacement exceeded mirror/wireline at 60 minute interval

PILE NO: \_\_\_\_\_ Test Pile \_\_\_\_\_

Urkkada Job No. 1905CS1373

Project: MTO 2018-2024

Date: Oct 9, 2019

Location: HWY 400&89

Start Time: 04:51 PM

Owner: MTO

Pile Size: 310x110

Contractor: Fermar Paving

Pile Type: H-Pile

Inspector: S. Ferguson/M. Ferguson

Embedment (m): 36.34

Date	Time		Applied Load (kN)	Gauge Reading (psi)	Test Pile												
					Vertical Gauge #1 (in)	Vertical Gauge #2 (in)	Gauge #1 Δ (mm)	Gauge #2 Δ (mm)	Average Δ Gauge (mm)	Lateral #1 (in)	Lateral #2 (in)	Wire Line Reading (cm)	Movement from Wire Line (cm)	Reaction Pile 1 (cm)	Reaction Pile 2 (cm)	Reaction Pile 3 (cm)	Reaction Pile 4 (cm)
	ZERO		0	0	1.991	3.819		-	-	0.400	0.736	27.20		42.6	47.2	54.2	52.8
2019-10-09	0 min	04:51 PM	1250	1350	1.555	2.167	40.31	41.96	41.14	0.383	0.871	22.90	4.30				
	2 min	04:53 PM	1178	1200 (+)	1.538	2.161	40.74	42.11	41.43	0.383	0.876	22.90	4.30				
	5 min	04:56 PM	1153	1200 (+)	1.533	2.157	40.87	42.21	41.54	0.384	0.878	22.90	4.30				
	10 min	05:01 PM	1131	1200 (-)	1.529	2.152	40.97	42.34	41.66	0.384	0.881	22.90	4.30				
	11 min	05:04 PM	1278	1300 (+)	1.272	1.892	47.50	48.95	48.22	0.389	0.889	22.20	5.00				
	20 min	05:11 PM	1164	1250	1.258	1.881	47.85	49.23	48.54	0.392	0.892	22.20	5.00				
	21 min	05:15 PM	1278	1300	1.155	1.777	50.47	51.87	51.17	0.385	0.889	22.00	5.20	41.8	46.5	53.7	52.2
	40 min	05:31 PM	1178	1250 (-)	1.140	1.763	50.85	52.22	51.54	0.384	0.890	21.90	5.30				
	41 min	05:34 PM	1282	1300	1.030	1.651	53.64	55.07	54.36	0.385	0.891	21.60	5.60				
	60 min	05:51 PM	1193	1250	1.015	1.639	54.03	55.37	54.70	0.384	0.892						
	61 min	05:53 PM	1301	1325	0.908	1.531	56.74	58.12	57.43	0.385	0.890						
	80 min	06:11 PM	1211	1250 (+)	0.894	1.519	57.10	58.42	57.76	0.388	0.816						
	100 min	06:21 PM	1194	1250	0.880	1.513	57.45	58.57	58.01	0.388	0.815						



## Unloading Cycle - 25% Decrements

PILE NO: \_\_\_\_\_ Test Pile \_\_\_\_\_  
Project: \_\_\_\_\_ MTO 2018-2024 \_\_\_\_\_  
Location: \_\_\_\_\_ HWY 400&89 \_\_\_\_\_  
Owner: \_\_\_\_\_ MTO \_\_\_\_\_  
Contractor: \_\_\_\_\_ Fermar Paving Limited \_\_\_\_\_  
Inspector: \_\_\_\_\_ S. Ferguson/M. Ferguson \_\_\_\_\_

Urkkada Job No. 1905CS1373  
Date: Oct 9, 2019  
Start Time: 06:38 PM  
Pile Size: 310x110  
Pile Type: H-Pile  
Embedment (m): 36.34

Date	Time		Applied Load (kN)	Gauge Reading (psi)	Test Pile									Reaction Pile 1 (cm)	Reaction Pile 2 (cm)	Reaction Pile 3 (cm)	Reaction Pile 4 (cm)	
					Vertical Gauge #1 (in)	Vertical Gauge #2 (in)	Gauge #1 Δ (mm)	Gauge #2 Δ (mm)	Average Δ Gauge (mm)	Lateral #1 (in)	Lateral #2 (in)	Wire Line Reading (cm)	Movement from Wire Line (cm)					
	ZERO		0	0	1.991	3.819		-	-	0.400	0.736	27.20		42.6	47.2	54.2	52.8	
2019-10-09		975 kN																
	0 min	06:38 PM	976	950 (+)	0.924	1.550	56.34	57.63	56.98	0.388	0.689							
	20 min	06:58 PM	985	950 (+)	0.924	1.549	56.34	57.66	57.00	0.389	0.689							
	40 min	07:18 PM	990	975	0.923	1.549	56.36	57.66	57.01	0.389	0.689							
	60 min	07:38 PM	995	975	0.923	1.549	56.36	57.66	57.01	0.390	0.689							
		650 kN																
	0 min	07:40 PM	623	650	1.034	1.668	53.54	54.64	54.09	0.397	0.780							
	20 min	08:00 PM	634	650	1.034	1.668	53.54	54.64	54.09	0.397	0.780							
	40 min	08:20 PM	637	650 (+)	1.033	1.667	53.57	54.66	54.11	0.398	0.779							
	60 min	08:40 PM	639	650 (+)	1.033	1.667	53.57	54.66	54.11	0.398	0.779							



# Unloading Cycle - 25% Decrements

PILE NO: Test Pile

Project: MTO 2018-2024

Location: HWY 400&89

Owner: MTO

Contractor: Fermax Paving Limited

Inspector: S. Ferguson/M. Ferguson

Urkkada Job No. 1905CS1373

Date: Oct 9, 2019

Start Time: 06:38 PM

Pile Size: 310x110

Pile Type: H-Pile

Embedment (m): 36.34

Date	Time		Applied Load (kN)	Gauge Reading (psi)	Test Pile								Reaction Pile 1 (cm)	Reaction Pile 2 (cm)	Reaction Pile 3 (cm)	Reaction Pile 4 (cm)		
					Vertical Gauge #1 (in)	Vertical Gauge #2 (in)	Gauge #1 Δ (mm)	Gauge #2 Δ (mm)	Average Δ Gauge (mm)	Lateral #1 (in)	Lateral #2 (in)	Wire Line Reading (cm)					Movement from Wire Line (cm)	
2019-10-09		325 kN																
	0 min	08:42 PM	331	350	1.164	1.816	50.24	50.88	50.56	0.410	0.761							
	20 min	09:02 PM	344	350 (+)	1.165	1.816	50.22	50.88	50.55	0.410	0.759							
	40 min	09:22 PM	345	350 (+)	1.166	1.816	50.19	50.88	50.53	0.410	0.759							
	60 min	09:42 PM	345	350 (+)	1.166	1.817	50.19	50.85	50.52	0.410	0.759							
		0 kN																
	0 min	09:46 PM	13	0	1.365	2.038	45.14	45.24	45.19	0.405	0.719	22.8	4.4	42.1	46.8	53.7	52.3	
	5 min	09:51 PM	15	0	1.369	2.041	45.03	45.16	45.10	0.408	0.719	22.8	4.4					
	12 hr	09:46 AM	2	0	1.477	2.148	42.29	42.44	42.37	0.402	0.715	23.0	4.2	40.4	44.8	51.8	51.0	

Figure 1: Load Movement Curve for from Static Load Test #1

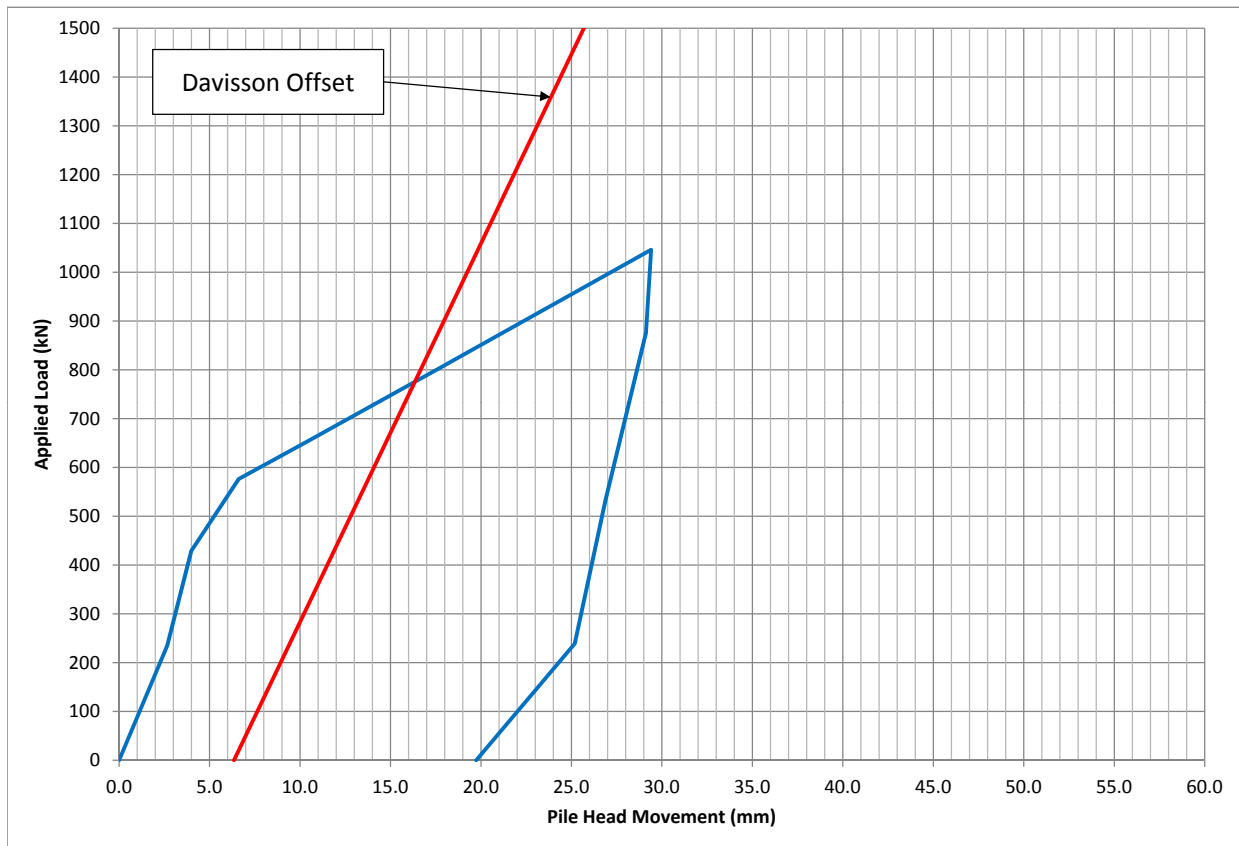


Table 1: Load Movement Summary

Load (kN)	Movement (mm)
0	0.0
235	2.7
429	4.0
576	6.6
654	10.5
802	17.6
1046	29.4
876	29.1
533	26.9
239	25.2



Figure 2: Load Movement Curve for from Static Load Test #2

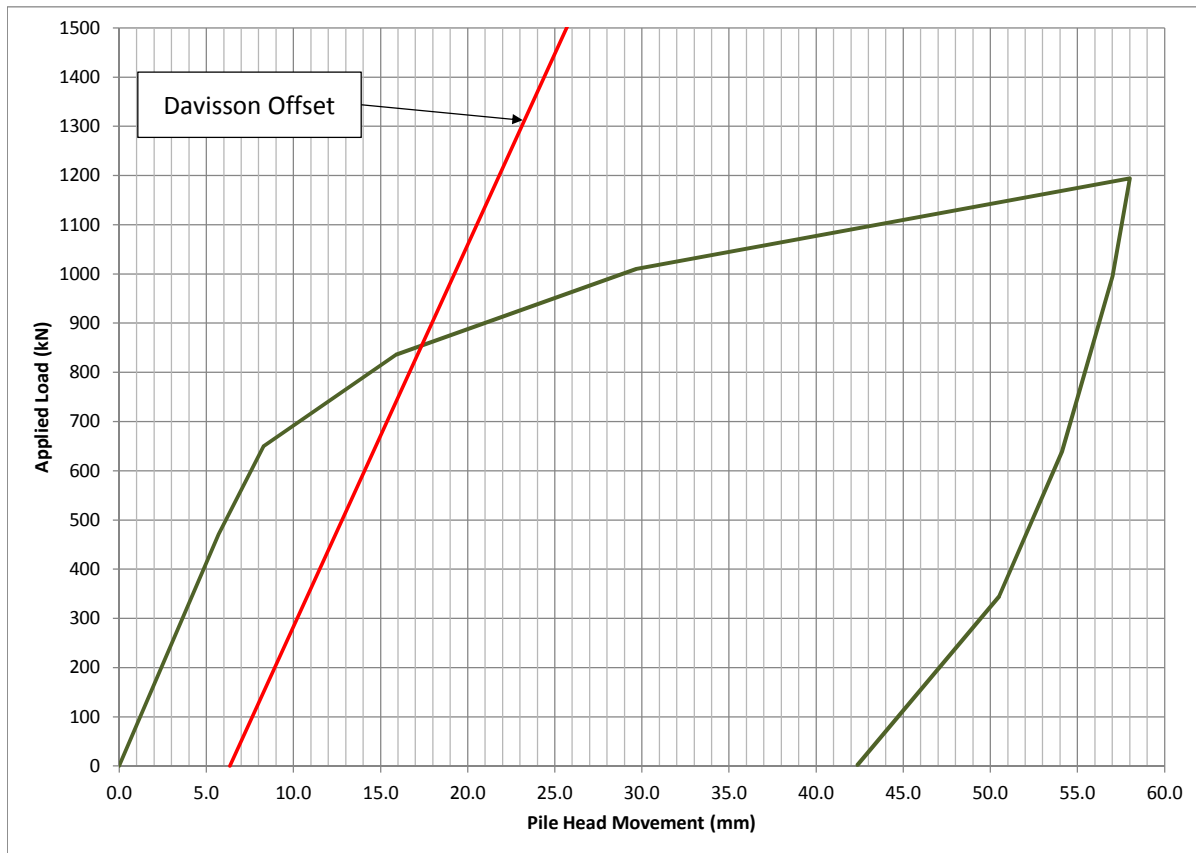
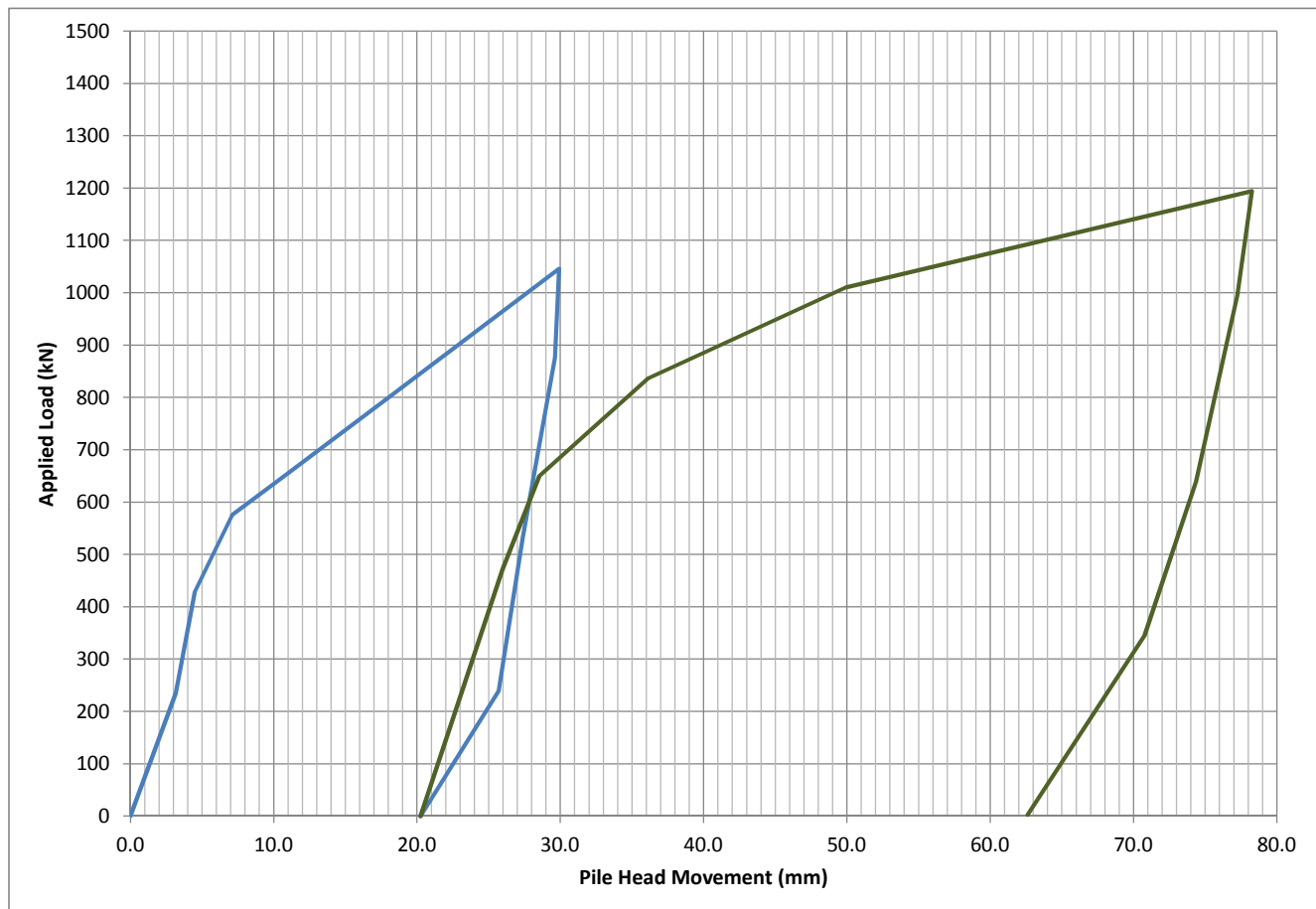


Table 2: Load Movement Summary

Load (kN)	Movement (mm)
0	0.0
471	5.7
650	8.3
836	15.9
1010	29.7
1194	58.0
995	57.0
639	54.1
345	50.5
2	42.4

Figure 3: Load Movement Curve for from Static Load Tests #1 and #2





**Load Increment 300 kN**

PILE NO: Test Pile

Urkkada Job No. 1905CS1373

Project: MTO 2018-2024

**Date:** Oct 28, 2019

**Location:** HWY 400 & 89

**Start Time:** 11:21 AM

Owner: MTO

**Pile Size:** 310x110

**Contractor:** Fermar Paving Limited

**Pile Type:** H-Pile

Inspector: M. El Kotob

Embedment (m): 50.80

[illegible]



**Load Increment 600 kN**

PILE NO: Test Pile

Urkkada Job No. 1905CS1373

Project: MTO 2018-2024

**Date:** Oct 28, 2019

Location: HWY 400 & 89

**Start Time:** 11:47 AM

Owner: MTO

**Pile Size:** 310x110

**Contractor:** Fermar Paving Limited

**Pile Type:** H-Pile

Inspector: M. El Kotob

Embedment (m): 50.80

[illegible]



**Load Increment 900 kN**

PILE NO: Test Pile

Urkkada Job No. 1905CS1373

Project: MTO 2018-2024

**Date:** Oct 28, 2019

Location: HWY 400 & 89

**Start Time:** 12:13 PM

Owner: MTO

**Pile Size:** 310x110

**Contractor:** Fermar Paving Limited

**Pile Type:** H-Pile

Inspector: M. El Kotob

Embedment (m): 50.80

[illegible]



**Load Increment 1200 kN**

PILE NO: Test Pile

Urkkada Job No. 1905CS1373

Project: MTO 2018-2024

**Date:** Oct 28, 2019

Location: HWY 400 & 89

**Start Time:** 01:16 PM

Owner: MTO

**Pile Size:** 310x110

**Contractor:** Fermar Paving Limited

**Pile Type:** H-Pile

Inspector: M. El Kotob

Embedment (m): 50.80

[illegible]



**Load Increment 1500 kN**

PILE NO: Test Pile

**Urkkada Job No.** 1905CS1373

**Project:** MTO 2018-2024

**Date:** Oct 28, 2019

**Location:** HWY 400 & 89

**Start Time:** 02:20 PM

Owner: MTO

**Pile Size:** 310x110

**Contractor:** Fermar Paving Limited

**Pile Type:** H-Pile

**Inspector:** S. Ferguson/M. El Kotob

Embedment (m): 50.80

[illegible]



Load Increment 1700 kN

Load was increased back to 1700 kN at 12 hr and 16 hr

PILE NO: \_\_\_\_\_ Test Pile \_\_\_\_\_

Urkkada Job No. 1905CS1373

Project: MTO 2018-2024

Date: Oct 28/29, 2019

Location: HWY 400 &amp; 89

Start Time: 03:47 PM

Owner: MTO

Pile Size: 310x110

Contractor: Fermar Paving Limited

Pile Type: H-Pile

Inspector: S. Ferguson/ M. Ferguson

Embedment (m): 50.80

Date	Time		Applied Load (kN)	Gauge Reading (psi)	Test Pile												
					Vertical Gauge #1 (in)	Vertical Gauge #2 (in)	Gauge #1 Δ (mm)	Gauge #2 Δ (mm)	Average Δ Gauge (mm)	Lateral #1 (in)	Lateral #2 (in)	Wire Line Reading (cm)	Movement from Wire Line (cm)	Reaction Pile 1 (cm)	Reaction Pile 2 (cm)	Reaction Pile 3 (cm)	Reaction Pile 4 (cm)
	ZERO		0	0	3.393	3.325	-	-	-	0.365	0.683	82.80	-	45.7	45.8	53.2	53.8
2019-10-28	0 min	15:47	1796	1850	1.961	1.826	36.37	38.07	37.22	0.316	0.781	86.20	-3.40				
	2 min	15:49	1762	1850	1.954	1.821	36.55	38.20	37.38	0.316	0.781	86.20	-3.40				
	5 min	15:52	1746	1850	1.951	1.819	36.63	38.25	37.44	0.316	0.781	86.30	-3.50				
	10 min	15:57	1730	1800	1.949	1.815	36.68	38.35	37.52	0.315	0.780	86.30	-3.50				
	20 min	16:07	1720	1800	1.946	1.810	36.75	38.48	37.62	0.314	0.778	86.30	-3.50				
	40 min	16:27	1708	1800	1.940	1.805	36.91	38.61	37.76	0.314	0.776	86.30	-3.50	45.1	45.1	52.5	53.2
	60 min	16:47	1704	1800	1.936	1.803	37.01	38.66	37.83	0.315	0.777	86.30	-3.50				
	80 min	17:07	1702	1800	1.934	1.800	37.06	38.74	37.90	0.316	0.777	86.30	-3.50				
	100 min	17:27	1701	1800	1.932	1.797	37.11	38.81	37.96	0.315	0.777	86.30	-3.50				
	120 min	17:47	1701	1800	1.930	1.794	37.16	38.89	38.02	0.316	0.778	86.40	-3.60				
	3 hr	18:47	1698	1800	1.925	1.788	37.29	39.04	38.16	0.317	0.777	86.40	-3.60				
	4 hr	19:47	1694	1800	1.922	1.785	37.36	39.12	38.24	0.318	0.777	86.40	-3.60				
	5 hr	20:47	1689	1800	1.921	1.783	37.39	39.17	38.28	0.320	0.777	86.40	-3.60				
	6 hr	21:47	1685	1750	1.919	1.782	37.44	39.19	38.32	0.319	0.777	86.40	-3.60				
	7 hr	22:47	1681	1700	1.918	1.782	37.47	39.19	38.33	0.322	0.777	86.40	-3.60	45.1	45.4	52.7	53.3
	8 hr	23:47	1677	1700	1.918	1.782	37.47	39.19	38.33	0.323	0.777	86.40	-3.60				





Load Increment 1700 kN  
 Load was increased back to 1700 kN at 12 hr and 16 hr

PILE NO: Test Pile  
 Project: MTO 2018-2024  
 Location: HWY 400 & 89  
 Owner: MTO  
 Contractor: Fermar Paving Limited  
 Inspector: S. Ferguson/ M. Ferguson

Urkkada Job No. 1905CS1373  
 Date: Oct 28/29, 2019  
 Start Time: 03:47 PM  
 Pile Size: 310x110  
 Pile Type: H-Pile  
 Embedment (m): 50.80

29/10/2019	9 hr	00:47	1671	1650	1.918	1.781	37.47	39.22	38.34	0.324	0.777	86.40	-3.60				
	10 hr	01:47	1665	1600	1.918	1.781	37.47	39.22	38.34	0.324	0.778	86.40	-3.60				
	11 hr	02:47	1656	1550	1.919	1.782	37.44	39.19	38.32	0.325	0.778	86.40	-3.60				
	12 hr	03:47	1646	1500	1.920	1.783	37.41	39.17	38.29	0.325	0.777	86.40	-3.60				
	12 hr	03:48	1697	1800	1.908	1.772	37.72	39.45	38.58	0.325	0.776	86.40	-3.60				
	13 hr	04:47	1677	1700	1.906	1.770	37.77	39.50	38.63	0.325	0.776	86.40	-3.60				
	14 hr	05:47	1670	1600	1.906	1.770	37.77	39.50	38.63	0.326	0.776	86.40	-3.60				
	15 hr	06:47	1661	1550	1.906	1.770	37.77	39.50	38.63	0.326	0.776	86.40	-3.60				
	16 hr	07:47	1650	1550	1.907	1.771	37.74	39.47	38.61	0.326	0.777	86.40	-3.60				
	16 hr	07:48	1701	1800	1.896	1.761	38.02	39.73	38.87	0.325	0.775	86.40	-3.60				



## Unloading Cycle - 25% Decrements

PILE NO: \_\_\_\_\_ Test Pile \_\_\_\_\_  
Project: \_\_\_\_\_ MTO 2018-2024 \_\_\_\_\_  
Location: \_\_\_\_\_ HWY 400&89 \_\_\_\_\_  
Owner: \_\_\_\_\_ MTO \_\_\_\_\_  
Contractor: \_\_\_\_\_ Ferman Paving Limited \_\_\_\_\_  
Inspector: \_\_\_\_\_ M. El Kotob \_\_\_\_\_

Urkkada Job No. 1905CS1373  
Date: Oct 29, 2019  
Start Time: 08:07 AM  
Pile Size: 310x110  
Pile Type: H-Pile  
Embedment (m): 50.80

Date	Time		Applied Load (kN)	Gauge Reading (psi)	Test Pile													
					Vertical Gauge #1 (in)	Vertical Gauge #2 (in)	Gauge #1 Δ (mm)	Gauge #2 Δ (mm)	Average Δ Gauge (mm)	Lateral #1 (in)	Lateral #2 (in)	Wire Line Reading (cm)	Movement from Wire Line (cm)	Reaction Pile 1 (cm)	Reaction Pile 2 (cm)	Reaction Pile 3 (cm)	Reaction Pile 4 (cm)	
	ZERO		0	0	3.393	3.325		-	-	0.365	0.683	82.80	-	45.7	45.8	53.2	53.8	
2019-10-29		1250 kN																
	0 min	08:07	1251	1000	2.080	1.940	33.35	35.18	34.26	0.359	0.758	86.00	-3.20					
	20 min	08:27	1261	1000	2.081	1.940	33.32	35.18	34.25	0.362	0.757	86.10	-3.30					
	40 min	08:47	1261	1000	2.082	1.940	33.30	35.18	34.24	0.362	0.757	86.10	-3.30					
	60 min	09:07	1259	1000	2.084	1.941	33.25	35.15	34.20	0.359	0.759	86.10	-3.30					
		850 kN																
	0 min	09:09	845	680	2.356	2.217	26.34	28.14	27.24	0.384	0.727	85.30	-2.50					
	20 min	09:29	853	680	2.360	2.219	26.24	28.09	27.17	0.382	0.728	85.30	-2.50					
	40 min	09:49	854	680	2.359	2.218	26.26	28.12	27.19	0.383	0.726	85.30	-2.50					
	60 min	10:09	850	680	2.363	2.219	26.16	28.09	27.13	0.379	0.729	85.30	-2.50					



## Unloading Cycle - 25% Decrements

PILE NO: Test Pile

Urkkada Job No. 1905CS1373

Project: MTO 2018-2024

Date: Oct 29, 2019

Location: HWY 400&amp;89

Start Time: 08:07 AM

Owner: MTO

Pile Size: 310x110

Contractor: Fermar Paving Limited

Pile Type: H-Pile

Inspector: M. El Kotob

Embedment (m): 50.80

2019-10-29		425 kN															
	0 min	10:15	430	325	2.645	2.522	19.00	20.40	19.70	0.408	0.709	84.60	-1.80				
	20 min	10:35	447	325	2.644	2.523	19.02	20.37	19.70	0.410	0.706	84.60	-1.80				
	40 min	10:55	451	325	2.642	2.523	19.08	20.37	19.72	0.412	0.705	84.60	-1.80				
	60 min	11:15	456	325	2.641	2.523	19.10	20.37	19.74	0.415	0.704	84.60	-1.80				
		0 kN															
	0 min	11:20	2	0	2.932	2.849	11.71	12.09	11.90	0.452	0.682	84.00	-1.20				
	5 min	11:25	0	0	2.938	2.858	11.56	11.86	11.71	0.453	0.682	83.90	-1.10	45.6	45.7	53.1	53.7
	12 hr	23:25	27	0	2.946	2.861	11.35	11.79	11.57	0.451	0.671	84.00	-1.20	45.6	45.7	53.1	53.7

Figure 1: Load Movement Curve for from Static Load Test #3

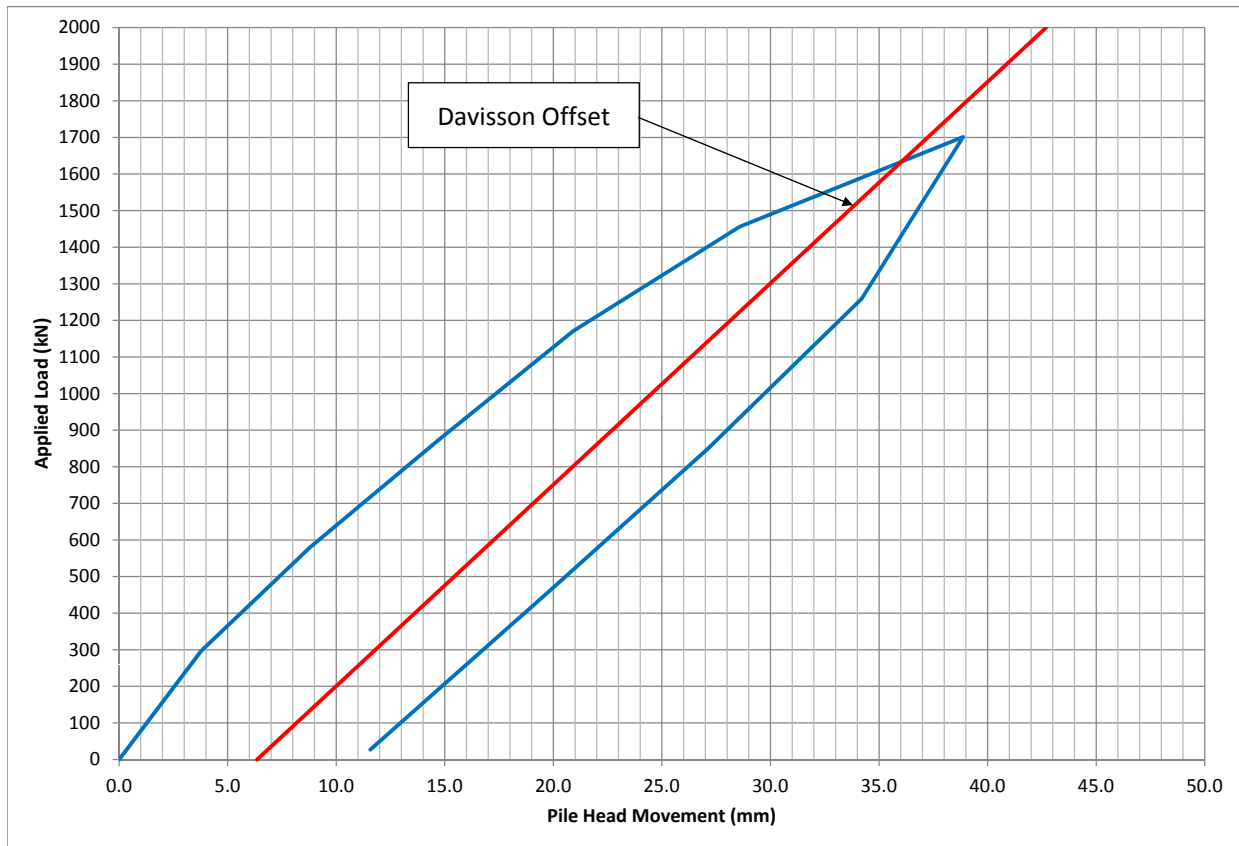
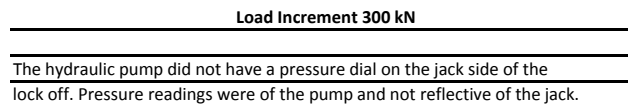


Table 1: Load Movement Summary

Load (kN)	Movement (mm)
0	0.0
297	3.8
580	8.8
873	14.7
1171	20.9
1456	28.6
1701	38.9
1259	34.2
850	27.1
456	19.7
27	11.6





**Load Increment 600 kN**

PILE NO: Test Pile

Urkkada Job No. 1905CS1373

See sheet 300 kN for comments on Gauge Pressure

Project: MTO 2018-2024

**Date:** November 12, 2019

**Location:** HWY 400 & 89

**Start Time:** 10:49

Owner: MTO

**Pile Size:** 310x110

**Contractor:** Fermar Paving Limited

**Pile Type:** H-Pile

Inspector: S. Ferguson/ M. Ferguson

Embedment (m): 50.80

[illegible]



**Load Increment 900 kN**

PILE NO: Test Pile

Urkkada Job No. 1905CS1373

See sheet 300 kN for comments on Gauge Pressure

Project: MTO 2018-2024

**Date:** November 12, 2019

Location: HWY 400 & 89

Start Time: 11:52

Owner: MTO

**Pile Size:** 310x110

**Contractor:** Fermar Paving Limited

**Pile Type:** H-Pile

Inspector: M. Ferguson

Embedment (m): 50.80

[illegible]



Load Increment 1200 kN

PILE NO: \_\_\_\_\_ Test Pile \_\_\_\_\_

Urkkada Job No. 1905CS1373

See sheet 300 kN for comments on Gauge Pressure

Project: MTO 2018-2024

Date: November 12, 2019

Location: HWY 400 &amp; 89

Start Time: 12:55

Owner: MTO

Pile Size: 310x110

Contractor: Fermar Paving Limited

Pile Type: H-Pile

Inspector: M. Ferguson

Embedment (m): 50.80

Date	Time		Applied Load (kN)	Gauge Reading (psi)	Test Pile									Reaction			
					Vertical Gauge #1 (in)	Vertical Gauge #2 (in)	Gauge #1 Δ (mm)	Gauge #2 Δ (mm)	Average Δ Gauge (mm)	Lateral #1 (in)	Lateral #2 (in)	Wire Line Reading (cm)	Movement from Wire Line (cm)	Reaction Pile 1 (cm)	Reaction Pile 2 (cm)	Reaction Pile 3 (cm)	Reaction Pile 4 (cm)
	ZERO		0	0	2.957	3.626	-	-	-	0.533	0.391	83.90	-				
2019-11-12	0 min	12:55	1203	1200	2.199	2.803	19.25	20.90	20.08	0.429	0.444	85.50	-1.60				
	2 min	12:57	1193	1200	2.198	2.803	19.28	20.90	20.09	0.425	0.444	85.50	-1.60				
	5 min	13:00	1183	1200	2.198	2.803	19.28	20.90	20.09	0.425	0.442	85.50	-1.60				
	10 min	13:05	1178	1200	2.198	2.802	19.28	20.93	20.10	0.421	0.440	85.50	-1.60				
	20 min	13:15	1174	1150	2.198	2.801	19.28	20.96	20.12	0.417	0.437	85.50	-1.60				
	40 min	13:35	1167	1150	2.198	2.801	19.28	20.96	20.12	0.411	0.435	85.50	-1.60				
	60 min	13:55	1160	1100	2.200	2.802	19.23	20.93	20.08	0.410	0.432	85.50	-1.60				
	90 min	14:25	1159	1100	2.201	2.803	19.20	20.90	20.05	0.408	0.431	85.50	-1.60				
	120 min	14:55	1154	1100	2.202	2.803	19.18	20.90	20.04	0.407	0.431	85.50	-1.60				





**Load Increment 1500 kN**

PILE NO: Test Pile

Urkkada Job No. 1905CS1373

See sheet 300 kN for comments on Gauge Pressure

Project: MTO 2018-2024

**Date:** November 12, 2019

Location: HWY 400 & 89

**Start Time:** 15:10

Owner: MTO

**Pile Size:** 310x110

**Contractor:** Fermar Paving Limited

**Pile Type:** H-Pile

Inspector: M. Ferguson

Embedment (m): 50.80

[illegible]



Load Increment 1800 kN

PILE NO: \_\_\_\_\_ Test Pile \_\_\_\_\_

Urkkada Job No. 1905CS1373

See sheet 300 kN for comments on Gauge Pressure

Project: MTO 2018-2024

Date: November 12, 2019

Location: HWY 400 &amp; 89

Start Time: 16:14

Owner: MTO

Pile Size: 310x110

Contractor: Fermar Paving Limited

Pile Type: H-Pile

Inspector: M. Ferguson

Embedment (m): 50.80

Date	Time		Applied Load (kN)	Gauge Reading (psi)	Test Pile									Reaction			
					Vertical Gauge #1 (in)	Vertical Gauge #2 (in)	Gauge #1 Δ (mm)	Gauge #2 Δ (mm)	Average Δ Gauge (mm)	Lateral #1 (in)	Lateral #2 (in)	Wire Line Reading (cm)	Movement from Wire Line (cm)	Reaction Pile 1 (cm)	Reaction Pile 2 (cm)	Reaction Pile 3 (cm)	Reaction Pile 4 (cm)
	ZERO		0	0	2.957	3.626	-	-	-	0.533	0.391	83.90	-	56.0	56.1	63.5	64.1
2019-11-12	0 min	16:14	1791	1900	1.611	2.205	34.19	36.09	35.14	0.381	0.470	87.00	-3.10				
	2 min	16:16	1765	1900	1.608	2.202	34.26	36.17	35.22	0.381	0.469	87.00	-3.10				
	5 min	16:19	1749	1850	1.605	2.200	34.34	36.22	35.28	0.381	0.469	87.00	-3.10				
	10 min	16:24	1734	1850	1.603	2.197	34.39	36.30	35.34	0.380	0.469	87.00	-3.10				
	20 min	16:34	1719	1800	1.601	2.194	34.44	36.37	35.41	0.379	0.469	87.10	-3.20				
	40 min	16:54	1707	1800	1.598	2.190	34.52	36.47	35.50	0.378	0.470	87.20	-3.30				
	60 min	17:14	1700	1800	1.597	2.189	34.54	36.50	35.52	0.377	0.470	87.20	-3.30				
	80 min	17:34	1697	1800	1.596	2.188	34.57	36.53	35.55	0.376	0.470	87.20	-3.30	55.8	55.9	63.3	63.9
	100 min	17:54	1692	1750	1.597	2.188	34.54	36.53	35.53	0.375	0.470	87.20	-3.30				
	120 min	18:14	1688	1750	1.597	2.186	34.54	36.58	35.56	0.375	0.470	87.20	-3.30				



### Load Increments 1900 and 2000 kN

PILE NO: Test Pile

Urkkada Job No. 1905CS1373

See sheet 300 kN for comments on Gauge Pressure

Project: MTO 2018-2024

**Date:** November 12, 2019

**Location:** HWY 400 & 89

**Start Time:** 18:37

Owner: MTO

**Pile Size:** 310x110

**Contractor:** Fermar Paving Limited

**Pile Type:** H-Pile

Inspector: M. Ferguson

Embedment (m): 50.80

[illegible]



Load Increment 2100 kN

PILE NO: \_\_\_\_\_ Test Pile \_\_\_\_\_  
 Project: \_\_\_\_\_ MTO 2018-2024 \_\_\_\_\_  
 Location: \_\_\_\_\_ HWY 400 & 89 \_\_\_\_\_  
 Owner: \_\_\_\_\_ MTO \_\_\_\_\_  
 Contractor: \_\_\_\_\_ Fermar Paving Limited \_\_\_\_\_  
 Inspector: \_\_\_\_\_ M. Ferguson \_\_\_\_\_

Urkkada Job No. 1905CS1373  
 Date: November 12, 2019  
 Start Time: 19:02  
 Pile Size: 310x110  
 Pile Type: H-Pile  
 Embedment (m): 50.80

See sheet 300 kN for comments on Gauge Pressure

Date	Time		Applied Load (kN)	Gauge Reading (psi)	Test Pile												
					Vertical Gauge #1 (in)	Vertical Gauge #2 (in)	Gauge #1 Δ (mm)	Gauge #2 Δ (mm)	Average Δ Gauge (mm)	Lateral #1 (in)	Lateral #2 (in)	Wire Line Reading (cm)	Movement from Wire Line (cm)	Reaction Pile 1 (cm)	Reaction Pile 2 (cm)	Reaction Pile 3 (cm)	Reaction Pile 4 (cm)
	ZERO		0	0	2.957	3.626	-	-	-	0.533	0.391	83.90	-	56.0	56.1	63.5	64.1
	0 min	19:02	2100	2225	1.125	1.719	46.53	48.44	47.49	0.357	0.470	88.10	-4.20				
	5 min	19:07	2009	2200	1.109	1.700	46.94	48.92	47.93	0.356	0.473	88.10	-4.20				
	10 min	19:12	1992	2150	1.106	1.697	47.02	49.00	48.01	0.356	0.474	88.20	-4.30				
	11 min	19:13	2060	2150	1.055	1.645	48.31	50.32	49.31	0.355	0.470	88.30	-4.40				
	16 min	19:18	2102	2200	1.012	1.607	49.40	51.28	50.34	0.355	0.462	88.40	-4.50				
	20 min	19:22	2045	2150	1.005	1.594	49.58	51.61	50.60	0.355	0.466	88.50	-4.60				
	40 min	19:42	2005	2100	0.997	1.589	49.78	51.74	50.76	0.352	0.468	88.50	-4.60	55.7	55.8	63.2	63.8
	60 min	20:02	1988	2100	0.995	1.584	49.83	51.87	50.85	0.351	0.470	88.50	-4.60				
	61min	20:04	2102	2250	0.925	1.516	51.61	53.59	52.60	0.347	0.460	88.50	-4.60	55.7	55.8	63.2	63.8
	80 min	20:22	2037	2200	0.911	1.504	51.97	53.90	52.93	0.346	0.467	88.60	-4.70				
	93 min	20:35	2104	2250	0.880	1.468	52.76	54.81	53.78	0.346	0.463	88.80	-4.90	55.7	55.8	63.2	63.8
	100 min	20:42	2062	2200	0.875	1.462	52.88	54.97	53.92	0.346	0.466	88.80	-4.90				
	120 min	21:02	2042	2200	0.873	1.460	52.93	55.02	53.98	0.346	0.468	88.80	-4.90				



# Load Increments 2200 and 2300 kN

Maximum vertical movement limit increased by Golder to 78 mm, required

\*Vertical Gauge #1 to be adjusted to allow for increased movement

See sheet 300 kN for comments on Gauge Pressure

PILE NO: \_\_\_\_\_ Test Pile \_\_\_\_\_  
 Project: \_\_\_\_\_ MTO 2018-2024 \_\_\_\_\_  
 Location: \_\_\_\_\_ HWY 400 & 89 \_\_\_\_\_  
 Owner: \_\_\_\_\_ MTO \_\_\_\_\_  
 Contractor: \_\_\_\_\_ Fermar Paving Limited \_\_\_\_\_  
 Inspector: \_\_\_\_\_ M. Ferguson / S. Ferguson \_\_\_\_\_

Urkkada Job No. \_\_\_\_\_ 1905CS1373 \_\_\_\_\_  
 Date: \_\_\_\_\_ November 12, 2019 \_\_\_\_\_  
 Start Time: \_\_\_\_\_ 21:11 \_\_\_\_\_  
 Pile Size: \_\_\_\_\_ 310x110 \_\_\_\_\_  
 Pile Type: \_\_\_\_\_ H-Pile \_\_\_\_\_  
 Embedment (m): \_\_\_\_\_ 50.80 \_\_\_\_\_

Date	Time		Applied Load (kN)	Gauge Reading (psi)	Test Pile												
					Vertical Gauge #1 (in)	Vertical Gauge #2 (in)	Gauge #1 Δ (mm)	Gauge #2 Δ (mm)	Average Δ Gauge (mm)	Lateral #1 (in)	Lateral #2 (in)	Wire Line Reading (cm)	Movement from Wire Line (cm)	Reaction Pile 1 (cm)	Reaction Pile 2 (cm)	Reaction Pile 3 (cm)	Reaction Pile 4 (cm)
	ZERO		0	0	2.957	3.626	-	-	-	0.533	0.391	83.90	-	56.0	56.1	63.5	64.1
2019-11-12		2200 kN			*1.386 = 52.93 mm travel												
	0 min	21:11	2207	2250	1.359	1.331	53.62	58.29	55.95	0.342	0.461	89.30	-5.40	55.7	55.8	63.2	63.8
	5 min	21:16	2203	2250	1.328	1.300	54.40	59.08	56.74	0.342	0.461	89.30	-5.40	55.7	55.8	63.2	63.8
	11 min	21:22	2207	2250	1.190	1.260	57.91	60.10	59.00	0.340	0.460	89.60	-5.70	55.7	55.8	63.2	63.8
	20 min	21:31	2207	2250	1.162	1.232	58.62	60.81	59.71	0.340	0.460	89.70	-5.80				
		2300 kN															
	0 min	21:43	2304	2400	1.035	1.105	61.85	64.03	62.94	0.340	0.454	89.90	-6.00	55.6	55.7	63.2	63.8
	3 min	21:46	2306	2400	0.986	1.055	63.09	65.30	64.20	0.335	0.455	90.10	-6.20				
	7 min	21:50	2305	2400	0.955	1.024	63.88	66.09	64.98	0.336	0.456	90.10	-6.20	55.6	55.7	63.2	63.7
	13 min	21:56	2305	2400	0.926	0.995	64.61	66.83	65.72	0.335	0.459	90.20	-6.30				



**Load Increment 2400 kN**

\*1 - Movement exceed reading area of Lateral #2. Reset at 16 min.

\*2 - Movement exceeded reading area of wireline

See sheet 300 kN for comments on Gauge Pressure

PILE NO: \_\_\_\_\_ Test Pile \_\_\_\_\_  
 Project: \_\_\_\_\_ MTO 2018-2024 \_\_\_\_\_  
 Location: \_\_\_\_\_ HWY 400 & 89 \_\_\_\_\_  
 Owner: \_\_\_\_\_ MTO \_\_\_\_\_  
 Contractor: \_\_\_\_\_ Fermar Paving Limited \_\_\_\_\_  
 Inspector: \_\_\_\_\_ S. Ferguson \_\_\_\_\_

Urkkada Job No. 1905CS1373  
 Date: Nov. 12-13, 2019  
 Start Time: 22:02  
 Pile Size: 310x110  
 Pile Type: H-Pile  
 Embedment (m): 50.80

Date	Time		Applied Load (kN)	Gauge Reading (psi)	Test Pile									Reaction			
					Vertical Gauge #1 (in)	Vertical Gauge #2 (in)	Gauge #1 Δ (mm)	Gauge #2 Δ (mm)	Average Δ Gauge (mm)	Lateral #1 (in)	Lateral #2 (in)	Wire Line Reading (cm)	Movement from Wire Line (cm)	Reaction Pile 1 (cm)	Reaction Pile 2 (cm)	Reaction Pile 3 (cm)	Reaction Pile 4 (cm)
	ZERO		0	0	2.957	3.626	-	-	-	0.533	0.391	83.90	-	56.0	56.1	63.5	64.1
2019-11-12	0 min	22:02	2406	2500	0.760	0.831	68.83	70.99	69.91	0.336	0.452	90.70	-6.80				
	16 min	22:18	2410	2500	0.623	0.689	72.31	74.60	73.46	0.337	*10.422	*2					
	21 min	22:23	2406	2500	0.583	0.648	73.33	75.64	74.48	0.330	0.424						
	32 min	22:34	2405	2500	0.545	0.607	74.29	76.68	75.49	0.340	0.430			55.5	55.6	63.1	63.5
	43 min	22:45	2400	2500	0.509	0.577	75.21	77.44	76.33	0.339	0.431						
	60 min	23:02	2350	2450	0.504	0.566	75.33	77.72	76.53	0.338	0.434						
	80 min	23:22	2358	2450	0.459	0.521	76.48	78.87	77.67	0.337	0.435						
	100 min	23:42	2367	2450	0.429	0.490	77.24	79.65	78.45	0.333	0.436						
Nov-13	120 min	00:02	2352	2450	0.427	0.486	77.29	79.76	78.52	0.326	0.437						



# Unloading Cycle - 25% Decrements

PILE NO: \_\_\_\_\_ Test Pile \_\_\_\_\_

Project: \_\_\_\_\_ MTO 2018-2024 \_\_\_\_\_

Location: \_\_\_\_\_ HWY 400&89 \_\_\_\_\_

Owner: \_\_\_\_\_ MTO \_\_\_\_\_

Contractor: \_\_\_\_\_ Fermar Paving Limited \_\_\_\_\_

Inspector: \_\_\_\_\_ S. Ferguson \_\_\_\_\_

Urkkada Job No. \_\_\_\_\_ 1905CS1373 \_\_\_\_\_

Date: \_\_\_\_\_ November 13, 2019 \_\_\_\_\_

Start Time: \_\_\_\_\_ 00:08 \_\_\_\_\_

Pile Size: \_\_\_\_\_ 310x110 \_\_\_\_\_

Pile Type: \_\_\_\_\_ H-Pile \_\_\_\_\_

Embedment (m): \_\_\_\_\_ 50.80 \_\_\_\_\_

\*1 - Pump was not used for unloading, pressure remained at 2450 in pump

Date	Time		Applied Load  (kN)	Gauge Reading  (psi)	Test Pile													
					Vertical Gauge #1 (in)	Vertical Gauge #2 (in)	Gauge #1 Δ (mm)	Gauge #2 Δ (mm)	Average Δ Gauge (mm)	Lateral #1 (in)	Lateral #2 (in)	Wire Line Reading (cm)	Movement from Wire Line (cm)	Reaction Pile 1 (cm)	Reaction Pile 2 (cm)	Reaction Pile 3 (cm)	Reaction Pile 4 (cm)	
	ZERO		0	0	2.957	3.626	-	-	-	0.533	0.391	83.90	-	56.0	56.1	63.5	64.1	
2019-11-13		1800 kN																
	0 min	00:08	1742	*1	0.742	0.802	69.29	71.73	70.51	0.323	0.441							
	20 min	00:28	1754		0.746	0.802	69.19	71.73	70.46	0.322	0.444							
	40 min	00:48	1754		0.746	0.802	69.19	71.73	70.46	0.321	0.443							
	60 min	01:08	1754		0.746	0.802	69.19	71.73	70.46	0.321	0.444							
		1200 kN																
	0 min	01:14	1208		1.192	1.254	57.86	60.25	59.05	0.319	0.413	89.40	-5.50	55.8	55.9	63.2	63.7	
	20 min	01:34	1223		1.194	1.255	57.81	60.22	59.02	0.319	0.413	89.40	-5.50					
	40 min	01:54	1228		1.195	1.255	57.78	60.22	59.00	0.318	0.414	89.40	-5.50					
	60 min	02:14	1228		1.195	1.257	57.78	60.17	58.98	0.318	0.414	89.40	-5.50					

**Unloading Cycle - 25% Decrements**

PILE NO: \_\_\_\_\_ Test Pile \_\_\_\_\_

Urkkada Job No. 1905CS1373

\*1 - Pump was not used for unloading, pressure remained at 2450 in pump

Project: MTO 2018-2024

Date: November 13, 2019

Location: HWY 400&amp;89

Start Time: 00:08

Owner: MTO

Pile Size: 310x110

Contractor: Fermar Paving Limited

Pile Type: H-Pile

Inspector: S. Ferguson

Embedment (m): 50.80

2019-11-13		<b>600 kN</b>															
	0 min	02:24	606		1.675	1.748	45.59	47.70	46.65	0.331	0.380	88.20	-4.30				
	20 min	02:44	630		1.678	1.752	45.51	47.60	46.56	0.331	0.377	88.20	-4.30				
	40 min	03:04	635		1.678	1.752	45.51	47.60	46.56	0.331	0.376	88.20	-4.30				
	60 min	03:24	635		1.679	1.753	45.49	47.57	46.53	0.331	0.375	88.20	-4.30				
		<b>0 kN</b>															
	0 min	03:30	2		2.117	2.250	34.36	34.95	34.66	0.505	0.362	87.10	-3.20	56.0	56.1	63.5	63.9
	12 hr	15:30	26		2.134	2.274	33.93	34.34	34.14	0.510	0.353	87.10	-3.20	56.0	56.1	63.5	64.0



Figure 1: Load Movement Curve for from Static Load Test #4

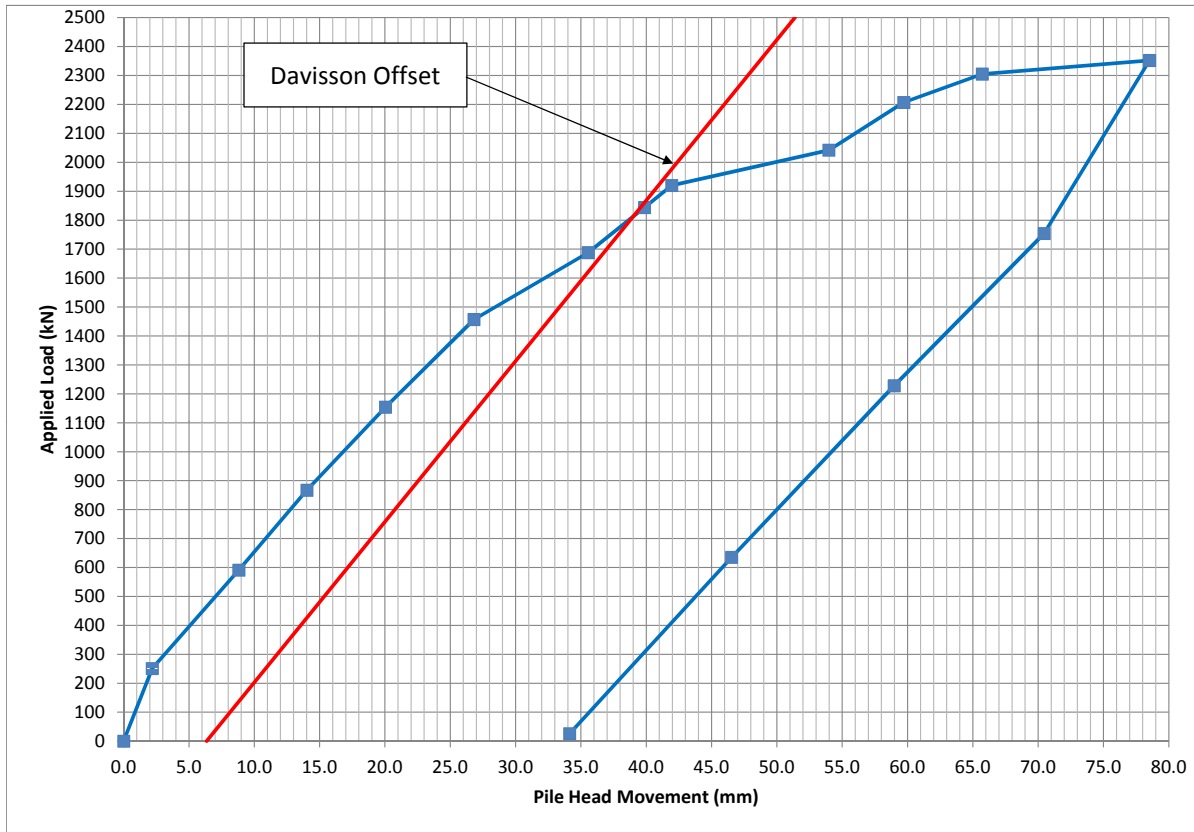


Table 1: Load Movement Summary

Load (kN)	Movement (mm)
0	0.0
251	2.2
591	8.8
867	14.0
1154	20.0
1457	26.8
1688	35.6
1844	39.9
1920	41.9
2042	54.0
2207	59.7
2305	65.7
2352	78.5
1754	70.5
1228	59.0
635	46.5
26	34.1

**f. Hwy 417 – Ramsayville**

Figure 1: Load Movement Curve for from Static Load Test

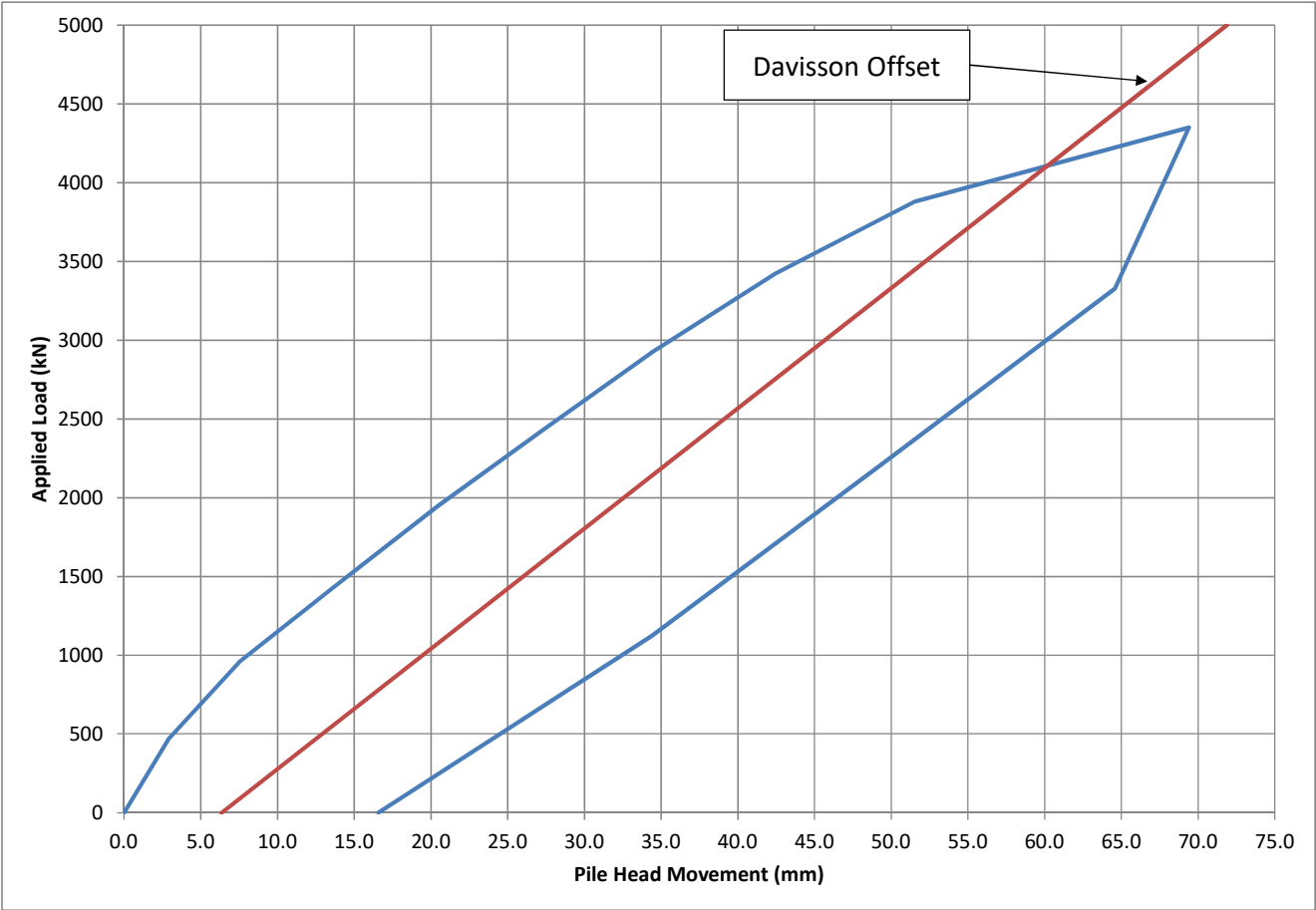


Table 1: Load Movement Summary

Load (kN)	Movement (mm)
0	0.0
471	2.9
954	7.5
1,432	13.7
1,945	20.4
2,430	27.3
2,927	34.5
3,422	42.4
3,880	51.5
4,350	69.4
3,328	64.6
2,238	49.7
1,122	34.4
0	16.6

**g. Hwy 400 - Essa Rd**

**Survey Monitoring of Micropiles**  
**Static Pile Load Testing: Procedure A - Quick Test**  
December 10, 2019

	Movement (mm)			
Time	MP-1A	MP-1B	MP-2A	MP-2B
1115	0	0	10	5
1130	10	10	5	5
1145	0	0	0	0
1200	0	5	0	0
1215	0	0	0	0
1230	0	0	0	0
1245	0	0	0	0
1300	0	0	0	0
1315	0	0	0	0
1330	0	0	0	0
1345	0	0	0	0
1400	0	0	0	0
1415	0	0	0	0
1430	0	0	0	0
<b>Total</b>	10	15	15	10

Note: 1. Time is in 24-hour format

STATIC PILE LOAD TEST RECORD - PROCEDURE A - QUICK TEST

Project:	Highway 400 and Essa	Pile Type/Size:	HP310x110	Golden Staff A.Poliack / C.Cornish	Target Load (kN):	3600
Project No.:	18105050	Pile embedment / Stickup (m):	31.8 / -0.1	Contractor:	GFL	Max tolerable Mvmt : 10-15% of Pile Width (45 mm)
Test Date:	December 10, 2019	Procedure :	A	Client:	Stantec / MTO	Max Rate of Mvmt: 0.0002 in per min . 0.004 mm per min

LOAD NO.	TIME			GAUGE READING (KIP)	Actual Applied Load (kN)	PILE MOVEMENT								WIRE LINE		
	START	Cumulative Time (hrs)	Target Load (kN)			DIAL # 1		DIAL #2		DIAL #3		DIAL #4		Average Cumulative Displacement (mm)	Reading (mm)	Cumulative Displacement (mm)
						Reading (mm)	Cumulative Displacement (mm)	Reading (mm)	Cumulative Displacement (mm)	Reading (mm)	Cumulative Displacement (mm)	Reading (mm)	Cumulative Displacement (mm)			
LOADING																
1	0	0.0	11:05	34	150	6.045		17.297		59.487			10.719			
	1	0.0	11:06		145											
	2	0.0	11:07		145	6.020	0.025	17.297	0.000	59.487	0.000	0.000	10.744	-0.025	0.000	
	4	0.1	11:09	29	130	6.033	0.013	17.297	0.000	59.500	-0.013	-0.006	10.744	-0.025	-0.006	
	8	0.1	11:13		127	6.045	0.000	17.272	0.025	59.500	-0.013	-0.003	10.744	-0.025	-0.003	
	15	0.3	11:20	28	125	6.083	-0.038	17.285	0.013	59.512	-0.025	-0.032	10.795	-0.076	-0.032	5.561
2	0	0.3	11:20	65	290	5.144	0.902	16.408	0.889	58.115	1.372	0.502	11.875	-1.156	0.502	
	1	0.3	11:21		290											
	2	0.3	11:22		290	5.105	0.940	16.345	0.953	58.115	1.372	0.527	11.875	-1.156	0.527	
	4	0.3	11:24		290	5.080	0.965	16.332	0.965	58.115	1.372	0.536	11.877	-1.158	0.536	
	8	0.4	11:28		290	5.080	0.965	16.332	0.965	58.115	1.372	0.537	11.875	-1.156	0.537	1.000
	15	0.5	11:35		290	5.080	0.965	16.332	0.965	58.115	1.372	0.536	11.877	-1.158	0.536	2.000
3	0	0.5	11:35	106	471	3.480	2.565	14.859	2.438	56.210	3.277	2.305	9.779	0.940	2.305	3.000
	1	0.5	11:36		467	3.454	2.591	14.834	2.464	56.210	3.277	2.318	9.779	0.940	2.318	
	2	0.5	11:37		464	3.454	2.591	14.834	2.464	56.210	3.277	2.324	9.754	0.965	2.324	
	4	0.6	11:39		462	3.429	2.616	14.757	2.540	56.210	3.277	2.350	9.754	0.965	2.350	3.000
	8	0.6	11:43	100	443	3.404	2.642	14.757	2.540	56.210	3.277	2.356	9.754	0.965	2.356	3.000
	15	0.8	11:50	99	440	3.404	2.642	14.757	2.540	56.210	3.277	2.356	9.754	0.965	2.356	
4	0	0.8	11:50	139	620	1.727	4.318	13.259	4.039	54.356	5.131	4.763	5.156	5.563	4.763	4.000
	1	0.8	11:51	138	615	1.702	4.343	13.246	4.051	54.356	5.131	4.778	5.131	5.588	4.778	5.000
	2	0.8	11:52		613	1.676	4.369	13.246	4.051	54.356	5.131	4.788	5.118	5.601	4.788	5.000
	4	0.8	11:54		611											
	8	0.9	11:58	137	607	1.676	4.369	13.208	4.089	54.356	5.131	4.797	5.118	5.601	4.797	5.000
	15	1.0	12:05	136	603	1.651	4.394	13.183	4.115	54.331	5.156	4.763	5.334	5.385	4.763	5.000
5	0	1.0	12:05	179	794	0.000	6.045	11.862	5.436	50.978	8.509	6.896	3.124	7.595	6.896	7.000
	1	1.0	12:06		782											
	2	1.0	12:07	173	770	-0.025	6.071	11.862	5.436	50.978	8.509	6.902	3.124	7.595	6.902	7.000
	4	1.1	12:09		765	-0.025	6.071	11.862	5.436	50.978	8.509	6.902	3.124	7.595	6.902	7.000
	8	1.1	12:13	171	760	-0.025	6.071	11.862	5.436	50.978	8.509	6.902	3.124	7.595	6.902	7.000
	15	1.3	12:20	171	762	-0.025	6.071	11.849	5.448	50.978	8.509	6.906	3.124	7.595	6.906	7.000

STATIC PILE LOAD TEST RECORD - PROCEDURE A - QUICK TEST

Project:	Highway 400 and Essa	Pile Type/Size:	HP310x110	Golder Staff A.Poliack / C.Comish	Target Load (kN):	3600
Project No.:	18105050	Pile embedment / Stickup (m):	31.8 / -0.1	Contractor:	GFL	Max tolerable Mvmt : 10-15% of Pile Width (45 mm)
Test Date:	December 10, 2019	Procedure :	A	Client:	Stantec / MTO	Max Rate of Mvmt: 0.0002 in per min . 0.004 mm per min

LOAD NO.	TIME		Gauge Reading (kN)	Actual Applied Load (kN)	PILE MOVEMENT												WIRE LINE	
	START	Cumulative Time (hrs)			DIAL # 1			DIAL #2			DIAL #3			DIAL #4			Average Cumulative Displacement (mm)	Cumulative Displacement (mm)
6	0	1.3	12:20	226	1005	-2.184	8.230	9.804	7.493	47.727	11.760	0.521	10.198	9.420	5.552	9.000		
	1	1.3	12:21		997													
	2	1.3	12:22		989	-2.210	8.255	9.779	7.518	47.701	11.786	0.508	10.211	9.442	5.552	9.000		
	4	1.3	12:24	219	973	-2.235	8.280	9.716	7.582	47.701	11.786	0.495	10.224	9.468	5.552	9.000		
	8	1.4	12:28	218	968	-2.261	8.306	9.703	7.595	47.676	11.811	0.483	10.236	9.487	5.552	9.000		
7	15	1.5	12:35	217	964	-2.261	8.306	9.703	7.595	47.650	11.836	0.483	10.236	9.493	5.552	9.000		
	0	1.5	12:35	272	1208	-4.470	10.516	7.696	9.601	45.288	14.199	-2.108	12.827	11.786	5.550	11.000		
	1	1.5	12:36		1197													
	2	1.5	12:37	267	1186	-4.483	10.528	7.671	9.627	45.288	14.199	-2.108	12.827	11.795	5.550	11.000		
	4	1.6	12:39	266	1181	-4.496	10.541	7.645	9.652	45.263	14.224	-2.134	12.852	11.817	5.550	11.000		
8	8	1.6	12:43	264	1176	-4.509	10.554	7.633	9.665	45.237	14.249	-2.134	12.852	11.830	5.550	11.000		
	15	1.8	12:50	263	1169	-4.534	10.579	7.620	9.677	45.212	14.275	-2.146	12.865	11.849	5.550	11.000		
	0	1.8	12:50	313	1391	-6.452	12.497	5.817	11.481	43.155	16.332	-4.343	15.062	13.843	5.548	13.000		
	1	1.8	12:51		1383													
	2	1.8	12:52		1374	-6.502	12.548	5.791	11.506	43.129	16.358	-4.343	15.062	13.868	5.548	13.000		
9	4	1.8	12:54	305	1356	-6.502	12.548	5.766	11.532	42.875	16.612	-4.369	15.088	13.945	5.548	13.000		
	8	1.9	12:58	303	1347	-6.528	12.573	5.740	11.557	43.078	16.408	-4.394	15.113	13.913				
	15	2.0	1:05	301	1339	-6.541	12.586	5.728	11.570	43.078	16.408	-4.394	15.113	13.919	5.548	13.000		
	0	2.0	1:05	355	1578	-8.776	14.821	3.505	13.792	40.615	18.872	-6.883	17.602	16.272	5.546	15.000		
	1	2.0	1:06		1570													
10	2	2.0	1:07		1562	-8.814	14.859	3.480	13.818	40.589	18.898	-6.896	17.615	16.297				
	4	2.1	1:09	347	1545	-8.865	14.910	3.429	13.868	40.589	18.898	-6.909	17.628	16.326	5.546	15.000		
	8	2.1	1:13	345	1534	-8.890	14.935	3.404	13.894	40.513	18.974	-6.947	17.666	16.367				
	15	2.3	1:20	344	1529	-8.890	14.935	3.366	13.932	40.513	18.974	-6.960	17.678	16.380	5.545	16.000		
	0	2.3	1:20	402	1788	-11.455	17.501	0.838	16.459	37.770	21.717	-9.703	20.422	19.025	5.543	18.000		
10	1	2.3	1:21		1776													
	2	2.3	1:22		1764	-11.506	17.551	0.762	16.535	37.719	21.768	-9.728	20.447	19.075	5.543	18.000		
	4	2.3	1:24	391	1740	-11.557	17.602	0.737	16.561	37.668	21.819	-9.779	20.498	19.120	5.543	18.000		
	8	2.4	1:28	389	1729	-11.570	17.615	0.686	16.612	37.643	21.844	-9.817	20.536	19.152	5.543	18.000		
	15	2.5	1:35	387	1722	-11.595	17.640	0.673	16.624	37.617	21.869	-9.817	20.536	19.167	5.543	18.000		



STATIC PILE LOAD TEST RECORD - PROCEDURE A - QUICK TEST

Project:	Highway 400 and Essa	Pile Type/Size:	HP310x110	Golder Staff A.Poliacik / C.Comish	Target Load (kN):	3600
Project No.:	18100500	Pile embedment / Stickup (m):	31.8 / -0.1	Contractor:	GFL	Max tolerable Mvmt : 10-15% of Pile Width (45 mm)
Test Date:	December 10, 2019	Procedure :	A	Client:	Stantec / MTO	Max Rate of Mvmt: 0.0002 in per min . 0.004 mm per min

LOAD NO.	TIME			Target Load (kN)	GAUGE READING (kN)	Actual Applied Load (kN)	PILE MOVEMENT								WIRE LINE		
	START	Cumulative Time (hrs)	TIME				DIAL #1		DIAL #2		DIAL #3		DIAL #4		Average Cumulative Displacement (mm)	Reading (mm)	Cumulative Displacement (mm)
							Reading (mm)	Cumulative Displacement (mm)	Reading (mm)	Cumulative Displacement (mm)	Reading (mm)	Cumulative Displacement (mm)	Reading (mm)	Cumulative Displacement (mm)			
11	0	2.5	1:35		448	1993	-14.326	20.371	-2.057	19.355	34.696	24.790	-12.725	23.444	21.990	5.540	21.000
	1	2.5	1:36			1978	-14.376	20.422	-2.134	19.431	34.646	24.841	-12.776	23.495	22.047	5.540	21.000
	2	2.5	1:37	1980		1962	-14.478	20.523	-2.210	19.507	34.620	24.867	-12.776	23.495	22.098		
	4	2.6	1:39		434	1932	-14.478	20.523	-2.210	19.507	34.595	24.892	-12.827	23.546	22.117	5.540	21.000
	8	2.6	1:43		432	1919	-14.529	20.574	-2.286	19.583	34.519	24.968	-12.903	23.622	22.187	5.540	21.000
12	15	2.8	1:50		430	1912	-14.580	20.625	-2.311	19.609	34.468	25.019	-12.929	23.647	22.225	5.540	21.000
	0	2.8	1:50		496	2205	-17.983	24.028	-5.461	22.758	31.191	28.296	-16.307	27.026	25.527	5.536	25.000
	1	2.8	1:51			2200											
	2	2.8	1:52			2194	-17.882	23.927	-5.588	22.885	31.090	28.397	-16.332	27.051	25.565	5.536	25.000
	4	2.8	1:54	2160		2183	-17.932	23.978	-5.639	22.936	31.064	28.423	-16.408	27.127	25.616		
13	8	2.9	1:58			2161	-17.958	24.003	-5.664	22.962	31.013	28.473	-16.459	27.178	25.654	5.536	25.000
	15	3.0	2:05			2122	-18.085	24.130	-5.817	23.114	30.886	28.600	-16.510	27.229	25.768	5.536	25.000
	20	3.1	2:10		471	2094	-18.110	24.155	-5.817	23.114	30.886	28.600	-16.510	27.229	25.775		
	0	3.1	2:10		536	2383	-20.955	27.000	-8.700	25.997	27.991	31.496	-19.558	30.277	28.692	5.533	28.000
	1	3.1	2:11			2376											
13	2	3.1	2:12	2340		2368	-21.057	27.102	-8.738	26.035	27.940	31.547	-19.609	30.328	28.753	5.533	28.000
	4	3.2	2:14			2354	-21.107	27.153	-8.763	26.060	27.889	31.598	-19.685	30.404	28.804		
	8	3.2	2:18			2324	-21.133	27.178	-8.839	26.137	27.813	31.674	-19.710	30.429	28.854	5.533	28.000
	15	3.3	2:25		511	2273	-21.234	27.280	-8.915	26.213	27.711	31.775	-19.812	30.531	28.950	5.533	28.000
	UNLOADING																
1	0	3.3	3:00		479	2129	42.469	27.076	54.737	26.060	27.889	31.598	43.942	30.277	28.753	5.534	27.000
	1	3.4	3:01			2129	42.469	27.076	54.737	26.060	27.889	31.598	43.942	30.277	28.753		
	2	3.4	3:02	1950		2129	42.469	27.076	54.737	26.060	27.889	31.598	43.942	30.277	28.753		
	4	3.4	3:04			2129	42.469	27.076	54.762	26.035	27.889	31.598	43.955	30.264	28.743		
	8	3.5	3:08		479	2131	42.469	27.076	54.762	26.035	27.889	31.598	43.967	30.251	28.740	5.534	27.000
2	15	3.6	3:15		479	2131	42.494	27.051	54.762	26.035	27.889	31.598	43.967	30.251	28.734		
	0	3.6	3:15		389	1730	43.790	25.756	55.829	24.968	28.981	30.505	47.777	26.441	26.918	5.535	26.000
	1	3.6	3:16			1733				80.797		59.487		74.219			
	2	3.6	3:17	1560	390	1735	43.790	25.756	55.829	24.968	29.007	30.480	47.777	26.441	26.911		
	4	3.7	3:19			1736	43.790	25.756	55.855	24.943	29.007	30.480	47.803	26.416	26.899	5.535	26.000
	8	3.7	3:23			1737	43.790	25.756	55.867	24.930	29.020	30.467	47.828	26.391	26.886	5.535	26.000
	15	3.8	3:30		391	1739	43.790	25.756	55.880	24.917	29.032	30.455	47.866	26.353	26.870	5.535	26.000

STATIC PILE LOAD TEST RECORD - PROCEDURE A - QUICK TEST

Project: Highway 400 and Essa

Project No.: 18105050

Test Date: December 10, 2019

Pile Type/Size: HP310x110

Pile embedment / Stickup (m): 31.8 / -0.1

Procedure : A

Golder Staff A.Poliack / C.Comish

Contractor: GFL

Client: Stantec / MTO

Target Load (kN): 3600

Max tolerable Mvmt : 10-15% of Pile Width (45 mm)

Max Rate of Mvmt: 0.0002 in per min . 0.004 mm per min

LOAD NO.	TIME			GAUGE READING (KIP)	Actual Applied Load (kN)	PILE MOVEMENT												WIRE LINE	
	START	TIME				DIAL #1			DIAL #2			DIAL #3			DIAL #4		Average Cumulative Displacement (mm)	Reading (mm)	Cumulative Displacement (mm)
		Cumulative Time (hrs)	TIME			Reading (mm)	Cumulative Displacement (mm)	Reading (mm)	Cumulative Displacement (mm)	Reading (mm)	Cumulative Displacement (mm)	Reading (mm)	Cumulative Displacement (mm)	Reading (mm)	Cumulative Displacement (mm)				
	0	3.8	3:30	1170	289	1286	46.507	23.038	58.344	22.454	31.674	27.813	50.673	23.546	24.213	5.537	24.000		
	1	3.9	3:31			1287	69.545			80.797	59.487		74.219						
	2	3.9	3:32			1288	69.545			80.797	59.487		74.219						
	4	3.9	3:34			1288	23.038	58.445	22.352	31.699	27.788	50.749	23.470	24.162	5.537	24.000			
	8	4.0	3:38		291	1294	46.507	23.038	58.801	21.996	31.687	27.800	50.749	23.470	24.076				
	15	4.1	3:45	780	291	1294	46.507	23.038	58.471	22.327	31.699	27.788	50.749	23.470	24.155	5.537	24.000		
	0	4.1	3:45		194	863	50.394	19.152	18.821	35.585	23.901	54.813	19.406	20.320	5.541	20.000			
	1	4.1	3:46			867	50.419	19.126	62.001	18.796	35.585	23.901	54.889	19.329	20.288				
	2	4.1	3:47			872	50.419	19.126	62.128	18.669	35.598	23.889	54.889	19.329	20.253	5.541	20.000		
	4	4.2	3:49		198	881	50.419	19.126	62.128	18.669	35.598	23.889	54.889	19.329	20.253	5.541	20.000		
	8	4.2	3:53	390	198	881	50.419	19.126	62.128	18.669	35.598	23.889	54.902	19.317	20.250	5.541	20.000		
	15	4.3	4:00		199	883	50.444	19.101	62.154	18.644	35.611	23.876	54.915	19.304	20.231	5.541	20.000		
	0	4.3	4:00		96	425	55.194	14.351	66.612	14.186	40.665	18.821	60.325	13.894	15.313	5.546	15.000		
	1	4.4	4:01			426	55.207	14.338	66.650	14.148	40.665	18.821	60.325	13.894	15.300				
	2	4.4	4:02			427	55.207	14.338	66.650	14.148	40.665	18.821	60.325	13.894	15.300				
	4	4.4	4:04	0		430	55.220	14.326	66.662	14.135	40.665	18.821	60.338	13.881	15.291	5.546	15.000		
	8	4.5	4:08			434	55.245	14.300	66.662	14.135	40.691	18.796	60.350	13.868	15.275	5.546	15.000		
	15	4.6	4:15		99	441	55.245	14.300	66.675	14.122	40.691	18.796	60.376	13.843	15.265	5.546	15.000		
	0	4.6	4:15		0	0	60.401	9.144	71.730	9.068	46.584	12.903	64.440	9.779	10.224	5.551	10.000		
	1	4.6	4:16			0	60.797	8.748	71.907	8.890	46.685	12.802	64.668	9.550	9.997	5.551	10.000		
6	2	4.6	4:17	0		0	60.884	8.661	71.933	8.865	46.736	12.751	64.694	9.525	9.950	5.551	10.000		
	4	4.7	4:19			0	60.935	8.611	71.958	8.839	46.787	12.700	64.770	9.449	9.900				
	8	4.7	4:23		0	0	60.985	8.560	71.984	8.814	46.838	12.649	64.834	9.385	9.852	5.551	10.000		
	15	4.8	4:30			0	61.138	8.407	72.034	8.763	46.888	12.598	64.897	9.322	9.773				

DIAL GAUGE SETUP:

- Dial Gauge #1 ACPG35
- Dial Gauge #2 ACPG26
- Dial Gauge #3 25-3041
- Dial Gauge #4 KXB634

Hwy 400



Essa Rd

Dial Gauge Locations

STATIC PILE LOAD TEST RESULTS - PROCEDURE A - QUICK TEST

PILE No.	PLT-1	DATE DRIVEN	04-Nov-19
PILE TYPE	310 mm x 110 mm		
SHOE DETAILS	NA		
FINAL LENGTH DRIVEN	31.8 m		
LENGTH AFTER CUT-OFF	31.7 m		
EMBEDDED LENGTH	31.5 m		
CUT-OFF ELEVATION	249.1 m		
TIP ELEVATION	215.9 m		

LOAD TEST RESULTS	
TEST No.	1
DATE	10-Dec-19
MAX LOAD APPLIED (kN)	2380
ESTIMATED FAILURE (kN) (Davisson Method)	2600
ESTIMATED FAILURE (kN) (10% of Pile Diameter)	2300

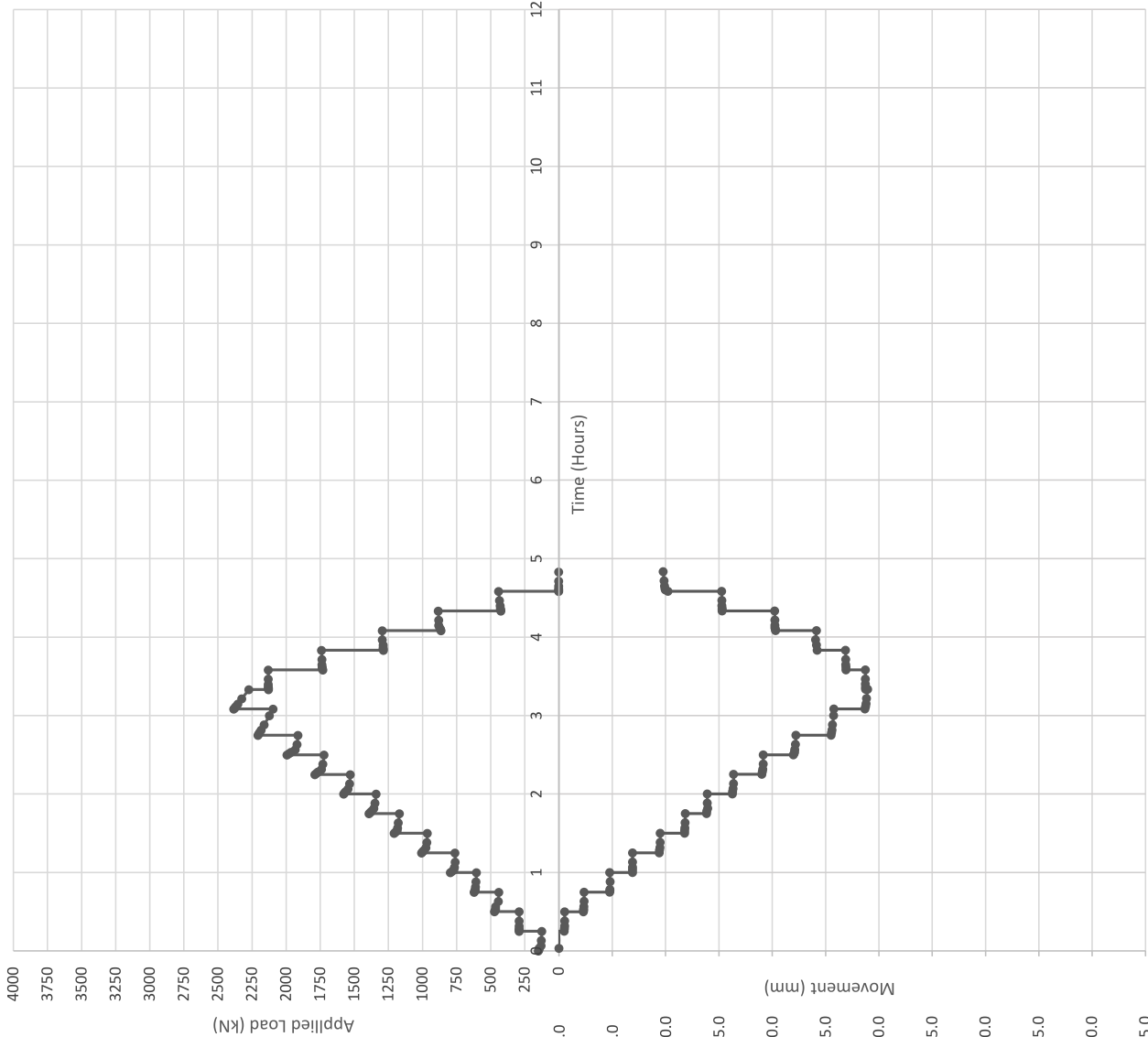
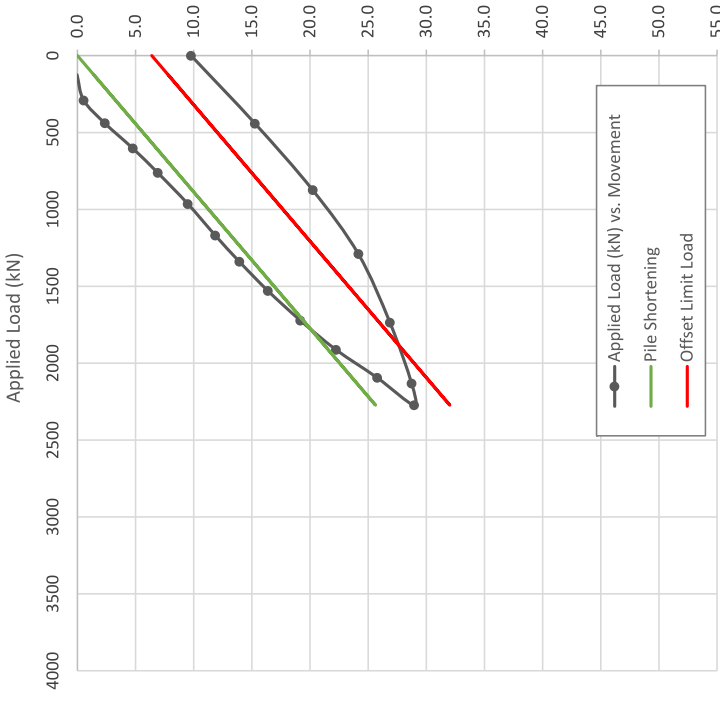


FIGURE F-1

**Survey Monitoring of Micropiles****Static Pile Load Testing: Procedure B - Maintained Test**

January 12 and 13, 2020

	<b>Movement (mm)</b>			
<b>Time</b>	<b>MP-1A</b>	<b>MP-1B</b>	<b>MP-2A</b>	<b>MP-2B</b>
1426	0	0	0	0
1440	0	0	0	0
1450	0	0	0	0
1500	0	0	0	0
1512	0	0	0	0
1522	0	0	0	0
1532	0	0	0	0
1542	0	0	0	0
1552	0	0	0	0
1602	0	0	0	0
1612	0	0	0	0
1624	0	0	0	0
1636	0	0	0	0
1648	0	0	0	0
1710	0	0	0	0
1740	0	0	0	0
1802	0	0	0	0
1835	0	0	0	0
1901	0	0	0	0
1945	0	0	0	0
2130	20	0	0	10
2210	0	10	0	0
2300	0	0	0	0
2330	0	0	0	0
2338	FAILED	FAILED	FAILED	FAILED
<b>Total*</b>	20	10	0	10

\*Prior to failure

Note: 1. Time is in 24-hour format

STATIC PILE LOAD TEST RECORD - PROCEDURE B - MAINTAINED TEST

Project:	Highway 400 and Essa	Pile Type/Size:	HP310x110	Golden Staff:	A.Pollack / C.Comish	Target Load (kN):	3600
Project No.:	18105050	Pile embedment / Stickup (m):	31.8 / -0.1	Contractor:	GFL	Max tolerable Mvmt :	10-15% of Pile Width (45 mm)
Test Date:	January 13 and 14, 2020	Procedure :	B	Client:	Stantec /MTO	Max Rate of Mvmt:	0.0002 in per min . 0.004 mm per min

#SPILL	TIME		Target Load (kN)	GAUGE READING (Digits)	Actual Applied Load (kN)	PILE MOVEMENT						WIRE LINE		
	START	Cumulative Time (hrs)				DIAL # 1		DIAL #2		DIAL #3		DIAL #4		Average Rate of Displacement (mm)
						Reading (mm)	Rate of Displacement (per min, per interval)	Reading (mm)	Rate of Displacement (per min, per interval)	Reading (mm)	Rate of Displacement (per min, per interval)	Reading (mm)	Rate of Displacement (per min, per interval)	Average Rate of Displacement (mm)
LOADING														
AL	0	0.00	0	850	64	80.670		88.824		55.347		93.345		0.557
	0	0.00		1355	450	77.521	-	85.928	2.896	52.527	2.819	90.195		0.554
	5	0.08		1356	451	77.343	-0.036	85.801	3.023	52.375	2.972	90.018	-0.036	0.554
	10	0.17		1351	447	77.241	-0.020	85.750	3.073	52.299	3.048	89.916	-0.020	0.554
	20	0.33	450	1355	450	77.216	-0.003	85.649	3.175	52.273	3.073	89.891	-0.003	0.554
1	40	0.67		1352	448	77.140	-0.004	85.573	3.251	52.248	3.099	89.814	-0.004	0.553
	60	1.00		1354	450	77.140	0.000	85.573	3.251	52.222	3.124	89.814	0.000	0.553
	0	1.00	15:18	1953	901	72.542	8.128	81.432	7.391	48.031	7.315	85.217	0.077	0.549
	5	1.08	15:23	1952	901	72.441	-0.020	81.407	7.417	47.955	7.391	85.115	-0.015	0.549
	10	1.17	15:28	1950	899	72.390	-0.010	81.382	7.442	47.879	7.468	85.065	-0.010	0.548
2	20	1.33	15:38	1949	899	72.365	-0.003	81.331	7.493	47.879	7.468	85.014	-0.005	0.548
	0	1.33	15:42	2553	1347	67.920	12.751	77.572	11.252	44.348	10.998	80.823		0.545
	5	1.42	15:47	2550	1345	67.767	-0.030	77.521	11.303	44.272	11.074	80.670	-0.030	0.544
	10	1.50	15:52	2549	1344	67.691	-0.015	77.470	11.354	44.221	11.125	80.594	-0.015	0.544
	20	1.67	16:02	2552	1346	67.615	-0.008	77.419	11.405	44.196	11.151	80.518	-0.008	0.544
3	40	2.00	16:22	2554	1348	67.564	-0.003	77.495	11.328	44.196	11.151	80.467	-0.003	0.544
	0	2.00	16:29	3163	1793	63.424	17.247	73.914	14.910	40.919	14.427	76.708		0.539
	5	2.08	16:34	3170	1798	63.195	-0.046	73.711	15.113	40.742	14.605	76.429	-0.056	0.539
	10	2.17	16:39	3174	1801	63.043	-0.030	73.609	15.215	40.640	14.707	76.302	-0.025	0.539
	20	2.33	16:49	3173	1800	62.941	-0.010	73.520	15.304	40.538	14.808	76.200	-0.010	0.539
4	40	2.67	17:09	3173	1800	62.814	-0.006	73.381	15.443	40.462	14.884	76.073	-0.006	0.539
	60	3.00	17:29	3173	1800	62.814	0.000	73.330	15.494	40.437	14.910	75.895	-0.001	0.539
	0	3.00	17:35	3797	2249	58.039	22.631	69.469	19.355		18.161	71.984		0.538
	5	3.08	17:40	3800	2251	57.658	-0.076	69.393	19.431	36.932	18.415	71.628	-0.071	0.538
	10	3.17	17:45	3793	2246	57.556	-0.020	69.063	19.761	36.830	18.517	71.552	-0.015	0.538
5	20	3.33	17:55	3797	2249	57.353	-0.020	68.872	19.952	36.678	18.669	71.374	-0.015	0.538
	40	3.67	18:15	3796	2248	57.201	-0.008	68.707	20.117	36.525	18.821	71.247	-0.008	0.538
	60	4.00	18:35	3797	2249	57.074	-0.006	68.580	20.244	36.424	18.923	71.120	-0.005	0.538
	80	4.33	18:55	3799	2250	57.010	-0.003	68.478	20.345	36.347	18.999	71.069	-0.003	0.538

STATIC PILE LOAD TEST RECORD - PROCEDURE B - MAINTAINED TEST

Project:	Highway 400 and Essa	Pile Type/Size:	HP310x110	Golden Staff:	A.Pollack / C.Comish	Target Load (kN):	3600
Project No.:	18105050	Pile embedment / Stickup (m):	31.8 / -0.1	Contractor:	GFL	Max tolerable Mvmt :	10-15% of Pile Width (45 mm)
Test Date:	January 13 and 14, 2020	Procedure :	B	Client:	Stantec / MTO	Max Rate of Mvmt:	0.0002 in per min . 0.004 mm per min

#Pile ID	TIME			Target Load (kN)	GAUGE READING (Digits)	Actual Applied Load (kN)	PILE MOVEMENT												Average Cumulative Displacement (mm)	Average Rate of Displacement (mm)	WIRE LINE	
	START	Cumulative Time (hrs)	TIME				DIAL # 1			DIAL # 2			DIAL # 3			DIAL # 4					Rate of Displacement (mm/min, per interval)	Cumulative Displacement (mm)
							Reading (mm)	Cumulative Displacement (mm)	Rate of Displacement (per min, per interval)	Reading (mm)	Cumulative Displacement (mm)	Rate of Displacement (per min, per interval)	Reading (mm)	Cumulative Displacement (mm)	Rate of Displacement (per min, per interval)	Reading (mm)	Cumulative Displacement (mm)	Rate of Displacement (per min, per interval)				
6	0	4.33	19:01	4436	2700		50.368	30.302	-0.102	62.941	25.883		31.648	23.698		65.151	28.194		27.019		0.526	0.310
	5	4.42	19:06	4430	2696		49.860	30.810	-0.102	62.535	26.289	-0.081	31.242	24.105	-0.081	64.745	28.600	-0.081	27.451	-0.086	0.526	0.310
	10	4.50	19:11	4437	2701		49.530	31.140	-0.066	62.281	26.543	-0.051	31.039	24.308	-0.041	64.465	28.880	-0.056	27.718	-0.053	0.525	0.320
	20	4.67	19:21	4434	2699		48.971	31.699	-0.056	61.773	27.051	-0.051	30.556	24.790	-0.048	63.932	29.413	-0.053	28.238	-0.052	0.524	0.330
	40	5.00	19:41	4432	2698	2700	48.463	32.207	-0.025	61.341	27.483	-0.022	30.099	25.248	-0.023	63.449	29.896	-0.024	28.708	-0.023	0.524	0.330
	60	5.33	20:01	4433	2698		48.158	32.512	-0.015	61.062	27.762	-0.014	29.845	25.502	-0.013	63.195	30.150	-0.013	28.981	-0.014	0.523	0.330
	80	5.67	20:21	4437	2701		47.981	32.690	-0.009	60.909	27.915	-0.008	29.718	25.629	-0.006	63.030	30.315	-0.008	29.137	-0.008	0.523	0.340
	100	6.00	20:41	4433	2698		47.854	32.817	-0.006	60.782	28.042	-0.006	29.616	25.730	-0.005	62.916	30.429	-0.006	29.254	-0.006	0.523	0.340
7	120	6.33	21:01	4436	2700		47.752	32.918	-0.005	60.681	28.143	-0.005	29.515	25.832	-0.005	62.840	30.505	-0.004	29.350	-0.005	0.523	0.340
	0	6.33	21:12	5084	3150		38.760	41.910		54.305	34.519		23.876	31.471		54.661	38.684		36.646		0.512	0.450
	5	6.42	21:17	5085	3151		37.490	43.180	-0.254	53.162	35.662	-0.229	23.114	32.233	-0.152	53.569	39.776	-0.218	37.713	-0.213	0.512	0.450
	10	6.50	21:22	5085	3151		36.982	43.688	-0.102	52.807	36.017	-0.071	22.758	32.588	-0.071	53.086	40.259	-0.097	38.138	-0.085	0.511	0.460
	20	6.67	21:34	5084	3150		36.246	44.425	-0.074	52.299	36.525	-0.051	22.327	33.020	-0.043	52.476	40.869	-0.061	38.710	-0.057	0.511	0.460
	40	7.00	21:52	5084	3150	3150	35.636	45.034	-0.030	51.892	36.932	-0.020	21.996	33.350	-0.017	51.968	41.377	-0.025	39.173	-0.023	0.510	0.470
	60	7.33	22:12	5083	3150		35.255	45.415	-0.019	51.587	37.236	-0.015	21.742	33.604	-0.013	51.587	41.758	-0.019	39.503	-0.017	0.510	0.470
	80	7.67	22:32	5082	3149		34.976	45.695	-0.014	51.435	37.389	-0.008	21.615	33.731	-0.006	51.384	41.961	-0.010	39.694	-0.010	0.510	0.470
	100	8.00	22:53	5084	3150		34.798	45.872	-0.009	51.257	37.567	-0.009	21.463	33.884	-0.008	51.232	42.113	-0.008	39.859	-0.008	0.509	0.480
	120	8.33	23:14	5085	3151		34.595	46.076	-0.010	51.562	37.262	0.015	21.361	33.985	-0.005	51.054	42.291	-0.009	39.903	-0.002	0.509	0.480
	140	8.67	23:32	5088	3132		34.493	46.177	-0.005	51.562	37.262	0.000	21.336	34.011	-0.001	50.952	42.393	-0.005	39.961	-0.003	0.509	0.480
	8	0	8.67	23:38	3600		NA	NA	NA	NA	NA	NA	NA	NA	NA	NA	NA	NA	NA	NA	NA	NA

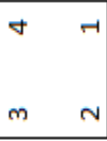
Notes:

1. Reaction Frame Failed at Time 23:38

DIAL GAUGE SETUP:

- Dial Gauge #1      ACPG26  
Dial Gauge #2      ACPG26  
Dial Gauge #3      25-3041  
Dial Gauge #4      ACPG45

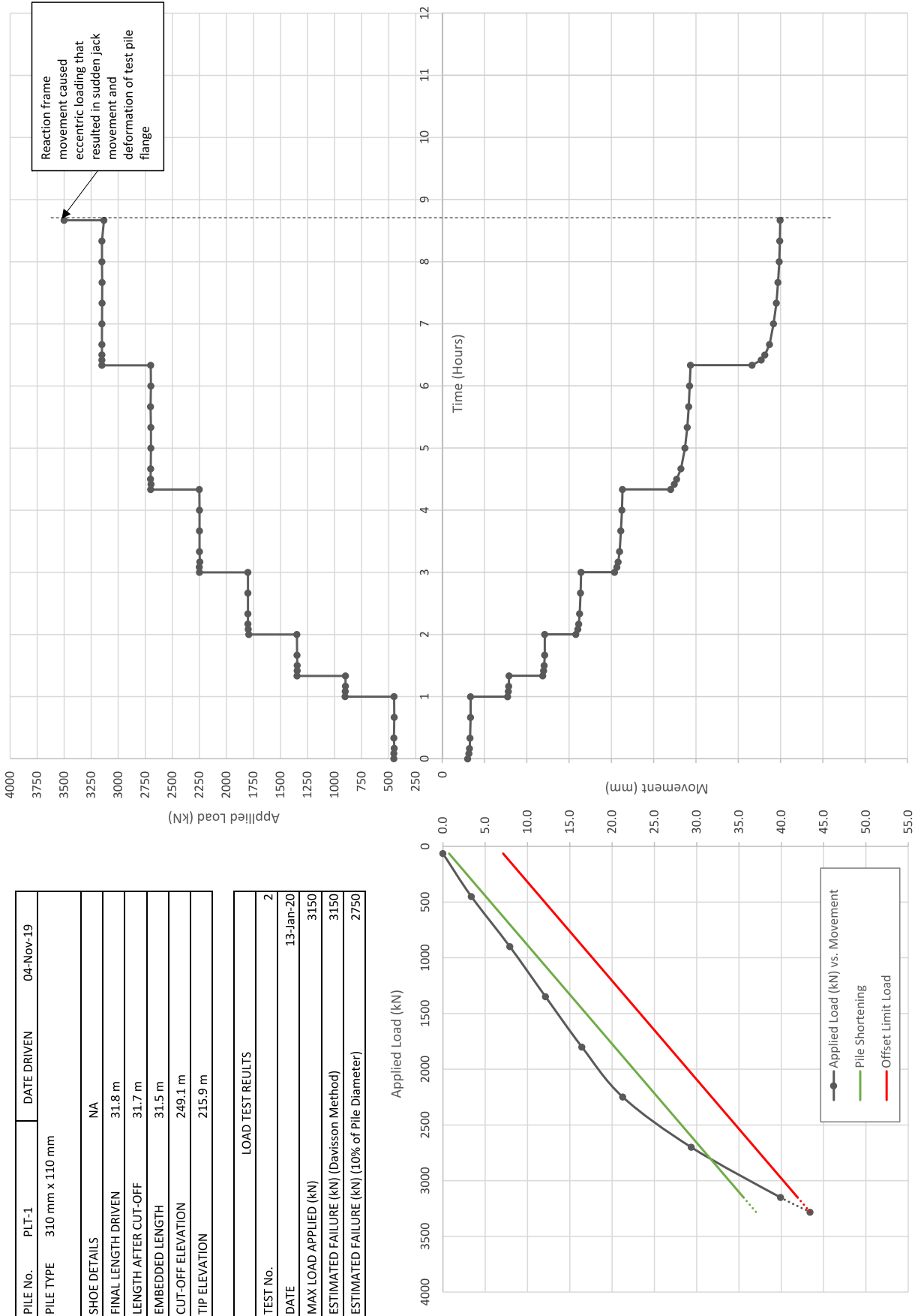
Hwy 400



Dial Gauge Locations

FIGURE F-2: STATIC PILE LOAD TEST RESULTS - PROCEDURE B - MAINTAINED TEST

PILE No.	PLT-1	DATE DRIVEN	04-Nov-19
PILE TYPE	310 mm x 110 mm		
SHOE DETAILS		NA	
FINAL LENGTH DRIVEN	31.8 m		
LENGTH AFTER CUT-OFF	31.7 m		
EMBEDDED LENGTH	31.5 m		
CUT-OFF ELEVATION	249.1 m		
TIP ELEVATION	215.9 m		
LOAD TEST RESULTS			
TEST No.	2		
DATE	13-Jan-20		
MAX LOAD APPLIED (kN)	3150		
ESTIMATED FAILURE (kN) (Davison Method)	3150		
ESTIMATED FAILURE (kN) (10% of Pile Diameter)	2750		



#### **h. Rainy River - Baudette River Interational Bridge**



AFT-Cell Gross Load vs Displacement  
Rainy River Bridge  
Test Pile

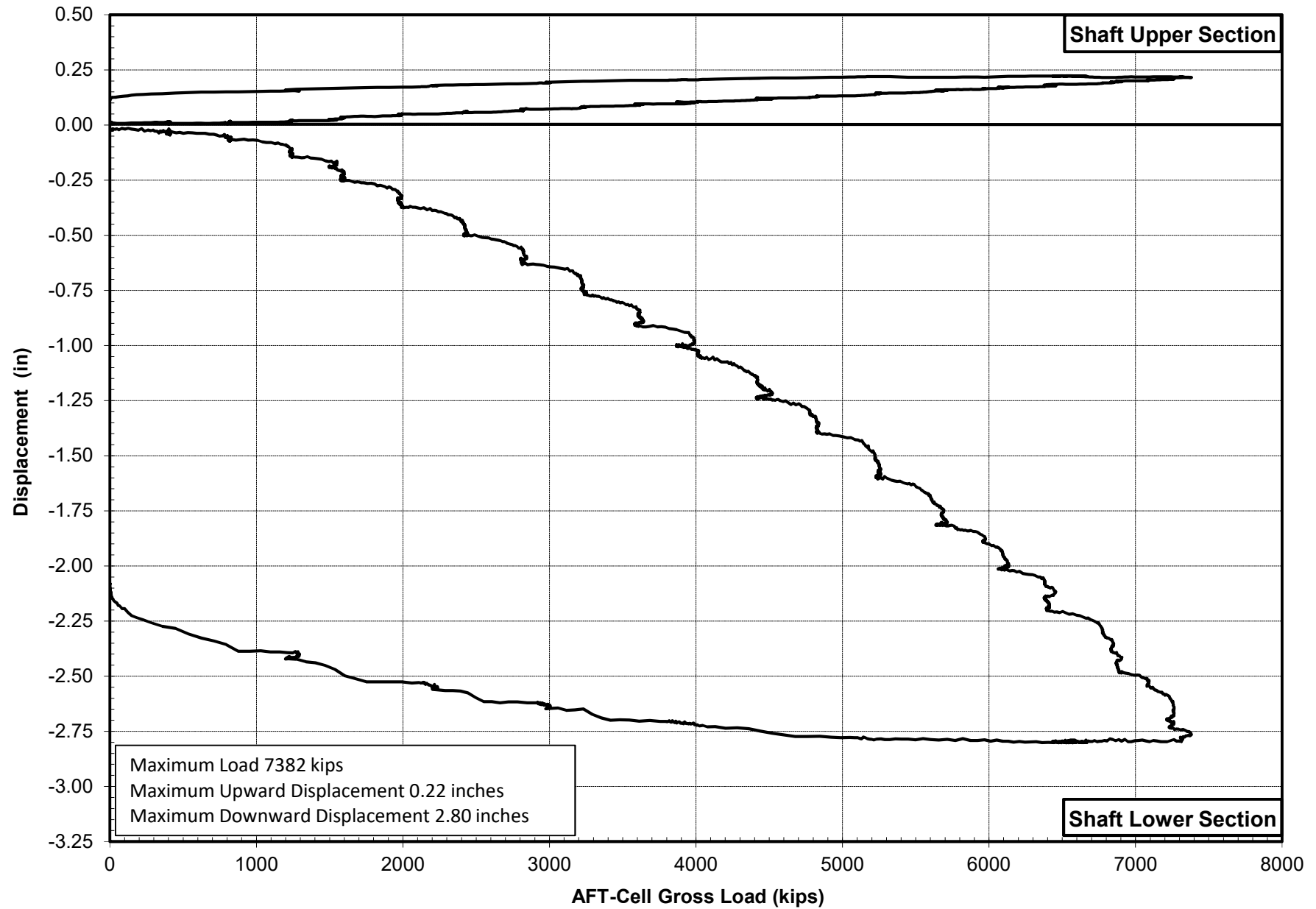


Figure 1



AFT-Cell Load vs Time  
Rainy River Bridge  
Test Pile

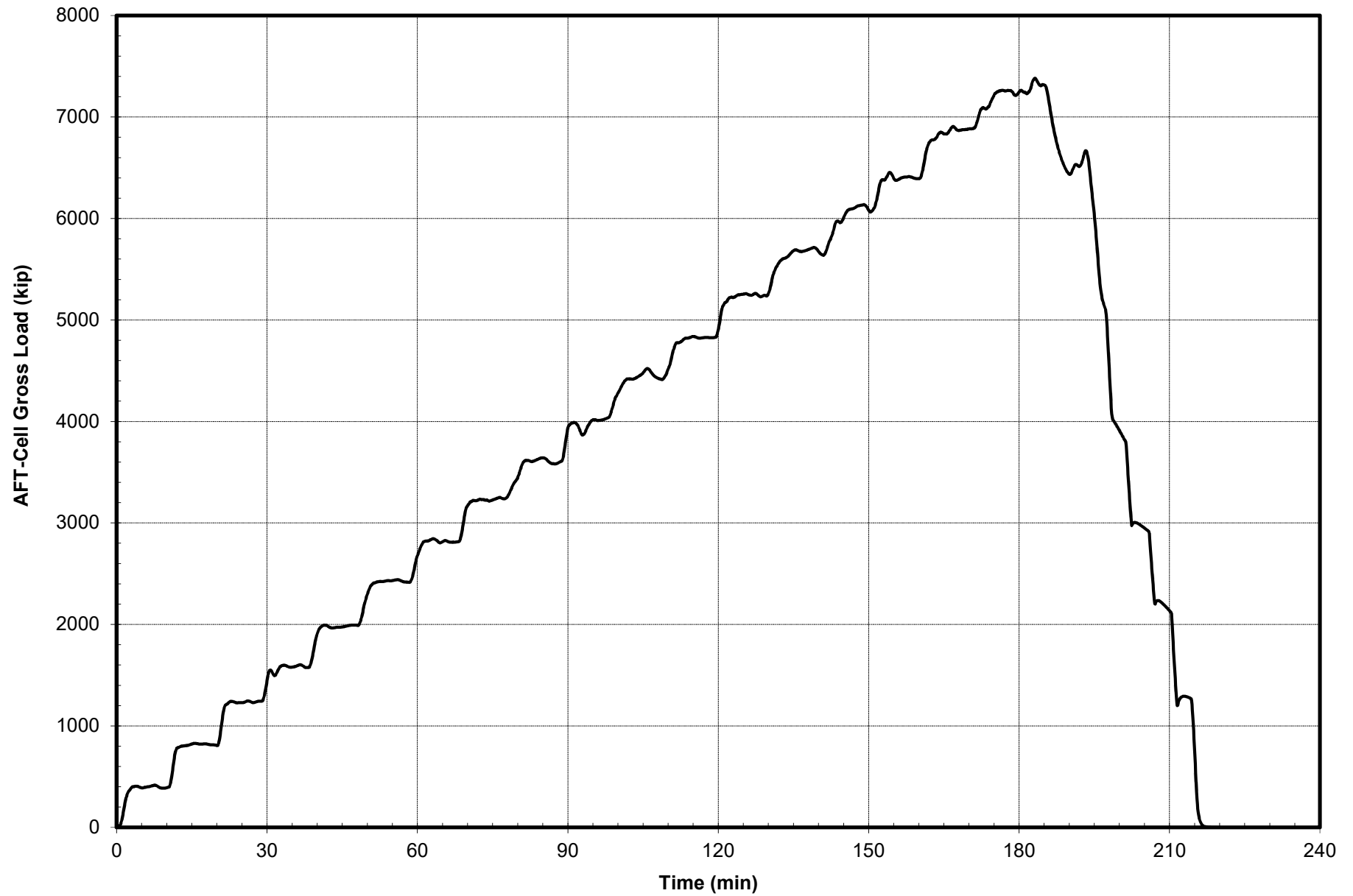


Figure 2

AFT-Cell Displacement vs Time  
Rainy River Bridge  
Test Pile

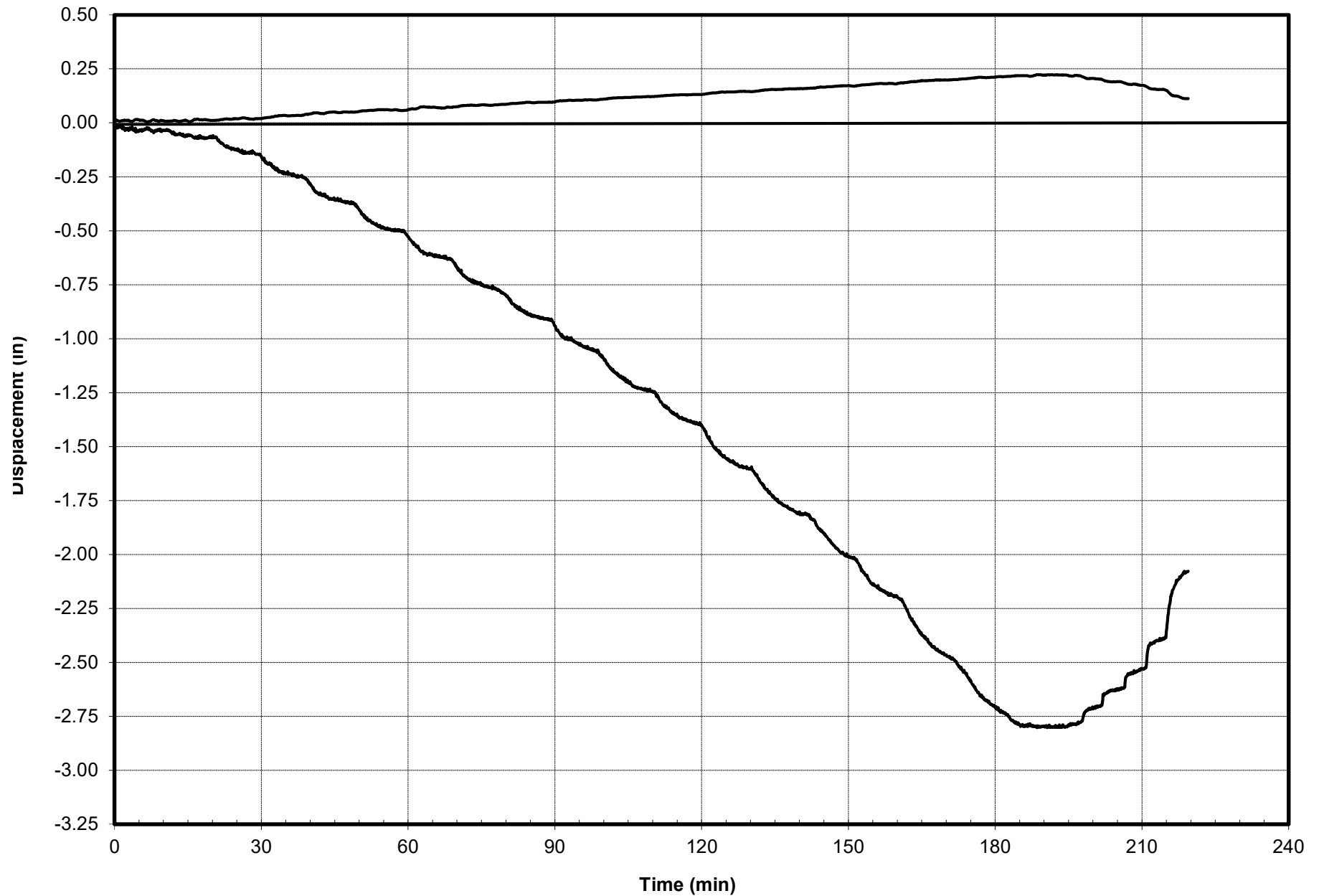


Figure 3

Upper Section Strain vs Time  
Rainy River Bridge  
Test Pile

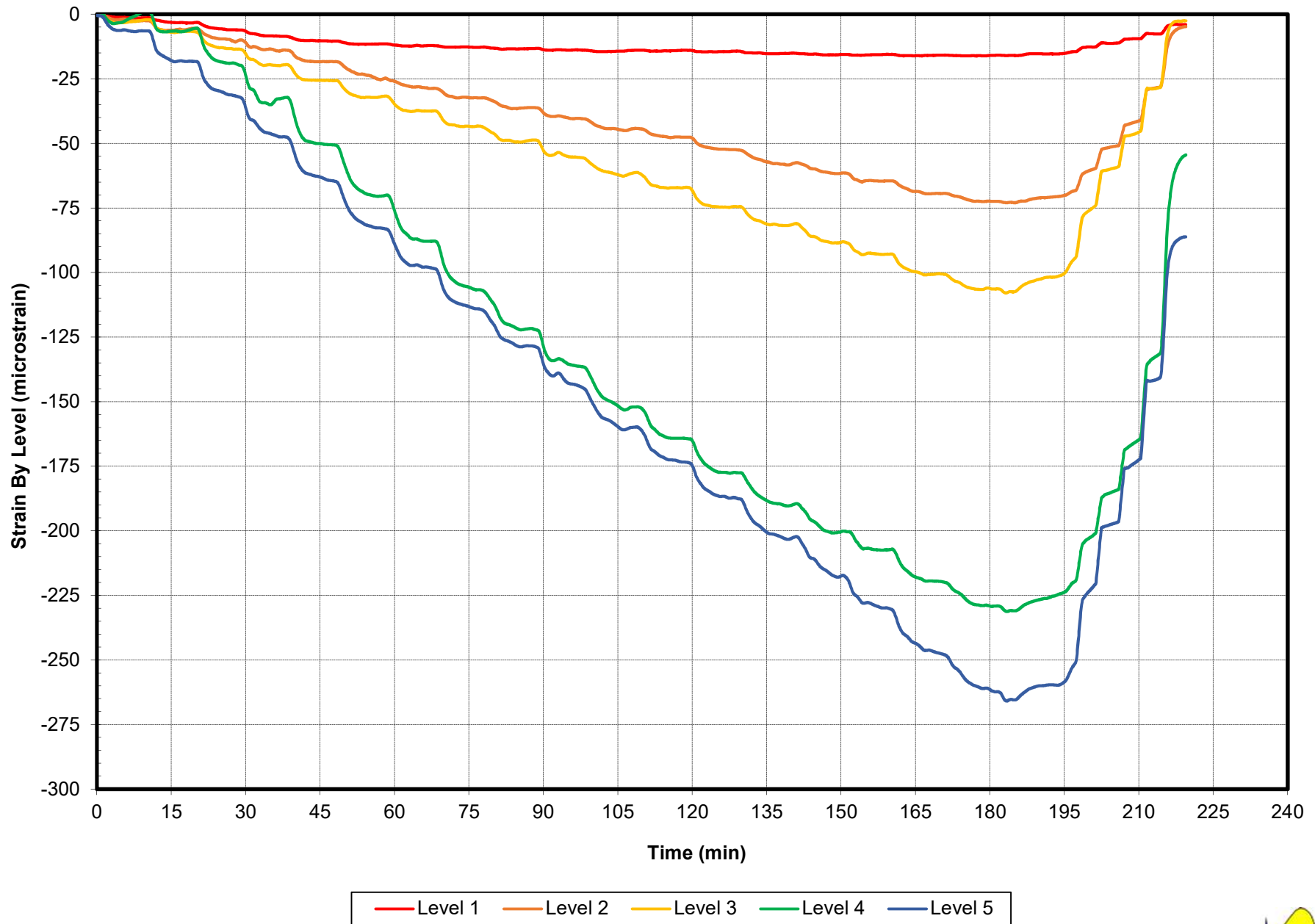


Figure 4

Upper Load Distribution vs Time  
Rainy River Bridge  
Test Pile

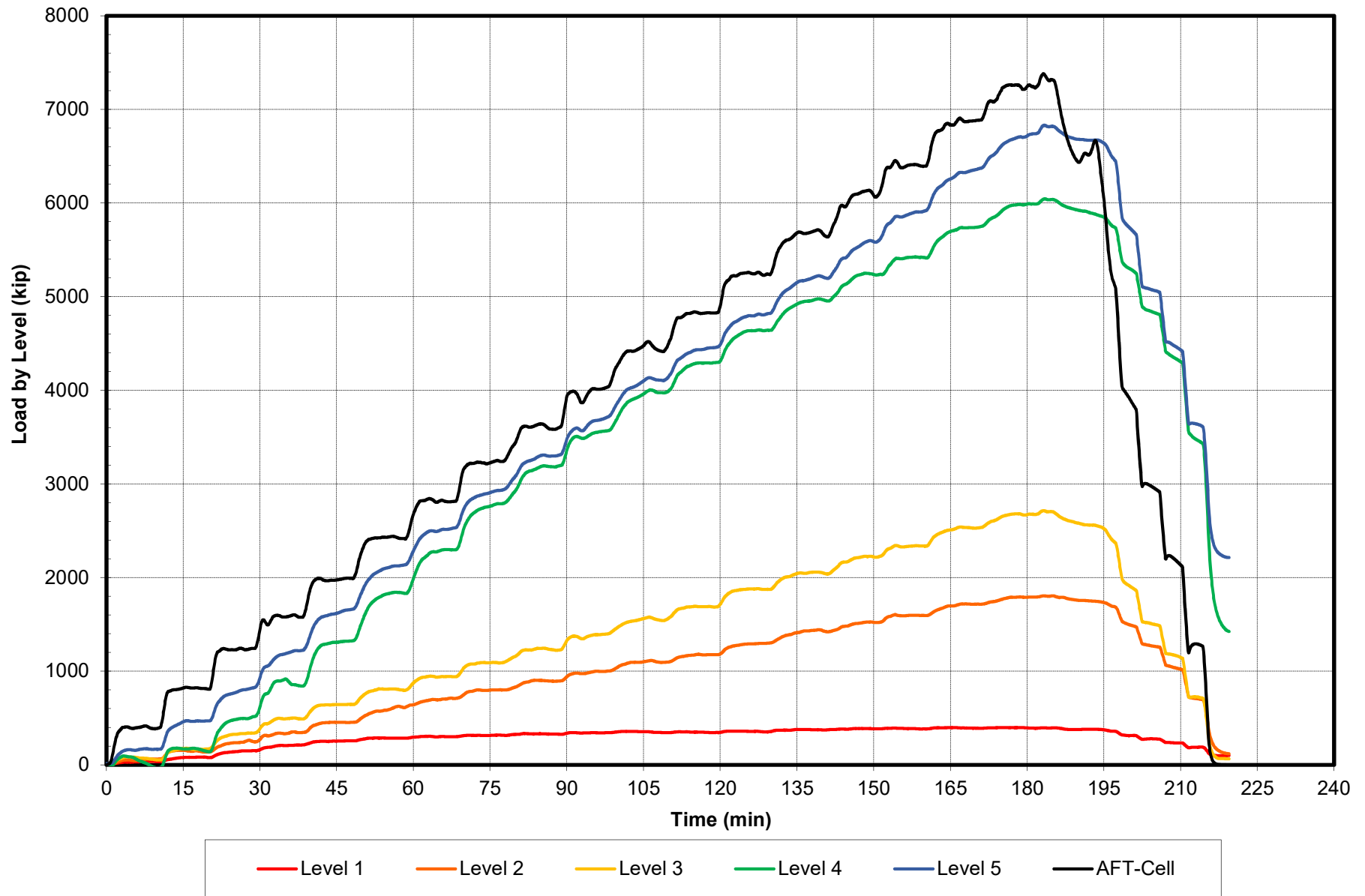


Figure 5



# Elevation Load Distribution Rainy River Bridge Test Pile

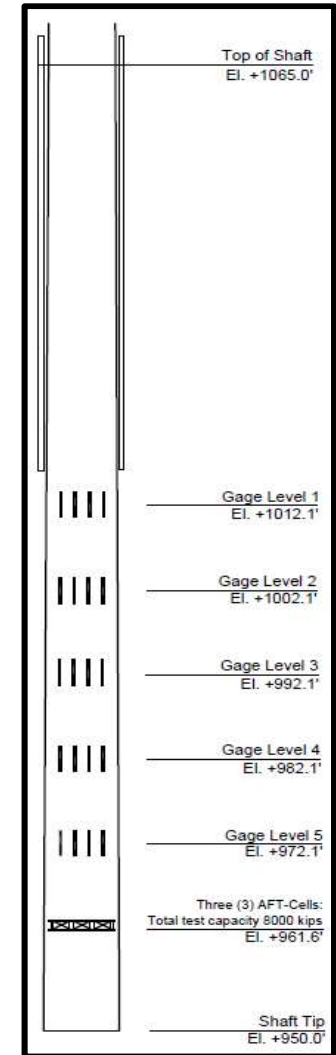
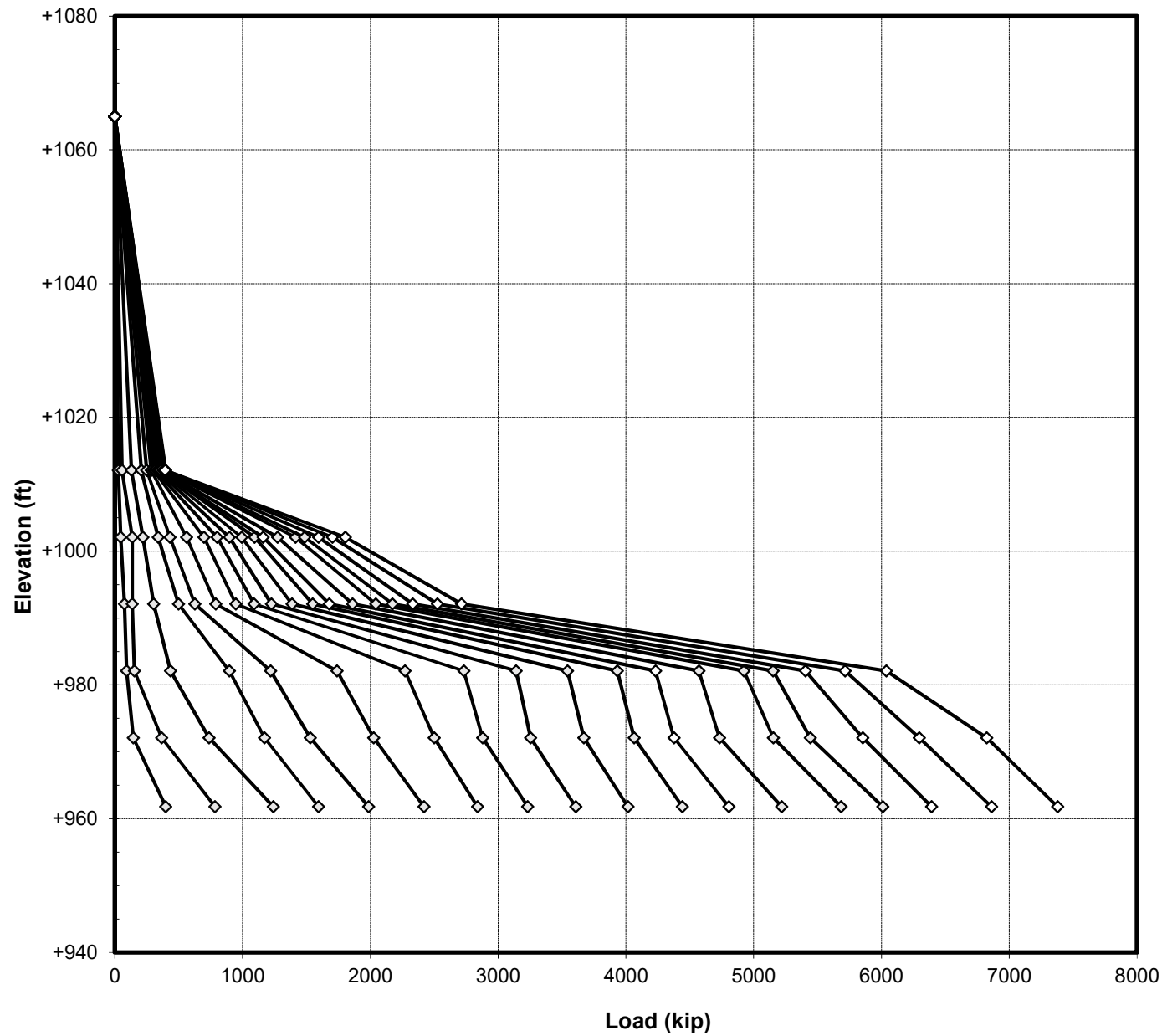


Figure 6

Upper Section Unit Side Shear ( $\tau_z$ )  
Rainy River Bridge  
Test Pile

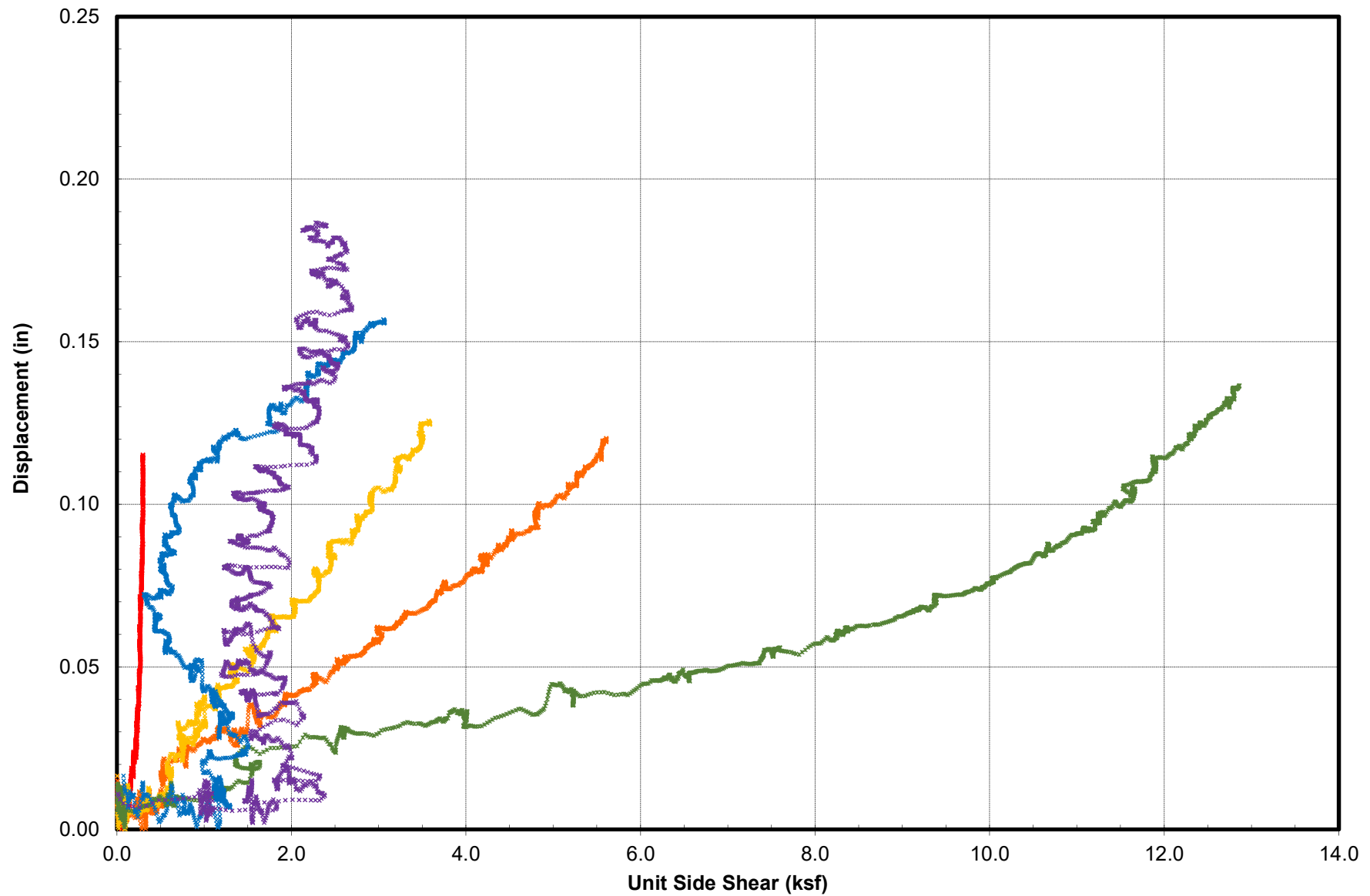


Figure 7

End Segment Resistance  
Rainy River Bridge  
Test Pile

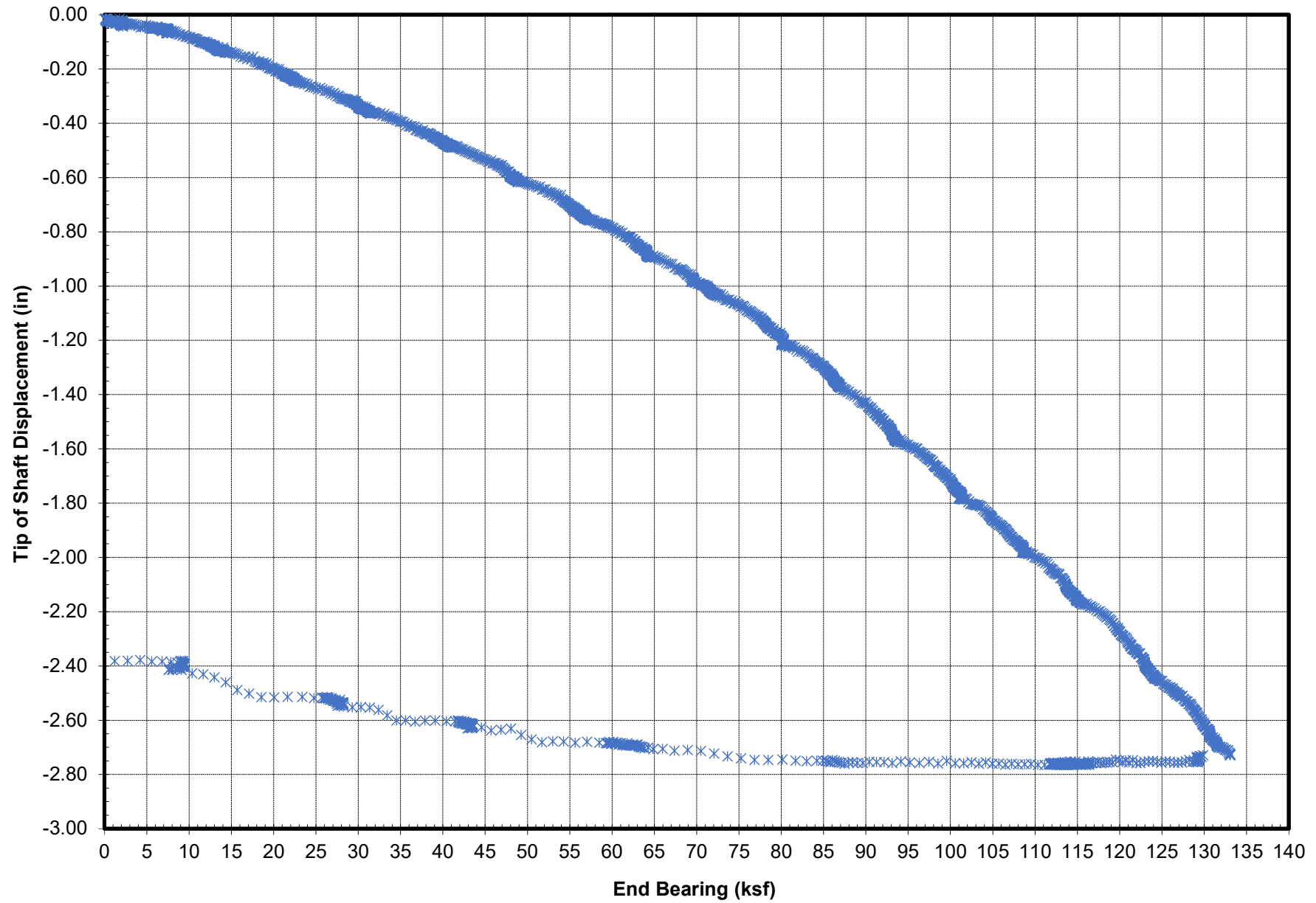


Figure 8



Equivalent Shaft Top Load vs Displacement  
Rainy River Bridge

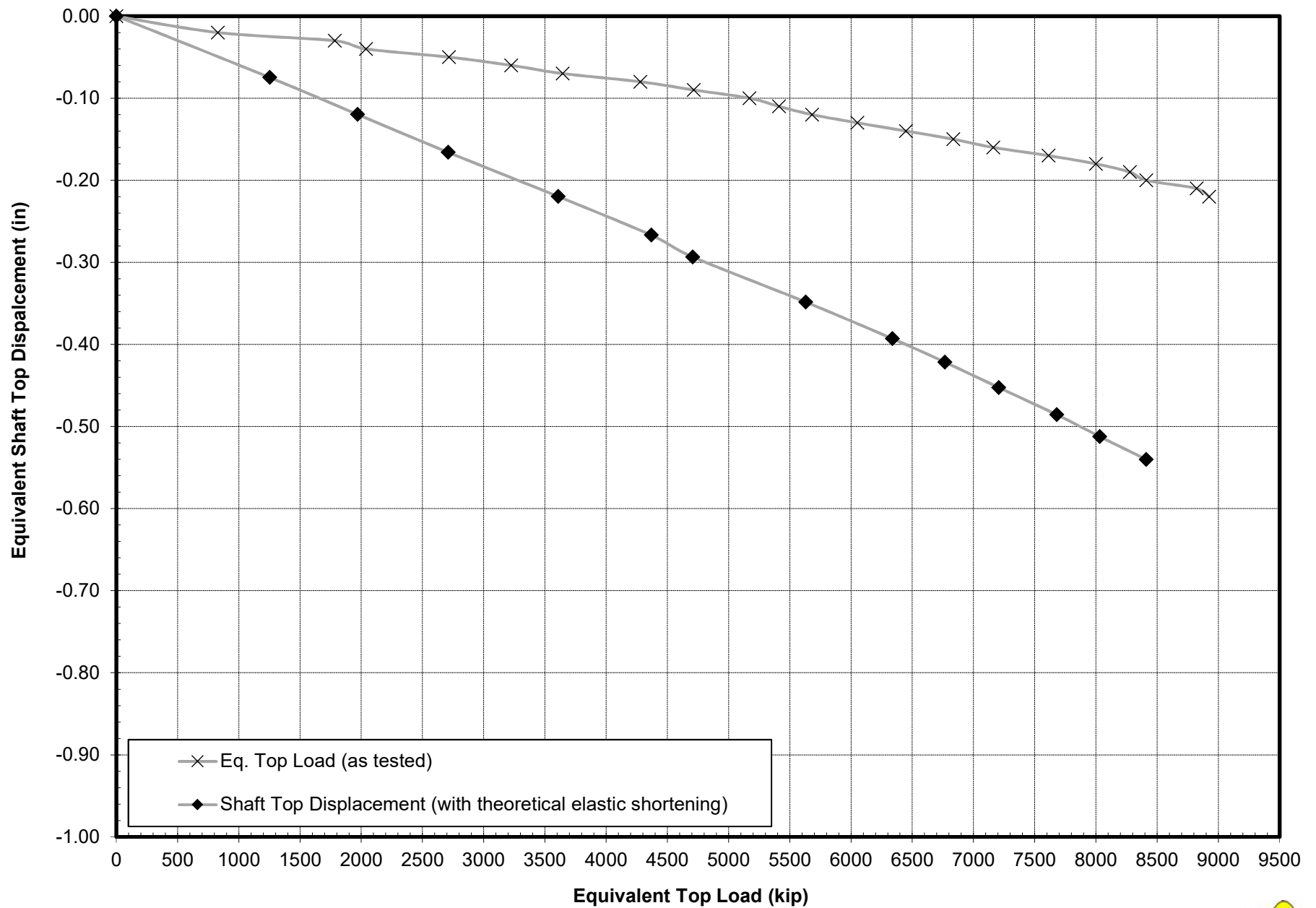


Figure 9

Creep Limit - Composite of All Stages  
Rainy River Bridge  
Test Pile

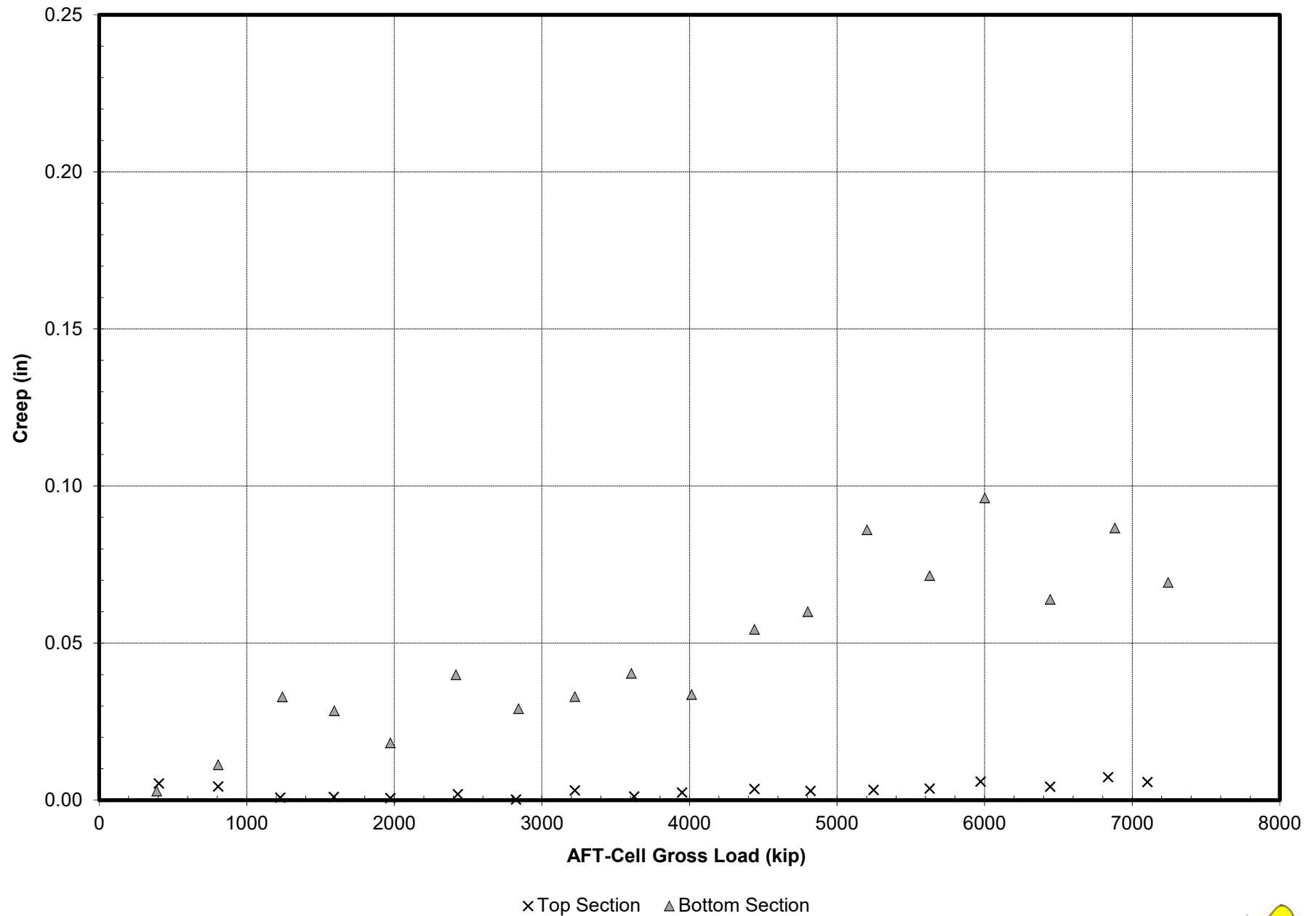


Figure 10

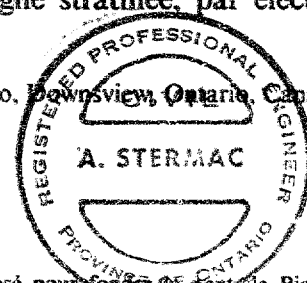


**i. Hwy 17 - Pic River**

# Capacity of Friction Piles in Varved Clay Increased by Electro-Osmosis

Augmentation de la force portante de pieux flottants, dans une argile stratifiée, par électro-osmose

by L. G. SODERMAN Principal Foundation Engineer, Department of Highways, Ontario, Downsview, Ontario, Canada  
and  
V. MILLIGAN Assistant Chief Engineer, Geocon Ltd, Rexdale, Ontario, Canada



## Summaries

The problem of founding the Big Pic River bridge on over 300 feet of soft varved clay and loose silt deposits is described in the paper. Details of the initial site investigation and pile driving and loading tests, together with adjacent piezometric observations during driving of the test piles are presented. It was found that, due to the presence of excess hydrostatic head within coarse silt layers at depth, the capacity of long friction piles was markedly less than that of short piles within the soft varved clay stratum; consequently, it was decided to found the structure on short steel 'H' section friction piles within the upper clay and to apply electro-osmotic treatment in the area of the bridge pier and abutment pile groups.

Further tests were carried out to determine the increase in pile capacity and the variation in piezometric levels in the general area both during and after treatment. Boring and sampling, together with additional laboratory testing, was also continued during the construction period to assess the changes in soil properties.

The overall effect of the electro-osmosis was to markedly increase the pile capacity, as determined from load tests. Detailed observations of the structure are being continued.

## Introduction

This paper describes the solution adopted for the substructure support at the Big Pic River Bridge, which is a three-span, through truss, cantilever structure, 600 feet in length. It is one of many along the route of the Trans-Canada Highway, which in part, skirts the north shore of Lake Superior.

Valleys in this area, of irregular volcanic and derived metamorphic Precambrian bedrock, are overlain by considerable thicknesses of stratified silts and clays deposited in post glacial Lake Algonquin. These soil conditions give rise to difficult foundation problems for embankments and structures, particularly at river crossings.

## Geological description

The subsoil stratigraphy at the site was defined by means of detailed sampled borings carried to a maximum depth of 300 feet. Bedrock surface was not determined. The upper strata were sampled using a Swedish Foil Sampler (KJELLMAN, KALLSTENIUS and WAGER, 1950) to a depth of 70 feet. Below 70 feet depth, sampling was carried out using thin walled and open drive samplers.

The upper stratum, 15 feet in thickness, consists of a

## Sommaire

Le problème qui s'est posé pour fonder le pont de Big Pic River au-dessus de trois cents pieds d'argile stratifiée et de dépôts de silts peu denses est décrit dans ce texte. Les détails de la première reconnaissance du site, du battage des pieux et des essais de chargement, ainsi que des observations piezométriques adjacentes pendant le battage des pieux sont présentés.

A cause de la présence d'une charge hydrostatique excessive dans les couches profondes de silts grossiers on a trouvé que la force portante des pieux longs était nettement plus faible que celles des pieux courts dans l'argile stratifiée molle. En conséquence, on a décidé de fonder la structure sur pieux métalliques flottants de section 'H' dans la couche supérieure de l'argile, et d'appliquer un traitement par l'électro-osmose à l'emplacement du pont et de l'ensemble des culées.

D'autres essais ont été faits pour déterminer l'augmentation de la force portante et la variation des niveaux d'eau dans le site général, tous deux pendant et après le traitement. Sondage, échantillonnage et essais additionnels en laboratoire, étaient encore continués pendant la période de construction pour être certains des changements des propriétés du sol.

L'effet général de l'électro-osmose a été d'augmenter d'une manière remarquable la force portante des pieux. Des observations détaillées de la structure seront continuées.

compact, fluvial silty sand. This is underlain by about 60 feet of medium to stiff, varved silty clay. The varves are composed of dark grey, brittle clay laminae, approximately 1 inch thick, and light grey, clayey silt laminae, typically 1/2 inch in thickness. The particle size distribution, determined from tests on individual laminae, is shown in Figure 1. This distribution falls within similar type curves reported by COOLING, 1959. The variations in Atterberg Limits, water content and undrained triaxial and in-situ vane shear strength with depth, are shown in Fig. 2.

The varved clay stratum grades into a grey, stratified coarse silt which becomes a silty fine sand with increasing depth. Between depths of 67 and 170 feet, the standard penetration resistance or "N" values ranged from 20 to 10 blows per foot, gradually decreasing with depth. Artesian conditions were observed on first encountering the silt stratum at 67 feet depth, elevation 546. This condition became more pronounced with depth, as reflected in the decrease in "N" values. The maximum artesian head rose to 20 feet above existing ground level at a depth of 250 feet. At this depth and below, the "N" values were sensibly zero due to piping in boreholes.

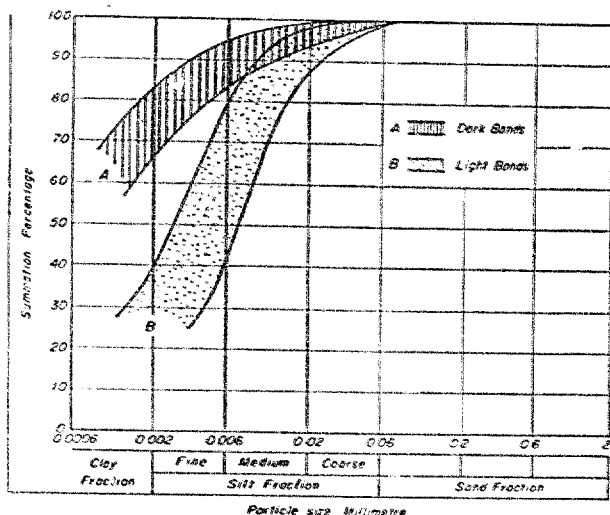


Fig. 1 Grain size distribution curves for varved clay.  
Courbes granulométriques de l'argile stratifiée.

### Initial Pile Tests

Due to the low strength and high compressibility of the deposits, a friction pile foundation was adopted. Initially, twelve 12-inch  $\times$  53 lb. "H" piles, varying in embedded

length from 55 feet to 166 feet, were driven. Open tube Casagrande type piezometers, (CASAGRANDE, 1949) installed to record pore water pressure due to pile driving, were positioned at distances of 5 to 18 feet from a test pile location, with tip elevations as shown in Fig. 3.

Piles were driven with a 2-ton drop hammer, developing 32,000 ft. lbs. energy per blow at a frequency of 15 blows per minute. The driving resistance increased linearly to a value of 20 blows per foot at a depth of 166 feet.

The increase in pore water pressure above existing hydrostatic head was measured during driving of the test piles and has been plotted as a function of horizontal distance away from a pile in Fig. 3. At a distance of 16 feet away from the test pile, no excess pore water pressure was recorded. The maximum increase in pore water pressure at any elevation within the varved clay stratum due to the cumulative effect of several piles within the radius of 16 feet from a piezometer, did not exceed 9 pounds per square inch. In no instance, did driving of a pile affect the pore water pressure when the pile tip was below the piezometer tip elevation. Dissipation of 90 per cent of the excess pore water pressure occurred within 3 days after driving. These findings agree in part with observations by BJERRUM and JOHANNSEN, 1960.

Typical results of static load tests on piles of varying lengths, are summarized in Fig. 4. These tests show that static pile capacity generally decreased with an increase in embedded length. This is believed due to artesian effects at depth. Piles tested up to 400 days after driving, showed no significant increase in capacity above that measured 5 days after driving.

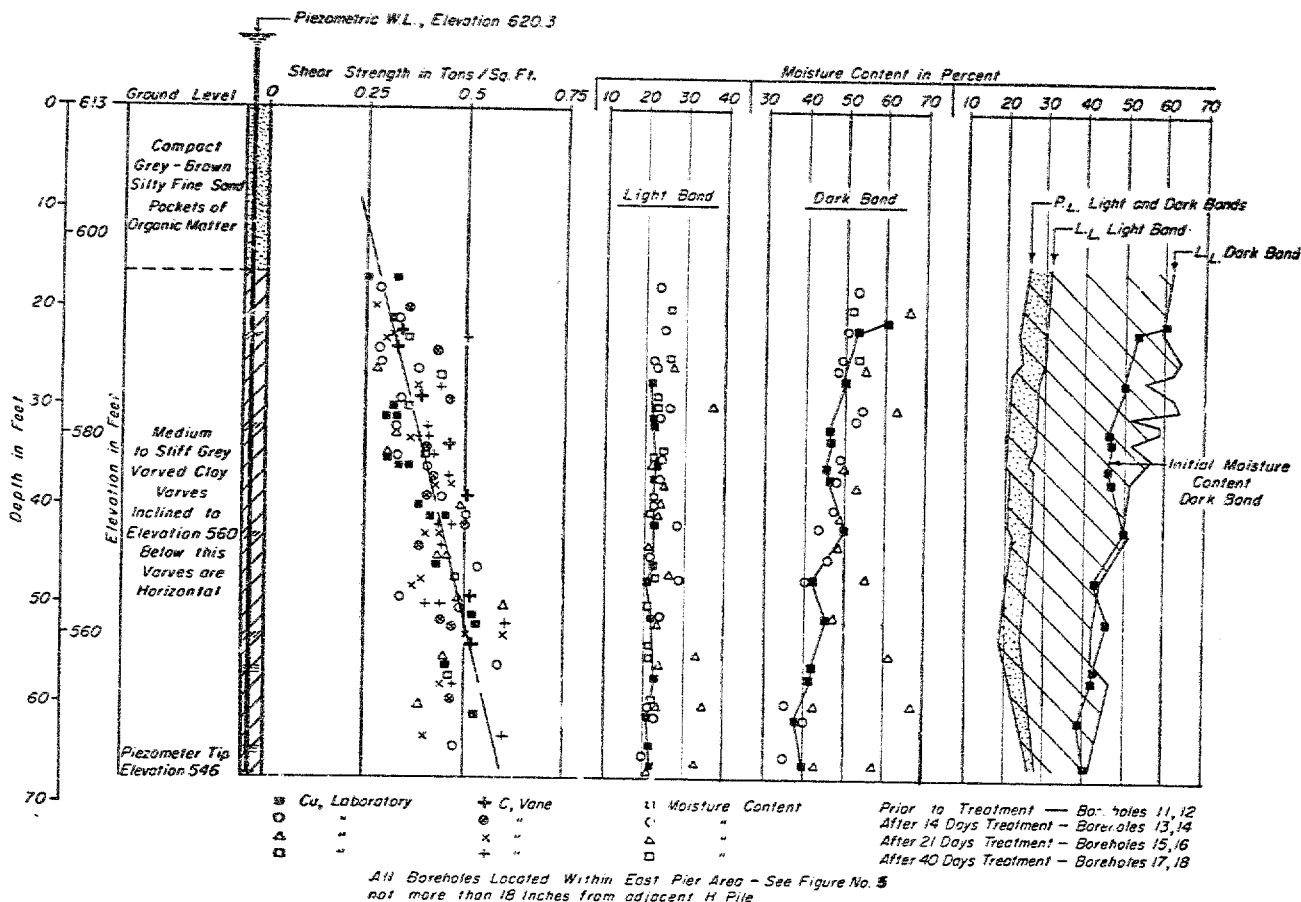


Fig. 2 Variation in water content, Atterberg Limits, and shear strength with depth.

Variation de la teneur en eau, des limites d'Atterberg, et de la résistance au cisaillement en fonction de la profondeur.

OVER

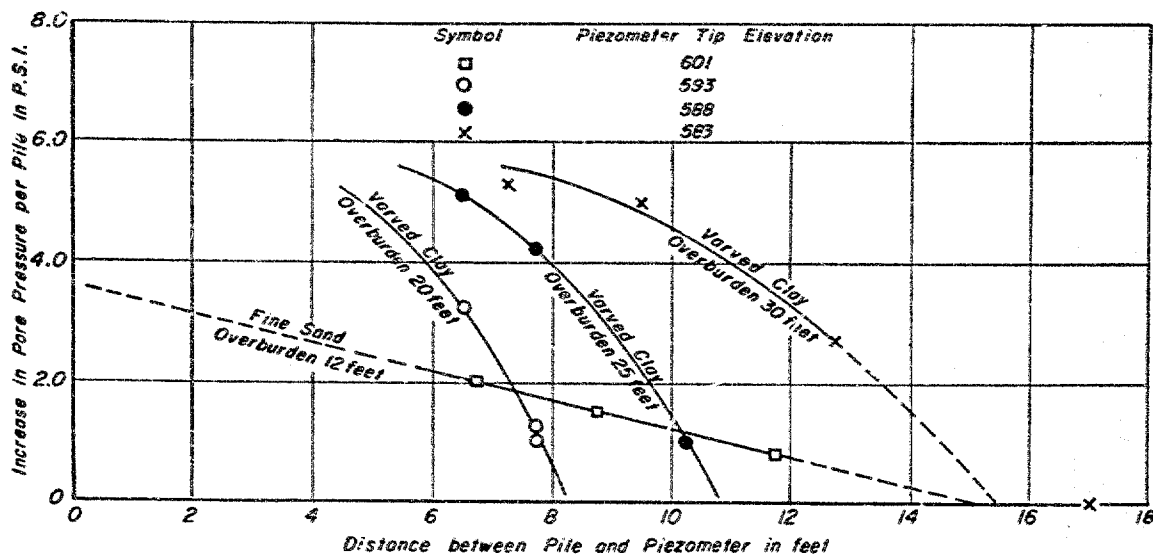


Fig. 3 Summary of pore water pressures during pile driving.  
Résumé de la pression interstitielle pendant le battage des pieux.

An analysis of the elastic compression showed that the pile capacities resulted from resistance within the upper strata. To increase the capacity of friction piles founded in the upper strata, the positive terminal of an electric arc welding machine with a maximum output of 374 amperes at 115 volts was connected to a test pile and the negative terminal to an adjacent pile. After 3 hours of treatment, the pile was retested and the capacity was found to have increased from 30 tons to 60 tons. Laboratory tests were carried out by Dr. L. Casagrande on undisturbed samples of the varved clay confirming that electro-osmosis would be effective in this soil type. It was therefore decided to found the structure on  $H^{25}$  piles, 12 x 12 inches in section at 53 lb. per foot, 55 feet long. To increase pile capacity and possibly reduce the

high compressibility of the varved clay stratum electro-osmotic treatment was applied.

#### Electro-Osmotic Treatment

The general arrangement of perimeter cathodes, 70 feet in length, at the east pier and abutment is shown in Fig. 5. Prior to pouring the reinforced concrete pile caps, each pile was individually wired as an anode. The test piles were boxed out for future testing. A 70-120 volt, 1 000-600 ampere direct current diesel generator was used as a power source for electro-osmotic treatment. Initially, it was attempted to treat the pile group as a whole. However, apparent shielding effects took place and in order to apply sufficient amperage to each pile, it was found necessary to disconnect the exterior piles. The treatment was continued working from the interior of the group outwards. Typical current measurements on an individual pile are given in Fig. 6. The total period of treatment for each group was 1960 hours.

#### Control Tests

The results of static load tests carried out during treatment are summarized in Fig. 6. It was found possible to continue treatment of the pile group during pile testing by placing insulation between the test pile head and the loading jack. This prevented the test pile from becoming cathodic. The typical ultimate capacity obtained, as for test pile E-16, was in excess of 100 tons.

Sampled borings were carried out at distances of between 12 and 18 inches away from specific piles before, during and immediately after treatment. The results of detailed laboratory tests on thin walled tube samples are summarised in Fig. 2. It may be observed that no definite trend in decrease of moisture content or increase of shear strength was measured within 12 to 18 inches from a pile. The measured shear strength gave good agreement with values obtained prior to pile driving. It is also significant to note that strength values from both in-situ vane tests and laboratory compression tests on undisturbed samples, are of the same order. No visible distortion of laminae in the undisturbed samples could be detected.

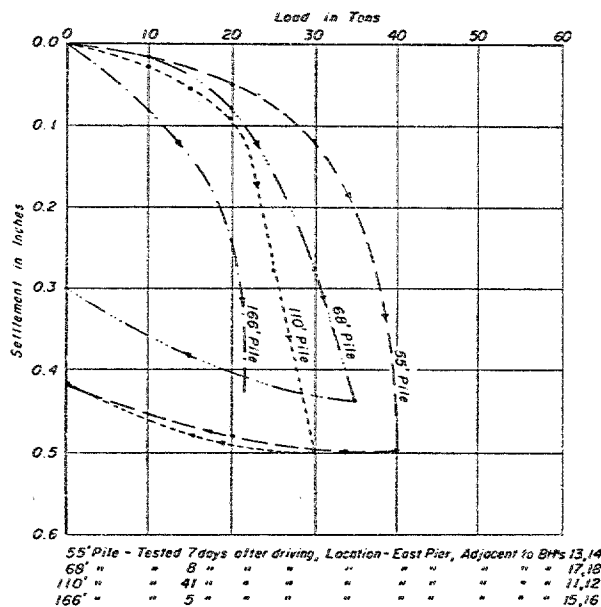


Fig. 4 Typical results of initial static load pile tests.  
Résultats typiques des premiers essais de chargement statique de pieux.

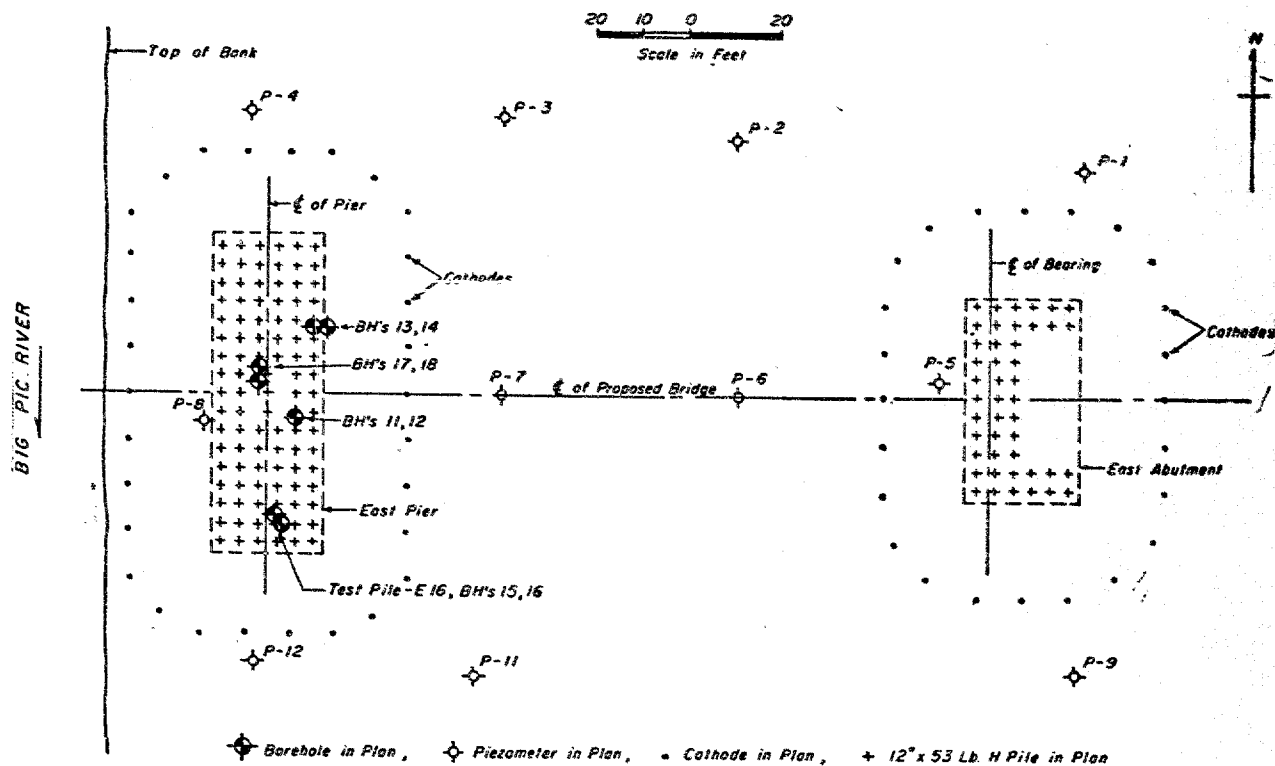


Fig. 5 Plan of East Pier and East Abutment.  
Plan de la pile Est et de la culée Est.

## Pore Pressure Measurement

In order to record changes in pore water pressure during and after electro-osmotic treatment, piezometers were installed both within and outside the pile group. The location of the piezometers is shown in Fig. 5. The piezometer tips were placed above the pile tips and thus above elevation 546 where artesian pressures were first observed. Prior to treatment normal ground water level was established at elevation 611 or 2 feet below general ground level.

The piezometer installed within the east pier pile group, adjacent to borehole 18 and with tip elevation 560, indicated a depressed piezometric level of 30 feet below normal water level at the end of treatment. Recovery of the piezometer to normal piezometric level was complete 90 days after treatment was stopped.

Piezometer P4, tip elevation 570 and located outside the perimeter cathodes, showed an increase in piezometric level of 7 feet above normal ground water level at the end of treatment. Recovery of the piezometer took place within 100 days after stopping treatment. This effect is also typical of the response measured in piezometers P1, P7, P9 and P12.

The variation in water levels in the remaining piezometers P2, P6 and P11 located outside the cathodes was insignificant.

Piezometer readings taken up to 400 days after completion of treatment showed no change from the normal piezometric level at elevation 611, as recorded prior to treatment. One piezometer with tip elevation below elevation 546 still indicated the artesian effect previously observed at this level.

## Settlement

Settlement observations during treatment, showed that the top of the pile cap at the east pier settled 1.2 inches, while ground level below the underside of the pile cap settled 3 inches. An irregular pattern of cracking of the ground surface developed between the east pier and east abutment during treatment.

Settlement observations are being continued.

## Conclusions

The effect of electro-osmotic treatment was to markedly increase pile capacity when the steel piles were used as anodes. The results of control testing indicate that the treatment affected only that soil within a distance of 1 diameter from each pile. It is further inferred that remoulding of the varved clay due to pile driving was confined to the soil within 1 diameter of the pile. Horizontal stratification of the varved clay served to accelerate the dissipation of pore pressures set up by pile driving and by electro-osmotic treatment. The permanence of the treatment with respect to pile capacity is being determined by further long term testing.

## Acknowledgment

This paper is presented with the approval of Mr. W. A. Clarke, Chief Engineer, Department of Highways, Ontario. The authors are indebted to Mr. A. Prior and Dr. F. A. De Lory for their careful supervision of control testing, to Dr. L. Casagrande for his invaluable advice and to Mr. J. Alexander for his assistance in the preparation of this paper.

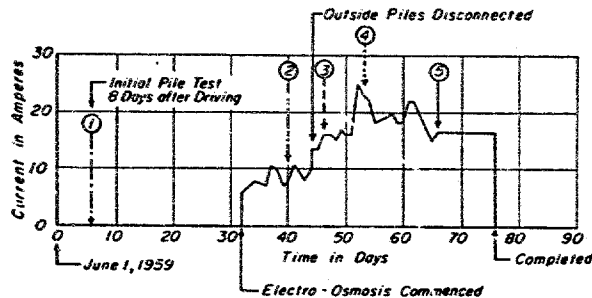
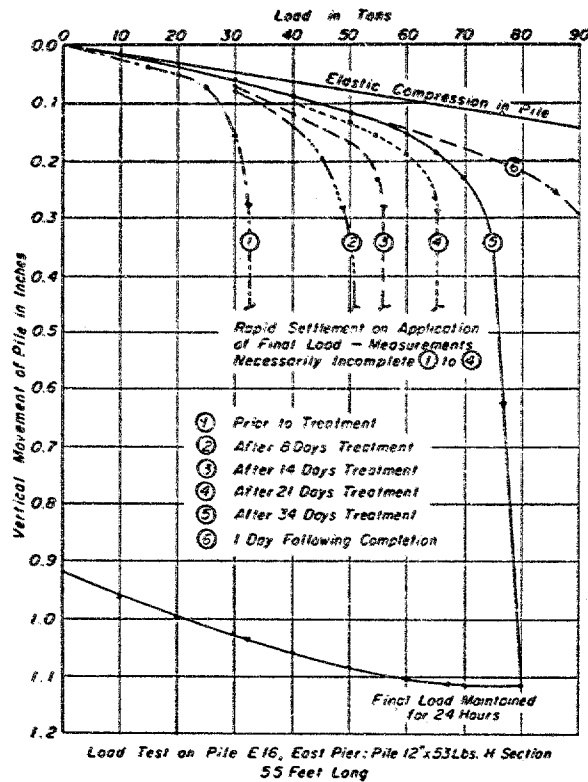


Fig. 6 Typical results of control static load pile tests.  
Résultats typiques de contrôle par essais de chargement statique sur pieux.

#### References

- [1] BJERRUM, L. and JOHANNSEN, I. (1960). Pore Pressures resulting from driving piles in soft clay. *Pore Pressure and Suction in Soils, Conference*, London, 1960.
- [2] CASAGRANDE, A. (1949). Soil Mechanics in the Design and Construction of the Logan Airport. *Journal Boston Society of Civil Engineers* 1941-1953.
- [3] COOLING, L. F. (1959). Soil Engineering at Steep Rock Iron Mines, Ontario, Canada. *Discussion to paper by R. F. Leggc., Proceedings Institution of Civil Engineers*, vol. II, 1958.
- [4] KJELLMAN, W. KALLSTENIUS, T., and WAGER, O. (1950). Soil Sampler with Metal Foils. *Royal Swedish Geotechnical Institute, Proceedings*, No. 1.



INCREASE OF BEARING CAPACITY  
OF FRICTION PILES BY ELECTRO-OSMOSIS

by

L. Casagrande<sup>1)</sup>

L.G. Soderman<sup>2)</sup>

R.W. Loughney<sup>3)</sup>

Presented at the ASCE Convention  
in Boston, Mass.  
October 11, 1960

- 1) Consulting Engineer, Gordon McKay Visiting  
Professor of the Practice of Foundation  
Engineering, Harvard University
- 2) Principal Foundation Engineer, Ontario  
Department of Highways, Toronto, Canada
- 3) Vice-President, Wellpoint Dewatering  
Corporation, N.Y.

## SYNOPSIS

The first part of this paper reviews the most important findings of past investigations concerning the strength increase of fine-grained soils achieved by means of electro-osmotic treatment, and with particular attention to possible applications for the increase of bearing capacity of friction piles. In the second part is described a full-scale application of this method in connection with the foundations for a bridge in Canada. The third part discusses the development of a novel type of friction pile which would lend itself well to application of electro-osmosis.

# I. COMMENTS ON THE ELECTRO-OSMOTIC STRENGTH INCREASE OF FINE-GRAINED SOILS

When applying direct current to a pair of electrodes driven into a reasonably homogeneous mass of clay or silt, the soil surrounding the anode and frequently also surrounding the cathode will gradually increase in strength. As illustrated in Fig. 1, this strength increase progresses with time from the electrodes radially outward. The rate at which a noticeable strength increase progresses depends on the electrical potential gradient and the duration of electrical treatment. The increase in strength of these zones is due to the following phenomena:

1. Water is transported from one electrode to the other, with few exceptions the flow being from the anode toward the cathode.
2. Base exchange takes place in the soil along the path of the electric current, i.e., low valence ions, such as sodium, attached loosely by molecular forces to the surface of clay particles, are replaced by ions of higher valence such as aluminum or iron. (1) <sup>\*)</sup>
3. In the pores of the soil surrounding the anode, metal derivatives are deposited (as a result of the gradual decomposition of the metallic anode) which act as cementing agents between soil particles. (1), (2)

---

<sup>\*)</sup> Numerals in parentheses refer to items in the list of references.

4. Remolded clay soils treated by electro-osmosis gradually develop a type of structure which resembles that of an undisturbed, sensitive clay. (3)
5. When free calcium is present in the soil it leads to the formation of calcium carbonate deposits in the soil surrounding the cathode.

These phenomena take place simultaneously. Usually the first three of the phenomena listed above are dominant in clay soils. However, even if the water content is not reduced, such as may happen in stratified soils with high permeability parallel to stratification (e.g. in some varved clays) which have a tendency of partially or fully replenishing pore water which is being removed by electro-osmosis, base exchange and cementation by metallic deposits will still be effective and cause an increase in strength.

Since the time, thirty years ago, when these basic observations were made by the senior author, a number of investigators have conducted laboratory and field tests in order to study the feasibility of increasing the bearing capacity of friction piles by electro-osmosis. The results of several of these investigations were published, (4) to (9), while other important work was compiled in the form of reports and has not yet been made available to the profession. In the majority of these investigations the anodic piles consisted of aluminum because of the early discovery that the aluminates

deposited in the soil adjacent to the anode are more effective in cementing the soil particles than the derivatives of iron anodes. (2)

In the photograph in Fig. 2 is shown the effect of electro-osmosis on a 3-inch diameter steel pipe, serving as anode, driven to a depth of approximately twelve feet into a man-made fill of soft, very sandy clay, mixed with calcium carbonate wastes.

About 10 ft to the right of the three-inch steel pipe was driven a 1.5-inch diameter steel pipe of equal length to serve as cathode. DC current with a potential of approximately 70 volts was applied for a period of 10 days. At the beginning 16.4 amps passed through these two electrodes and the current dropped gradually to less than 1.5 amps after 10 days. Attempts to increase the conductivity by adding sodium chloride or other salts to the soil near the anode were effective only for a duration of several hours after which the resistivity of this system increased again to the value established prior to the addition of salts.

The anodic pipe was load-tested after it had been in place for a period of 6 hours, but prior to application of electro-osmosis. The ultimate bearing capacity was 177 pounds which included the weight of the 3-inch pipe. At this load the settlement progressed steadily and had reached 3.3 inches when the load test was discontinued.

After 10 days of electrical treatment the load test was repeated and failure occurred rather suddenly after the load had been increased to 3470 pounds and the total settlement had reached 1.2 inches.

After completion of this load test the anodic pipe was pulled. As can be seen in Fig. 2 a cemented clay cylinder of about 10 inches in diameter had formed around the pipe. The upper portion of this cylindrical body of soil was removed by means of hammer blows and subjected to laboratory testing.

## II. PRACTICAL APPLICATION FOR INCREASING THE BEARING CAPACITY OF FRICTION PILES

Despite the fact that all investigations which have come to the authors' attention proved the feasibility of substantially increasing the bearing capacity of friction piles by means of electro-osmosis at reasonable cost, this method encountered barely more than theoretical interest amongst practicing engineers. This is primarily due to the fact that the substantial increase in bearing capacity of friction piles resulting from electro-osmosis does not eliminate the problem of settlements due to consolidation of compressible strata beneath the pile points.

The first application of this method was completed about one year ago in connection with the foundations of a bridge over the Big Pic River near Marathon, Ontario, for the Trans-Canada Highway. (10) As illustrated in Fig. 3, the foundation soils at this location consist of a few feet

of sand and gravel fill followed by a 10 to 20 foot stratum of fluvial deposits of silty clay and fine sand which are underlain by 40 to 60 feet of varved clay of soft to medium strength. The varved clay, consisting of alternating layers of clay and silt, is underlain by a very thick deposit of rock flour which at the depth of approximately 250 feet changes gradually into silty fine sand. The borings were stopped at a depth of 300 feet without reaching bedrock. In the silt and fine sand strata artesian pressure was encountered.

Because of the excessive depth to bedrock and the sensitive character of the varved clay, the original design called for the bridge footings to be founded on 110-foot long, 12-inch, 53-pound steel H-piles driven as friction piles through the clay into the underlying silt stratum, and using a design load of 40 tons per pile. Several load tests on such piles gave ultimate bearing capacities ranging as low as 20 tons. Repetitions of load tests after the piles had been in place for a period of over one year did not show any increase in bearing capacity.

In order to avoid a radical change in the design of this bridge at this late stage, the Ontario Department of Highways decided to attempt to increase the frictional resistance of the piles by applying electro-osmosis. A preliminary field test was arranged utilizing two 56-foot long test piles as electrodes. With a potential of

115 volts the bearing capacity of the anodic pile, which prior to treatment had carried an ultimate load of barely 30 tons, showed an increase to approximately 60 tons after three hours of treatment. Subsequent laboratory tests indicated that with longer duration of treatment even better results could be anticipated. On the basis of these favorable results it was decided to use 56-foot long piles which would not extend into the silt stratum beneath the varved clay.

In Fig. 4 is shown the electrical installation for the West Pier, including the arrangement of the cathodes relative to the H-piles, to be utilized as anodes. The average distance between the electrodes was slightly over 23 feet. The layout for the electrical treatment at the East Pier was similar to that at the West Pier as can be seen in the photograph in Fig. 5. In order to prevent clogging of the cathodic pipes with calcium carbonate, a combination of steel pipes and plastic pipes was used as shown in the photograph in Fig. 6. Numerous small holes were drilled into the plastic pipe to allow the water (carried by electro-osmosis toward the cathode) to penetrate the plastic pipe and to discharge on the surface. Three diesel generators with an output of 70 to 120 volts and 1000 to 600 amps per unit were used. The average current consumption per H-pile for a potential of 100 volts amounted to 15 amps.



A number of H-piles in the foundations for the piers and one abutment had been boxed out in order to enable performance of load tests during and after electrical treatment. In this manner it was possible to follow the progress of the increase in bearing capacity with the duration of treatment. The results for a typical test pile are plotted in Fig. 7 showing an increase in ultimate bearing capacity from 30 tons before electrical treatment to 100 tons after a treatment lasting four weeks. On the basis of such tests it was possible to decide on the necessary duration of electro-osmotic treatment. While the H-piles closest to the cathodes were treated for approximately two weeks, the piles located farthest from the cathodes had to be treated for a period of approximately 6 weeks.

The total cost of this electro-osmotic treatment, performed by the Wellpoint Dewatering Corporation of New York, was approximately \$55,000, i.e. a fraction of the savings which had accrued due to the use of much shorter piles than the original design had called for.

### III. DEVELOPMENT OF A NEW TYPE OF FRICTION PILE

In an attempt to develop a friction pile which would combine the qualifications of causing minimum disturbance to sensitive soils during driving with a maximum benefit from electro-osmotic treatment, the senior author developed a skeleton-type pile. As shown in the photograph in Fig. 8, it consists of a series of rods or pipes which are

welded to spacers made of short sections of pipe. The appreciable reduction in displacement of soil, and therefore in disturbance caused by the driving of such a skeleton pile as compared to conventional piles, is illustrated by the model tests shown in the photograph in Fig. 9.

A semi-cylinder, which is closed in front with a lucite wall, was filled with bentonite clay of very soft consistency. Embedded in this clay were thin layers of brown, fine sand, spaced approximately 2 inches. On the left side of the photograph is shown the effect of pushing into the clay a full-displacement pile. It consists of a thin-wall aluminum tube which was cut in half lengthwise and filled with plaster-of-paris. The other half of this aluminum tube was pushed <sup>in</sup> as an "open-ended pipe pile", and is shown in the center of the photograph. On the right side a half-section of a skeleton pile was pushed in. During pushing of the full-displacement and open-end piles the surface of the clay heaved and cracked, and below the bottom ends of these piles the clay mass deformed to a depth of several pile diameters. Inside the open pipe the clay had risen to less than one-half of the length of the pile, when the friction between the inside of the tube and the clay plug had increased to a magnitude which caused the pile to be driven further as a full displacement pile. In contrast, the pushing of the skeleton pile into the clay (which was done after the installation of the other two piles) created hardly noticeable disturbance of the clay,

and the surface of the clay plug inside the skeleton was practically at the same elevation as the clay on the outside. This skeleton pile was pushed to the same depth as the other two piles. Nevertheless, below its tip no additional deflection of the sand layers was created.

All three piles were 1.5 inches in diameter. The skeleton pile consisted of six 1/8-inch diameter rods. It was cut lengthwise so that two half-rods were in contact with the lucite plate. These rods were held in place by four thin steel collars 1/4 inches high. The force necessary to push the skeleton pile down was one-fifth of the force required for the open-ended pipe, and one-sixth of the force required to push the solid pipe down to the same depth.

For the sake of interest, buckling tests were made on single 1/8-inch diameter rods (of which the skeleton pile was built) and on the entire skeleton pile. It was found that the buckling strength, tested without confinement in clay, was for the skeleton pile 8.4 times greater than the combined buckling strength of six individual rods of equal length.

While the surface area of such a skeleton pile is only a fraction of a conventional pile of similar diameter, it lends itself well to an increase in bearing capacity by electro-osmotic treatment. As shown in Fig. 10, the cylindrical bodies of cemented soil surrounding each rod or pipe of this pile will gradually meet and form one unit which

contribute to the bearing capacity of the pile. Model tests have shown that already before these hardened cylinders (indicated by dashed line in Fig. 10) grow into one unit, the larger circumferential surface area indicated by a full line in Fig. 10 will govern its bearing capacity.

The effect of electro-osmosis on such a skeleton pile in a model test in Boston Blue Clay is shown in Fig. 11. The 1.5-inch diameter skeleton pile was pushed into a uniform mass of remolded clay having an average water content of 43.8 per cent. The liquid limit of this clay was 47.6 and the plastic limit 23.3. The clay was tilled into a plastic bucket. The skeleton pile in the center of the clay mass served as anode and two 1/8-inch diameter rods were arranged on two opposite sides of the anode, next to the wall of the bucket, to serve as cathodes. A potential of 6 volts was supplied by a storage battery for a duration of approximately 2 weeks. A number of load tests were made before and during treatment and the results, expressed in unit frictional resistance, are recorded in the diagram in Fig. 12.

After the last load test was completed, electro-osmosis was applied for several additional hours. Then an attempt was made to pull the skeleton pile from the body of clay. This resulted in the full content of the bucket to be pulled up with the pile. Although it may be startling to see a weight of 40 pounds of clay hanging on a few thin rods, this result is not unexpected if compared with the bearing

capacities recorded in Fig. 12. The same block opened up along a vertical plane is shown in Fig. 13. It can be seen that the clay has developed a structure with distinct conchoidal stratification and fissuring. Along the outer zone the water content of the clay was still near the liquid limit, but it developed substantial strength and a structure which was quite sensitive to remolding.

#### IV. CONCLUSIONS

From laboratory and field investigations, including one full-scale application, it may be concluded that (1) the bearing capacity of friction piles can be increased greatly and economically by the use of electro-osmosis, and (2) the ideal type of friction pile for this purpose would be a skeleton pile of the type discussed above and shown in Fig. 8.

## REFERENCES

- (1) K. Endell, Beitrag zur Chemischen Erforschung und Behandlung von Tonböden, Bautechnik, Vol. 13, Berlin, 1935.
- (2) L. Casagrande, Die Elektrochemische Bodenverfestigung, Bautechnik, Vol. 17, Berlin, 1935.
- (3) L. Casagrande, Structures Produced in Clays by Electric Potentials and Their Relation to Natural Structures, Nature, Vol. 160, p. 470, 1947.
- (4) L. Erlenbach, Anwendung der Elektrochemischen Verfestigung auf Schwimmende Pfahlgründungen, Bautechnik, Vol. 14, pp. 257-259, Berlin, 1936.
- (5) L. Casagrande, Grossversuch zur Erhöhung der Tragfähigkeit von Schwebenden Pfahlgründungen durch Elektrochemische Behandlung, Bautechnik, Vol. 17, pp. 228-230, Berlin, 1939.
- (6) E. Kumutat, Über die Elektrochemische Bodenverfestigung nach dem Verfahren von L. Casagrande, Angewandte Chemie, Vol. 53, No. 15-16, 1940.
- (7) L. Bendel, Ergebnisse von Belastungsproben bei Pfahlfundationen, Schweiz. Techn. Zeitschrift, p. 41, Zürich, 1941.
- (8) M.G. Spangler and H.L. King, Electrical Hardening of Clays Adjacent to Aluminum Friction Piles, Proc. Highway Research Board, Vol. 29, pp. 589-599, 1949.
- (9) A.B. Bridgwater, Electro-Kinetic Phenomena in Soils, Civil Engineering and Public Works Review, Vol. 45, 1950.

REFERENCES (Cont.)

- (10) L.G. Soderman and V. Milligan, Capacity of Friction Piles in Varved Clay Increased by Electro-Osmosis. Paper submitted to the Fifth International Conference on Soil Mechanics and Foundation Engineering, Paris, 1961.

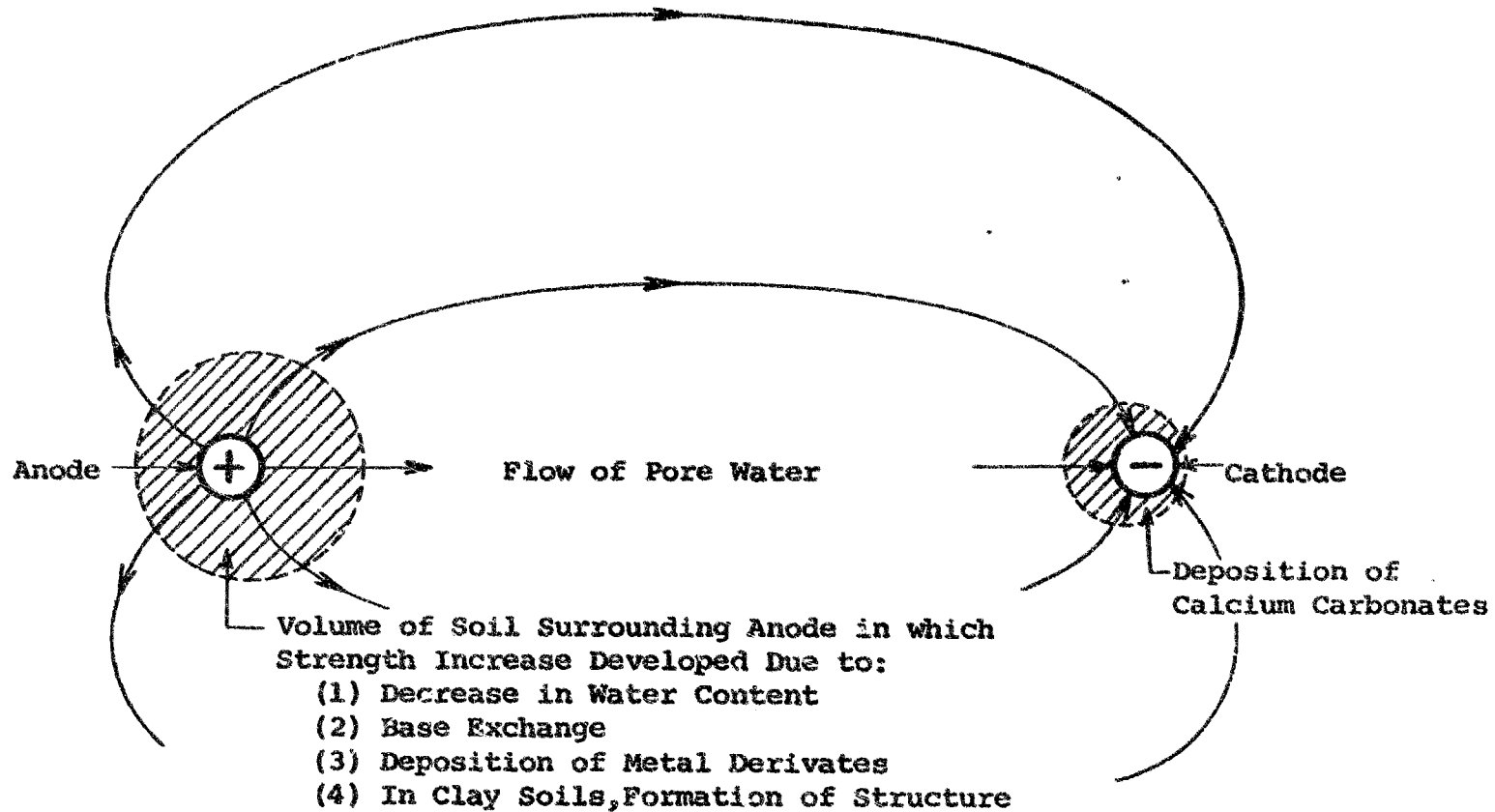


FIG.1.- PROGRESS OF STRENGTH INCREASE OF SOIL SURROUNDING ELECTRODES





FIG.2.- CEMENTED CLAY CYLINDER FORMED AROUND ANODIC PILE  
AFTER TEN DAYS OF TREATMENT

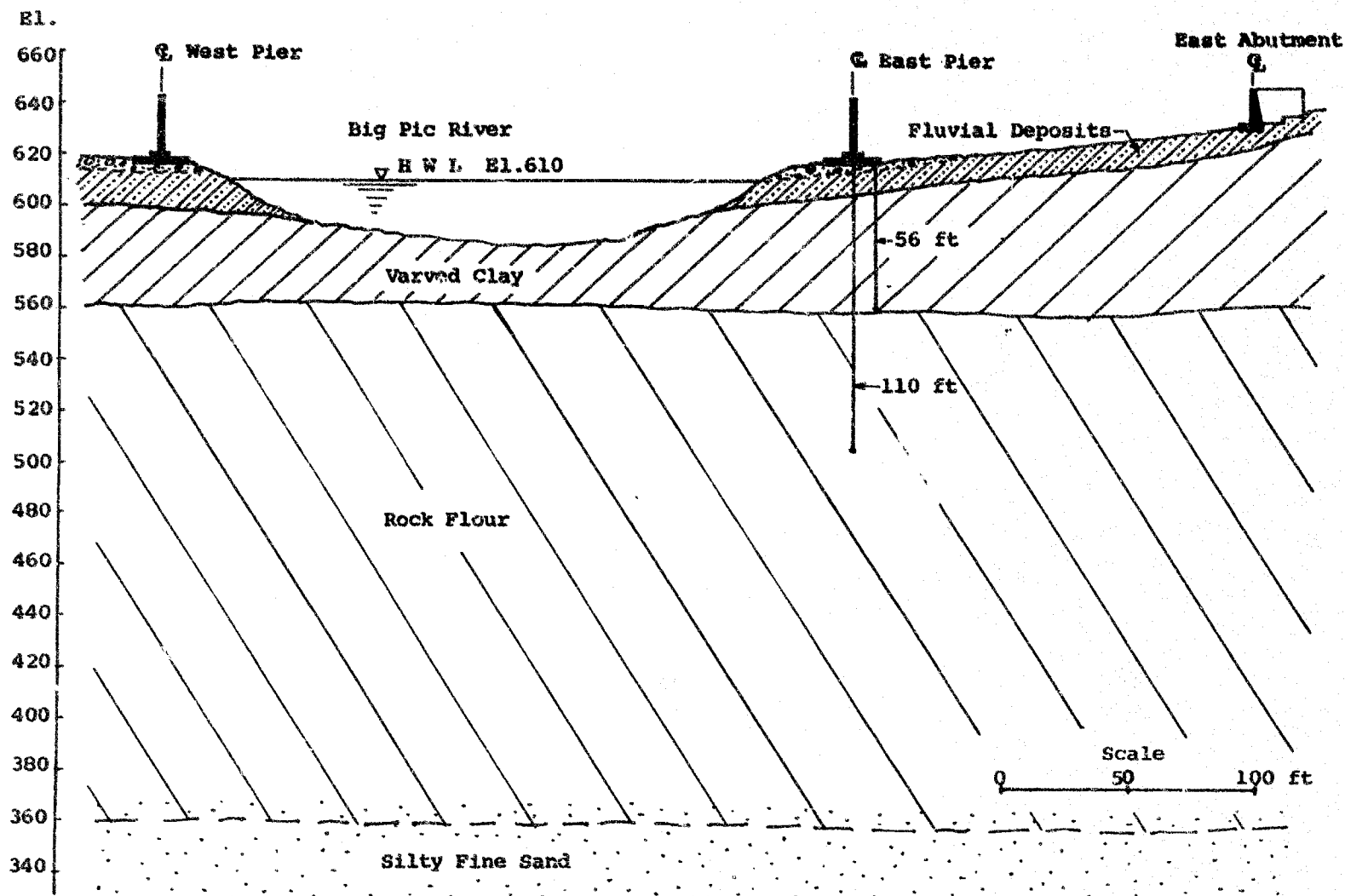


FIG.3.- SUBSOIL PROFILE AT BIG PIC RIVER BRIDGE, MARATHON, ONTARIO

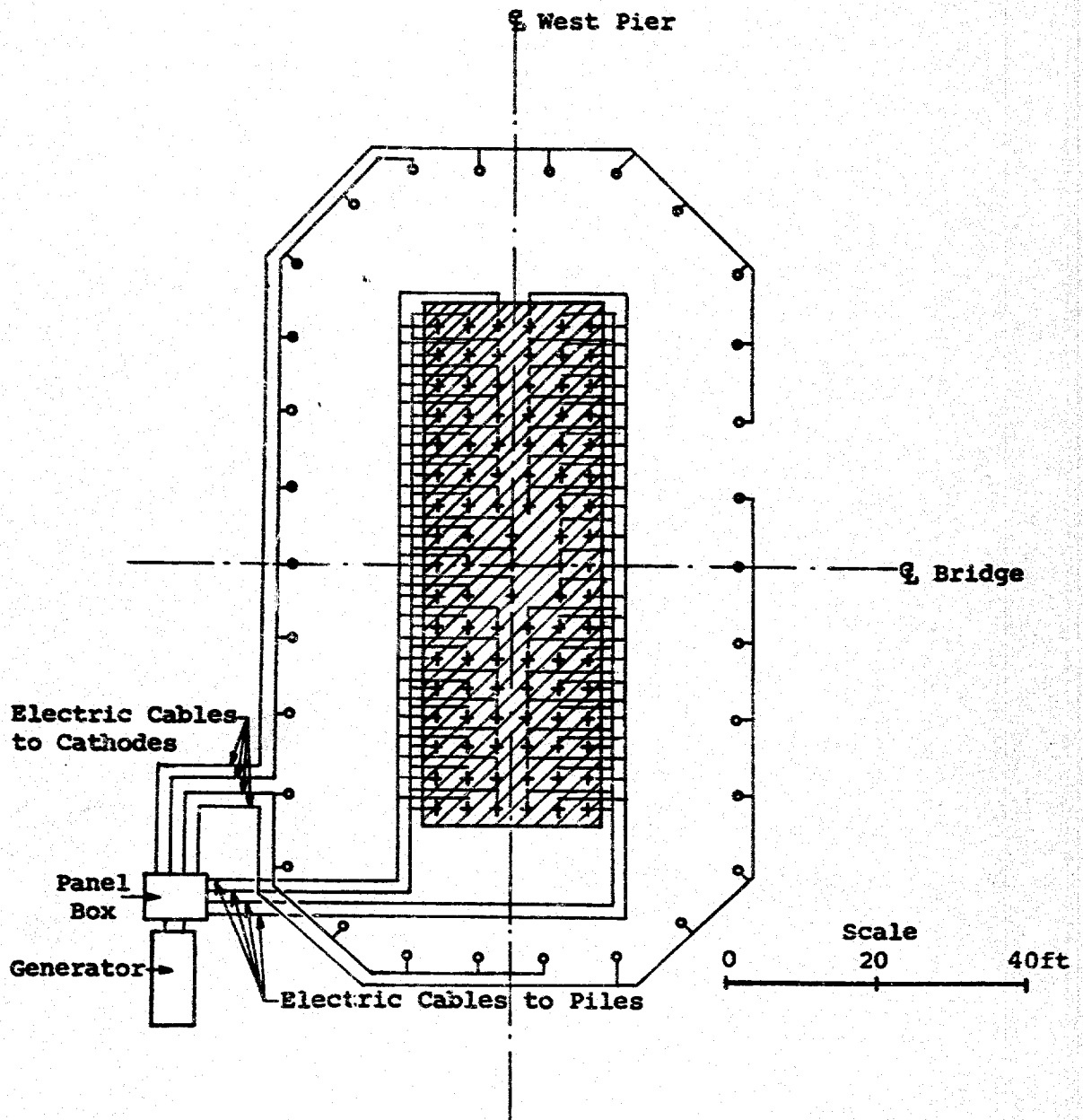


FIG.4.- ELECTRICAL INSTALLATION AT WEST PIER OF BIG PIC RIVER BRIDGE,  
MARATHON, ONTARIO

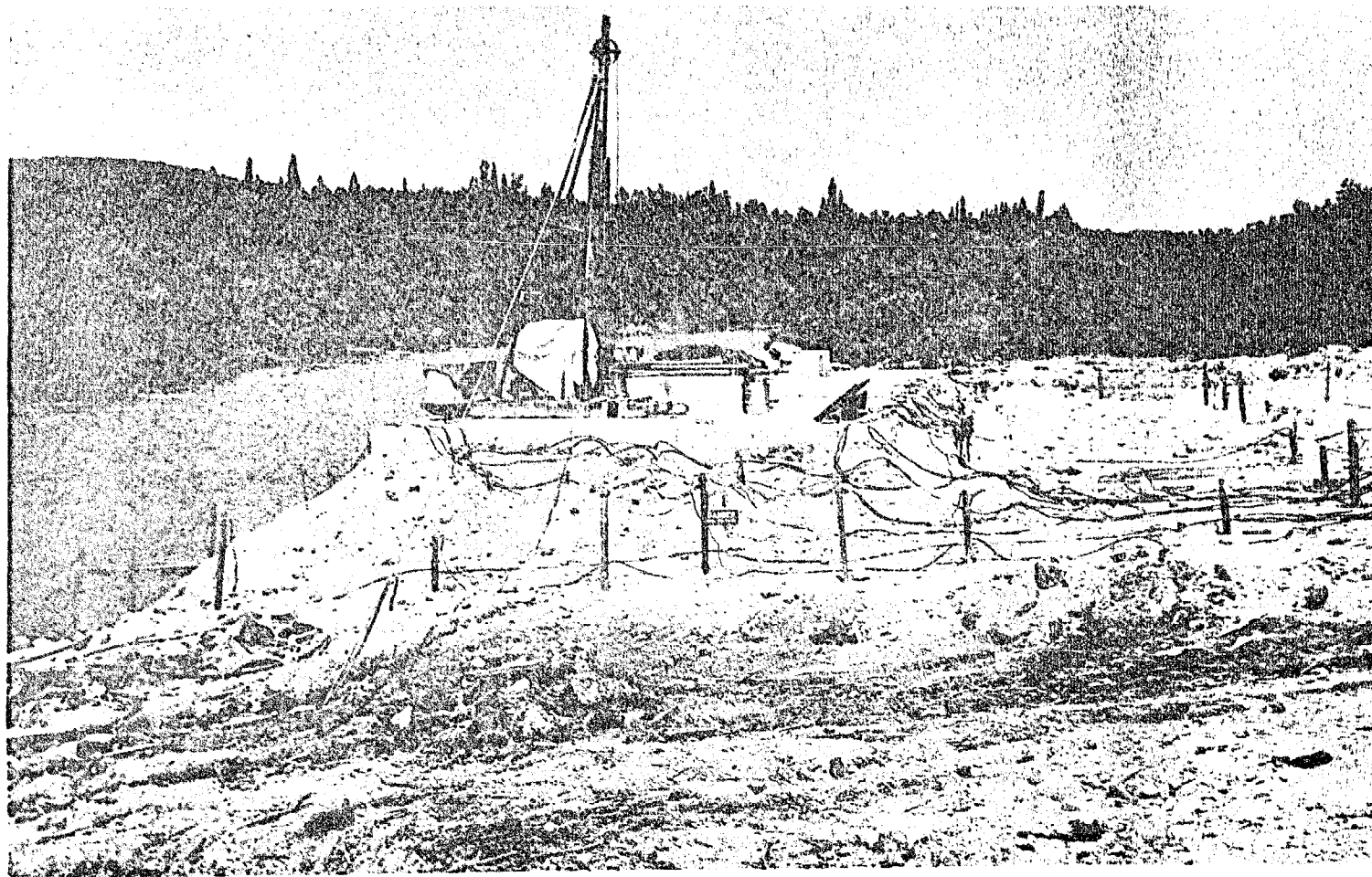


FIG.5.- VIEW OF ELECTRICAL INSTALLATION AT EAST PIER, BIG PIC RIVER BRIDGE,  
MARATHON, ONTARIO

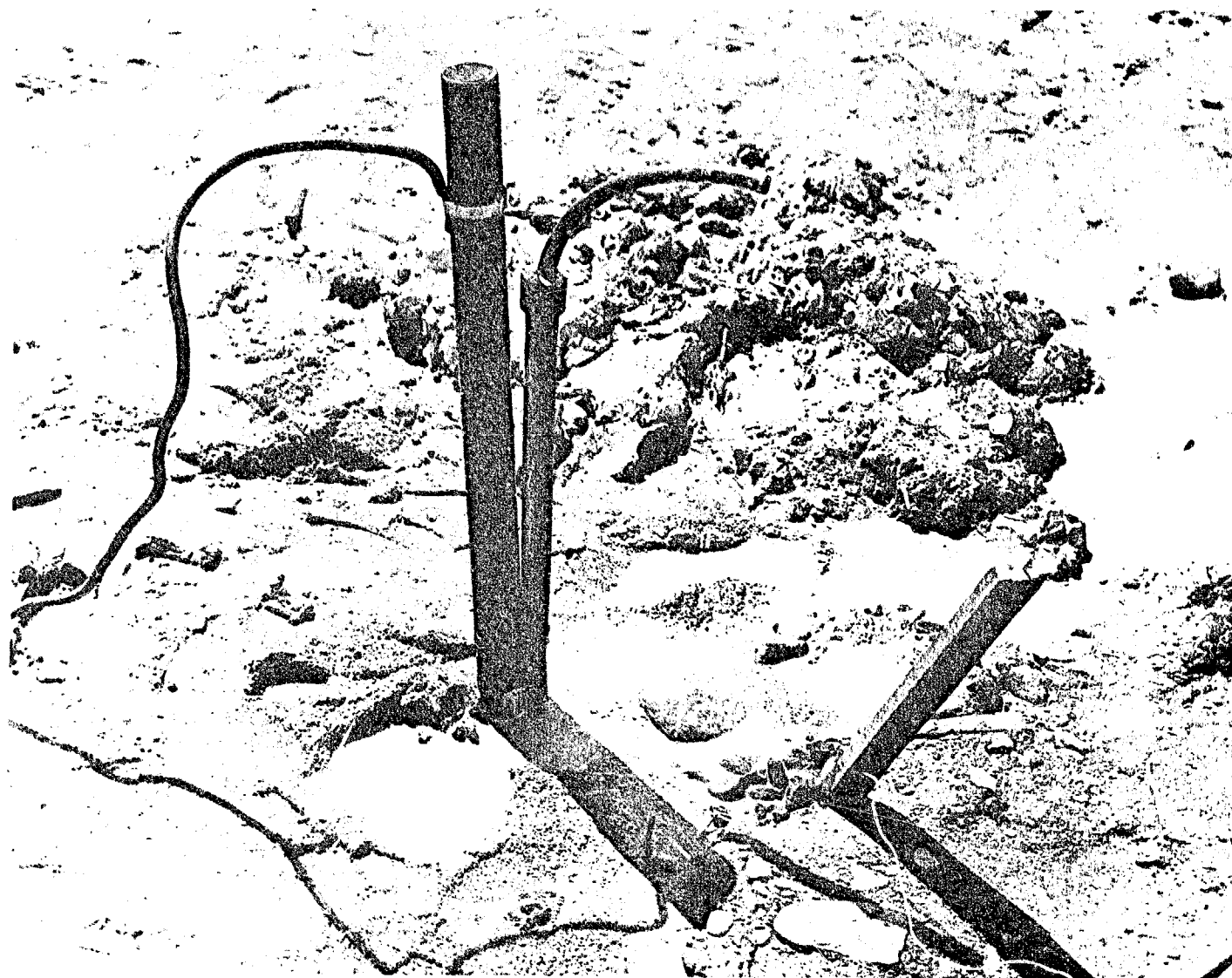


FIG.6.- DRAINAGE FROM CATHODIC PIPE AT BIG PIC RIVER BRIDGE, MARATHON, ONTARIO

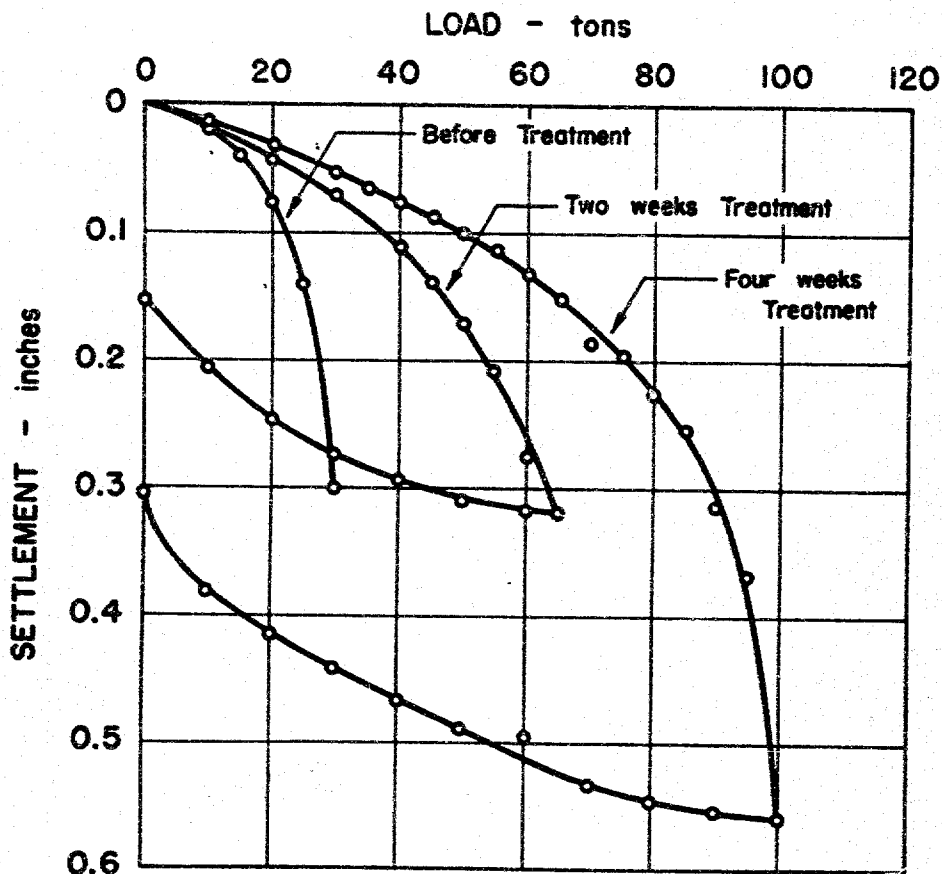


FIG.7.- LOAD TESTS ON TYPICAL PILE BEFORE AND DURING TREATMENT.  
BIG PIC RIVER BRIDGE, MARATHON, ONTARIO



FIG.8.- MODEL OF SKELETON-TYPE PILE

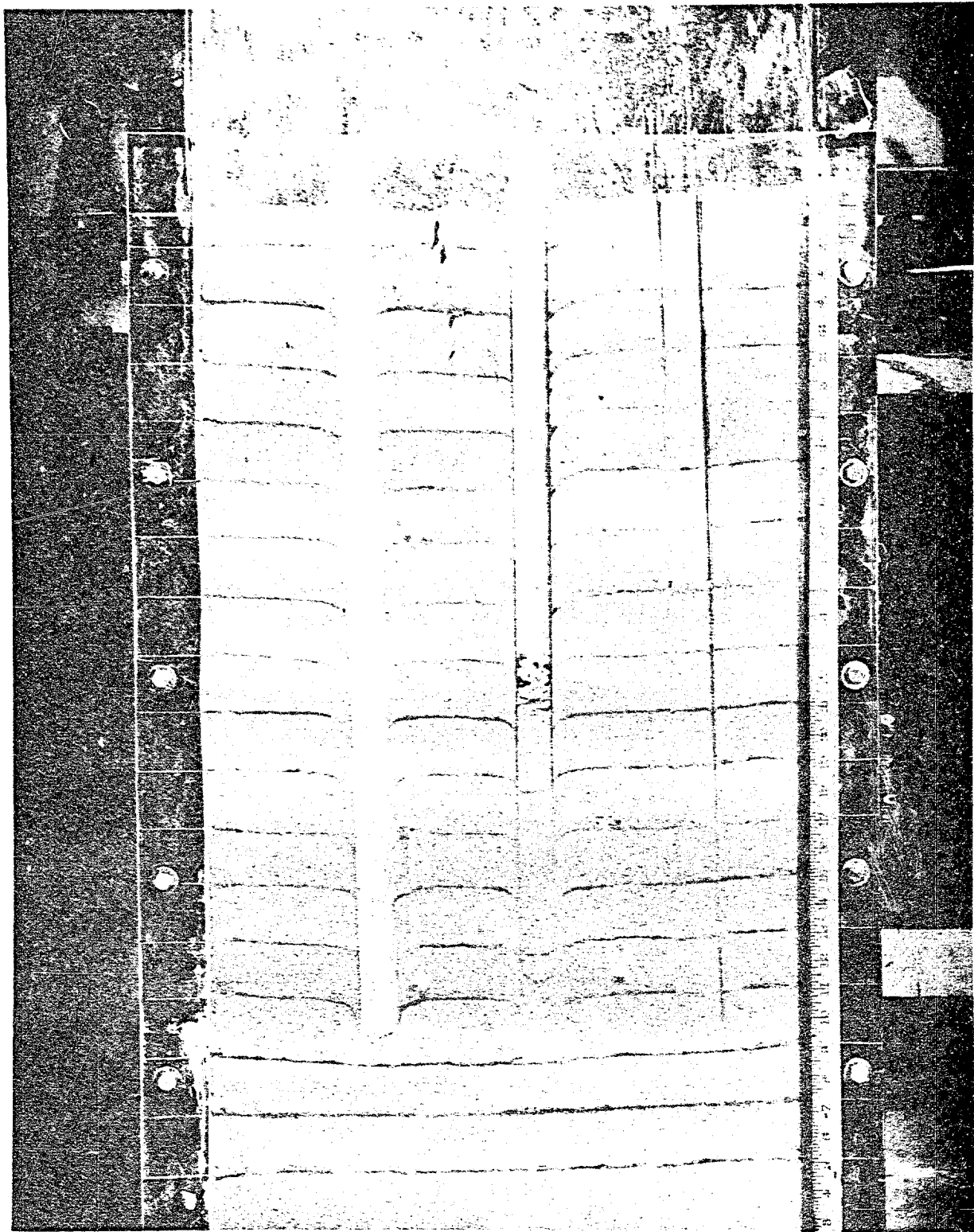


FIG.9.- DISPLACEMENT TESTS OF CONVENTIONAL PILES  
AND SKELETON-TYPE PILE



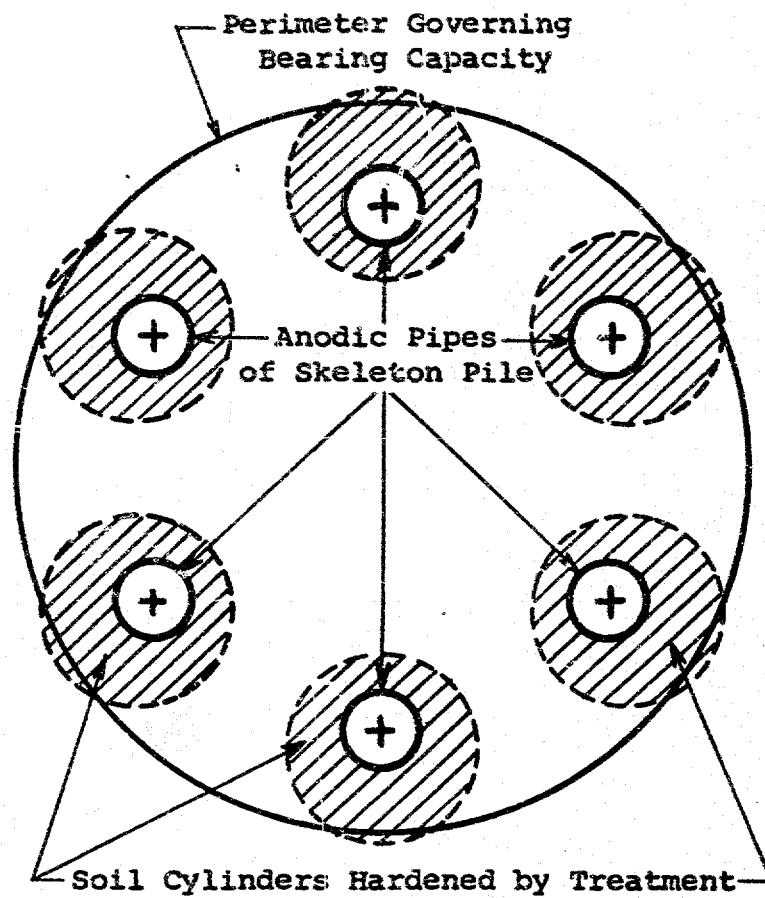


FIG.10.- STRENGTH INCREASE OF SOIL SURROUNDING SKELETON PILE  
DURING ELECTRICAL TREATMENT

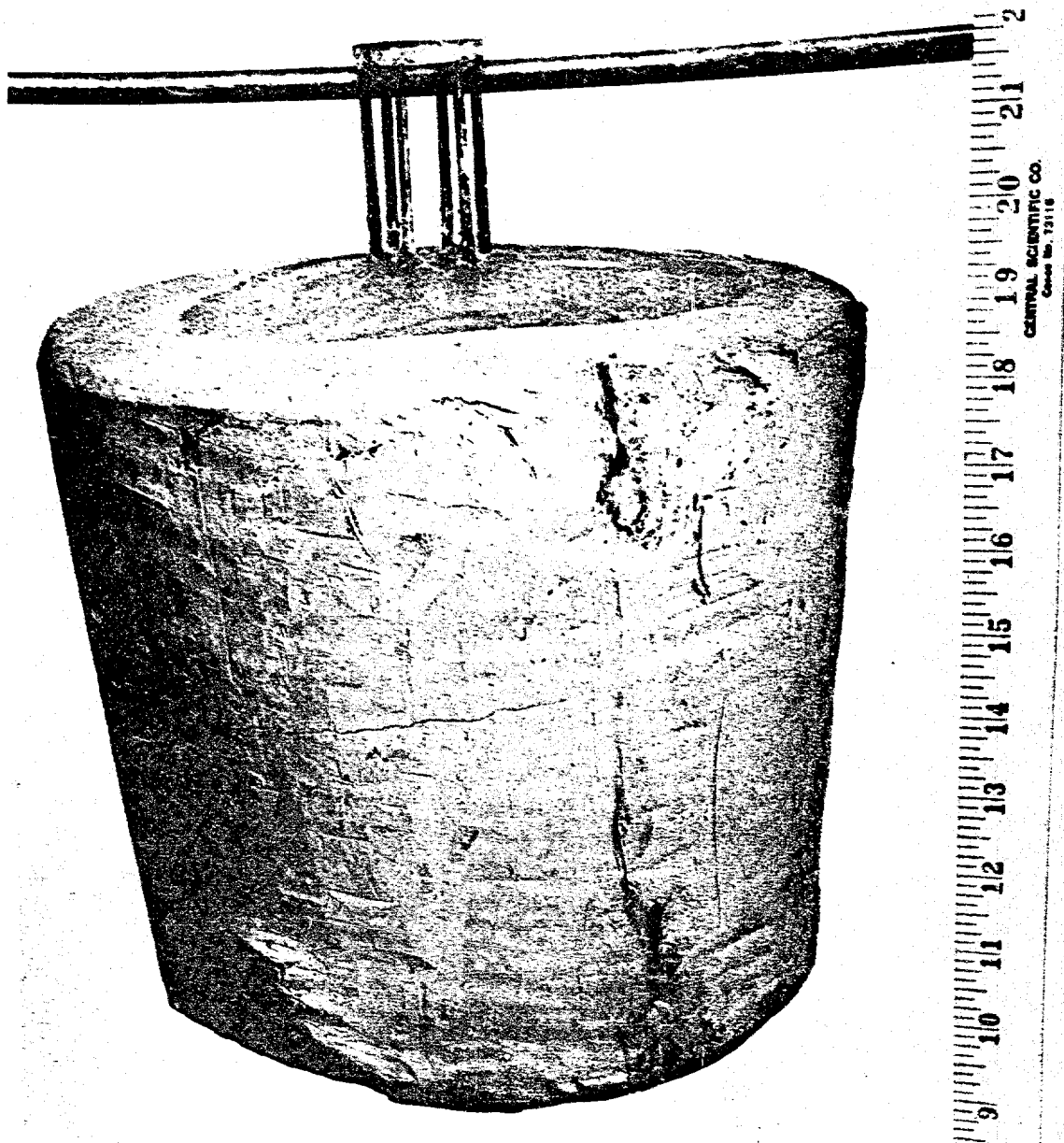


FIG.11.- EFFECT OF ELECTRO-OSMOSIS ON SKELETON PILE MODEL  
IN BOSTON BLUE CLAY

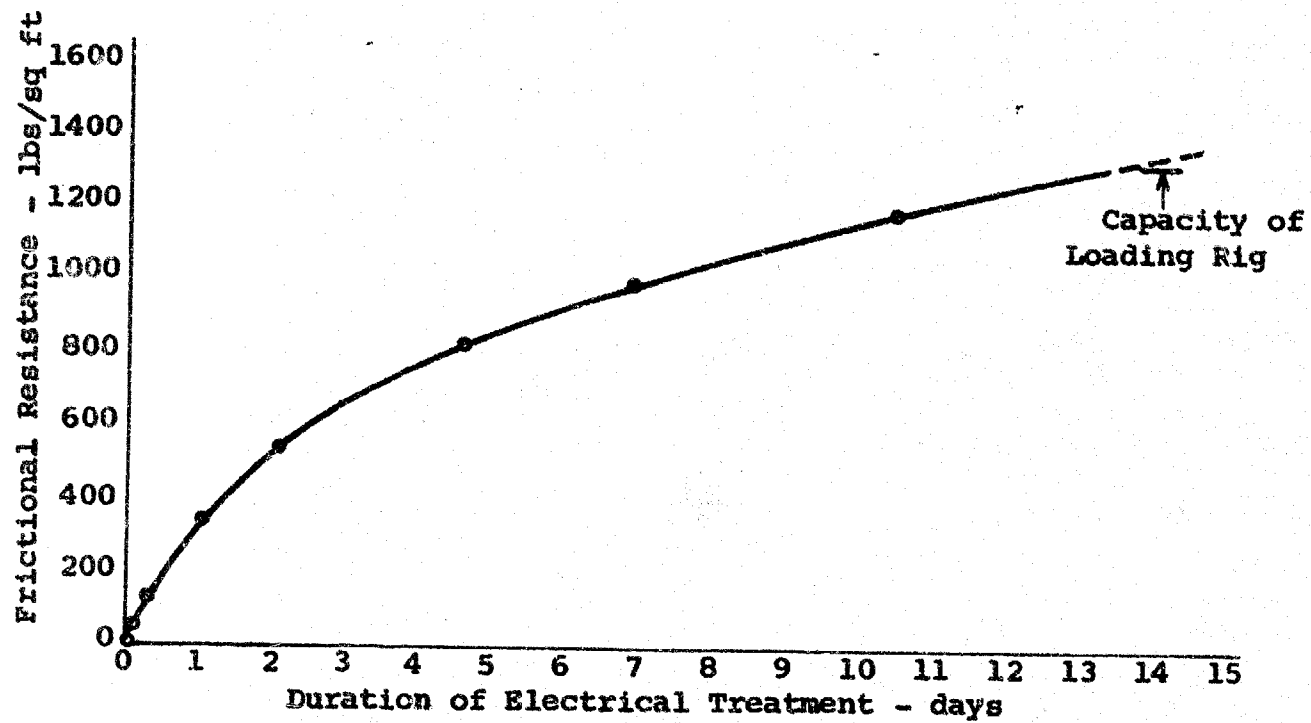


FIG.12.- INCREASE OF UNIT FRICTIONAL RESISTANCE OF MODEL PILE  
WITH DURATION OF TREATMENT

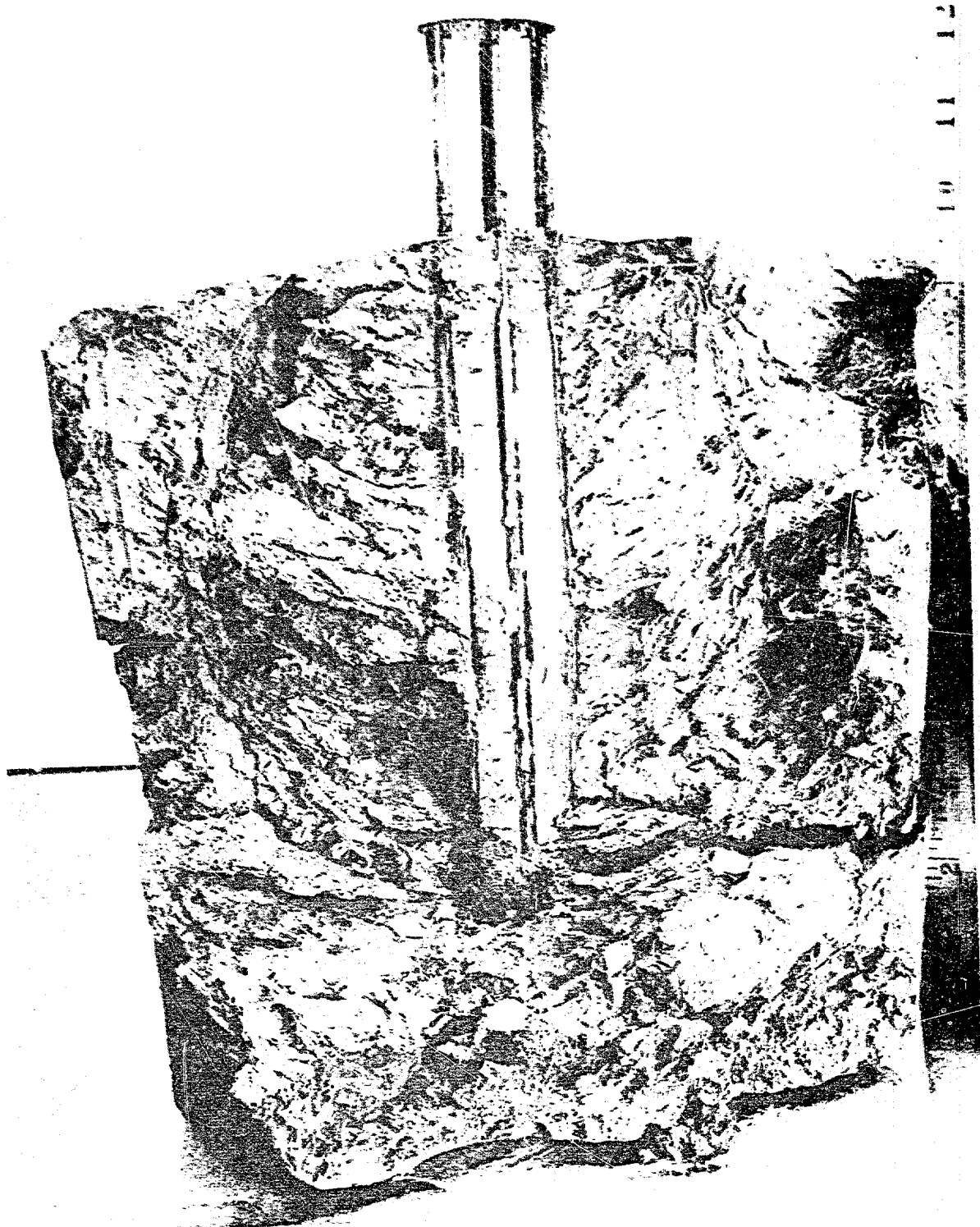


FIG.13.- DEVELOPMENT OF SOIL STRUCTURE BY ELECTRICAL TREATMENT



## **Sustained Capacity of Friction Piles in a Clay Deposit Treated by Electro-Osmosis: Observations over Five Decades**

P.K. Chatterji, Murray Anderson, Keli Shi  
*Thurber Engineering Ltd., Oakville, Ontario*  
Ken Ahmad  
*MTO Pavements and Foundations Section, Toronto, Ontario*  
Tae C. Kim  
*exp Services Inc., Brampton, Ontario*  
*(formerly with MTO Pavements and Foundations Section)*

### **ABSTRACT**

The 178 m long, three-span Pic River Bridge near Marathon, Ontario is founded on relatively short friction piles driven into an 18 m deep soft to firm varved silty clay layer underlain by over 70 m of stratified silt and silty fine sand deposits under a maximum 6 m of artesian head. Due to the artesian pressure at depth, the capacity of long friction piles driven into the silt and sand deposits was determined by load testing to be significantly less than that of short friction piles installed within the clay deposit. The original foundation design in 1959 was therefore based on 16.5 m long friction piles installed within the clay deposit. The clay properties were improved by applying electro-osmotic treatment at the two piers and east abutment. The electro-osmotic treatment doubled the ultimate pile capacity from 300 to 600 kN per pile. Subsequent load tests on selected piles conducted from 1961 to 1992 indicated that the increased pile capacities were being sustained.

Rehabilitation of the bridge involving a superstructure replacement was carried out in 2015 and 2016 along with settlement monitoring of the existing foundations. Static pile load tests were conducted on selected piles in 2013 to confirm that the pile capacities have not diminished with time. The results indicate that the pile capacity improvements achieved by the electro-osmotic treatment of the clay have been sustained over a 54-year period. Static cone penetration tests and shear vane tests were also undertaken near the test piles to assess the improvement of clay properties due to the electro-osmotic treatment. Pre-rehabilitation settlement analyses predicted negligible immediate settlement and 10 to 20 mm of long-term settlement in 25 years. The monitoring data collected between 2015 and 2017 indicated generally less than 5 mm of settlement at abutments and piers.

### **RÉSUMÉ**

Le pont de la rivière Pic à trois travées de 178 m de long, près de Marathon, en Ontario, est fondé sur des pieux de friction relativement courts enfoncés dans une couche d'argile molle à ferme de 18 m de profondeur reposant sur plus de 70 m de dépôts de limon stratifié et de sable fin limoneux sous un maximum de 6 m de tête artésienne. En raison de la pression artésienne en profondeur, la capacité des longs pieux à friction enfoncés dans les dépôts de limon et de sable a été déterminée par les tests de charge comme étant nettement inférieure à celle des pieux à friction courts installés dans le dépôt d'argile. La conception originale de la fondation en 1959 était donc basée sur des pieux de friction de 16,5 m de long installés dans le gisement d'argile. Les propriétés de l'argile ont été améliorées en appliquant un traitement électroosmotique aux deux piliers et au pilier est. Le traitement électroosmotique a doublé la capacité ultime de la pile de 300 à 600 kN par pile. Des tests de charge ultérieurs sur des pieux sélectionnés effectués de 1961 à 1992 ont indiqué que l'augmentation des capacités des pieux se maintenait.

La réhabilitation du pont impliquant un remplacement de la superstructure a été réalisée en 2015 et 2016 ainsi que le suivi de la colonisation des fondations existantes. Des tests statiques de charge de pieux ont été effectués sur des pieux sélectionnés en 2013 pour confirmer que les capacités des pieux n'ont pas diminué avec le temps. Les résultats indiquent que les améliorations de la capacité du pieu obtenues par le traitement électroosmotique de l'argile se sont maintenues sur une période de 54 ans. Des tests statiques de pénétration au cône et des tests avec des aubes de cisaillement ont

également été effectués près des pieux pour évaluer l'amélioration des propriétés de l'argile due au traitement électroosmotique. Les analyses de peuplement avant la réhabilitation ont prédit un peuplement immédiat négligeable et 10 à 20 mm de peuplement à long terme en 25 ans. Les données de surveillance collectées entre 2015 et 2017 indiquent généralement moins de 5 mm de tassement au niveau des culées et des piles.

## 1 INTRODUCTION

The Pic River Bridge on Highway 17 near Marathon, Ontario, constructed in 1959, is founded on relatively short friction piles driven into an 18 m deep soft to firm varved silty clay layer which was treated by electro-osmosis to increase the carrying capacity of the piles. Bridge rehabilitation involving a superstructure replacement was completed in 2017. The superstructure replacement involved a 15% increase in pile load at the piers. In order to confirm that the pile capacities have not diminished with time and that the pier piles can carry the additional load, static pile load tests were conducted on selected piles in 2013. The load tests supplemented periodic load testing carried out on the piles since construction to establish a period of 54 years of monitoring pile capacities. Static cone penetration tests and shear vane tests were also undertaken in the vicinity of the test piles to assess the improvement of clay properties due to electro-osmotic treatment.

The results of these load tests over 5 decades are summarized in this paper to demonstrate that the pile capacities have not diminished with time and that the pier piles can accommodate the load increase imposed by superstructure replacement.

## 2 SITE DESCRIPTION AND GEOLOGY

The Pic River Bridge is located on Highway 17 approximately 8 km east of Marathon, Ontario. The highway crosses the Pic River over a three-span steel truss structure supported on two piers and two abutments. The bridge is about 178 m long and 11.7 m wide. The approach fill height ranges up to 3.5 m at the west abutment and 2.5 m at the east abutment. A snowmobile trail bridge exists to the north of the highway bridge.

The river channel at the bridge is approximately 67 m wide and 7.5 m deep. The river flows to the south and is relatively fast flowing at this location. Rock fill erosion protection is visible above the river level in the lower parts of the approach embankment and valley slope. A photograph of the site is shown in Figure 1.

The river valley is underlain by approximately 18 m thick deposit of soft to firm varved clay, grading to stratified silt and then to silty fine sand at 70 to 80 m depth. The depth to bedrock is greater than 80 m and was not determined at the site. Artesian water pressure was encountered in the silt strata. The maximum artesian head was 6 m above ground surface at a depth of 80 m as reported in the original 1958 investigation.

## 3 FOUNDATION DESIGN BACKGROUND

The piers and abutments of the Pic River Bridge are supported on steel H Piles (12BP53/HP310x79) driven

into the clay deposit at the piers and east abutment and into the underlying silt strata at the west abutment.



Figure 1. Looking east from west bank of Pic river (2011)

During the original bridge design in 1959, the planned design load for the piles was set at 350 kN per pile. Initially the piles were driven to lengths ranging from 16.5 to 50.5 m using a 2-ton drop hammer falling 2.5 m. Load tests on these initial piles indicated ultimate pile capacities of 135 to 355 kN which did not meet the planned design load of 350 kN. The load tests also showed that the pile capacity decreased with an increase in pile embedment depth due to artesian pressures at depth. Piles tested up to 400 days after initial driving showed no significant increase in capacity when compared to the capacity measured 5 days after initial driving (Milligan, 1994).

In response to the low pile capacities, and in order to increase pile capacity, Ministry of Transportation Ontario (MTO) carried out electro-osmotic treatment of the foundation clay at selected foundation elements. The purpose of the electro-osmotic treatment was not only to increase the pile capacity but also to reduce the potential for foundation settlement and to avoid redesign of the foundation system.

For an initial test run of the electro-osmotic treatment, an electric arc welder with a maximum capacity of 375 Amperes at 115 Volts was used. The anode of the welder was hooked up to the test piles and the cathode was connected to the head frame connecting the two anchor piles. At the west pier, the energy source was connected to a 50 m long test pile group and the current maintained for 2.5 hours. At the east pier, electro-osmosis was similarly applied for 3 hours to a 20 m long test pile. At the end of this time period of application of electro-osmosis, the anodic test pile capacities increased from 150 kN to 350 kN for an untreated pile at the west pier and from 350 kN to more than 500 kN at the east pier (Geocon 1959). MTO consulted with late Professor Leo



Casagrande on the design of the electro-osmotic treatment.

Based on these favourable load test results of the treated test piles, MTO decided to apply electro-osmotic treatment to the foundation clay at the east abutment, east pier and west pier. The test pile at the west abutment was first tested after 8 days following initial driving and the load carrying characteristics of this pile had markedly improved when retested 54 days after driving. Therefore, the piles at the west abutment did not warrant electro-osmotic treatment. At the final design stage, a pile length of 16.5 m was selected to prevent penetration into the underlying silt deposit which was under artesian pressure. The foundation design resulted in using 95 friction piles at the two piers, and 33 and 22 friction piles at east and west abutments, respectively. The pile spacing ranged from 1.0 to 1.8 m. A pile capacity of 135 kN per pile was adopted for final design, even after improvement of foundation soils by electro-osmotic treatment. The design capacity was likely selected based on application of a safety factor to the measured post-treatment capacity and considerations for limiting

settlement of the pile group. Details and description of the pile load tests during original bridge design described in the 1959 report by Geocon.

As part of the original foundation design in 1959, MTO installed a number of additional piles at each pier which were isolated from the load bearing pile group by boxing out access portals in the pile cap to permit load testing during and after completion of electro-osmotic treatment of the foundation clay. A reaction beam was cast into the pile cap above each test pile to enable application of static load on the piles. Subsequent to electro-osmotic treatment, static load testing of selected piles was carried out by MTO in 1961, 1968, 1971, and 1992 to confirm that the load capacity was sustained. The results of the load tests are available in MTO files and summarized in a paper by Milligan (1994). Rehabilitation of the bridge in 2015/2016 included replacement of the bridge deck and modifications to the abutments and piers. The new deck will generally increase the loads on the piles from an original design load of 135 kN to the following loads:

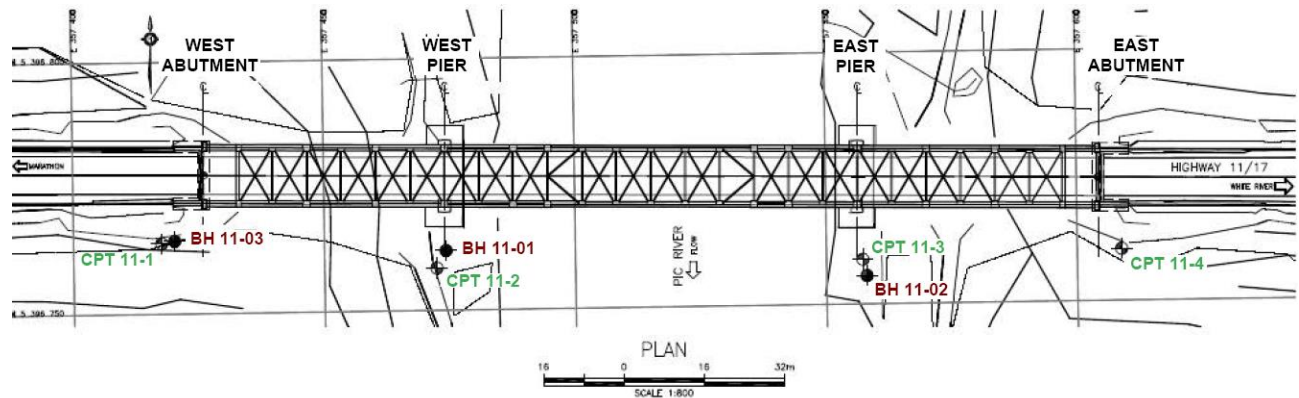


Figure 2. Locations of boreholes and piezocones (2011)

Table 1. Design loads of the replacement bridge

Foundation Element	ULS (kN)	SLS (kN)
West Abutment	215	143
West and East Piers	209	156
East Abutment	143	95

Assuming that the SLS loads are similar to working stress design load in the original design, this implies a load increase of 15% on the piles at the piers and a load decrease of 30% at the east abutment. The new SLS load at the west abutment is essentially same as the original design load. In light of this requirement MTO initiated a program in 2013 to carry out static pile load tests on three selected piles at the piers to confirm that the ultimate pile capacities are being maintained and to assess the current pile capacity and evaluate the load displacement behavior of the test piles some 50 years after construction. An in-situ program of piezocone and vane shear testing was also undertaken to evaluate the condition of the foundation clay that was treated by electro-osmosis.

#### 4 INVESTIGATION PROGRAM

The investigation program consisted of the following components:

- Borehole Drilling Program
- Static Pile Load Tests
- Piezocone and Field Vane Testing

##### 4.1 Borehole Drilling Program

A foundation investigation, carried out in April 2011, consisted of drilling three boreholes to depths of 26.5 to 46.3 m near the west pier, the east pier and the west abutment. Standard Penetration tests and shear vane tests were carried out at selected intervals in each borehole. Undisturbed Shelby tube samples of the foundation clay were collected from the boreholes. Piezocone testing was conducted near each foundation element to complement borehole information. Figure 2 shows the approximate locations of the boreholes and piezocones.

The samples collected from the boreholes were subjected to water content and index tests consisting of gradation and Atterberg Limit tests.

#### 4.2 Static Pile Load Tests

Static Pile Load tests were conducted on the following piles:

- East Pier: Pile Nos. G-5 and E-16
- West Pier: Pile No. E-2

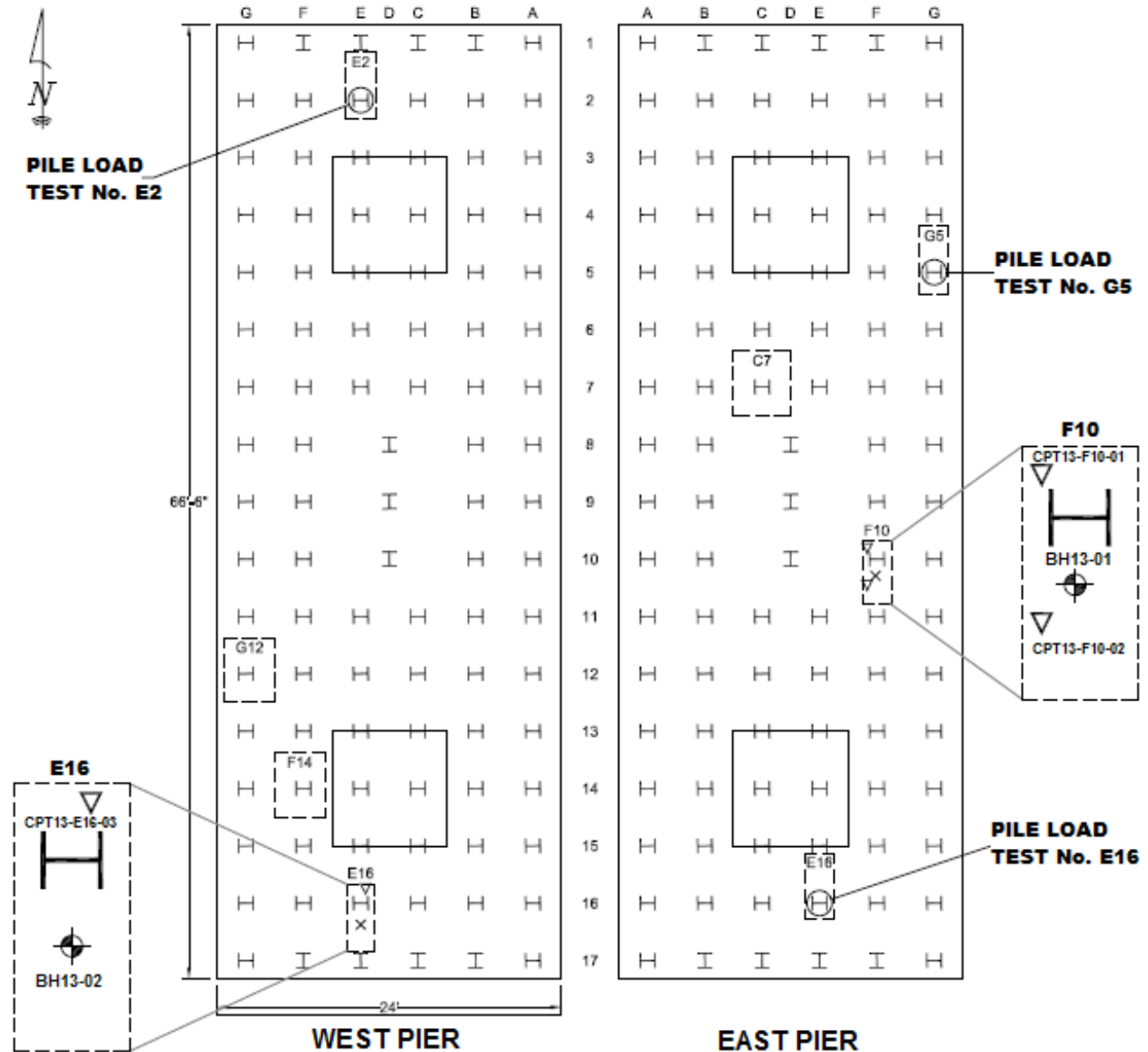


Figure 3. Locations of test piles, boreholes and piezocones (2013)

#### 4.3 Piezocone and Field Vane Testing

In addition to the pile load testing program, static piezocone tests (CPT) were conducted at two locations within the east pier (CPT 13-F, 10-01 and 10-02) and one location within the west pier (CPT 13-E16-03). The CPT

The location of the test piles at each pier is shown on Figure 3.

Each pile was loaded to a maximum load ranging from 700 kN to greater than 900 kN and settlement of each pile was recorded at prescribed intervals under each load increment. A photograph of the load test set up is presented in Figure 4.

test locations are shown on Figure 3.

The piezocones were pushed to a depth of 11.8 m. One of the CPT tests was pushed 0.23 m from the centre of a pile while the second test was pushed 0.56 m away from the pile to compare soil properties within and outside the zone of electro-osmotic treatment. Pore



pressure dissipation tests were conducted at selected depths within the foundation clay.

Field vane shear tests were conducted at 0.75 m depth intervals to 12 m depth in pile access portal F10.



Figure 4. Pile load test set-up at Pile E-16, East Pier

## 5 INVESTIGATION RESULTS

### 5.1 Stratigraphy

Figure 5 presents a stratigraphic profile at the bridge site.

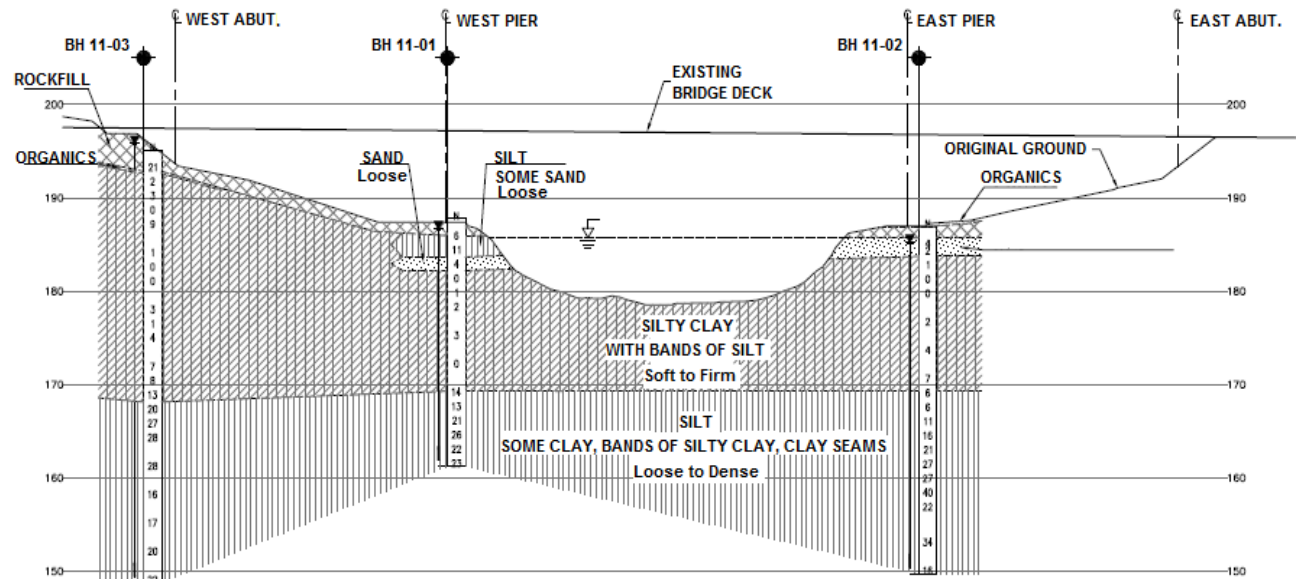


Figure 5. Stratigraphic profile at the Pic River site

### 5.2 Static Pile Load Tests

The results of the static pile load tests on the three piles are plotted on the load-settlement curves in Figures 6, 7 and 8 along with the historical load test curves. A review of the pile load test data indicated the following:

- 1) The interpreted ultimate capacity of Piles G-5 and E-16 at the east pier ranges between 550 and 600 kN.
- 2) The load/deformation behavior of the test piles at the east pier is essentially elastic below 600 kN and the pile settlements are less than 5 mm. The settlement

The stratigraphy encountered in the boreholes consisted of 1 to 2 m of rockfill overlying 2 to 4 m of loose sand and silt which was overlying the varved silty clay.

The silty clay deposit, about 13 to 25 m thick, is soft to stiff. The deposit contains 5 to 10 mm thick varves of silt. The clay deposit transitions to a compact silt layer with clay bands below a depth of 18 to 27 m.

The varved clay is of intermediate to high plasticity. The approximately 25 mm thick dark grey silty clay bands exhibited moisture contents of 35 to 65%, a clay content of 70%, and a silt content of about 30%, while the typically 12 mm thick light grey clayey silt bands exhibited moisture contents of 20 to 30%, a clay content of 30% and a silt content of 70%. The undrained shear strength of the clay ranged from about 16 to 40 kPa in the upper 4.5 m of the deposit and increased to 32 to 76 kPa below this level.

The underlying silt layer is loose to dense with moisture content of 20 to 40%. The silt gradation includes 83 to 96% silt sized particles with 4 to 17% clay size fraction.

The piezometer installed in the silt deposit in the borehole indicated a piezometric level of 1.6 m below ground surface to a small artesian load of 1 m above the ground surface. It should be noted that the maximum artesian head was 6 m above ground surface in the silt strata at a depth of 80 m during the 1958 investigation.

increased more rapidly with each load increment over 600 kN, reaching a maximum of 19 to 20 mm (indicating pile failure) at applied loads of 690 and 750 kN before the load test was discontinued.

3) The load test for Pile E-2 at the west pier indicated that the pile did not reach failure at a loading of 900 kN and the pile settlement at this loading was in the order of 8 mm.

4) Each pile was unloaded and reloaded at one point during the load tests and the resulting load settlement behavior remained essentially elastic.

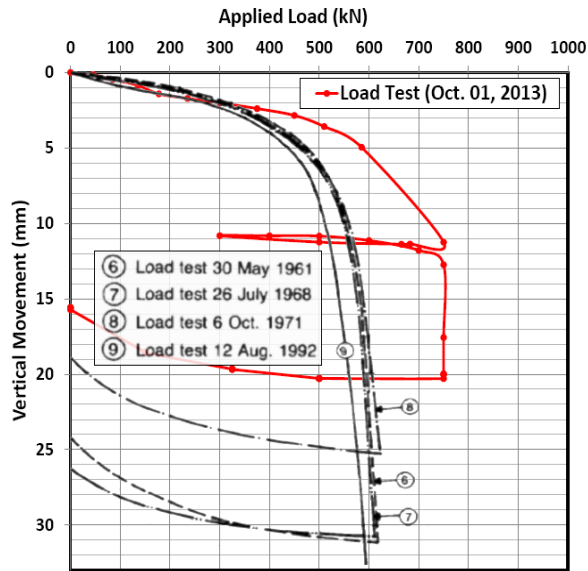


Figure 6. Load deformation curves of East Pier G-5

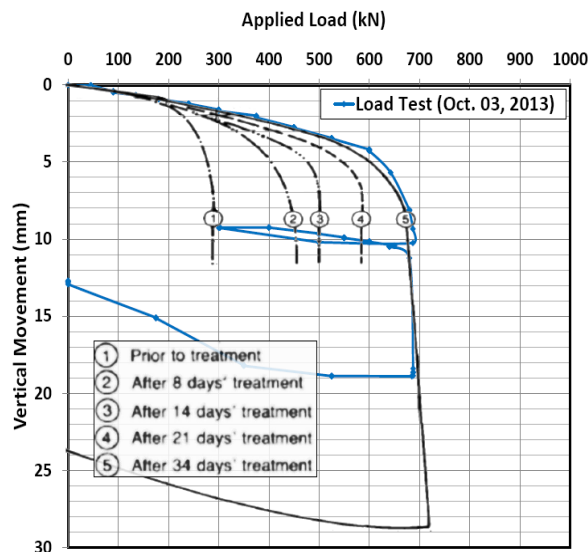


Figure 7. Load deformation curves of East Pier E-16

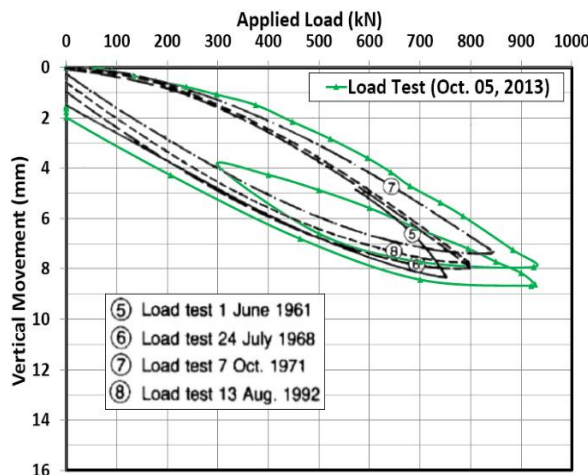


Figure 8. Load deformation curves of West Pier E-2

### 5.3 Piezometer and Vane Tests

The results of piezocone tests are presented in Figures 9 and 10. The results of field vane tests indicate undrained shear strengths of the treated clay from 48 to 80 kPa at the east pier and 53 to 75 kPa at the west pier.

Figures 9 and 10 present a comparison of undrained shear strength ( $S_u$ ) of the untreated clay (outside pile group) versus the undrained shear strength of the treated clay around the piles (within pile group) of the east and west piers, respectively. The average  $S_u$  profile from the original 1958 investigation appears very similar to the  $S_u$  profile of the untreated clay outside the pile group tested in 2011. At both pier locations,  $S_u$  for the untreated clay ranges from 20 to 58 kPa, while the  $S_u$  values of the treated clay ranged from 50 to 70 kPa. This data tends to indicate an increase in the clay strength by about 50% after electro-osmotic treatment.

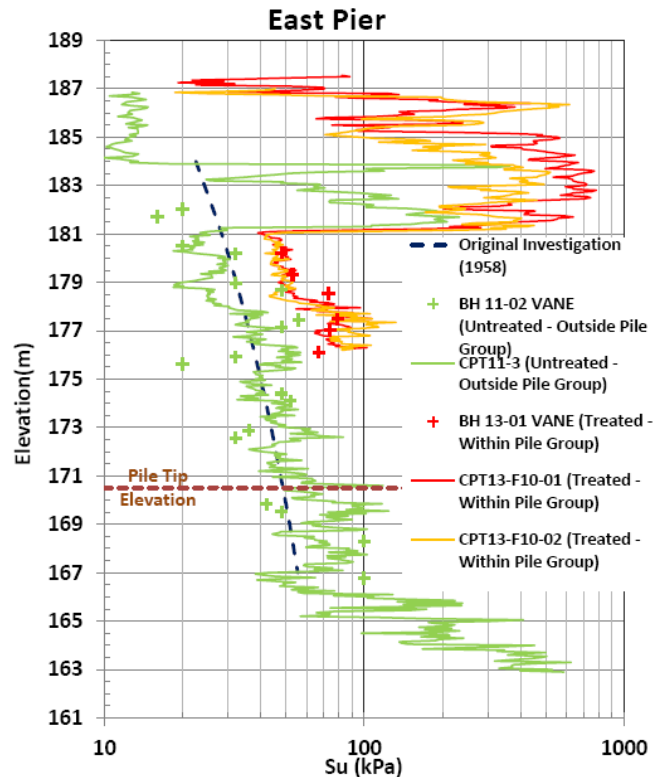


Figure 9. Comparison of undrained shear strengths of untreated clay and treated clay at the East Pier

## 6 GEOTECHNICAL ASSESSMENT

### 6.1 Pile Load Tests

The load settlement curves from the current load tests in Figures 6, 7 and 8 are plotted along with the load settlement curves previously conducted in 1961, 1968, 1971, and 1992. The results indicate that the ultimate pile capacities of all three piles have been maintained and appear to have increased for piles G-5 and E-2.

Based on the results of the pile load tests, an ultimate capacity of 600 kN per pile may be assumed for a single pile within the east and west pier pile groups. The factored geotechnical resistance at Ultimate Limit State (ULS) per pile is therefore 360 kN (600 kN x resistance factor of 0.6). Based on the load-settlement curves, the immediate (elastic) settlement of a single pile subjected the increased design load of 156 kN per pile will be 2 mm or less.

The load test results indicate that a single pile at the piers can accommodate an increase in design load from 135 kN to 156 kN per pile.

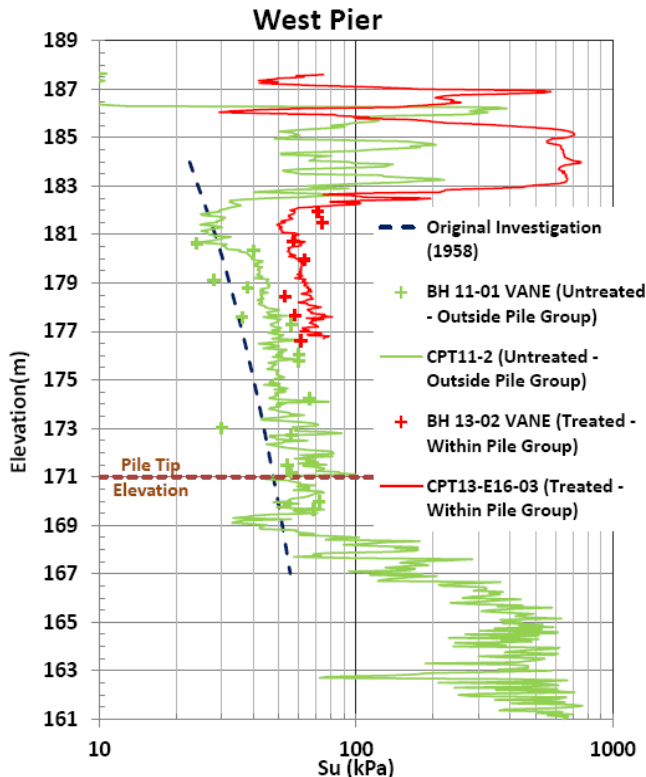


Figure 10. Comparison of undrained shear strengths of untreated clay and treated clay at the West Pier

The assessment of carrying capacities was followed by an estimation of settlement of the pile groups under the new bridge deck load resulting from the rehabilitation of the bridge. The total settlement will include both immediate (elastic) settlement of the pile groups as well as post-construction consolidation and creep settlement in the clay. Geotechnical programs including GROUP (developed by Ensoft) and Settle<sup>3D</sup> (developed by Rocscience) were used to carry out the settlement analysis. The settlements tabulated below are estimated for a design service load of 175 kN per pile:

The above settlement estimates are within the settlement tolerance that can be accommodated by the rehabilitated bridge.

Table 2. Estimated settlements of the pile groups

Foundation Element	Estimated Settlement (mm)			
	Immediate (elastic)	25-year	50-year	75-year
West Abutment	1	10	15	19
West Pier	2	15	20	25
East Pier	3	20	25	30
East Abutment	2	16	23	28

## 6.2 Monitoring During Bridge Rehabilitation

The performance of the foundations of the existing bridge were monitored during and subsequent to the rehabilitation of the bridge between approximately May 2015 and July 2017. This included settlement monitoring of the abutment and pier caps by surveying of settlement monitoring points. In addition, the pore pressure response of the foundation clay near the foundation elements was monitored using vibrating wire piezometers.

Settlement monitoring points were installed near the centre and at the corners of each concrete pile cap. Accuracy of the settlement survey was maintained at  $\pm 2$  mm. The results of the settlement monitoring collected over the 2-year period indicated less than 5 mm of settlement at each foundation element. This observation agreed well with the estimated foundation settlements presented in Table 2.

A total of eight vibrating wire piezometers were installed in the clay deposit with two near each foundation element. The piezometer tips were located at depths ranging from 7 to 14 m below ground surface. Each pair of piezometers were typically spaced at 3 m in depth between the two. The measured pore pressures in the clay during the bridge rehabilitation generally fluctuated with the hydrostatic pressure in the ground.

## 7 CONCLUSIONS

The existing Pic River Bridge is supported on pile groups consisting of steel H-piles driven into soft to stiff varved clay. During initial construction, electro-osmotic treatment was applied to the foundation clay to improve pile capacity and settlement characteristics of the foundation clay.

Proposed rehabilitation of the bridge would include deck replacement and an increased load on the existing pier piles by up to 15%. Confirmation was required that the existing pile foundations could accommodate the increased loading at the piers and had maintained the improved capacity realized by electro-osmotic treatment.

The results of a foundation investigation program and static load tests on selected test piles in 2013 led to the following conclusions:

1. The pile capacity improvements realized by electro-osmotic treatment have been maintained since original construction in 1959. Test pile G-5 at the east pier showed about 25% higher capacity than the previous load test results. The mechanism behind the

post electro-osmosis capacity increase is not well understood but it is postulated that this may be attributed to shaft shear setup associated with aging effect of driven piles in clay. However, the capacity increase was not observed for the test pile E-16 within the same pile group.

2. The piezocone and vane shear strength testing indicate that the strength of the clay within the entire block of the pile group has been significantly improved by the electro-osmotic treatment.

3. The pile load tests indicate that the existing pier piles will be able to carry the 15% load increase.

4. Based on the results of the pile load tests and computation of pile group settlements, the settlement estimates due to increased pile loads are within the settlement tolerance of the rehabilitated bridge.

5. Settlement and pore pressure response were monitored during the rehabilitation of the bridge. Minimal settlements of the foundation elements were noted under the increased load from the new bridge deck. No discernable increase in pore pressure was noted in the foundation clay during the bridge rehabilitation work.

It should be noted that the success of electro-osmotic treatment in improving driven pile capacity in varved clay deposit at the Pic River Bridge is a very site-specific case study and may not be replicated at other sites with differing soil conditions. An extensive field and laboratory testing program will be necessary to prove the applicability of the electro-osmotic treatment for a particular site. In addition, post-treatment monitoring should be implemented to confirm retention of the improvements in soil properties and foundation capacity in the long term.

## 8 ACKNOWLEDGMENTS

The authors would like to thank the Ministry of Transportation (MTO) for their support and funding for the work and their permission to publish this paper. The assistance of Ben Huh, Lead Bridge Engineer, MTO Bridge Branch and Anna Piascik, formerly with MTO Pavements and Foundation Group are gratefully acknowledged. The authors also wish to thank Dick Dykstra, Head of Geotechnical Section, MTO Northwest Region for his support.

The static pile load tests were conducted by Geo-Foundations Contractors Inc, of Acton, Ontario. CPT testing was performed by ConeTec Investigations Ltd. of Richmond Hill Ontario. The drill rig used to push the cones was supplied by TBT Engineering of Thunder Bay, Ontario. The assistance of Tulloch Engineering, the Contract Administrator for the project in obtaining geotechnical instrumentation readings is gratefully acknowledged.

The pile load tests, CPT testing and installation of instruments were supervised by Mark Farrant of Thurber Engineering. Monitoring of geotechnical instruments were supervised by Luke Gilarski, formerly with Thurber Engineering.

## 9 REFERENCES

- Milligan, V. 1994. *First application of Electro-Osmosis to improve friction pile capacity - three decades later*. In Proceedings of the 13th International Conference on Soil Mechanics and Foundation Engineering, New Delhi, India, 1994.
- Geocon Ltd., 1958. *Soil Conditions and Engineering Study, Proposed Big Pic River Bridge, Highway 17, Marathon, Ontario*. Report submitted by Geocon Ltd. to MTO on Sep. 19, 1958. Geocres No. 42D-7.
- Geocon Ltd., 1959. *Pile Driving, Pile Loading and Piezometric Observation, Proposed Pic River Bridge, Highway 17, Marathon, Ontario*. Report submitted by Geocon to MTO, March 3, 1959, Geocres No. 42D-11.
- Ministry of Transportation Ontario, 1993. *MTO Pile Load and Extraction Tests, 1954-1992*, Foundation Design Section, Report EM-48, Rev. 199.
- Randolph, M.F., Carter, J.P. and Wroth, C.P. 1979. Driven Pile in Clay – The Effects of Installation and Subsequent Consolidation. *Geotechnique*, 29(4): 361-393
- Poulos, H.G. and Davis E.H. 1980. *Pile Foundation Analysis and Design*. The University of Sydney.
- Edil, T.B. and Mochtar, I.B. 1988. Creep Response of Model Pile in Clay. *Journal of Geotechnical Engineering*, ASCE, 114(11): 1245-1260.
- Lo, K.Y., Inculet, I.I. and Ho, K.S. 1991. Electroosmotic Strengthening of Soft Sensitive Clays. *Canadian Geotechnical Journal*, 28: 62-73.
- Doherty, P. and Gavin, K. 2013. Pile Aging in Cohesive Soils. *Journal of Geotechnical and Geoenvironmental Engineering*, ASCE, 139(9): 1620-1624.



# First application of electro-osmosis to improve friction pile capacity—three decades later

V. Milligan, MSc, CEng, DSc, DEng, MICE

It is the intention of the Editorial Panel occasionally to publish Papers which have been published elsewhere, are of particular interest and would not easily be accessible to the readership of this Journal. This short Paper was presented at the 13th International Conference on Soil Mechanics and Foundation Engineering in New Delhi early in 1994 and it is of interest because it provides a long-term case study of pile load bearing behaviour, following the use of electro-osmosis to improve the friction capacity of steel H-piles in soft varved clay and silt soils.

- **The problem of founding the Big Pic River Bridge on some 100 m of soft varved clay and loose silt deposits is described. Due to the presence of excess hydrostatic head at depth, the capacity of long friction piles was markedly less than that of short piles; consequently, it was decided to found the structure on short, steel H-section friction piles within the upper clay and to apply electro-osmotic treatment. The overall effect of the electro-osmosis was markedly to increase the pile capacity. It is believed that this is the first example of electro-osmosis being used to improve friction pile capacity. Further tests have since been carried out over the past 33 years to assess the permanence of the increase in pile capacity. No reduction in the load bearing capacity of the piles has been measured over this period and recorded settlement of the bridge foundations has been minimal.**

## Introduction

This Paper describes the use of electro-osmosis to increase the bearing capacity of friction piles for the substructure support at the Big Pic River Bridge, which is a three-span, through truss steel cantilever structure, over 180 m in length. It is one of many along the route of the Trans-Canada Highway which, in part, skirts the north shore of Lake Superior. Valleys in this area, of irregular volcanic Precambrian rock, are infilled by considerable thicknesses of stratified glacial lake silts and clays. Electro-osmosis was used when the original foundation design, which called for friction piles driven into the silts at depth, proved to be inadequate.

2. Load tests carried out over a period of 33 years since the original treatment in 1959 have

demonstrated that pile capacities have not diminished with time.

## Site geology

3. The subsoil stratigraphy at the site is illustrated in Fig. 1. Bedrock surface was not determined. The upper several metres consist of a compact, fluvial silty sand. This is underlain by about 18 m of medium to stiff, varved silty clay. The varves are composed of dark grey, brittle clay laminae, approximately 25 mm thick, and light grey, clayey silt laminae, typically 12 mm in thickness. The particle size distribution, determined from tests on individual laminae, is shown in Fig. 2. The variations in Atterberg Limits, water content and undrained triaxial and in-situ vane shear strength with depth, are shown in Fig. 3.

4. The varved clay stratum grades into a grey, stratified coarse silt which becomes a silty fine sand with increasing depth. Between depths of 20 m and 50 m, the standard penetration resistance, or  $N$  values, ranged from 20–10 blows per 300 mm, gradually decreasing with depth. Artesian conditions were observed on first encountering the silt stratum at 50 m depth. This condition became more pronounced with depth, as reflected in the decrease in  $N$  values. The maximum artesian head rose to 6 m above existing ground level at a depth of 80 m. At this depth and below, the  $N$  values were sensibly zero due to piping in boreholes.

## Pile load tests

5. Because of the low strength, high compressibility and excessive depth of the deposits, a friction pile foundation was chosen in 1959. Steel H-section piles, 300 × 300 mm, 79 kg/m, varying in embedded length from 16.5 to 50.5 m, were driven using a 2 t drop hammer falling 2.5 m. The driving resistance increased linearly



Victor Milligan,  
formerly of  
Golder Associates  
Ltd, Mississauga,  
Canada

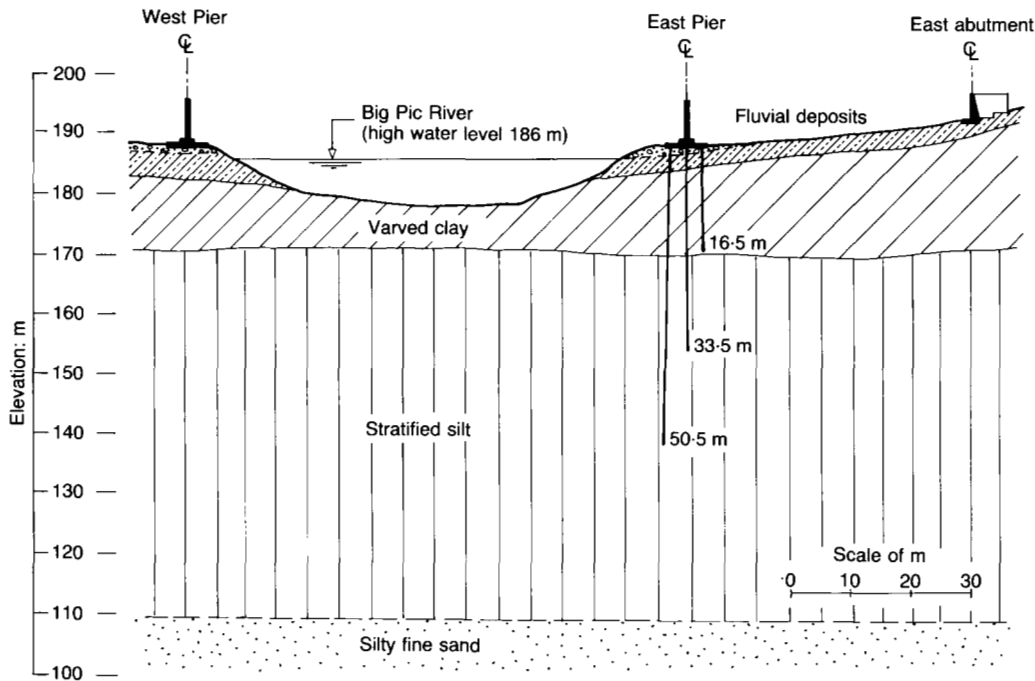


Fig. 1. Subsoil profile at Big Pic River, Marathon, Ontario

with depth to a maximum resistance of about 20 blows for 300 mm penetration at a depth of 50.5 m.

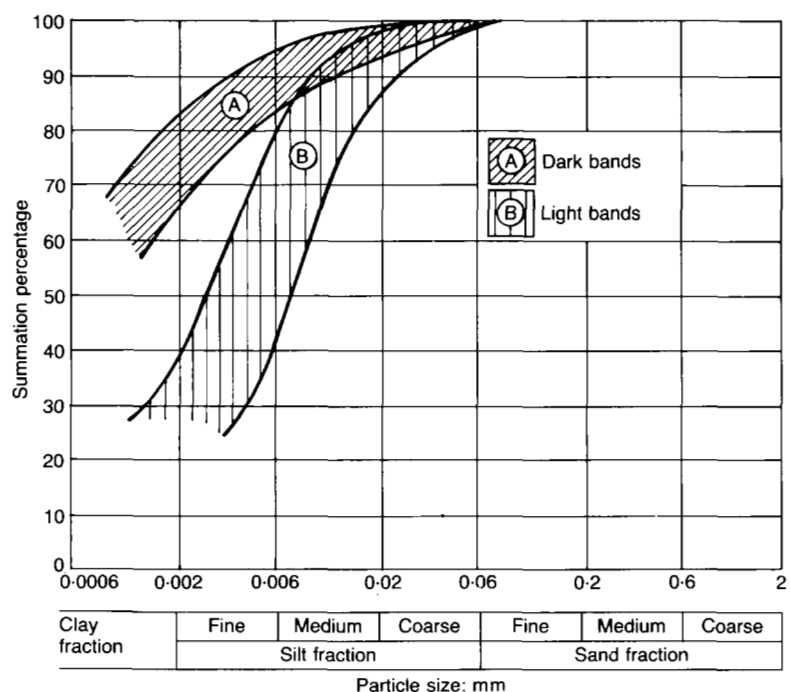
6. The planned design load was to be 350 kN, but load tests on initial piles driven at the site indicated pile capacities of about half this amount. Typical results of static load tests on piles of varying lengths are summarized in Fig. 4. These tests show that static pile capacity actually decreased with an increase in embedded length, due to artesian effects at depth. Piles tested up to 400 days after driving showed no significant increase in capacity above that measured 5 days after driving.

### Electro-osmotic treatment

7. In order to avoid a radical change in the design of the bridge at this late stage, it was decided to attempt to increase the frictional resistance of the piles by applying electro-osmosis. A preliminary field test was carried out utilizing two 16.5 m long test piles as electrodes. Under a potential of 115 volts applied by electric arc welding equipment on site, the bearing capacity of the anodic pile, which prior to treatment had carried an ultimate load of barely 260 kN, showed an increase to approximately 500 kN after three hours of treatment. Subsequent laboratory tests by Dr L. Casagrande at Harvard University indicated that with longer duration of treatment even better results could be anticipated. On the basis of these favourable results it was decided to use 16.5 m long piles which would not penetrate into the silt stratum beneath the varved clay and a design load of 135 kN per pile.

8. In Fig. 5, the installation for the West Pier is shown including the arrangement of the cathodes relative to the H-piles, utilized as anodes. The average distance between the electrodes was about 7 m. The layout for the electrical treatment at the East Pier was similar to that at the West Pier. In order to prevent clogging of the cathodic pipes with calcium carbonate, a combination of steel pipes and plastic pipes was used and small holes were drilled

Fig. 2. Grain size distribution for varved clay



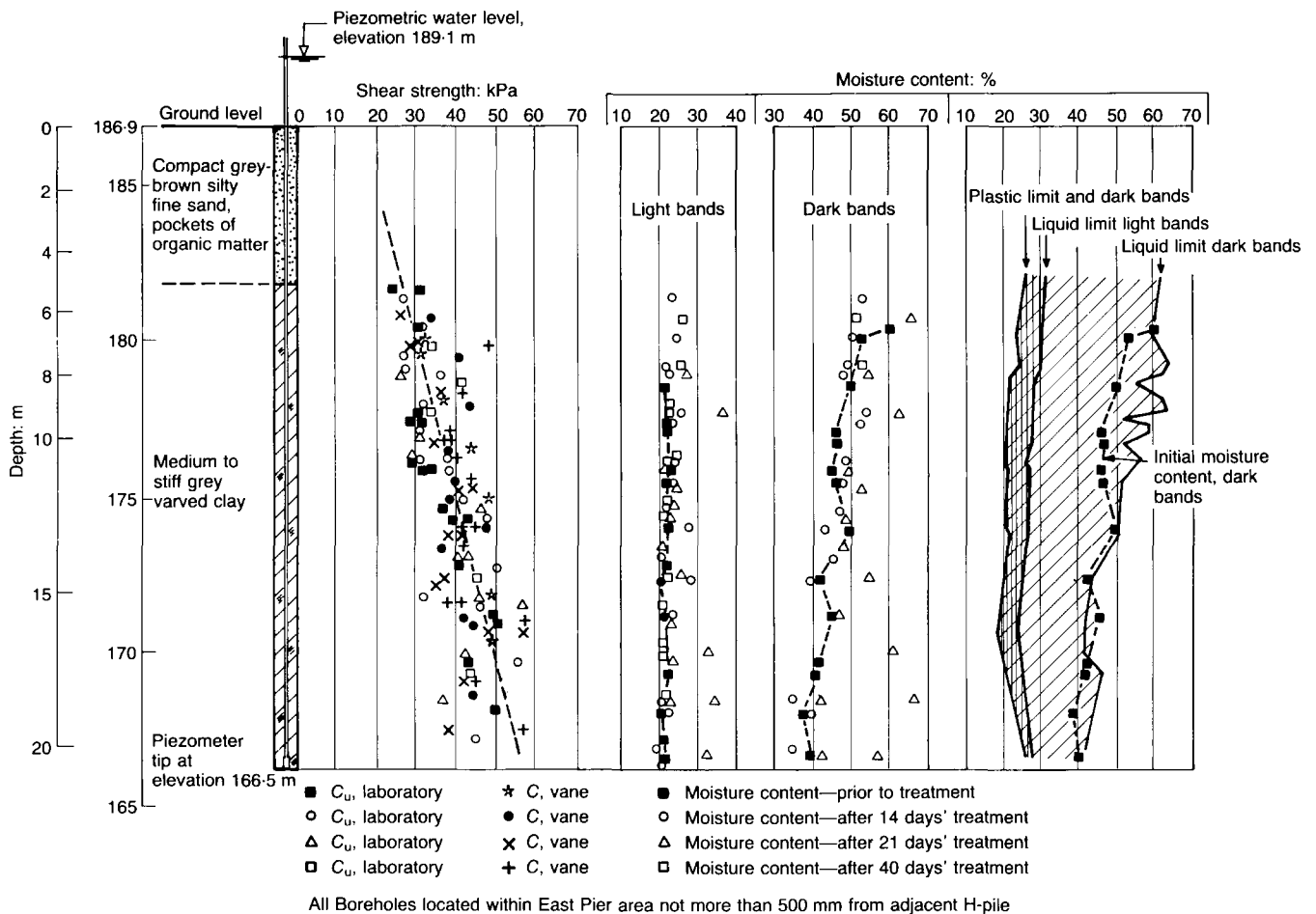


Fig. 3. Geotechnical properties of varved clay

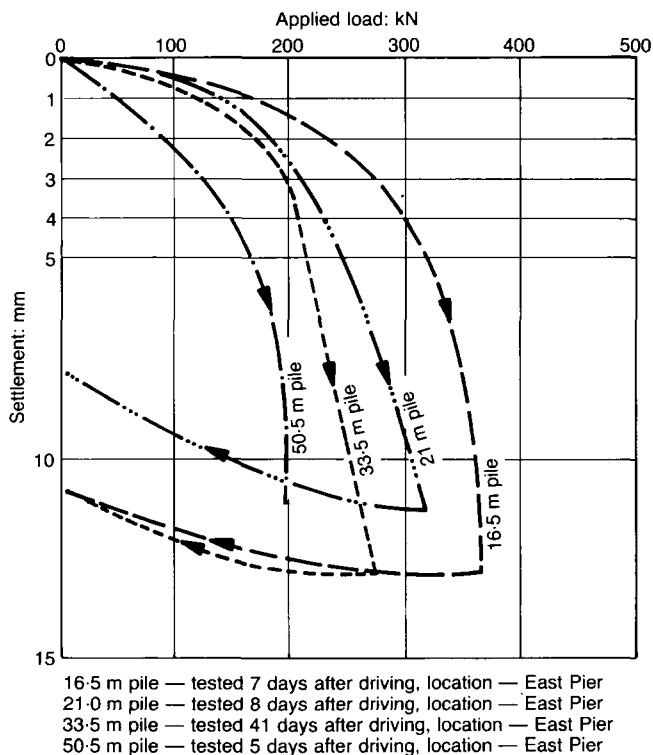


Fig. 4. Typical results of initial static load tests

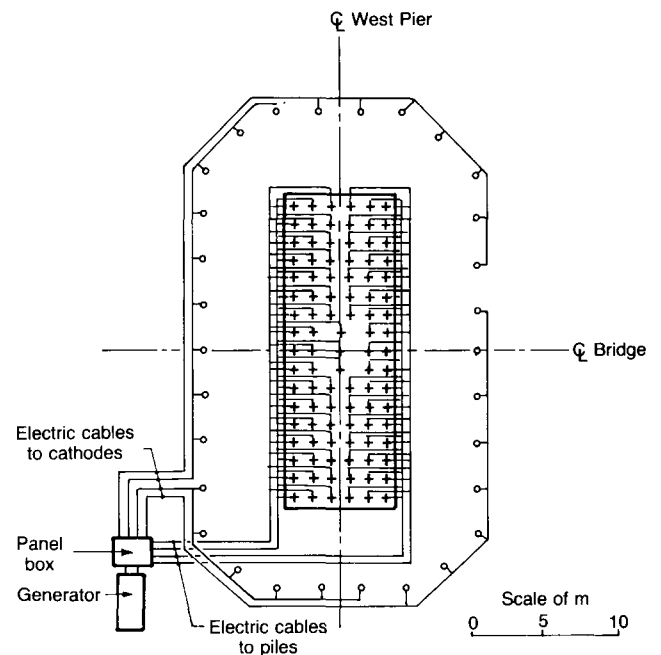


Fig. 5. Electrical layout at West Pier

into the plastic pipe to allow the water (carried by electro-osmosis toward the cathode) to penetrate the plastic pipe and to discharge on the surface. Three diesel generators with an output of 70–120 volts and 1000–600 amps per unit were used. The average current consumption per H-pile for a potential of 100 volts amounted to 15 amps. (Further details of the site and of the pile treatment are given in Soderman and Milligan, 1961,<sup>1</sup> and in Casagrande *et al.*, 1960.<sup>2</sup>)

### Control tests (1959) and subsequently (1960–92)

9. Several H-piles in the foundations of each of the piers were boxed out in order to permit pile load tests to be carried out during and after

electrical treatment. Thus, the progress of increase in bearing capacity with the duration of treatment could be monitored. The results for test pile E-16 in the East Pier are plotted in Fig. 6 and demonstrated a remarkable increase in ultimate bearing capacity from less than 300 kN to over 600 kN, over a period of treatment in 1959 lasting five weeks.

10. Subsequent pile load tests on adjacent pile G-5, also in the East Pier and of the same length, carried out in the period 1960–92, are shown in Fig. 7. It may be seen that there has been no reduction in capacity with time.

11. Load test results in 1959 for test pile E-2 in the West Pier are shown in Fig. 8. Load tests for the period 1961–92 are shown in Fig. 9. Even though pile load capacities are, in this

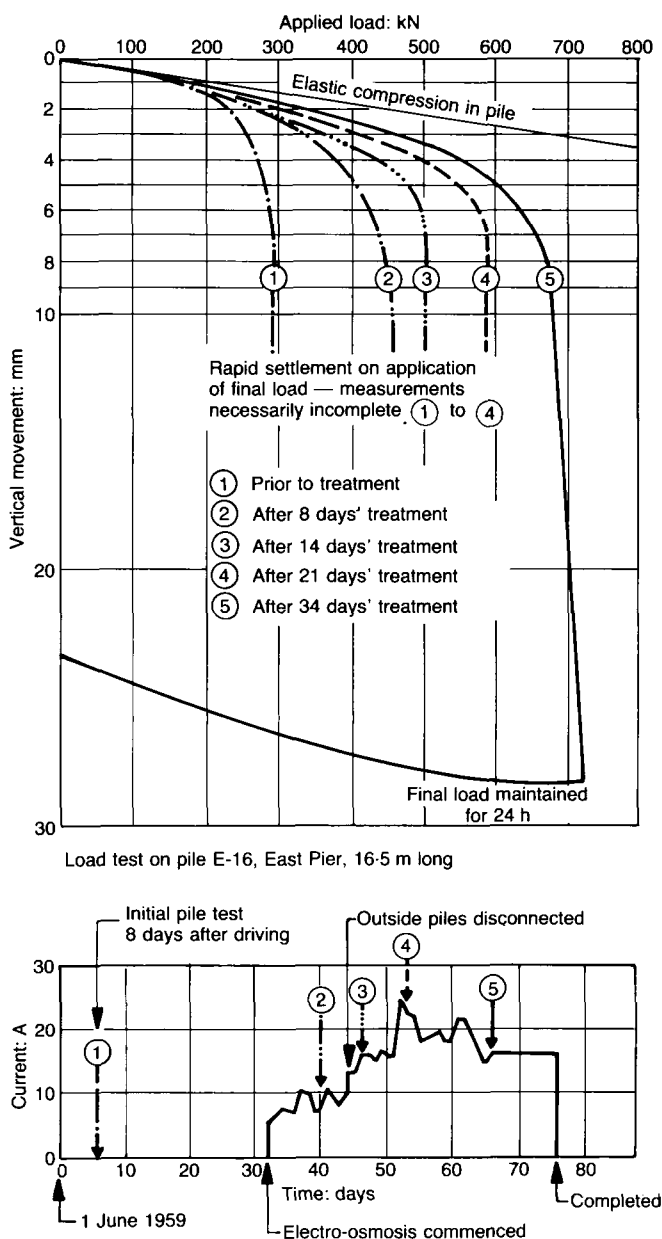


Fig. 6. Pile load tests (1959)—East Pier

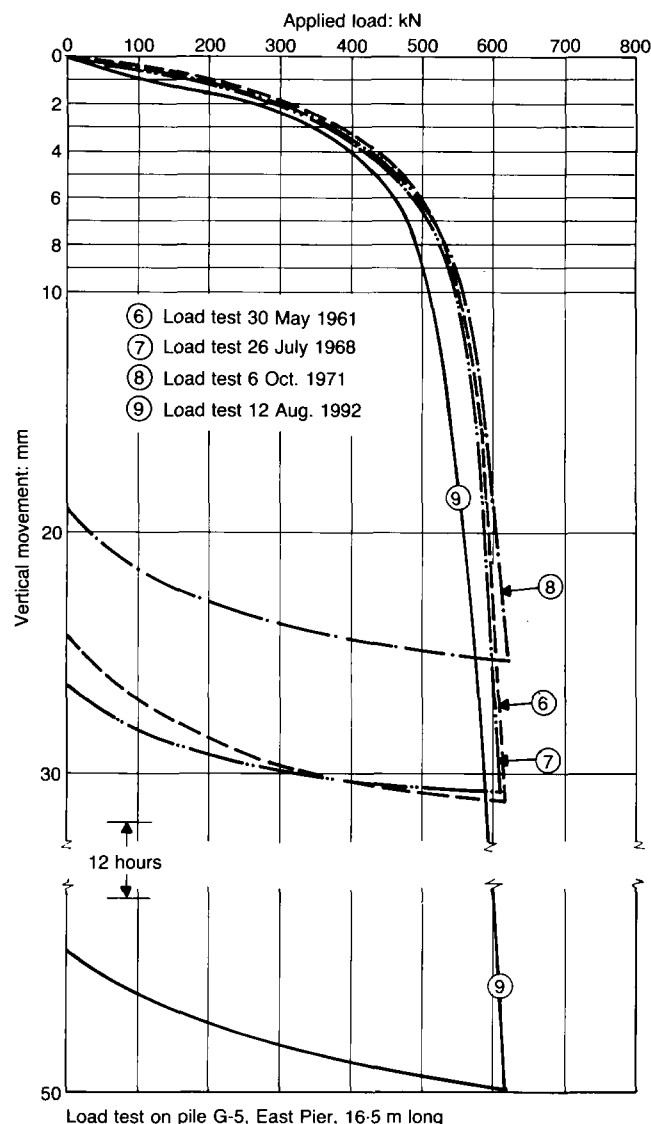


Fig. 7. Pile load tests (1961–1992)—East Pier



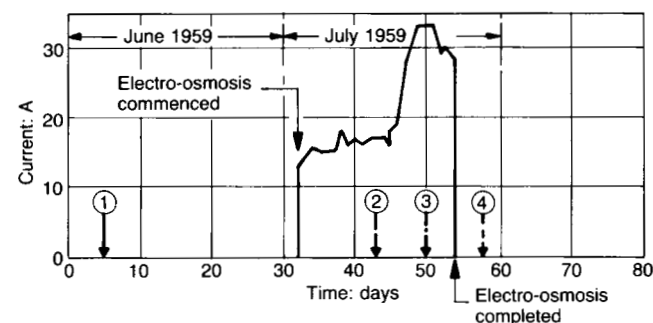
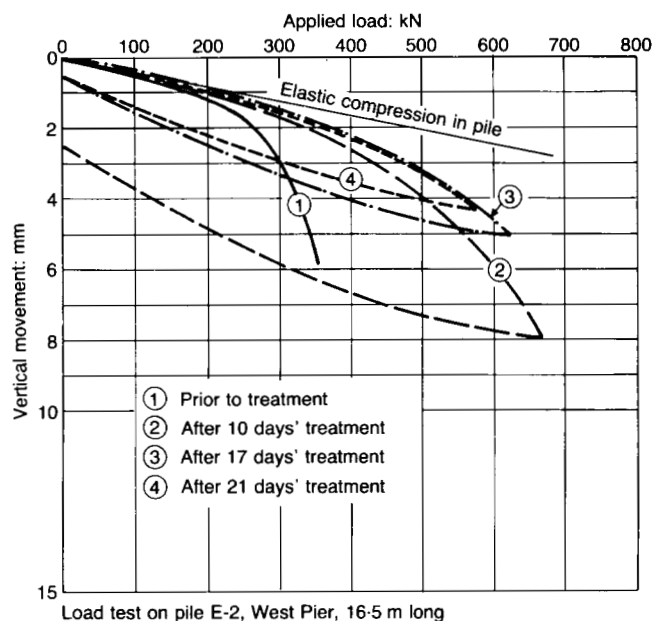


Fig. 8. Pile load tests (1959)—West Pier

case, slightly higher, it can be noted that again there is no reduction in pile capacity with time.

### Settlement

12. Recorded settlements of the pier pile caps during treatment (1959) were generally less than 40 mm. Bridge foundation settlements over the past 30 year period have been of the same order and well within acceptable limits for the structure.

### Conclusions

13. Electro-osmosis was originally developed as a means of dewatering fine-grained soils (Casagrande, 1952).<sup>3</sup> It has also been used to strengthen soft sensitive clays (Bjerrum *et al.*, 1967;<sup>4</sup> Lo *et al.*, 1991<sup>5</sup>); however, it is believed that this is the first example of it being used to increase friction pile capacity. The significance of these data is extremely important. The fact that load tests have been carried out over a period of some 30 years following treatment and that they have demonstrated the undiminished integrity of the

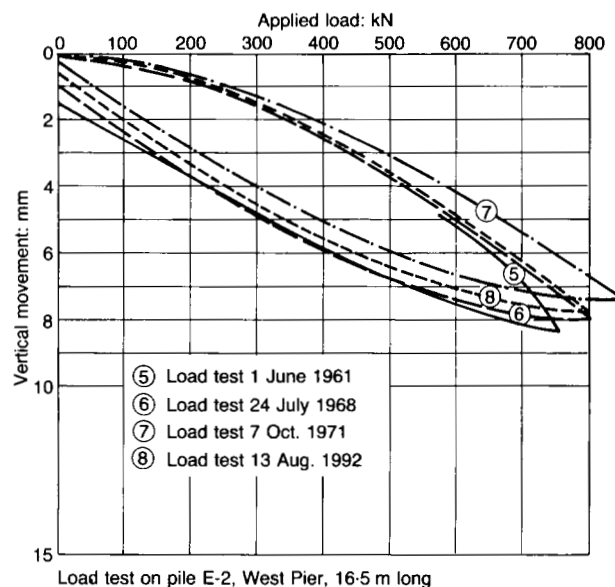


Fig. 9. Pile load tests (1961–1992)—West Pier

foundation is remarkable. Early speculation concerning the long-term effectiveness of electro-osmotic treatment at this site has been answered and the permanence of the process established.

### Acknowledgements

14. This Paper is published with the approval of the Ministry of Transportation, Ontario, Chief Foundations Engineer, Mr M. Devata, who, with his able staff, Ms E. Bennet and Mr Tae Kim, was responsible for the recent pile load tests. The Author is also indebted to many friends and colleagues associated with the Big Pic project over the past 35 years; in particular to Mr A. G. Stermac and to the late L. G. Soderman and Dr L. Casagrande for their invaluable advice and counsel.

### References

1. SODERMAN L. G. and MILLIGAN V. Capacity of friction piles in varved clay increased by electro-osmosis. *Proc. 5th Int. Conf. on Soil Mechanics and Foundation Engineering, Paris, 1961*. Vol. 2, 143–148.
2. CASAGRANDE L. *et al.* Increase in bearing capacity of friction piles by electro-osmosis. Paper presented at the American Society of Civil Engineers Convention, Boston, Mass., 11 Oct. 1960.
3. CASAGRANDE L. Electro-osmosis stabilization of soils. *J. Boston Soc. Civ. Engrs*, 1952, **39**, No. 1, 51–83.
4. BJERRUM L. *et al.* Application of electro-osmosis to a foundation problem in a Norwegian quick clay. *Géotechnique*, 1967, **17**, 214–235.
5. LO K. Y. *et al.* Electro-osmotic strengthening of soft sensitive clay. *Canadian Geotech. J.*, 1991, **28**, 62–73.



## **Appendix C**

### **Summary of the Suggested Design Methods**

# Summary

## Shaft Resistance in Soil

### Cohesionless Soil

Unit Shaft Resistance ( $F_s$ ) =  $K(h) \cdot \tan(\delta) \times \sigma_v' \times A_s$

$$K(h) = K_{\min} + (K_{\max} - K_{\min}) e^{-(\mu h/D)}$$

- Friction Fatigue (Randolph et. al. 1994)

$K_{\min}$  = active earth pressure coefficient

$$K_{\max} = S_t \times N_q$$

$$S_t = 0.1 \exp(-3 \cdot \tan \phi)$$

$\mu$  = decay rate parameter

= 0.03 to 0.05 → for compact to very dense silty sand to sandy silt,

= 0 to 0.03 → for very loose to loose soil, very loose to very dense gravel or silt,

= 0 → for caissons

$h$  = height above the tip of pile

$D$  = pile diameter

### Cohesive Soil

Total Stress Approach ( $\alpha$  method)

$$F_s = \alpha \cdot S_u \cdot A_s$$

Effective Stress Approach ( $\alpha$  method)

$$F_s = \beta \cdot \sigma_v \cdot A_s$$

-  $\alpha$  = Adhesion factor

-  $\beta$  = Shaft friction coefficient

1.  $\alpha$ -methods: Kolk and Van Der Velde (1996) and Karlsrud (2012) provide the best match with the measured shaft resistance.

2.  $\beta$ -methods: Burland (1993) and Karlsrud (2012) provide the best match with the measured shaft resistance.

3. The shaft resistance value should be the minimum predicted resistance obtained from the aforementioned methods.

# Summary

## End Bearing in Soil

### Cohesionless Soil

$$\text{End Bearing} = q_b \times A_b$$

Where: Unit End Bearing Resistance ( $q_b$ ):

$$q_{b1} = N_q \times \sigma_v'$$

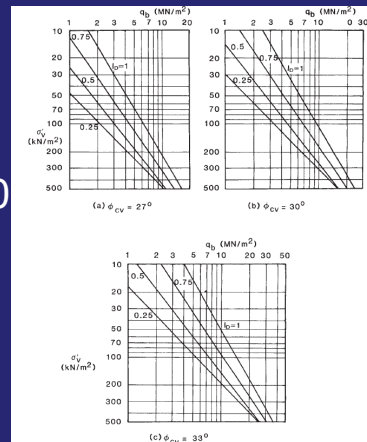
minimum of

**Table C6.11.2.1(a)**  
The values of  $N_q$  for various  $\phi'$  values and pile types (after NAVFAC DM 7.2)

$\phi'$	26	28	30	31	32	33	34	35	36	37	38	39	40
$N_q$ (for driven piles)	10	15	21	24	29	35	42	50	62	77	86	120	145
$N_q$ (for bored piles)	5	8	10	12	14	17	21	25	30	38	43	60	72

$q_{b2}$  = as per Fleming et al. (2009)

- For open end driven piles (small displacement piles) → Multiply  $q_{b2}$  value by a factor of 0.4 to 1.0
- For piles (no-displacement piles) → Multiply  $q_{b2}$  value by a factor of 0.5 to 0.7



### Cohesive Soil

The ultimate toe resistance may be estimated from:

$$R_t = N_s A_t$$

where

$R_t$  = toe resistance

$A_t$  = cross-sectional area of pile at toe

$s_u$  = minimum undrained shear strength of the clay at pile toe

$N_s$  = a bearing capacity coefficient that is a function of the pile diameter, as follows:

Pile toe diameter  $N_s$   
 smaller than 0.5m 9  
 0.5 m to 1 m 7  
 larger than 1m 6

# Summary

## Geotechnical Resistance for Piles in Till

- The recommended design methods for piles driven through and founded on soil were found to be applicable for glacial till deposits.
- The glacial till deposits are typically overconsolidated. Therefore, obtaining the geotechnical design parameters shall be done through a comprehensive field and laboratory investigation program.
- During the preliminary design stage, it is possible to obtain design parameters using empirical correlations specifically developed for glacial till deposits (e.g., Laifa et al., 2015). Additionally, information from field and laboratory testing conducted on glacial till and reported in relevant literature (e.g., Manzari et al., 2014) can also be utilized to inform the design process.

# Summary

## Driven Piles Rest on Bedrock

Predicting the geotechnical capacity of piles rest on sound or fractured bedrock can be computed via following equation.

$$Q_{ult} \text{ (kN)} = N_{cr} \cdot q_u \cdot A_p$$

where:

$A_p$  = toe resisting area

$q_u$  = unconfined compressive strength of rock

For piles rest on sound bedrock:  $N_{cr} = 7.5$

For piles rest on fractured bedrock:  $N_{cr} = \tan^2(45 + \phi/2) + 1$

# Summary

## Driven Piles Rest on Bedrock

- The geotechnical capacity of piles driven to found within the completely weathered bedrock (i.e., residual soil) can be obtained using the design methodologies for piles driven to found on soil.
- The pile geotechnical capacity shall be estimated considering that the entire thickness of completely weathered bedrock will act like soil with both plastic and non-plastic behaviour.

# Summary

## Capacity of Rock Sockets

- Ultimate end bearing and shaft resistance using the equations presented in the CFEM:

### End Bearing

$$q_a = \sigma_c K_{sp} d \quad \text{X3 [to obtain unfactored ultimate resistance]} \quad (18.42)$$

where

$q_a$  = allowable bearing pressure

$\sigma_c$  = average unconfined compressive strength of rock core, from ASTM D2938

$K_{sp}$  = empirical factor, as given in Section 9.2 and including a factor of safety of 3

$d$  = depth factor =  $1 + 0.4 \frac{L_s}{B_s} \leq 3$

$L_s$  = depth (length of the socket)

$B_s$  = diameter of the socket

### Shaft Resistance

$$Q_s = \pi B_s L_s q_s \quad (18.43)$$

where

$B_s$  = diameter of the socket

$L_s$  = length of the socket

$q_s$  = average unit shear resistance along the socket



# Summary

## Capacity of Rock Sockets



Ultimate geotechnical capacity = minimum of the following:

- Peak shaft resistance + mobilized end bearing at peak shaft resistance level of displacement.
- Ultimate end bearing + post-peak shaft resistance

# Summary

## Strength Gain

The semi-empirical method proposed by NGI provides good estimate for the change in the capacity of piles driven into cohesive soil deposits with time.

# Summary

## Relaxation

- Piles driven into dense to very dense saturated fine sands and silts, heavily over-consolidated clays, or weak laminated bedrocks may experience relaxation.
- When relaxation is anticipated, it is recommended to postpone static load testing or restriking of piles a week to two weeks after driving, or even longer if feasible.
- When piles are driven into materials that are prone to relaxation, it is advisable to drive the piles to a capacity higher than the required ultimate capacity to accommodate for some later magnitude of relaxation.